DEVELOPMENT OF RISK ANALYSIS TECHNIQUE AND ITS APPLICATION TO GEO-DISASTER MANAGEMENT IN INDONESIA

サモドラ, グル

https://doi.org/10.15017/1470585

出版情報：九州大学, 2014, 博士（工学）, 課程博士
バージョン：
権利関係：全文ファイル公表済

DEVELOPMENT OF RISK ANALYSIS TECHNIQUE AND ITS APPLICATION TO GEO-DISASTER MANAGEMENT IN INDONESIA

GURUH SAMODRA

DEVELOPMENT OF RISK ANALYSIS TECHNIQUE AND ITS APPLICATION TO GEO-DISASTER MANAGEMENT IN INDONESIA

A Thesis Submitted
In Partial Fulfillment of the Requirements
For the Degree of
Doctor of Engineering

By
GURUH SAMODRA

to the
DEPARTMENT OF CIVIL AND STRUCTURAL ENGINEERING
GRADUATE SCHOOL OF ENGINEERING
KYUSHU UNIVERSITY
Fukuoka, Japan
August, 2014

DEPARTMENT OF CIVIL AND STRUCTURAL ENGINEERING
GRADUATE SCHOOL OF ENGINEERING
KYUSHU UNIVERSITY
Fukuoka, Japan

CERTIFICATE

The undersigned hereby certify that they have read and recommended to the Graduate School of Engineering for the acceptance of this thesis entitled, "***Development of risk analysis technique and its application to geo-disaster management in Indonesia***" by **Guruh Samodra** in partial fulfillment of the requirements for the degree of **Doctor of Engineering**.

Dated: August, 2014

Thesis Supervisor:

_____
Prof. Guangqi CHEN, Dr. Sci.

Examining Committee:

_____
Prof. Yasuhiro MITANI, Dr. Eng.

_____
Prof. Yujing JIANG, Dr. Eng.

teruntuk Bangsa dan Tanah Airku

ABSTRACT

Even though not always as spectacular as earthquakes and tsunami, landslide is of the serious natural hazards since rainfall-induced landslides frequently occur during the rainy season in Indonesia. There are 3307 fatalities caused by landslides from 1998 to 2013 with annual average of 207 fatalities per year. Indonesia is also listed as the top three countries with the highest percentage of landslide fatalities in 2003, 2007 and 2008. Therefore, landslide risk management is an important issue to mitigate disaster and there is an increasing awareness toward the need of landslide prediction and risk assessment tools due to the high number of annual fatalities in Indonesia.

The shift from focusing on disaster response to enhancing risk reduction of disasters has been started for disaster mitigation paradigm since 2007 when a law called *Undang-Undang* 24/2007 was enacted, which was driven by scientific society and government awareness after post-tsunami 2004 emergency response and subsequent rehabilitation and reconstruction phase. Risk analysis, as a basis for risk management, is an important issue in the Law. However, compared with developed countries, the developing country like Indonesia has no adequate landslide inventory available, which is essential for hazard and risk analysis. Also, the technology and know-how of quantitative landslide risk analysis are not well established in Indonesia. For this reason, this study aims at (1) proposing an approach for field investigation to obtain the landslide data and generating a landslide inventory database which is necessary in risk analysis; (2) developing a technique of landslide susceptibility zoning based on the inventory map; (3) proposing a technique to infer rockfall source from rockfall inventory (4) developing rockfall risk zoning based on the distribution of rock boulders from the past rockfall events and the landform classification.

The thesis comprises the following chapters.

Chapter 1 introduces (1) disaster in Indonesia, (2) the shifting disaster mitigation policy in Indonesia, (3) the problems in landslide risk zoning in Indonesia, (4) the scope and objectives of this study, and (5) the organization of the thesis.

Chapter 2 reviews terminologies used in landslide risk analysis and risk management. Although some terminologies are often used interchangeably, the terminology misconception can generate confusion for the decision maker, urban planner, stakeholders and even young engineer. Thus, this chapter attempts to overview the difference between susceptibility, hazard and risk in landslide studies.

Chapter 3 proposes an approach for landslide inventory mapping considering conditions in Indonesia. It includes (1) a plan of items and parameters to be investigated which are necessary in risk analysis; (2) a field investigation procedure which combines the traditional geomorphological field survey method involving active participation from communities with the use of an innovative technology; (3) inventory mapping methods for both landslide and rockfall, which provide information related to location, landslide typology, landslide extents and elements at risk information; (4) statistical analysis to obtain necessary relationships between factors. The so-called *participatory landslide inventory mapping* method is expected to solve the problem of insufficiency of landslide inventory in Indonesia.

Chapter 4 develops a technique of data driven landslide susceptibility zoning based on the inventory map. The key issues in susceptibility zoning are (1) what susceptibility analysis

method should be used and (2) what landslide causative factors should be considered. This chapter, at first, makes a comparison between the three widely used methods: a bivariate method called weight of evidence, a multivariate method called logistic regression and a soft computing called artificial neural network by using landslide data obtained from the participatory landslide inventory mapping. The merits and demerits of each method are summarized, so that the most suitable method may be taken and necessary landslide causative factors may be considered in Indonesia, which is important in particular to the data availability and the characteristic of the study area. And then, a technique is proposed by combining the bivariate method of *weight of evidence* and the *logistic regression* based on the comparison analysis. Finally, landslide susceptibility maps are made using different method. It is shown that landslide susceptibility map using the proposed technique is of the highest accuracy by means of the success rate.

Chapter 5 proposes a rockfall susceptibility analysis method based on rockfall boulder inventory. The rockfall susceptibility analysis is generally carried based on potential rockfall sources which is identified by field investigation. However, field investigation of rockfall source is not always possible for some areas in Indonesia. Thus, how to analyze rockfall susceptibility without the data of potential rockfall source is a great challenge. In this study, at first, a back analysis technique of GIS rockfall simulation is proposed for identifying potential rockfall source based on the distribution of boulders from the past rockfall events. Sensitivity analysis is conducted to discuss the effect of restitution coefficient, a major parameter related to the rebounding characteristic of a falling boulder in the simulation. And then, reliable trajectories, frequency and energy of rockfall are estimated once the potential rockfall sources are identified. Both frequency and energy map obtained from trajectory simulation represent the physical characteristic of rockfall movement and rockfall susceptibility degree.

Chapter 6 develops a technique of quantitative rockfall risk analysis by combining statistical and physical models based on landform classification. Since the movement behaviors of a falling boulder such as flying, rolling, sliding and bouncing are related to landform, firstly, an automated landform classification is proposed by applying unsupervised fuzzy k means based on a modified 9-unit model. And then, a practical formula of rockfall risk is presented based on landform classes. The trajectories and dynamic behavior of boulder when travel along the slope, and its interaction where elements are at risk are calculated based on the landform classes and they are used to evaluate the occurrence probability with particular boulder size in space and time. Finally, the risk to building and the risk to person inside the building are calculated based on the chance of loss (in monetary term) during a specified time. The results show that landform class significantly influences the calculated risk and the chance of loss is the highest in the landform of transportational middle slope. Since the result from rockfall risk analysis indicates the chance of loss during a specified time, it is very useful and helpful in landuse planning and in cost-benefit analysis of disaster mitigation countermeasure.

Chapter 7 summarizes and concludes the results and achievements of the study. Problems are also highlighted for future studies.

ACKNOWLEDGEMENTS

Praise and gratitude to Allah Almighty, because of God's mercy and blessing, this thesis has been completed properly. I owe a debt of gratitude to many people when the dissertation is finished, and I would like to mention a few of those by name. Without their encouragement, patience, effort and good guidance, this study could have never been finished.

First, I express my sincere gratitude to my supervisor, Prof. Guangqi Chen, for his valuable support, kind advises, comments and particularly his enormous encouragement which actually contributed a lot to improve the quality of this work. He also provides me the best scientific research environment and provided me many chances to take part in international conferences and course. LARAM course 2012 (International school on Landslide Risk Assessment and Mitigation) was the turning point of my research. It provided an environment to exchange thoughts and ideas in the field of landslide risk assessment and mitigation.

I would like to express my sincerely gratitude to members of the thesis committee, Prof. Yasuhiro Mitani and Prof. Yujing Jiang for their treasure time in review, evaluation and valuable comments on my thesis. I also deeply appreciate Assoc. Prof. Kiyonobu Kasama, who is so kindly that more like a friend to introduce me about Japanese culture and education. Also, great thanks to Staff Yuichi Yahiro for his enthusiasm, help and kindness.

I am deeply indebted to Prof. Junun Sartohadi and Dr. Danang Sri Hadmoko, my former supervisors in Universitas Gadjah Mada, Yogyakarta for their support during my study.

I would like to extend my grateful acknowledgement to AUN/SEED-Net JICA for providing me the opportunity and scholarship to pursue my study at Kyushu University.

I would like to thank all the students whom I have been studying with at Geo-disaster Prevention Laboratory, where I really enjoy my life in Japan. Thanks to Yinbin Zhang, Yange Li, Hong Zhang, Zheng Han, Fusong Fan, Wang Wei, and Jing Peideng for their joke, cooperation, dissertation printing, etc. I also thank

Koyanagi-san, Kawakami-san, Nakamura-san, Inoue-san, and Naotsuka-san for the *Nihon-go* practice, softball and football game. I was really enjoying it. For Indonesian friends, Pak Syahminan, Pak Agung P, Pak Very, Pak Hariyadi, Pak Agus Didit, Pak Islamy, Pak Taufik and Mas Iping; without all of you my life would not have been comfortable and happy.

I am indebted to my parents and my sister for their love and encouragement for my life. My parents play an important role in nourishing my interest in science and education. Finally, there are too numerous persons who help the author during research and writing to be thanked individually. The author praises that their help will get the return from no one except Allah Almighty.

TABLE OF CONTENTS

LIST OF FIGURES

LIST OF TABLES

CHAPTER 1

INTRODUCTION

1.1 BACKGROUND

1.1.1 DISASTER IN INDONESIA

Indonesia has been laid by a sequence of plate movements over time. There is a place of outstanding geological process related to the active plate tectonic movement (Figure 1.1). The Australian Plate is converging at an average rate of 70 mm/year in the 3° direction (Hutchinson, 2003) along the Java trench. It produces Sunda Arc which extends westward from Sumba passing through Java, Sumatera and Andaman Islands. Along the Timor trench, The Australian Plate is converging at an average 80 mm/year (Hamilton, 1979) which produces Sangihe and Halmahera arc and Sulawesi Arc. It is also the home of 127 active volcanoes located along Sumatra, Java, Bali, North Sulawesi, Sangihe and Halmahera islands as a part of the Pacific Ring of Fire. Those make Indonesian region, which is characterized by complicated seismological features causing several disasters, including the latest deadly disaster Aceh Tsunami in December 2004 affecting 173,741 deaths and Yogyakarta Earthquake affecting 5737 fatalities and 8904 injuries.

Indonesia is also prone to disaster due to climatic condition. The variation of rainfall is often linked with the monsoons because it lies between Asia in the northwest and Australia in the southeast. High pressure in the Asian continent during winter (December to February) forces the wind to blow to the southeast where there is low pressure during summer in Australia. This west monsoon causes rainy season in Indonesia during October to March because the wind crosses the South China Sea. In contrast, the monsoons reverse direction from Australia to Asia, called as

east-monsoons, which causes dry season during April to September. Indonesia receives on average 1755 mm of precipitation annually or 146 mm each month. Drought usually occurs during the dry season; and sediment related disaster and flood usually occur during the rainy season.

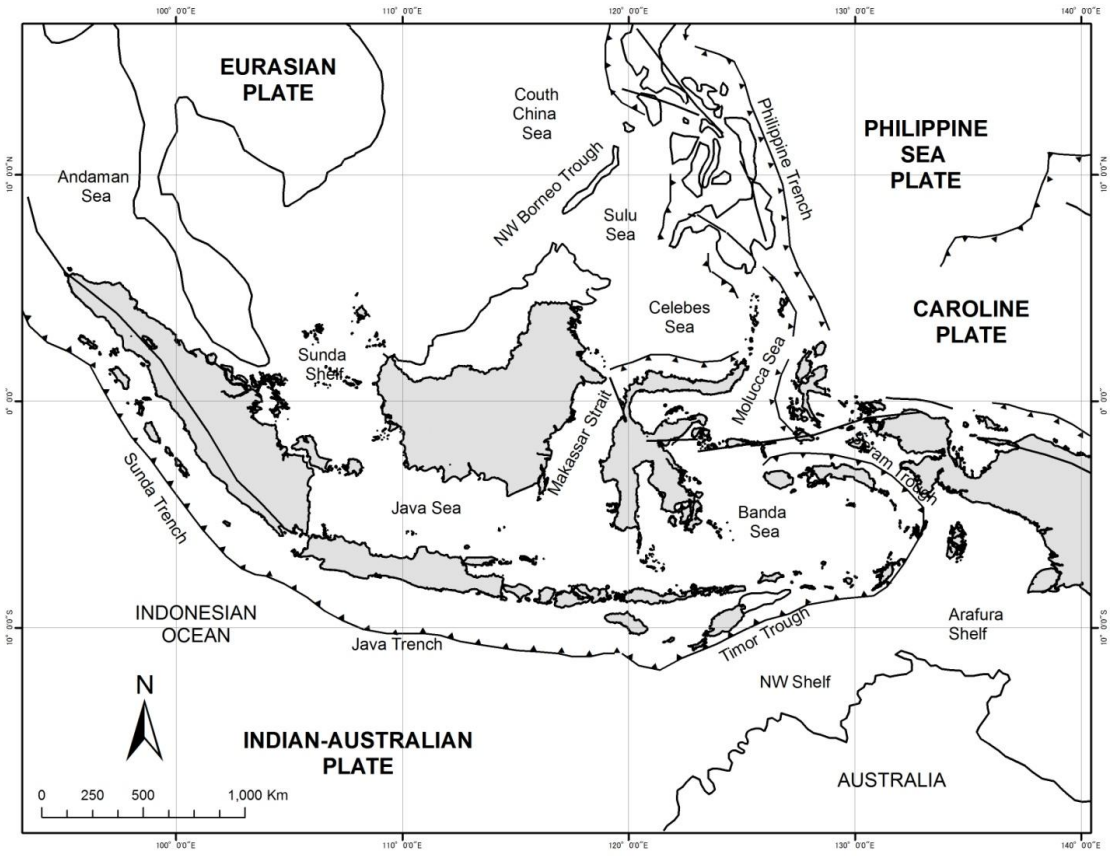

Figure 1.1 Regional Tectonic Setting of Indonesia

Indonesia's island arc and mountain range lying in the complex tectonic setting and high variation of rainfall are subjected to natural disasters, including geophysical disaster and hydro-meteorological disaster, killing 182.783 people during 1996-2014. Most of which are killed by geophysical disaster such as tsunami (92%), earthquake (5%) and volcanic eruption (0.2%). But, the high percentage of fatalities on geophysical disaster is due to Aceh Tsunami 2004 and Yogyakarta Earthquake 2006. Intense rainfall and weathering process may cause hydro-meteorological disaster such as landslide and flood which affect 1.9% and 1.2% fatalities respectively. Floods and landslides periodically occur in Indonesia. Landslides is ranked as the highest average annual occurrences and fatalities in Indonesia.

Even though not always as spectacular as earthquakes and tsunami, rainfall-induced landslides frequently occur in Indonesia during rainy season. The annual frequency, calculated from DIBI (Indonesian Disaster Database) 1998-2013, is 158 events/year (Figure 1.2). However, this data may be underestimated since landslides occurrences reported by DIBI are based on provincial and regency report. Smaller scale landslide without fatalities may not be reported in DIBI. Landslides caused 3432 loss lives with annual frequency fatalities 214 people/year (Table 1.1). Indonesia is also listed as the top three countries with the highest percentage of landslide fatalities in 2003, 2007 and 2008 (Kirschbaum, 2010).

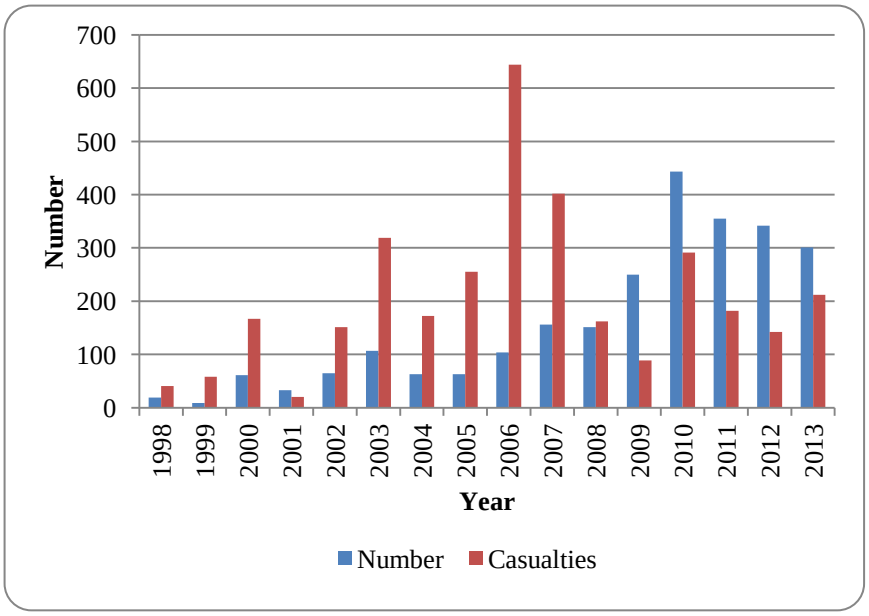

Figure 1.2 Number of Landslides and Fatalities in Indonesia (DIBI, 2014)

Along with the increasing number of material and fatalities due to the landslide occurrence, there is increasing awareness toward the need of landslide prediction and risk reduction tools. Prevention and remediation as hard countermeasure are not always possible, especially in the rural area where settlement/housing is spread out. Hard measures installation in each single building will cost too much and not feasible. Practical considerations for the establishment of countermeasures is an important issue for administrators and stakeholders in the landslide prone area. It is feasible to map major instable areas and to take measures for avoidance, prevention or remediation of landslide occurrences based on observation, analysis and research. An integrated strategy for observation, research, assessment and management includes

landslide hazard mitigation from a spatial zoning point of view. The decision for avoidance, prevention and remediation is well approached by landslide risk analysis.

Table 1.1 Ranking of Major Natural Hazards by Fatalities and Injuries in Indonesia (DIBI, 2014)

Rank	Disaster Type	Fatalities	Injuries
1	Tsunami	167,780	18,860
2	Earthquake	8,950	58,993
3	Landslide	3,432	42,875
4	Flood	2,190	190,333
5	Volcanic Eruption	429	3,472
6	Drought	2	0
Total		314,533	533,416

Source: Indonesian Disaster Database (http://dibi.bnpb.go.id/DesInventar/dashboard.jsp)

1.1.2 DISASTER MANAGEMENT POLICY IN INDONESIA

The shift in disaster management paradigm from focusing on disaster response to enhancing disaster risk reduction has been started in 2007 by enactment of *Undang-Undang* (Law) 24/2007. It was driven by scientific society and government awareness after post-tsunami emergency response and subsequent rehabilitation and reconstruction phase. The momentum was also appeared by the experiences of Nabire Earthquake 2004, Nias Earthquake 2005, and Yogyakarta Earthquake 2006 emergency response. However, the initiative to reform the Disaster Management Law has been started before the earthquake and tsunami of 26 December 2004. There were a discussion forum between BAKORNAS PB (National Disaster Management Coordination and Agency), NGO's and MPBI (Indonesian Society for Disaster Management) to promote national disaster management. Before the enactment Law 24/2007, the disaster management in Indonesia were focusing on crisis management and disaster response coordinated by BAKORNAS PB.

The Disaster Management Law 24/2007 enforces a systematic approach in disaster risk reduction that contains three phases of the disaster management cycle as follows:

1. pre-disaster planning and preparedness, including disaster risk reduction, mitigation, preparedness, risk assessment and contingency planning
2. emergency response, including evacuation, search and rescue, providing immediate assistance, assessing damage and disaster relief
3. post disaster management, including rehabilitation and reconstruction.

The law also mandates the creation of the "new BAKORNAS PB", later called as BNPB (National Disaster Management Agency), as a national coordinating agency for disaster management that is responsible for pre disaster planning, emergency response and post disaster management. BNPB must coordinate all contingencies, preparedness, mitigation, prevention, disaster management training, risk assessment and risk zoning. In the emergency response phase, BNPB has a responsibility to coordinate government, NGO's and international organization during the emergency response phase. BNPB must also coordinate damage and loss assessment and coordinate rehabilitation and reconstruction in the post disaster phase.

However, with the high responsibility for conducting disaster management, BNPB needs partners to provide all the technical support, to train technical personnel, and to create preventive disaster risk reduction culture in Indonesia. One of the representative partners to provide technical expertise in the full spectrum of disaster related fields is the university partner. It is expected to be an intellectual capital, which is able to provide technical assistance in disaster risk reduction including the research and technology development of early warning systems, damage assessment and risk analysis.

Risk analysis, as a basis for disaster risk reduction, is an important issue in the Law 24/2007. Disaster prevention planning should include disaster risk data documentation and risk analysis. Development activities which may have high risk must be equipped with risk analysis. The implementation of risk analysis is closely related to spatial planning or landuse planning. Two other laws were also enacted in 2007 i.e. Law 26/2007 about spatial planning and Law 27/2007 about coastal zone management and small islands. Both have a strong attachment to disaster mitigation. Law 26/2007 dictates that spatial plan documents should be based on the consideration of disaster mitigation measures. Law 27/2007 states that disaster reduction strategy has to be included in the coastal zones and small islands spatial

plan. Spatial planning at national, provincial and regency level is developed for 20 years and can be reviewed once in 5 years. If a disaster happens due to the development in a high risk area which is not equipped with disaster risk analysis, the responsible parties can be fined for up to US$ 26000 or jailed up to 3 years.

Thus, spatial planning based on disaster risk reduction is one of the primary issues of the Indonesia's national development agenda to promote sustainable development due to the increasing frequency of disasters and continuing environmental degradation. In terms of landslide disaster risk reduction, regional development and disaster mitigation are well approached by landslide susceptibility, hazard and risk zoning.

1.1.3 Landslide Risk Analysis: the Problems in an Incomplete-data Environment

Landslide risk analysis involves several steps, i.e. scope definition, landslide hazard identification and risk estimation. Scope definition addresses several issues including delineating the study area, elements at risk identification, and methodology selection. Landslide hazard identification addresses several issues on understanding physical characteristic of study area regarding to landslide processes such as understanding geology, geomorphology, hydrogeology and climate. It also includes collecting landslide data, such as landslide classification, area, volume, travel distance, date occurrence, and elements at risk. Hazard identification activities are mostly related to landslide inventory. Risk estimation deals with consequence analysis and frequency analysis.

Landslide inventory is very important in the landslide risk analysis because it gives information related to frequency of occurrences, landslide typology, landslide extents and damage of elements at risk. Estimation of spatial probability, temporal, probability and magnitude probability is not possible without landslide inventory containing sufficient data of past landslide events. In Indonesia, especially where this research was undertaken, adequate landslide inventory is not available. It is a central problem of quantitative landslide risk analysis in Indonesia. Thus, producing landslide inventory maps and developing approaches of using those maps for landslide risk zoning in Indonesia are challenging task that this research focuses on.

1.2 SCOPE AND OBJECTIVES

Landslide is defined, as general terminology, to describe the movement of rock, debris or soil down a slope due to gravitational process (Fell et al., 2008). However, the terminology of landslide, in this research, is used interchangeably to define rotational and translational slide. For the movement of the rock, we used word "rockfall". Landslide hazard and risk analysis, as a soft preventive countermeasure, is a vital tool for disaster risk reduction in Indonesia because of the shifting paradigm of its disaster management from focusing on disaster response to enhancing disaster risk reduction. However, the major drawback of generating landslide risk analysis is the unavailability of landslide inventory data, which makes difficulties in estimating spatial probability, temporal probability and magnitude probabilities. This research will distinguish its analysis based on typology i.e. landslide (focusing on rotational and translational slide) and rockfall. Thus, the objectives of this research are:

(1) to propose a method of landslide inventory mapping based on available information or archives in Indonesia. These inventory data should include landslide extents and date of occurrences that can be used to estimate spatial, temporal and magnitude probabilities;

(2) to compare existing landslide susceptibility zoning method using the proposed landslide inventory technique, to analyze the spatial association between landslide and a set of controlling factor, and to propose a technique how to improve the accuracy of the model based on the evaluation of existing landslide susceptibility zoning;

(3) to propose a back analysis technique to infer rockfall source from rockfall inventory;

(4) to develop rockfall risk zoning based on the distribution of rock boulders from the past rockfall events and the landform classification.

1.3 THESIS ORGANIZATION

The thesis comprises the following chapters.

Chapter 1 introduces (1) disaster in Indonesia, (2) the shifting disaster mitigation policy in Indonesia, (3) the problems in landslide risk zoning in Indonesia, (4) the scope and objectives of this study, and (5) the organization of the thesis.

Chapter 2 reviews terminologies used in landslide risk analysis and risk management. Although some terminologies are often used interchangeably, the terminology misconception can generate confusion for the decision maker, urban planner, stakeholders and even young engineer. Thus, this chapter attempts to overview the difference between susceptibility, hazard and risk in landslide studies.

Chapter 3 proposes an approach for landslide inventory mapping considering conditions in Indonesia. It includes (1) a plan of items and parameters to be investigated which are necessary in risk analysis; (2) a field investigation procedure which combines the traditional geomorphological field survey method involving active participation from communities with the use of an innovative technology; (3) inventory mapping methods for both landslide and rockfall, which provide information related to location, landslide typology, landslide extents and elements at risk information; (4) statistical analysis to obtain necessary relationships between factors. The so-called *participatory landslide inventory mapping* method is expected to solve the problem of insufficiency of landslide inventory in Indonesia.

Chapter 4 develops a technique of data driven landslide susceptibility zoning based on the inventory map. The key issues in susceptibility zoning are (1) what susceptibility analysis method should be used and (2) what landslide causative factors should be considered. This chapter, at first, makes a comparison between the three widely used methods: a bivariate method called weight of evidence, a multivariate method called logistic regression and a soft computing called artificial neural network by using landslide data obtained from the participatory landslide inventory mapping. The merits and demerits of each method are summarized, so that the most suitable method may be taken and necessary landslide causative factors may be considered in Indonesia, which is important in particular to the data availability and the characteristic of the study area. And then, a technique is proposed by combining the bivariate method of *weight of evidence* and the *logistic regression* based on the comparison analysis. Finally, landslide susceptibility maps are made using different method. It is shown that landslide susceptibility map using the proposed technique is of the highest accuracy by means of the success rate.

Chapter 5 proposes a rockfall susceptibility analysis method based on rockfall boulder inventory. The rockfall susceptibility analysis is generally carried based on

potential rockfall sources which is identified by field investigation. However, field investigation of rockfall source is not always possible for some areas in Indonesia. Thus, how to analyze rockfall susceptibility without the data of potential rockfall source is a great challenge. In this study, at first, a back analysis technique of GIS rockfall simulation is proposed for identifying potential rockfall source based on the distribution of boulders from the past rockfall events. Sensitivity analysis is conducted to discuss the effect of restitution coefficient, a major parameter related to the rebounding characteristic of a falling boulder in the simulation. And then, reliable trajectories, frequency and energy of rockfall are estimated once the potential rockfall sources are identified. Both frequency and energy map obtained from trajectory simulation represent the physical characteristic of rockfall movement and rockfall susceptibility degree.

Chapter 6 develops a technique of quantitative rockfall risk analysis by combining statistical and physical models based on landform classification. Since the movement behaviors of a falling boulder such as flying, rolling, sliding and bouncing are related to landform, firstly, an automated landform classification is proposed by applying unsupervised fuzzy k means based on a modified 9-unit model. And then, a practical formula of rockfall risk is presented based on landform classes. The trajectories and dynamic behavior of boulder when travel along the slope, and its interaction where elements are at risk are calculated based on the landform classes and they are used to evaluate the occurrence probability with particular boulder size in space and time. Finally, the risk to building and the risk to person inside the building are calculated based on the chance of loss (in monetary term) during a specified time. The results show that landform class significantly influences the calculated risk and the chance of loss is the highest in the landform of transportational middle slope. Since the result from rockfall risk analysis indicates the chance of loss during a specified time, it is very useful and helpful in landuse planning and in cost-benefit analysis of disaster mitigation countermeasure.

Chapter 7 summarizes and concludes the results and achievements of the study. Problems are also highlighted for future studies.

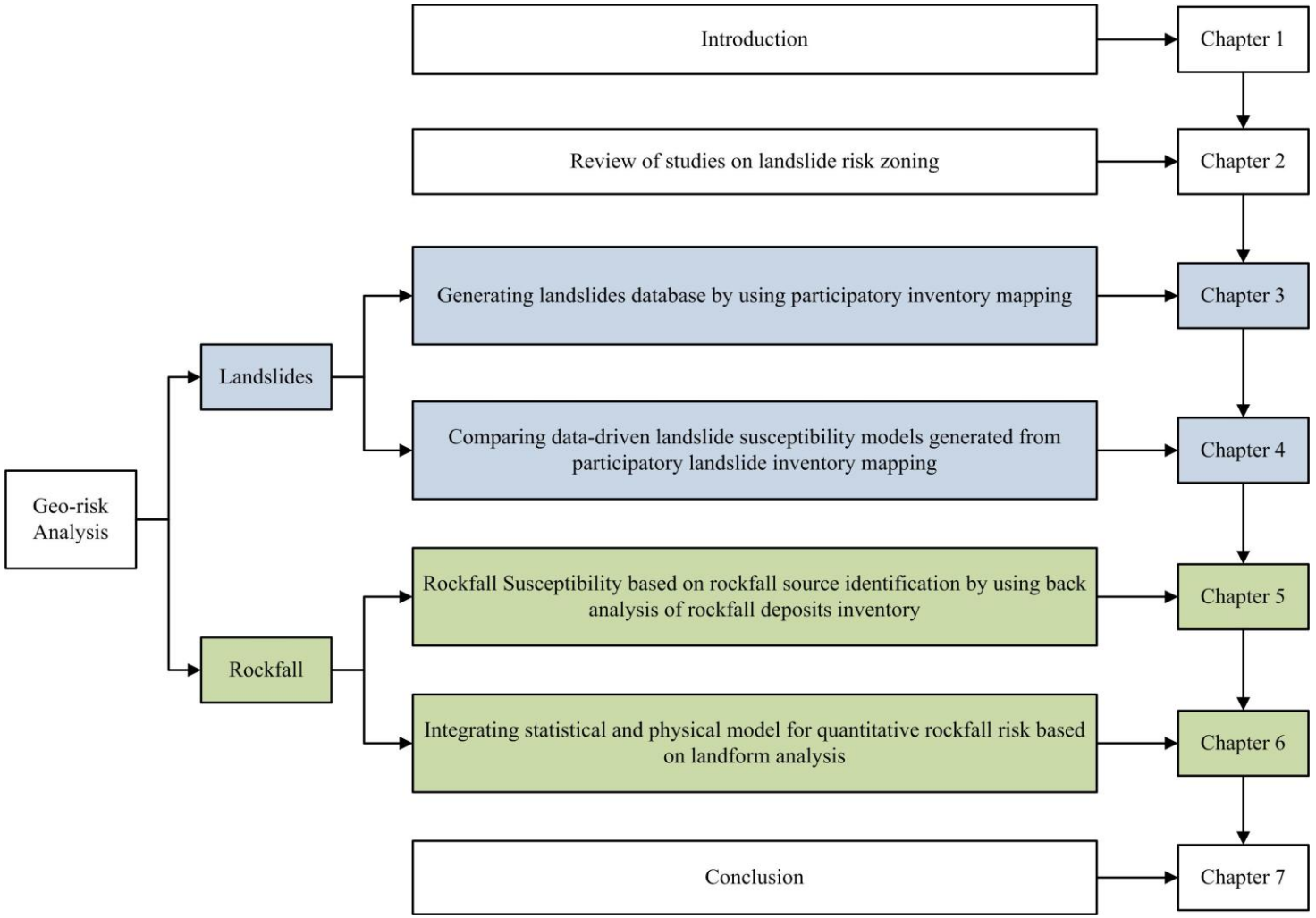

Figure 1.3 The Thesis Organization

REFERENCES

Anonym. 2007. Undang-Undang Nomor 24 Tahun 2007 tentang Penanggulangan Bencana, Lembaran Negara Republik Indonesia tahun 2007 nomor 66, Jakarta.

Anonym. 2007. Undang-Undang Nomor 26 Tahun 2007 tentang Penataan Ruang, Lembaran Negara Republik Indonesia tahun 2007 nomor 68, Jakarta.

Anonym. 2007. Undang-Undang Nomor 27 Tahun 2007 tentang Pengelolaan Wilayah Pesisir dan Pulau-pulau Kecil, Lembaran Negara Republik Indonesia tahun 2007 nomor 84, Jakarta.

DIBI. 2014. Indonesian Landslide Disaster Database 1998-2013. Accessed on March 2014 from http://dibi.bnpb.go.id/DesInventar/dashboard.jsp

Fell, R., Corominas, J., Bonnard, C., Cascini, L., Leroi, E., and Savage,W. Z. 2008. "Guidelines for landslide susceptibility, hazard and risk zoning for land use planning". *Eng. Geol.*, 102, 85–98,.

Hamilton, W. 1979. Tectonics of the Indonesian Region. U.S. Geological Survey Profesiional Paper 1078. US Government Printing Office. Washington.

Hutchinson, C, S. 2003. in Gupta, A.(Ed.), 2003. *The physical geography of Southeast Asia*. Oxford Univercity. Press,

Kirschbaum, D.B., Adler, R., Hong, Y., Hill, S., dan Lerner-Lam, A. 2009. A Global Landslide Catalog for Hazard Application: Method, Result, and Limitations. *Journal of Natural Hazard* doi 10.1007/s11069-009-9401-4.

CHAPTER 2

REVIEW OF STUDIES ON LANDSLIDE RISK ZONING

2.1 INTRODUCTION

Risk is defined, in the Oxford dictionary of English, as possibility of future harms viewed from the present (Soanes and Steventon, 2005). The concept of risk is also used by various disciplines resulting many definitions and paradigms on how it is calculated either qualitative, semi-quantitative or quantitative. For example, in Economics and finance, risk is defined as the probability of financial asset return or the probability that an actual return on a financial investment will be lower than the expected return (Andersen, et al., 2013). In natural hazard, risk is defined as the probability and severity of a future harm to health, property or the environment (IUGS, 1997; Fell et al., 2008). More specific to the effect of natural disaster, risk is defined as the expected number of lives lost, injured persons, damage to property, or disruption of economic activity due to a natural phenomenon (Varnes, 1984; Cardona, 2003). In application of risk analysis, they generally involve more mathematical term dealing with term "probability" which depend on hazard, vulnerability and elements at risk. Assuming their independency, it is described by the product of elements at risk (E), vulnerability (V) and hazard (H), expressed by the following formula (Varnes, 1984; Ebert *et al*., 2009):

$$Risk = f(hazard, vulnerability, element\ at\ risk) \quad (2.1.)$$

Risk can be qualitative, semi-quantitative and quantitative. Qualitative risk uses a descriptive or word form to describe the degree of risk or the likelihood that potential

consequences will occur. Semi-quantitative risk is rather similar with qualitative risk, but it uses a numeric rating scale.

Nowadays, geographical data related to disasters can be handled in a GIS (Geographic Information System) environment, even by users who are not experts in GIS or natural hazard field due to the advanced development and more user friendly GIS software. However, the terminology and methodology in landslide risk studies may be diverse significantly from country to country and even within the same country such as Indonesia. The interchangeably terminology used of susceptibility and hazard in the scientific literature is one of the examples. Some literatures on landslide hazard zoning often discuss methods and techniques on landslide susceptibility zoning. Landslide susceptibility and landslide hazard are also often used as synonymous, even though those are rooted from different concept. The terminology misconception between susceptibility and hazard often generates confusion for the decision maker, urban planner, stakeholders and even young engineer.

Thus, this chapter attempts to overview the difference between landslide susceptibility, landslide hazard and landslide risk. The information on susceptibility involves mainly the spatial probability, whereas the information in hazard involves the spatial probability, temporal probability and landslide size (area or volume) probability. Some issues on landslide risk zoning are also highlighted.

2.2 LANDSLIDE RISK

In landslides studies, quantitative risk assessment has been applied and developed since long time ago by geotechnical engineer on a site investigation scale, such as pipeline, road, dam, oil platform, and housing. The analysis will be more focused on the hazard analysis of a specific slope. It uses deterministic (factor of safety, numerical analyses) and/or probabilistic methods, e.g. first order, second-moment (FOSM), first order reliability method (FORM), point estimate methods, and Monte Carlo Simulation (MCS). However, quantitative risk zoning in large areas for landuse planning in which this research focuses on seems still need improvement.

Similar to equation 2.1, landslide risk also involves hazard, vulnerability and elements at risk. It should comprise probability of landslide, run out behavior, vulnerability of property and people to landslide (Dai *et al*., 2002). IUGS Working Group on Landslides (1997) also proposed the overall framework for quantitative risk analysis of landslide as follows: (1) hazard analysis – analysis of the probability and the characteristics of the potential landslide (2) identification of elements at risk (3) analysis of the vulnerability of the elements at risk and (4) calculation of the risk from the hazard. Thus, landslide risk zoning assesses the loss of life or property or environmental features accounting for temporal probability, spatial probability, magnitude probability and vulnerability. In practice, it would not be simple to achieve and need detailed investigation on each risk element, i.e. hazard, vulnerability and element at risk.

2.2.1 LANDSLIDE HAZARD

Hazard can be defined as a potential condition as an effect of an occurrence to have an undesirable consequences or damage (IUGS, 1997). Furthermore, landslide hazard defined as the probability of occurrence within a specified period of time and within a given area of a potentially damaging phenomenon (Varnes, 1984) includes spatial, temporal and magnitude probability of landslide events. It is characterized by statements of ‘what’, ‘where’, ‘when’, ‘how strong’ and ‘how often’, demanding knowledge of variation in both spatial conditions, temporal and magnitude behavior (Glade et al., 2005). The information should include the location, size (area and or volume) classification and velocity of the potential landslides and any resultant detached material and the probability of their occurrence within a given period of time. It provides potential capability to describe landslide distribution spatially and temporally. The landslide hazard map is a tool used to portray the location of landslide, the predicted location of landslide, and can be used to divide the different level of risk areas (Guzzetti *et al*., 2000).

Landslide hazard is expected to answer temporal and magnitude probability which are not taken into account in landslide susceptibility zoning. Generating landslide hazard from landslide susceptibility requires estimation of spatial, temporal

and magnitude probabilities (Guzzetti et al., 1999; Glade et al., 2005; Fell et al., 2008; van Westen et al., 2008). Thus, landslide hazard analysis needs information about landslide susceptibility and landslide inventory containing the date of landslides events and area/volume of landslides. However, the date of the landslide events and area/volume of landslides are difficult to be included in most of landslide hazard maps because several factors, i.e. 1) absence of multi-temporal data of landslide events, 2) heterogeneity of the subsurface conditions, 3) scarcity of input data and 4) absence or insufficient length of historical records of triggering events (van Westen et al., 2006). Thus, generating landslide inventory is essential for landslide hazard analysis.

2.2.1.1 LANDSLIDE INVENTORY

A landslide inventory, called also as landslide map or just "inventory" (Guzetti et al. 2012), is the simplest form of landslide map (Hansen, 1984; Wieczorek, 1984; Guzetti et al., 1999). It is a data set that represents single or multiple events as well as shows the locations and outlines of landslides (Chacon 2006). Location, type of landslide, the volume, activity, date of occurrence and other characteristic of landslides in the area (Fell et al., 2008) as well as information on triggering factors (Godt et al., 2008) should be available in landslide inventory.

Landslide inventory is the basis for landslide susceptibility, hazard and risk zoning (Carrara and Merenda, 1976; Guzzetti et al., 2000; Brardinoni et al., 2003). It provides spatial distribution of landslide which is useful for landslide susceptibility; date of occurrences for generating landslide temporal probability and information of area or volume for generating magnitude probabilities. Without complete temporal archives, it is difficult to generate temporal probability by relative times. But some historical inventories obtained from well archived data will give information related to date of occurrences. There are several methods for preparing a landslide inventory such as traditional methods (field survey, interpretation of aerial photograph) and modern techniques (interpretation of very detailed DTMs and interpretation and analysis of satellite imagery) (Guzetti, 2006; van Westen et al., 2008).

Many attempts have been made to prepare landslide hazard maps based on traditional inventory method (Guzzetti et al., 2005; Pradhan, 2010; van Westen et al.,

2003). Traditional method based landslide inventory is produced by interpretation of aerial photographs coupled with field surveys. It can be defined as geomorphological inventories and can also be combined with collecting historical information on individual landslide events called as archive inventory (Guzetti et al., 2000; Malamud et al., 2004). According to the availability of temporal database, traditional method can be classified further as historical, event, seasonal or multi-temporal inventories. Temporal information is usually given in relative terms, i.e., recent, old or very old.

An event inventory informs landslide occurrences that caused by a single trigger, such as earthquake, a rainfall or snowmelt event showing the date of the landslides which corresponds to the date (or period) of the trigger event. Seasonal and multi-temporal inventories are obtained by interpretation multiple sets of aerial or satellite images of different dates. The main difference both of those inventories is the period (short/season or long period) of the triggering event. A seasonal inventory shows landslide triggered by single or multiple events during a single season or a few seasons, while multi-temporal inventory indicates landslide occurrences triggered by multiple events over longer periods. Similar to the event inventory, the seasonal and multi-temporal inventories inform the date of the landslides which corresponds to the period of the trigger event. Preparation of landslide inventories by traditional methods is a substantial challenge because it requires time and a team of experienced people. Galli et al. (2008) estimated that preparation of an inventory took an average one month per interpreter to cover 100 km^2 area in the Umbria region of Italy.

In some cases, it is difficult to obtain all the landslides by field survey and interpretation of aerial photograph, especially in a vastly inaccessible mountainous area. It is also often subjective, prone to error (Malamud et al., 2004), time consuming and difficult to carry out in forested terrain (Brardinoni et al., 2003; Van den Eeckhaut et al., 2005). Recent techniques of landslide inventory are comparatively fast, unbiased and data driven, and the outputs are also visually consistent. It involves interpretation of very detailed DTMs (Digital Terrain Models) and interpretation and analysis of satellite imagery which have been widely used to resolve this problem (Nichol and Wong, 2005; Mondini et al., 2011, Barlow et al., 2006; Martha et al., 2010b; Moine et al., 2009). Automatic identification was also

applied to identify landslides using satellite imagery data (Barlow et al., 2006; Borghuis et al., 2007; Martha et al., 2010b; Nichol and Wong, 2005b; Rosin and Hervas, 2005). However, it is data driven, cloud problem image in tropical country and still expensive in developing countries.

2.2.1.2 LANDSLIDE SUSCEPTIBILITY

Landslide susceptibility is an estimate of spatial distribution in which landslide potentially may occur in an area. It shows the likelihood of occurrence of landslide in a given location (Corominas and Moya, 2008) and takes the output of the landslide inventory mapping or by computing probability of failure of the slopes. Susceptibility poses the spatial probability in which the landslide may occur or an estimation "where" landslides are likely to occur. Landslide susceptibility does not consider "when", "how frequent" and "how large" landslides are likely to occur.

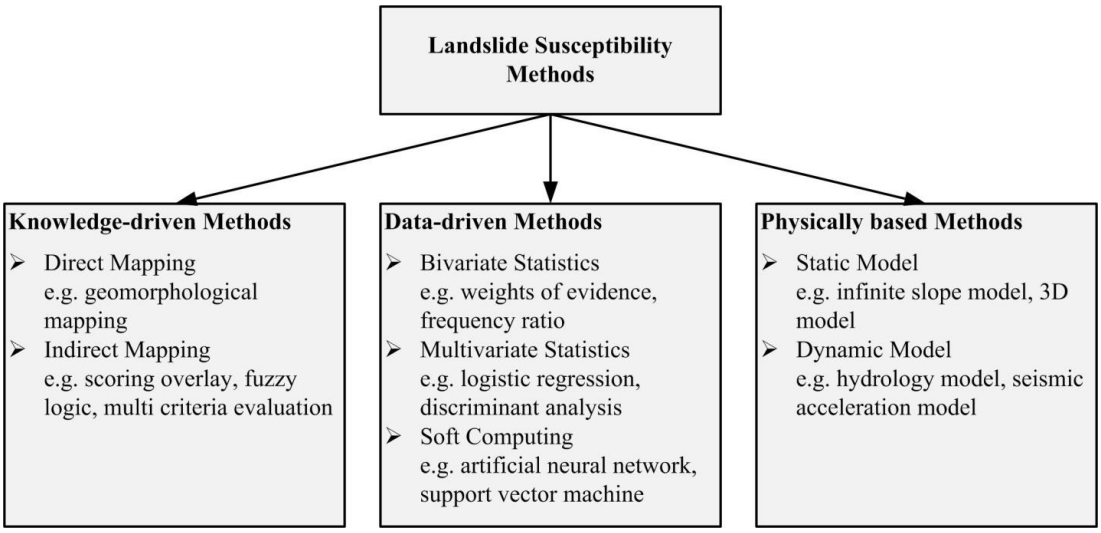

Figure 2.1 Methods for Landslide Susceptibility Assessment

Lanslide susceptibility zoning is usually carried out in GIS-based system. GIS (Geographic Information Systems) and remote sensing technology offer more effective and efficient data handling for modeling of the real world. It can support efficient and effective data capture, storage, management, retrieval, analysis, integration and display, and have shown great advantages to the study and mapping of landslide distributions and potential (Carrara *et al*., 1995). Recently, GIS technology has influenced the development of landslide susceptibility zoning and

given more benefits to model it (Atkinson and Massari, 1998; Westen *et al*., 2003; Huabin *et al*., 2005). Several methods of landslide susceptibility include knowledge driven, data driven, and physically based methods (Figure 2.1).

Knowledge-driven method is classified into qualitative, whereas data driven and physically based methods are classified as quantitative. The assessment of landslide susceptibility can also be classified based on the area extents i.e. in site-specific location and in wide areas. In the site-specific location, landslide susceptibility zoning is usually emphasized on the safety factor of the slope. In the other hand, the assessment of the wide area is usually represented by landslide susceptibility zoning either in qualitative, semi-quantitative or quantitative.

Knowledge-driven or heuristic method can be direct (i.e. geomorphology-landslide mapping) and indirect (i.e. index based, AHP, fuzzy logic and spatial multi criteria evaluation). Direct Geomorphological susceptibility zoning is a traditional method in landslide susceptibility zoning. It includes the identification of landforms related to landslide. Long experiments, fieldwork and laboratory analysis were done in order to provide a landslide hazard assessment. Some geomorphology features were analyzed, including soil properties related to the landslide. This work was especially done in specific geomorphology features presumed as the main factor of landslide such as in micrograben (Moeyersons *et al*., 2003). In Indonesia, direct geomorphological hazard zoning is usually combined with heuristic or index-based method (Priyono *et al*., 2006; Kumajas, 2006; Mardiatno, 2001; Sutikno *et al*., 2002).

Geomorphology features were analyzed through terrain mapping unit. Soil properties were analyzed based on terrain mapping unit in order to index the potential landslide hazard. This method usually did not analyze the past landslide occurrences or without landslide inventory mapping. It is very subjective and depends on the experience and the judgment of the researcher (Atkinson and Massari, 1998; Nagarajan *et al*., 2000; Huabin *et al*., 2005). However, it sometimes can be used to control mathematic or statistic procedure used in landslide susceptibility zoning or modeling (Westen *et al*., 2003; Guzzetti, 2005).

The more objective methods and quantitatively sound are geotechnical or physically based models and statistically based models. Geotechnical or physically

based models are usually based on the slope analysis, determining safety factor in the slope. It is usually applied in site-specific location (large scale mapping) and detail measurement of slope failure. The limitation of geotechnical models are that the model can only be applied in the homogeneous geological region (Dahal, *et al*., 2007), similar landslide mechanism, and cannot be analyzed easily (Huabin *et al*., 2005). It is not possible to be applied in the wide area because of the mechanical parameter of the slope cannot be extrapolated in the regional scale (Ruff and Czurda, 2007)

The statistical (data-driven) based model was widely used due to the development of GIS technology. The model is usually applied either based on bivariate, multivariate or soft computing. Bivariate involves weight of evidence (van Westen, 1993; Bonham-Carter, 1994; Suzen and Doyuran, 2004), likelihood ratio model (Lee, 2005), and favourability functions (Chung and Fabbri, 1993; Luzi, 1995). Multivariate model involves discriminant analysis (Carrara, 1983; Gorsevski et al., 2000) and logistic regression (Ohlmacher and Davis, 2003; Gorsevski et al., 2006). Soft computing involves ANN (Lee et al., 2004; Ermini et al., 2005; Kanungo et al., 2006) and SVM (Yao et al., 2008)

Landslide susceptibility is an initial step towards landslide hazard and risk, but it can also be an an end product that can be used in land use planning (Corominas et al., 2013). In Indonesia, geomorphological mapping combined with heuristic weighting is one of the most common methods of landslide susceptibility zoning due to unavailability of spatial past landslide inventory data. Geomorphology approach, focusing on landform, material, and geomorphic processes were used in order to construct a landslide susceptibility map (Sutikno, 1994). Either data driven method and physically based method are rarely applied in Indonesia. Comparison of quantitative method is essential to generate the most suitable method in landslide susceptibility zoning.

2.2.1.3 TEMPORAL PROBABILITY

It is difficult, up to now, to predict exactly when landslide will occur due to the limitations to human knowledge of nature. Temporal probability is used as an approach to estimate the occurrence of landslides during a specified time in a

particular area (Crovelli, 2000). It can be expressed in terms of frequency, return period or exceedance probability. Frequency, as annual frequency, represents the number of landslide event in a year in an area (i.e. number/km^2/year). The return period represents the average time interval of a landslide event expected to occur. It is an inverse of the annual probability. The exceedance probability expresses the probability that one or more events will occur in a certain period. Exceedance probability usually includes the magnitude of landslides which means the probability of landslides with magnitude equal or larger than a certain value in a certain period.

Temporal probability estimation is mainly based on the availability of past landslide data. Temporal probability or cumulative occurrence of landslide is estimated based on known intervals (Hungr et al., 1999; Guthrie and Evans, 2004; Jaiswal and Westen, 2009). Temporal probability can also be derived by establishing an empirical relation between landslides event and its triggering factor, i.e. intensity of rainfall or or earthquake, which later called as magnitude-frequency analysis (Crozier, 1999; van Westen, et al., 2006). Ghosh (2011) estimated temporal probability, by using landslide event-days and associated daily and antecedent rainfall to model the temporal relationship between landslide events and the amount of triggering rainfall. Keefer (2002) estimated landslide occurrences by using the intensity of the landslide and earthquake.

2.2.1.4 MAGNITUDE PROBABILITY

In natural hazard studies, the magnitude-frequency relationship has been observed based on complete past events data i.e. earthquake and floods. It describes the specific relationship between the frequency of events falling in different magnitude classes. The well-known magnitude-frequency relationship is a relation between earthquake magnitude and cumulative frequency expressed by Gutenberg equation as follows:

$$logN(m) = a - bM \quad (2.2)$$

where $N(m)$ is the cumulative number of earthquake events with magnitudes equal or greater than M, a and b are constant.

The magnitude of landslides refers to the volume of material which may fail, the velocity of movement during failure, and the land area which may be affected

(Fell, 1994; Crozier, 1995 and Hutchinson, 1995). It is usually represented by the statistics of landslide sizes (area or volume) either using the cumulative or the non-cumulative distribution. Both indicate landslides area or landslides volume, above threshold, is generally well approximated by negative power law (Brunetti, 2009). It is formally equivalent to the Gutenberg-Richter equation. The cumulative number of landslide is described by the equation as follows:

$$N_L = rV_L^{-\alpha} \tag{2.3}$$

where N_L is the cumulative number of landslides, V_L is the landslide volume, α is the cumulative power-law scaling exponent, and r is a constant. In the other hand, non-cumulative number-volume distribution also follows a power law:

$$N_L' = \frac{dN_L}{dV_L} = -\alpha r V_L^{-(\alpha+1)} = sV_L^{-\beta} \tag{2.4}$$

Where dN_L is the number of landslides in the volume interval $[V_L; V_L+dV_L]$ (i.e. in a "bin" size dV_L), β is the non-cumulative scaling exponent and s is a constant. Non-cumulative power law distribution with exponent β>1 has exponent α= β-1 (Guzzetti et al., 2002). Without the estimation of the expected annual frequency of landslide events of a given magnitude or exceeding magnitude threshold, quantitative hazard assessment is not feasible.

2.2.2 LANDSLIDE VULNERABILITY

The ability to measuring vulnerability has been increasing significantly through the increasing frequency of disasters and environmental degradation (Arakida, 2006; Wisner, 2006; Villagran de Leon, 2006). It has been increasing due to the undesirable for defining landslide primarily as a physical process. For example, factor safety is not always being able to perform the capabilities on inhibiting undesirable behavior (Morgenstern, 1997). It is traditionally that landslide was viewed as an isolated physical event and few linkages were made to link the landslide event with the people affected by the disaster (Bollin and Hidajat, 2006). As a kind of disaster, landslide is better viewed as a result of complex interaction among physical processes and social process. Vulnerability is an important thing to formulate social aspect as a result of interaction between landslide occurrence and potentially

damaging event.

The vulnerability in rural area more tends to have such a tendency rather randomly. Since the nature of people, social structure and culture were less influenced by the development of technology and modernization, the natural feature and condition would more dominantly influence the way of life. It is related to the preference of the people to build settlements in the hilly and rural area. According to Whynne-Hammond (1979) the growing of settlement (village) is based on the combination of four factors i.e. topographical, economic, historical, and cultural.

The conceptual framework of vulnerability has been proposed by several authors in order to systematize the definition and to make relevant indicators to measure it. (Birkmann, 2006) explains several conceptual framework of vulnerability, i.e. the double structure of vulnerability as defined by Bohle, vulnerability within the framework of hazard and risk, and vulnerability based on the UN/ISDR framework for disaster risk reduction.

The double structure of vulnerability indicates two major sides of vulnerability, i.e. internal and external side. Internal side relates to the capacity to anticipate, cope with, resist and recover from the impact of hazards; whereas external side relates to the exposure to risks as an impact of hazards. It seems that exposure, coping capacity, and response capacity should be analyzed simultaneously. In contrast, vulnerability within the framework of hazard and risk defines that vulnerability is defined separately with coping capacity and exposure. It results in the formulation of risk as the sum of hazard, exposure, vulnerability, and capacity measures. Therefore, vulnerability is defined as one component of disaster risk. Moreover, (UN/ISDR, 2004) defines vulnerability as a key factor, a tool, and a preconditioning to determine risk. It is divided into physical, environmental, social, and economic components.

Vulnerability can be defined as the condition increased the susceptibility of the community as the impact of hazard, which is determined by physical, social, economic and environmental factors or process (UN/ISDR, 2004). Similar with UN/ISDR, ADPC (2004) divides the factors of vulnerability into four types:

1. Physical vulnerability (building age, construction, material, infrastructures, lifeline facilities)

2. Social vulnerability (risk perception and way of life related to culture, religion, ethnicity, social interaction, age, gender, attitude of population property)
3. Economic vulnerability (income, investments, potential loss of stock)
4. Environmental vulnerability (water, air, land, flora and fauna)

Varnes, (1984) defines a vulnerability definition subjected to landslide as the degree of loss to a given element at risk resulted from the impact of the natural phenomenon of a given magnitude. The vulnerability degree is expressed on a scale from 0 (no damage) to 1 (total loss). Elements at risk of landslides can be settlement building, properties, population, and public services in a given area. Thus, landslide vulnerability can be viewed as intrinsic feature that determines the degree of loss to a given element at risk as an impact of landslide which can be measured through the proxies of physical, social, economic, and environmental dimension.

The landslide hazard map will be more valuable with the analysis of landslide vulnerability in order to develop landslide risk. Vulnerability is related to the consequences of the impact of disaster which is generally measured by damage or loss (Glade, 2003). Therefore, it is important to define the degree of vulnerability in each type of landslide. The degree of vulnerability will also be different related to the ability of individual, community, or society to cope and to anticipate the impact of disaster. When the disaster happens, more complex systems are usually involved to tackle down the problem (Bell and Glade, 2004). It includes the physical, social, economic, and environmental dimension. Both landslide vulnerability and landslide risk assessment will be more informative to be represented as a map processed by GIS.

2.3 CURRENT ISSUES IN LANDSLIDE RISK ANALYSIS

Several issues in quantitative landslide risk analysis include developing technique in inventory mapping, particularly in a data scarce environment, selecting methods for landslide susceptibility assessment, and developing approaches for landslide risk analysis. It varies depending on the availability of secondary data, geomorphological characteristic, and landslide typology. The availability of data input is very important prior to landslide risk analysis. It can affect the overall methodology or approaches applied in the landslide risk analysis. Despite the

availability of landslide inventory, geomorphological characteristic of the study area should also be considered prior to selecting suitable landslide susceptibility and risk analysis. Some approaches in landslide susceptibility and risk analysis can also not be applied in rockfall susceptibility and risk analysis. For example, landslide susceptibility assessment based on GIS and statistics uses landslide area represented by polygon to estimate susceptibility. Whereas, it is not suitable for rockfall susceptibility analysis because the dangerous zone in rockfall is represented by trajectory line.

2.3.1 INSUFFICIENT LANDSLIDES INVENTORY MAPPING

Generating landslide analysis is difficult in some areas because the unavailability of the landslide inventory map. However, the recent technology developments such as the availability of the modern field instrument, high resolution DTMs, high resolution satellite imagery, recent development on GIS and remote sensing technology have made generating landslide map easier. But, the selection of this technique should be carefully reviewed based on the purpose, the extent of the study area, the scale of base maps and analysis, resolution and characteristics of the available imagery, and the skill and experience of the interpreter (Guzetti et al., 2000; van Westen et al., 2006). Mapping landslide through field survey is the oldest technique for landslide inventory mapping and considered as the most accurate technique for mapping fresh landslide events. But it is difficult, by using field survey, to recognize old landslides in the field where the natural process (e.g. erosion, vegetation) and the anthropogenic activities (e.g. urbanization, road construction, ploughing) are exist. The use of aerial photograph interpretation is also difficult in Indonesia due to unavailability of multiple sets of aerial photograph in the same area and different time. In the other hand the use of recent technology such as very high resolution of DTMs and remote sensing imagery faces problems related to budget limitation and cloud problem in remote sensing images. Thus, combination techniques are needed to map landslide events either old or recent landslide events.

2.3.2 SELECTING METHOD IN LANDSLIDE SUSCEPTIBILITY

Quantitative statistical analysis has been widely applied as a standard method for landslide susceptibility zoning in wide areas (regional scale mapping). It includes bivariate statistic, multivariate statistic and soft computing. Bivariate analysis assumes that the presumed controlling factors of landslide are not interrelated each other (Suzen and Doyuran, 2004). It is a robust and flexible method, but has several limitations, including over simplification of input thematic data related to landslides and loss of data sensitivity of controlling factors (Thiery et al., 2007). Bivariate statistical methods can also be used to determine which factors or combination of factors play a role in the initiation of landslides.

In the other hand, multivariate analysis assumes that the presumed controlling factors of landslide are interrelated each other. It determines the relative contribution of each landslide causal factor in the presence or absence of past landslide events (Dai et al., 2001; Süzen and Doyuran, 2004; Ayalewand Yamagishi, 2005; Nandi and Shakoor, 2009). Multivariate statistical analysis can be used to predict a result measured by a binary variable such as the absence or presence of landslides based on a set of one or more landslide causal factors as independent variables. The independent variables can be nonlinear, continuous, categorical or a combination of both continuous and categorical; and does not to be normally distributed.

Soft computing techniques were used in the assessment of the landslide susceptibility because of a limitation such as insufficient knowledge about the area of interest. Its computing procedure has the ability to handle imprecise and fuzzy data with continuous, categorical and binary data without violating assumptions and also independent of the statistical distribution of the data. The purpose of soft computing technique, i.e. ANN, is to build a model of the data-generating process so that the network can generalize and predict outputs from inputs that it has not previously seen (Lee et al., 2001).

One of the main advantages of data driven landslide susceptibility is the easily updating of the landslide susceptibility assessment procedure and also relatively easy to apply for land-use planning. However, it can be affected by shortcomings such as the assumption that landslides occur due to the same combination of factors

throughout a study area, spatial factors can vary widely in areas with complex geomorphological settings, and the lack of suitable expert opinion on landslide processes and causal factors (Corominas et al., 2013). Selecting method, i.e. either bivariate, multivariate or soft computing is essential to apply for landuse planning based on complete landslide inventory.

2.3.3 ROCKFALL SUSCEPTIBILITY ZONING METHOD

Several attempts of rockfall susceptibility zoning have been carried out through several ways, relatively similar to landslide susceptibility zoning, i.e. heuristic, statistic and trajectory-energy/velocity approaches. Heuristic methods involve geomorphological analysis and rating based approaches. Field work and photo interpretation are the main sources of the geomorphological analysis for determining the trajectories of rockfall. Geomorphologic elements connected to rockfall are taken into account to delineate landscape that is susceptible to rockfall. It is subjective and need well experienced geomorphologist. Weight of each element is also added to determine the rockfall susceptibility based on rating approach (Romana, 1993; Pierson et al., 1990; Hoek, 2007). The mapping unit used in geomorphological approach is usually geomorphological unit or landform. For example, Sasaki et al., (2000) generated land condition map showing geomorphologic element which is susceptible to rockfall.

Statistic approaches such as logistic regression using pixel/mesh unit was also applied in rockfall susceptibility zoning (Shirzadi et al., 2012). But, it is not widely applied, as in landslide susceptibility zoning, due to difficulties in delineating rockfall affected area. Single rockfall may only affect a narrow area as a trajectory of rockfall movement. The most common method in rockfall susceptibility zoning is a trajectory-energy/velocity modeling (Guzzetti et al., 2002; Lan et al., 2007; Chen, 2003; Agliardi and Crosta, 2003). It is a quantitative approach employing computer simulation to calculate probability of reach, velocity and the kinetic energy distribution at each point of the slope. The propagation is dependent on slope topography, lithology, mass block shape and mass. Some GIS rockfall models do not include the shape and size of the rockfall. In a scarce data environments, problems

may arise because the mass and volume of rockfall are unknown and exact rockfall sources are difficult to be identified. Zoning area is sometimes not fixed due to many scenarios involved when running the simulation. Many uncertainties and assumptions (i.e. source area, input parameter, the number of runs) may affect the result.

2.4 CONCLUSIONS

Landslide risk analysis comprises several terminologies which are used interchangeably and often generates confusion. It includes risk, hazard, inventory, susceptibility, temporal probability, magnitude probability and vulnerability. Understanding terminologies in the landslide risk analysis is important in which allows scientists and engineer quantify landslide risk in an objective way, reproducible and the result can be compared from one region to another region. The confusion may also arise when there are available methodologies applied for different landslide mechanism and typology. Generating landslide inventory, distinguishing landslide typology for different method on risk analysis, and selecting an appropriate method for susceptibility are among the current issues which should be taken into account in the quantitative landslide risk analysis.

REFERENCES

ADPC. 2004. A Framework for Reducing Risk, in CBDRM Field Practitioners Handbook. Bangkok, Thailand. Accessed on September 2009 from http://www.adpc.net/PDR SEA/publications/12Handbk.pdf

Agliardi, F. and Crosta, G. 2003. High resolution three-dimensional numerical modelling of rockfalls. *Int. J. Rock Mech. Min., Sci.,* 40, 455–471.

Andersen, T., G., Bollerslev, T., Christoffersen, P. F., and Diebold, F. X. 2013. *Financial Risk Measurement and Management* in Constantinides, G. M., Harris, M., and Stulz, R. M (Eds.). Handbook of the Economics and Finances. Elsevier.

Anonym. 2007. Undang-Undang Nomor 24 Tahun 2007 tentang Penanggulangan Bencana, Lembaran Negara Republik Indonesia tahun 2007 nomor 66, Jakarta.

Arakida, M. 2006. Measuring Vulnerability: The ADRC Perspective for the Theoretical Basis and Principles of Indicator Development, edited by Birkmann, J. *Measuring Vulnerability to Natural Hazard: Towards Disaster Resilient Societies*. United Nation University Press. USA.

Atkinson, P. M. and Massari, R. 1998. Generalized Linear Modelling of Susceptibility to Landsliding in The Central Apennines, Italy. *Computers & Geosciences* vol. 24, no. 4:373-385.

Ayalew, L. and Yamagishi, H. 2005. The application of GIS-based logistic regression for landslide susceptibility zoning in the Kakuda-Yahiko Mountains, Central Japan. Geomorphology, 65, 15-31.

Barlow, J., Franklin, S., Martin, Y. (2006). "High spatial resolution satellite imagery, DEM derivatives, and image segmentation for the detection of mass wasting processes". Photogrammetric Engineering and Remote Sensing, 72, pp. 687-692.

Bell, R and Glade, T. 2004. Quantitative Risk Analysis for Landslides-Examples from Bildudalur, NW-Iceland. *Natural Hazards and Earth System Sciences (2004) 4*: *117–131*. European Geoscience Union, 2004.

Birkmann, Jorn. 2006. Measuring Vulnerability to Promote Disaster-Resilient Societies: Conceptual Framework and Definitions, edited by Birkmann, J. *Measuring Vulnerability to Natural Hazard: Towards Disaster Resilient Societies*. United Nation University Press. USA.

Bollin, C. and Hidajat, R. 2006. Community Based Disaster Risk Index: Pilot Implementation in Indonesia, edited by Birkmann, J. *Measuring Vulnerability to Natural Hazard: Towards Disaster Resilient Societies*. United Nation University Press. USA.

Bonham-Carter, G. F. 1994. Geographic Information Systems for Geoscientists: Modelling with GIS. Computer Methods in the Geosciences, 13: pp 267-302. Pergamon.

Borghuis, A. M., Chang, K., Lee, H. Y. 2007. Comparison between automated and manual mapping of typhoon-triggered landslides from SPOT-5 imagery". International Journal of Remote Sensing, 28, pp. 1843-1856.

Brardinoni, F., Slaymaker, O., Hassan, M. A. 2003. Landslide inventory in a rugged

forested watershed: a comparison between air-photo and field survey data. *Geomorphology* 54:179–196.

Cardona, O. D. 2003. *The Notion of Disaster Risk: Conceptual Framework for Integrated Risk Management*, IADB/IDEA Program on Indocators for Disaster Risk Management, Universidad Nacionalde Colombia, Manizales accessed from http://idea.manizales.unal.edu.co/Proyectos Especiales/adminIDEA/centroDocumentacion/DocDigitales/documentos/01%20Conceptual%20Framework%20IADB-IDEA%20Phase%20I.pdf

Carrara, A. and Merenda, L. 1976. Landslide inventory in northern Calabria, southern Italy. Geol Soc Am Bull. 87: 1153−1162.

Carrara, A., Cardinali, M., Guzzetti, F., and Reichenbach, P. 1995. GIS Technology in Mapping Landslide Hazard. In: Carrara, A. and Guzzetti, F. (eds.), *Geographical Information Systems in Assessing Natural Hazards* page: 135–175. Kluwer Academic Publisher, Dordrecht, the Netherlands.

Carrara A., *1983*. *Multivariate models* for landslide hazard evaluation. Mathematical Geol., v. 15, n. 3, p. 403-426.

Chacon, J., Irigaray, C., Fernandez, T., and El Hamdouni, R. 2006. Engineering geology maps: landslides and Geographical Information Systems (GIS), *Bull. Eng. Geol. Environ*., 65, 341–411.

Chen. G. 2003. Numerical Modelling of Rockfall using Extended DDA. *Chinese Journal of Rock Mechanics and Engineering*, 22 (6):926-931.

Chung, C. F. and Fabbri, A. G. 1993. The representation of geosciences information for data integration. *Nonrenewable Resources*, 2(2), PP.122-139.

Corominas J and Moya J. 2008. A review of assessing landslide frequency for hazard zoning purposes. Engineering Geology 102:193–213. doi: 10.1016/j.enggeo.2008.03.018.

Corominas, J., van Westen, C., Frattini, P., Cascini, L., Malet, J. P., Fotopoulou, S., Catani, F., Van Den Eeckhaut, Mavrouli, O., Agliardi, F., Pitilakis, K., Winter, M. G., Pastor, M., Ferlisi, S., Tofani, V., Hervas, J., Smith, J. T. 2014. Recommendations for the quantitative analysis of landslide risk. *Bulletin Engineering Geology and the Environment*. Vol. 73, Issue 2, pp 209-263.

Crovelli, R. A. 2000. *Probability models for estimation of number and costs of*

landslides. USGS Denver, Colorado.

Crozier, M. J. 1995. Landslide hazard assessment: a review of papers submitted to theme G4. Bell, D. H. (Ed.) Proceedings of the sixth International Symposium, 10-14 February 1992. Christchurch, New Zealand, A.A. Balkema, Rotterdam:1843-8.

Crozier MJ (1999) Prediction of rainfall-triggered landslides: A test of the antecedent water status model. *Earth Surface Processes and Landforms* 24:825-33.

Dahal, R.K., Hasegawa, S., Nonomura, A., Yamanaka, M., Masuda, T., Nishino, K. 2007. GIS Based Weights-of-Evidence Modeling of Rainfall Induced Landslides in Small Catchments for Landslide Susceptibility Mapping. *Environ Geol*, doi: 10.1007/s00254-007-0818-3

Dai, F.C., Lee, C.F., Li, J. and Xu, Z.W. 2001. Assessment of landslide susceptibility on the natural terrain of Lantau Island, Hong Kong. *Environmental Geology*, Vol. 40, 381- 391

Dai FC, Lee CF (2002) Landslide characteristics and slope instability modeling using GIS, Lantau Island Hongkong. *Geomorphology* 42:213-228.

Ebert, A., Kerle, N., & Stein, A. 2009. Urban Social Vulnerability Assessment with Physical Proxies and Spatial Metrics derived from Air- and Spaceborne Imagery and GIS Data. *Nat Hazards 48:275–294*.

Ermini, L., Catani, F., Casagli, N. 2005. Artificial neural networks applied to landslide susceptibility. *Geomorphology* 66:327-343.

Fell R, Corominas J, Bonnard C, Cascini L, Leroi E, Savage W.Z (2008) Guidelines for landslide susceptibility, hazard, risk zoning for land-use planning. *Engineering Geology* 102:99-111.

Fell, R. 1994. Landslide risk assessment and acceptable risk. *Canadian Geotechnical Journal* , 31: 261-272.

Galli M, Ardizzone F, Cardinali M, Guzzetti F, Reichenbach P (2008) Experimental acute renal failure. Dissertation, University of California. Comparing landslide inventory maps. *Geomorphology* 94:268–289.

Ghosh, S. 2011. Knowledge Guided Empirical Prediction of Landslide Hazard. *PhD Thesis*. University of Twente, Netherland.

Glade, T., Anderson, M., Crozier M.J. 2005. *Landslide hazard and Risk*. John

Wiley & Sons Ltd.

Glade, T. 2003. Vulnerability assessment in landslide risk analysis, *Die Erde*, 134, 2, 121–138, 2004b. Accessed February 2007 from homepage.univie.ac.at/thomas.glade/Publications/Glade2003b.pdf

Godt J.W., Baum R.L., Savage W.Z., Salciarini D, Schulz W.H., Harp E.L. 2008. Transient deterministic shallow landslide modeling: Requirements for susceptibility and hazard assessments in a GIS framework. *Engineering Geology* 102:214–226.

Gorsevski, P. V., Gessler, P., Foltz, R. B. 2000. Spatial prediction of landslide hazard using discriminant analysis and GIS. GIS in the Rockies 2000 Conference. Available online at http://www.fs.fed.us/rm/pubs_other/rmrs_2000_foltz_r001.pdf

Gorsevski, P.V., Gessler, P.E., Foltz, R.B.and Elliot, W.J. 2006. Spatial prediction of landslide hazard using logistic regression and ROC analysis. *Transactions in GIS* 10 (3), 395-415.

Guhtrie RH, Evans SG (2004) Analysis of landslide frequencies and characteristics in a natural system, coastal British Columbia. *Earth Surf. Process. Landforms* 29:1321–1339.

Guzetti, F., Carrara, A., Cardinali, M., Reinchenbach, P. 1999. Landslide hazard evaluation: a review of current techniques and their application in a multi-scale study, Central Italy. *Geomorphology* 31:181-216.

Guzzetti F., Cardinali M., Reichenbach P., Carrara A. 2000. Comparing landslide maps: a case study in the upper Tiber River Basin, Central Italy. *Environmental Management* 25 (3):247–363.

Guzzetti, F., Malamud, B., Turcotte, D. L., Reichenbach, P. 2002. Power–law correlations of landslide areas in central Italy. *Earth and Planetary Science Letters* 195:169–183.

Guzzetti, F., Reichenbach, P., Cardinali, M., Galli, M., Ardizzone, F. 2005. Probabilistic landslide hazard assessment at the basin scale. *Geomorphology* 72:272–299.

Guzzetti, F., Galli, M., Reichenbach, P., Ardizzone, F., Cardinali, M. 2006. Landslide hazard assessment in the Collazzone area, Umbria, central Italy. *Natural*

Hazards and Earth System Sciences 6:115–131.

Guzzetti F, Mondini A.C., Cardinali M, Fiorucci F, Santangelo M, Chang K.-T. 2012. Landslide inventory maps: New tools for an old problem. *Earth-Science Reviews* 112:42–66.

Hansen, A. (1984). "Strategies for classification of landslides". In: Brunsden, D., Prior, D.B. (Eds.), Slope Instability. Wiley, New York, pp. 523-602.

Hoek, E. 2007. Practical Rock Engineering. available online at : http://www.rocscience.com/hoek/pdf/Practical_Rock_Engineering.pdf

Huabin, W., Gangjun, W., Weiya, X., and Gonghui, W. 2005. GIS-based Landslide Hazard Assessment: an Overview. *Progress in Physical Geography* 29, 4 page 548-567

Hungr, O., Evans, S. G., and Hazzard, J. (1999). "Magnitude and frequency of rockfalls and rock slides along the main transportation corridors of south-western British Columbia". *Can. Geotech. J.*, 36, 224–238,.

Hutchinson, J. N.: Keynote paper: landslide hazard assessment, In: Landslides, (Ed.) Bell, Balkema, Rotterdam, 1805–1841, 1995

IUGS Working Group on Landslides. 1997. Quantitative Risk Assessment for Slopes and Landslides – The State of The Art in Cruden, D and Fell, R. (Eds). *Landslide Risk Assessment*. Balkema, Rotterdam. The Netherlands

Jaiswal, P. and van Westen, C.J. 2009. Estimating temporal probability for landslide initiation along transportation routes based on rainfall thresholds. *Geomorphology* 12, 1-2 pp. 96-105.

Kanungo, D. P., Arora, M. K., Sarkar, S., Gupta, R.P. 2006. Comparative study of conventional, ANN black box, fuzzy and combined neural and fuzzy weighting procedures for landslide susceptibility zonation in Darjeeling Himalayas. *Engineering Geology*, 85, pp. 347-366.

Keefer, D. K. 2000. Statistical analysis of an earthquake-induced landslide distribution of the 1989 Loma Prieta, California event. *Engineering Geology*, 58, pp. 231-249.

Kumajas, M. 2006. Inventarisasi dan Pemetaan rawan Longsor Kota Manado – Sulawesi Utara. *Forum Geografi*, vol. 20, no. 2, December 2006: 190-197.

Lan, H., Martin, C. D., and Lim, C. H. 2007. RockFall analyst: a GIS extension for

three-dimensional and spatially distributed rockfall hazard modeling. *Computer and Geoscience*., 33, 262–279.

Lee, S., Ryu, J., Min, K., Won, J. 2001. Development of two artificial neural network methods for landslide susceptibility analysis. Proceeding of Geoscience and Remote Sensing Symposium, IGARSS `01. IEEE 2001 International 5:2364-2366.

Lee, S., Ryu, J., Won, J., Park, H. (2004). Determination and application of weights for landslide susceptibility mapping using an artificial neural network. *Engineering Geology*, 71, pp. 289-302.

Lee, S. 2004. Application of likelihood ratio and logistic regression models to landslide susceptibility mapping using GIS. *Environmental Management* 34 (2), 223-232

Luzi, L., 1995, GIS for Slope StabilityZonaton in the Fabriano Area, Central Italy. ITC, Enschede, The Netherlands.

Malamud B.D., Turcotte D.L., Guzetti F, Reichernbach P (2004) Landslide inventories and their statistical properties. *Earth Surf. Process. Landforms* 29:687–711. 10.1002/esp.1064.

Mardiatno, D. 2001. Resiko Longsor di Kecamatan Girimulyo. *Thesis*. Fakultas Geografi UGM, Yogyakarta.

Martha T.R., Kerle N, Jetten V, van Westen C.J., Kumar K.V (2010) Characterising spectral, spatial and morphometric properties of landslides for semi-automatic detection using object-oriented methods. *Geomorphology* 116:24–36. doi: 10.1016/j.geomorph.2009.10.004.

Moeyersons, J., Trefois, Ph., Lavreau ,J., Alimasi, D., Badriyo, I., Mitima, B., Munadala, M., Munganga, D. O., Nahimana, L. 2004. A Geomorphological Assessment of Landslide Origin at Bukavu, Democratic Republic of the Congo. *Engineering Geology* 72, page 73-87.

Moine, M., Puissant, A., Malet, J. P. (2009). “Detection of landslides from aerial and satellite images with a semi-automatic method. Application to the Barcelonnette basin (Alpes-de-Haute-Provence, France)”. In: Malet, J.-P., Remaitre, A., Bogaard, T. (Eds.), Landslide Processes: From Geomorphological Mapping to Dynamic Modelling. CERG, Strasbourg,

France, pp. 63-68.

Mondini, A. C., Guzzetti, F., Reichenbach, P., Rossi, M., Cardinali, M., Ardizzone, F. (2011). Semi-automatic recognition and mapping of rainfall induced shallow landslides using satellite optical images. *Remote Sensing of Environment*, 115, pp. 1743-1757.

Morgenstern, N. R. 1997. Toward Landslide Risk Assessment in Practice in Cruden, D. M and Fell, R. (eds). *Landslide Risk Assessment*, Balkema: Rotterdam. The Netherlands.

Nagarajan, R., Roy, A., Vinod Kumar, R., Mukherjee, A., Khire, M. V. 2000. Landslide Hazard Susceptibility Mapping Based on Terrain and Climatic Factors for Tropical Monsoon Regions. *Bull Eng Geol Env* 58: 275-287. Springer-Verlaag

Nandi A, Shakoor A (2009) A GIS-based landslide susceptibility evaluation using bivariate and multivariate statistical analyses. *Engineering Geology* 110:11-20.

Nichol, J., Wong, M. S. (2005). Satellite remote sensing for detailed landslide inventories using change detection and image fusion. *International Journal of Remote Sensing*, 26, pp. 1913-1926.

Ohlmacher, C.G., Davis, C.J., 2003. Using multiple regression and GIS technology to predict landslide hazard in northeast Kansas, USA. *Engineering Geology* 69, 331–343

Pierson, L.A., Davis, S.A., Van Vickle, R. 1990. Rockfall Hazard Rating System Implementation Manual, Federal Highway Administration (FHWA) Report FHWA-OREG- 90-01, FHWA, United States Department of Transportation.

Pradhan B (2010) Remote sensing and GIS-based landslide hazard analysis and cross-validation using multivariate logistic regression model on three test areas in Malaysia. *Advance in Space Research* 45:1244-1256.

Priyono, D.K., Priyana, Y., Priyono. 2006. *Analisis Tingkat Bahaya Longsor Tanah di Kecamatan Banjarmangu Kabupaten Banjarnegara*. *Forum Geografi*, Vol. 20, No. 2, hal: 175 – 189.

Romana, M. 1993. A geomechanical classification for slopes: slope mass rating, *Comprehensive Rock Engineering*, Oxford, Pergamon.

Rosin, P.L., Hervás, J., 2005. Remote sensing image thresholding methods for determining landslide activity. *International Journal of Remote Sensing* 26 (6), 1075–1092.

Ruff, M. and Czurda, K. 2007. Landslide susceptibility Analysis with a Heuristic Approach at The Eastern Alps (Voralberg, Austria). *Geomorphology*, doi: 10.1016/j.geomorph.2006.10.032.

Sasaki, Y. Dobrev, N., Wakizaka, Y. 2002. The detailed Hazard Map of road Slopes in Japan, in Instability-Planning and Management, London, Thomas Telford, p.381-388. Eds: McInnes, R. G and Jakeways Jenny

Shirzadi, A., Saro, L., Joo, O. H., and Chapi, K. 2012. A GIS-based logistic regression model in rockfall susceptibility mapping along a mountainous road: Salavat Abad case study, Kurdistan, Iran. *Nat. Hazards*, 64, 1639–1656.

Soanes C, Stevenson A (eds) (2005) Oxford dictionary of English, (revised) 2nd edn. Oxford University Press, Oxford

Sutikno. 1994. Pendekatan Geomorfologi untuk Mitigasi Bencana Alam Akibat Gerakan Massa Tanah Batuan. *Makalah Simposium Nasional Mitigasi Bencana Alam*. Fakultas Geografi. Universitas Gadjah Mada, Yogyakarta.

Sutikno, Huda, M., Sarwondo, Triyono. 2002. Sistem Informasi Penanggulangan Bencana Alam Tanah Longsor Kabupaten Kulon Progo. *Simposium Nasional Pencegahan Bencana Alam*. ISDM Project. Yogyakarta.

Suzen, M. L. and Doyuran, V. 2004. Data Driven Bivariate Landslide Susceptibility Assessment Using GIS: a Method and Application to Asarsuyu Catchment, Turkey. *Engineering Geology* 71, pp 303-321.

Thierry, Y., Malet, J.P., Sterlacchini, S. Puisant, A., Maquaire, O. 2007. Landslide susceptibility assessment by bivariate methods at large scale: application to a complex mountainous environment. *Geomorphology, 92, 38-59.*

UN/ISDR (International Strategy for Disaster Reduction). 2004. *Living with Risk: A Global Review of Disaster Reduction Initiatives*. Geneva: UN Publications.

Van Den Eeckhaut M, Poesen J, Verstraeten G, Vanacker V, Moeyersons J, Nyssen J, Van Beek LPH (2005) The effectiveness of hillshade maps and expert knowledge in mapping old deep-seated landslides. *Geomorphology* 67: 351–363.

van Westen, C. J., Rengers. N., Soeters. R. 2003. Use of Geomorphological Information in Indirect Landslide Susceptibility Assessment. *Natural Hazard* 30: 399-419. Kluwer Academic Publishers. Netherlands.

van Westen CJ, Asch TWJ, Soeters R (2006) Landslide hazard and risk zonation-why is it still so difficult? *Bull Eng Geol Env* 65: 67-184

van Westen C.J., Castellanos E, Kuriakose S.L. 2008. Spatial Data For Landslide Susceptibility, Hazard, and Vulnerability Assessment: An Overview. *Engineering Geology* 102:112-131.

van Westen, C. J. 1993. Application of geographic information systems to landslide hazard zonation. *PhD dissertation*, Technical University Delft. ITC-publication number 15, ITC,

Varnes, D.J. (1984). *Landslide Hazard Zonation*: *a Review of Principles and Practice*. United Nations Educational, Scientific and Cultural Organization (UNESCO). Paris

Villagran de Leon, J. C. 2006. Vulnerability Assessment: The Sectoral Approach, in Birkmann, J. (eds). *Measuring Vulnerability to Natural Hazard*: *Towards Disaster Resilient Societies*. United Nation University Press. USA.

van Westen, C. J., Rengers. N., Soeters. R. 2003. Use of Geomorphology Information in Indirect Landslide Susceptibility Assessment. *Natural Hazard* 30: 399-419. Kluwer Academic Publishers. Netherlands.

Whynne-Hammond, C. 1979. *Elements of Human Geography*. George Allen and Unwin. London.

Wieczorek, G.F., 1984, Preparing a detailed landslide-inventory map for hazard evaluation and reduction: *Association of Engineering Geologists Bulletin*, v. 21, no. 3, p. 337–342

Wisner, B. 2006. Self-Assessment of coping capacity: Participatory, Proactive, and Qualitative Engagement of Communities in Their Own Risk Management, in Birkmann, J (eds). *Measuring Vulnerability to Natural Hazard*: *Towards Disaster Resilient Societies*. United Nation University Press. USA.

Yao, X., Tham, L. G., and Dai, F. C.: Landslide susceptibility mapping based on Support Vector Machine: A case study on natural slopes of Hong Kong, China, Geomorphology, 101, 572–582, 2008.

CHAPTER 3

GENERATING SPATIAL LANDSLIDE DATABASE BY USING PARTICIPATORY INVENTORY MAPPING: AN EXAMPLE IN PURWOSARI AREA, YOGYAKARTA, JAVA

3.1 INTRODUCTION

One of the recent progress of Indonesia's disaster management after the enactment of *Undang-Undang* (Law) 24/2007 is the availability of online Indonesian Disaster Data and Information Database (DIBI) in http://dibi.bnpb.go.id. DIBI was launched on 29 July 2008 and is housed within the newly established National Disaster Management Agency (BNPB). It is expected that, by utilizing DIBI, all relevant stakeholders can successfully implement disaster management planning at every stage of the disaster management cycle and support disaster reporting and monitoring at national and sub-national level. There is historical disaster information provided by DIBI, including the occurrence, magnitude and the impact of disaster for both natural and man made disaster.

The landslide database provided by DIBI includes date of occurrence, location, and impact. The impact information is more detail than others, including the number of deaths, missing, injured, affected, evacuated and elements at risk damaged/destroyed. Even though DIBI was intended to enhance disaster management planning at every stage of the management cycle, it still seems a step too far. Landslide database in DIBI is still focusing on disaster response rather than preparing data for pre-disaster planning and preparedness. The database is also limited to disaster with 1 or more people reported killed, 100 people reported affected, a call for international assistance and declaration of a state of emergency. Upgrading the landslide database in DIBI is needed to support pre-disaster planning

and preparedness, including disaster risk reduction, mitigation, preparedness, risk assessment and contingency planning.

For landslides database, the upgrading should include the information about location (coordinate), type of landslide, landslide volume, state of activity, date of occurrence and other characteristic of landslides in the area as well as information on triggering factors for all landslides, called as landslide inventory (Guzzetti, 2000; Fell et al., 2008). Landslide inventory is a pre-requisite for landslide susceptibility, hazard, and risk zoning. The spatial relationship between landslide area and the environmental causative factors is a key to investigate the landslide susceptibility, which later can be used to investigate landslide hazard by incorporating with recurrence or frequencies of landslides. Landslide inventory can also be utilized to investigate the statistics of landslides and the evolution of the landscape. There are several methods to prepare a landslide inventory such as geomorphological field mapping, visual interpretation of aerial photographs, interpretation of satellite imagery, and analysis of surface morphology (Guzzetti, 2014). However, these methods are sometimes not possible to be applied in Indonesia.

Landslide is an important geomorphological feature and must be included in geomorphological map. Thus, geomorphological field mapping is the oldest method of landslide inventory. It is the most possible method to be applied in Indonesia. However, previous report and landslide historical data should be available prior to geomorphological field mapping. It is sometimes difficult even costly and time consuming to find landslide location, especially for old landslide without initial data, such as previous reports, internal database or tentative landslide map obtained from the interpretation of ancillary data. Identifying the boundary of landslides through field investigation is also difficult where landslides are covered by vegetation or dismantled by erosion and human activities (Guzzetti, 20014).

Aerial photograph interpretation is the most popular method and has been used extensively to investigate landslide. The investigation is usually based on visual interpretation using a stereoscope. Simultaneous consideration and synthesis of multiple different criteria such as shape, pattern of objects, color/tone, shadow, texture and association/site of landslides are used to recognize landslides in the aerial photograph. The interpretation may vary among interpreter and prone to subjectivity

of interpreters because the unavailability of standard criteria. Generating temporal landslide inventory in Indonesia by aerial photograph interpretation seems also difficult due to unavailability of multi-temporal aerial photographs especially in hilly and mountainous area. The aerial photograph is often only available in a single year and is not regularly updated.

The unavailability of the temporal aerial photograph could be substituted by satellite imagery. Very high resolution (VHR) panchromatic may represent an alternative to conventional aerial photographs (Weirich and Blesius, 2007). Fused higher resolution panchromatic image with the lower resolution multispectral image to obtain a single high resolution color image is also possible in order to improve the visual interpretation capacity of satellite imagery. However, some problems may arise where most of the imagery covered by cloud since Indonesia is a tropical country. It is possible to remove cloud by some techniques with another scene of satellite imagery, but it can also remove landslide features. For example, if satellite imagery is not recorded after landslide happened, the old landslides are often partially or totally covered by vegetation. Mixed landuse in Indonesia can also affect misinterpretation of landslides feature using satellite imagery.

Analysis of surface morphology is the most recent trend in landslide inventory mapping due to the availability of very high resolution of DEMs (Digital Elevation Models) derived from airborne laser profiler or Light Detection and Ranging (LiDAR). After a landslide occurs, the surface topography changes and leaves a distinct signature (Pike, 1988). Digital representations of the topographic surface were employed to characterize and different landslide morphology and to investigate the location and distribution of landslide activity (Schulz, 2004; Chen et al., 2006; Schulz, 2007; Booth et al., 2009; Kasai et al., 2009; Derron and Jaboyedoff, 2010; Razak et al., 2011). It can be employed by visual interpretation (Haugerud et al., 2003; Chigira et al., 2004; Schulz, 2004; Chen et al., 2006; Haneberg et al., 2009) or automatic or semi-automatic (Sato et al., 2007; Booth et al., 2009; Kasai et al., 2009). Also, some authors integrated DEM with satellite imagery to obtain a 3D view of the terrain, which can be visually interpreted to identify landslides (e.g. Nichol et al., 2006). However, analysis of surface morphology by very high resolution of DEM is still expensive and not common in Indonesia.

In this paper, the author adapts several methods of landslide inventory and proposes a landslide inventory method, so called participatory landslide inventory mapping, in order to provide a nearly complete landslide inventory data over a 33 year period (1979 to 2013) in the Purwosari Area, Java, (Indonesia). The nearly complete landslide database is employed to generate statistics of landslides, including area, volume, slope, runout, and exceedance probability. It is also used as a basis for landslide susceptibility zoning (Chapter 4)

3.2 Participatory Landslide Inventory Mapping

Landslide inventory map is the simplest landslide map. This can be easily understood by earth scientist, city planners, and decision makers. Landslide inventory map shows the location and the type of landslide occurrences. Finally, it can be used as information to construct hazard map (Galli *et al*., 2007). The landslide inventory map can also record landslide occurrences for several years by compiling with historical landslide data. Conventional approaches to obtain landslide inventory maps are usually conducted by interpreter who interpret remote sensing data without profound knowledge of local resource conditions. Limited field experience possibly results in inaccurate delineation and misinterpretation of landslide polygon. The objective of participatory landslide inventory mapping is to enable villagers/local people to carry out the interpretation of aspects of their experience. In this process local people show the exact boundary of past landslide events. The information will later be digitized and geo-referenced. Involving local people as eyewitnesses are expected to improve the accuracy and precision of data measurement.

3.2.1 Data Source

An official landslide database provided by DIBI is adopted from DesInventar which is expected to collect disaster information at a local level (sub-district). The data are limited to the time, location, death toll, material/immaterial losses, and the number of affected people. In practical application, the landslide data is usually used to propose an aid which is distributed by the local government once landslide occur. The landslide database provided by DIBI also lacks a proper georeference and dimension (size and volume) that is essential for landslide hazard and risk

assessment. The problem also involves the difficult decision on what extend of landslide or people should be affected to be counted in the database. Thus, the landslide database provided by DIBI are also often different with the disaster register in the sub-district level or village level (some regions are not available).

The author employed a disaster register obtained from Purwosari Area local government as a basis of participatory landslide inventory mapping. The disaster register is a database generated by Purwosari local government based on the report from local people once a disaster occurs. It involves all disaster types. This data is used to distribute emergency response supplies such as medicine, blanket, instant noodle, rice, etc. Since the data focus on the emergency response phase, the information also mainly focuses on the time, location (name of the village), the number of people affected, and estimated loss. It provides a valid information on the occurrences, time, location, and estimated loss, but it lacks a proper georeference and dimension.

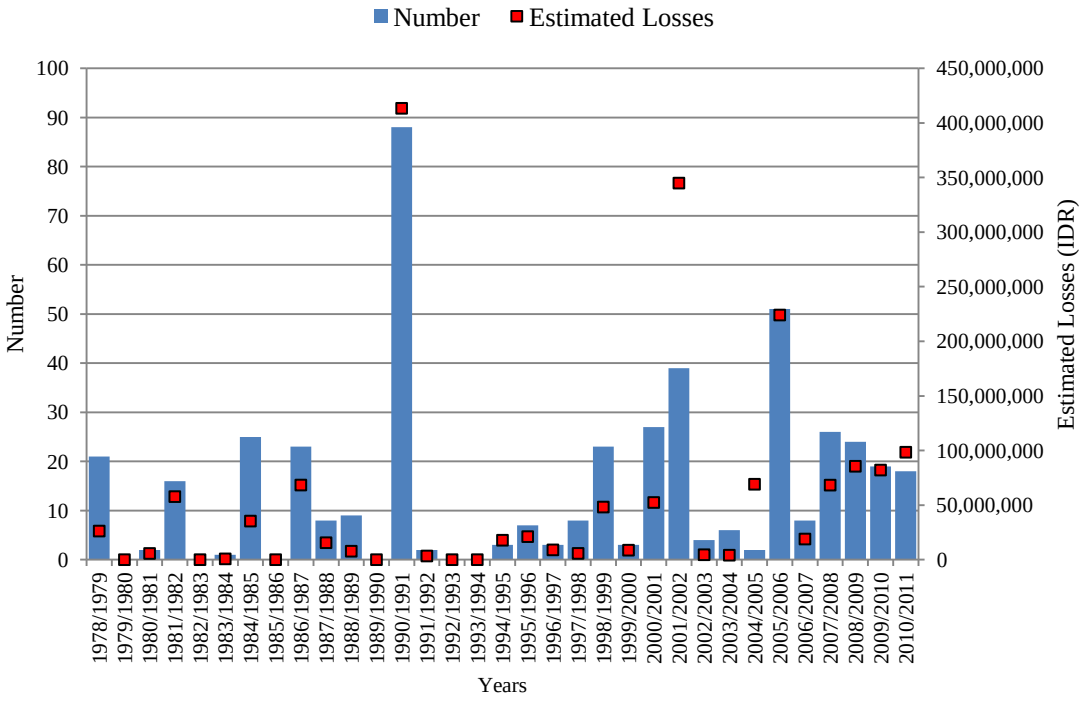

Figure 3.1 Number and Estimated Losses based on Purwosari Area Disaster Register

For landslide events, there were 472 landslides reported by local people from 1978-2011 with total loss 1,796,794,32 IDR. It means that there were 14 landslide

events/year with average loss 54,448,300 IDR/year and one landslide event can cause 4,057,350 IDR losses (Figure 3.1). It involves all of the reported landslide events by local people and without the verification on what extend of the size, area, landslide type, triggering factor, and accurate coordinate location.

Due to the lack of proper georeference and dimension, it is critical to conduct the ground check in order to provide the more complete accurate data inventory of landslide. In depth interview method and participatory mapping were employed to identify the dimension of landslides which are not documented by local government. Thus, the memory of key person and local people were used to improve the delineation of past landslide events by using GPS plotting and participatory mapping technique.

3.2.2 PARTICIPATORY FIELD MAPPING

Participatory landslide inventory mapping is a process, which can be used to generate a series of landslide inventory outputs to be transferred into a Geographic Information System (GIS). Landslide events catalogue obtained from disaster register needs to be checked through field mapping. Past landslides which are covered by vegetation or dismantled by erosion and human activities are not easily identified in the field. Boundary of past landslide sometimes can not be clearly defined. A help from eyewitnesses or landslide disaster victims is needed to reconstruct the boundary of past landslides. A combination between field survey method involving active participation from communities and the use of an innovative technology, i.e. laser range finder and GPS are employed to identify and measure the extents of past landslide.

There were three teams (two persons each) of well trained surveyor involved in landslide participatory landslide inventory mapping in Purwosari area. Semi closed questionnaire (Appendix A) was prepared to obtain information related landslide hazard and risk in particular landslide events. The unclear boundary of past landslide is able to be identified by using participatory landslide inventory mapping. Local people kindly showed the dimension of past landslide failure, including length, width, depth, and run out to the surveyor. Figure 2 shows the activities of participatory landslide inventory mapping in Purwosari Area. It shows that the dimension of

landslides can be measured directly in the recent landslide events and collaboration between surveyor and local people is needed to measure past landslide dimension.

Figure 3.2 Activities during Participatory Landslide Field Mapping

All of 472 landslide events reported by local people should be verified and the dimension of landslides should be mapped in order to be able to quantify both landslide susceptibility and hazard. The participatory landslide inventory mapping successfully verified 182 landslide events from 1978-2011. There are 267 misreport landslides and 23 unsuccessfully verified landslides. Misreport landslide means that the surveyor and local people could not find and recognize the name reported in the register; or reported landslides which have no dimension. Some people reported landslides when they found cracking on their house and the evidence of landslides was difficult to be recognized. Since there is no landslide failure on it, the author considers that it should not be included in the landslide inventory mapping. Unsuccessfully verified landslides mean that the evidence of past landslide could not be recognized anymore in the field and the eyewitnesses of landslides have already moved to another place. Thus, the author considers that the participatory landslide inventory mapping in Purwosari area is nearly complete.

Table 3.1 Descriptive Statistics of Landslide Inventory Mapping in Purwosari Area

Information	Number
Number of surveyor	6
Survey rate (#/2 men/day)	6-10
Database (man)	1
Database rate (days)	7
Number of landslides	182
Area total landslides (m^2)	44496.43
Landslide density #/km^2	13
Smallest area (m^2)	12.1
Largest area (m^2)	3036
Average area (m^2)	244.5

Participatory landslide inventory mapping in Purwosari Area required 21 days with 6 people surveyors. The average speed of survey is 6-10 landslides/team/day and the total area of landslide is 44496.43 m^2 (Table 3.1). Landslides length, width, depth and run out reconstruction took a long time because the evidence of past landslides in the field should be reconstructed based on visual observation both surveyor and local people. Errors may occur during this process, especially when measuring landslides in which the evidences are totally disappear. Geomorphological experience and knowledge and the memory of local people were combined to minimize errors during landslides boundary measurement.

3.2.3 GENERATION OF LANDSLIDES DATABASE

Some techniques applied during measuring the dimension of landslides were also employed to support the generation of landslide databases. It included coordinate plotting on the landslide crown or toe, sketching landslide area, placing landslide on the topographic map, taking pictures of landslides, recording the direction/orientation of landslides (dip and strike if possible). The generation of landslide database will be easier if these data are available. Landslide data from field mapping were transferred into GIS. On-screen digitizing was carried out on the basis of all information in the field mapping, topographic map and SPOT 5 imagery. This process used all information on the map, including the position of drainage line,

roads, building, landuse, etc. The author manually drew the boundaries on-screen by following the lines, shapes, pattern of the topographic map and SPOT 5 imagery on the screen.

Drawing landslide polygon on-screen was a time consuming process in landslide inventory mapping. Transferring information from field mapping onto GIS data file (e.g. shapefile) needs to be carefully checked. Topographic map and SPOT 5 imagery were the basis of placing the landslide in the right position. Coordinate record, landslide pictures, landslide orientation and landslide sketch were essential in order to accurately digitize landslide polygon in GIS layer. The average speed database generation was 26 landslides/day. Spatial data attribute of the landslide inventory map in Purwosari Area includes date of occurrence (some including time), coordinate, element at risk, estimated loss, number of pictures, orientation, lithology, landslide type, and landslide dimension. Once landslides are transferred to GIS, computation landslide susceptibility, hazard and risk is possible.

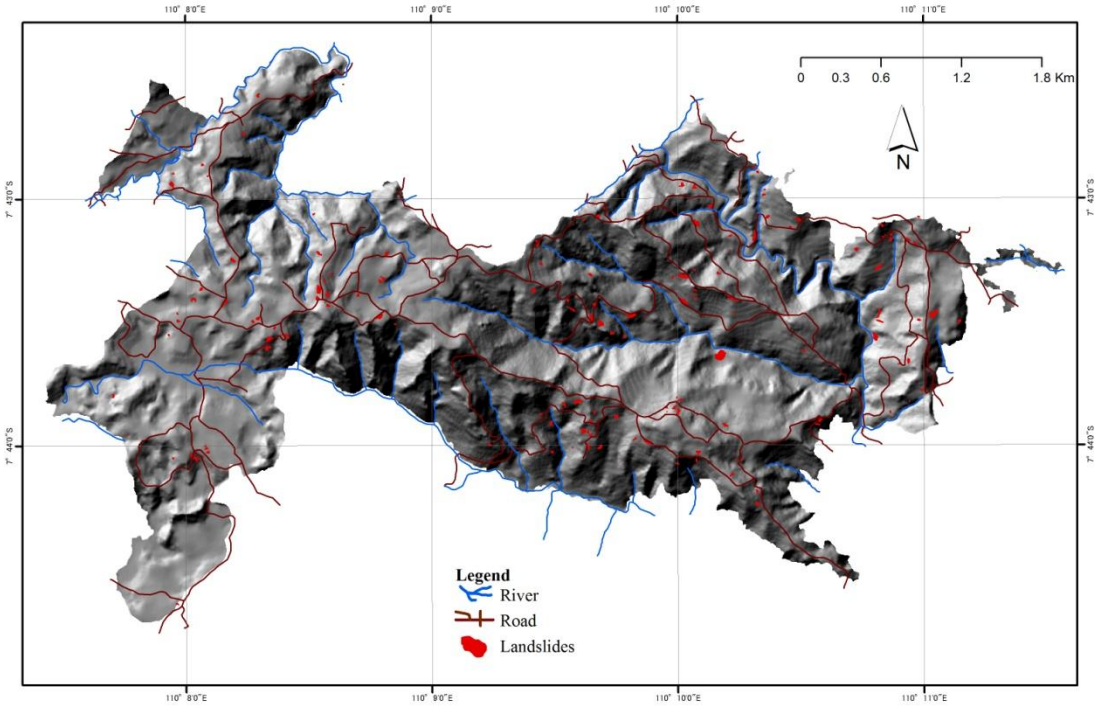

Figure 3.3 Landslide Inventory Map of Purwosari Area

3.3 ANALYSIS OF THE LANDSLIDE INVENTORY

There are many purposes of preparing a landslide inventory map such as (i)

documenting the landslide phenomena (ii) preparing preliminary step for susceptibility, hazard and risk (iii) investigating the distribution, types, and pattern of landslides and (iv) studying the evolution of landform dominated by mass wasting process (Guzzetti et al., 2012). Several empirical relationships can also be computed when the complete information on the landslide inventory map is available. It includes the height of the slope and run out, run out and volume, area and volume, and the probability distributions of landslide area and volume. Landslide inventory by using perticipatory mapping have been analyzed to describe possible correlation and empirical relationships.

The landslide typology in Purwosari area can be classified into translational and rotational slide. There were 10, 23, 1, and 148 landslides occurred in the public infrastructure area, dry cultivated area, paddy field, and settlement area respectively. An empirical relationship between height and run out might be useful to consider a safer place for the settlement area. Height of slope represents the difference between the highest altitude of the source area and the lowest part of the landslide deposit. Figure 3.4 shows that run out distance is proportional to the height of landslides. It also indicates that the run out around 20 m could be a threshold for building or infrastructure development with minimum structural measures. The empirical relationship can be a recommendation to improve landslide susceptibility or hazard zoning.

The correlation between height of the slope and run out shows a linear trend for both translational and rotational slide. The best interpolation obtained with the standard least square regression method gives the empirical relationship $L=1.65H+1.09$, where L and H are in meters. Figure 3.4 shows that Purwosari area is mostly dominated by short distance run out and height. Those were produced by landslides which mostly occurred in the populated area as an effect of a cut in the slope during development of a house. Landslides in Purwosari area can also be categorized as shallow landslide. Geomorphological processes influence the typology of landslide. Purwosari area is dominated by steep topography with strong dissection and V-shape valley caused by intensively valley deepening. Rill and gully erosion are dominant features identified in this area. Thus, soils are not well developed in the steep topography with high erosion process.

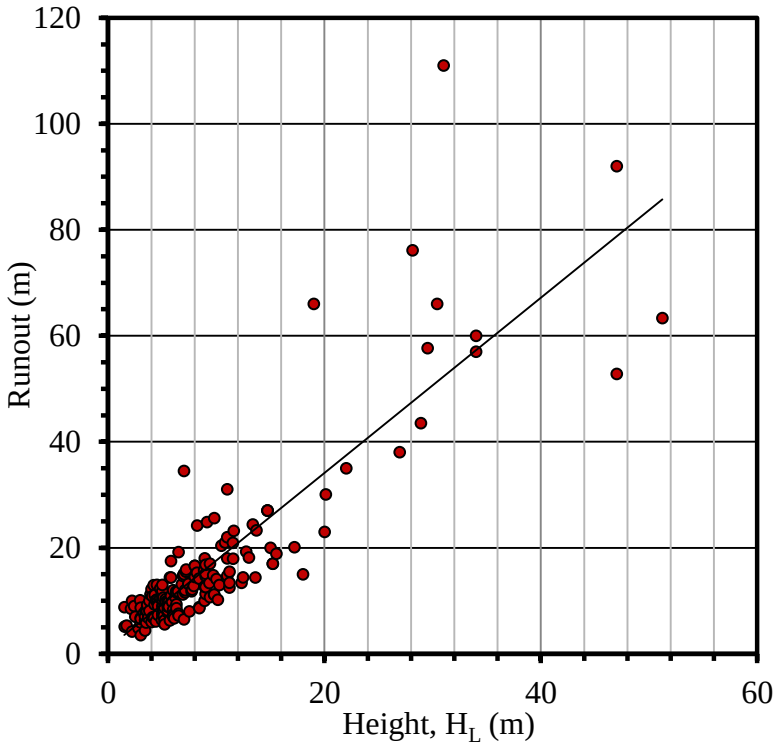

Figure 3.4 Relationship between Height and Run out Distance

Geomorphological processes and soil depth will contribute to landslide area and volume, which play a major role in landscape denudation and evolution. Determining landslide volumetrically may be difficult for past landslide which is usually identified by aerial photograph. Investigating landslide by aerial photograph can only delineate areas of landslide. Investigating the correlation between area and volume is an approach to find the empirical relationship between them.

The correlation between area and volume in Purwosari area may be reasonably calculated using the formula $V_L=0.053A_L^{1.6}$ with $12.1 \leq A_L \leq 3036$ m^2 (Figure 3.5). The average depth of landslide is 2.75 m. The similar trend can also be found in several places in the world (see Guzzetti, et al. 2009). This correlation could be used to infer the landslide volume in the area where landslide depth is unknown. But, this correlation should be used with care in order to avoid over exaggeration. Consideration about the similarity of the characteristics of an area such as geomorphological condition, lithology, landslide typology and landslide character should also be employed.

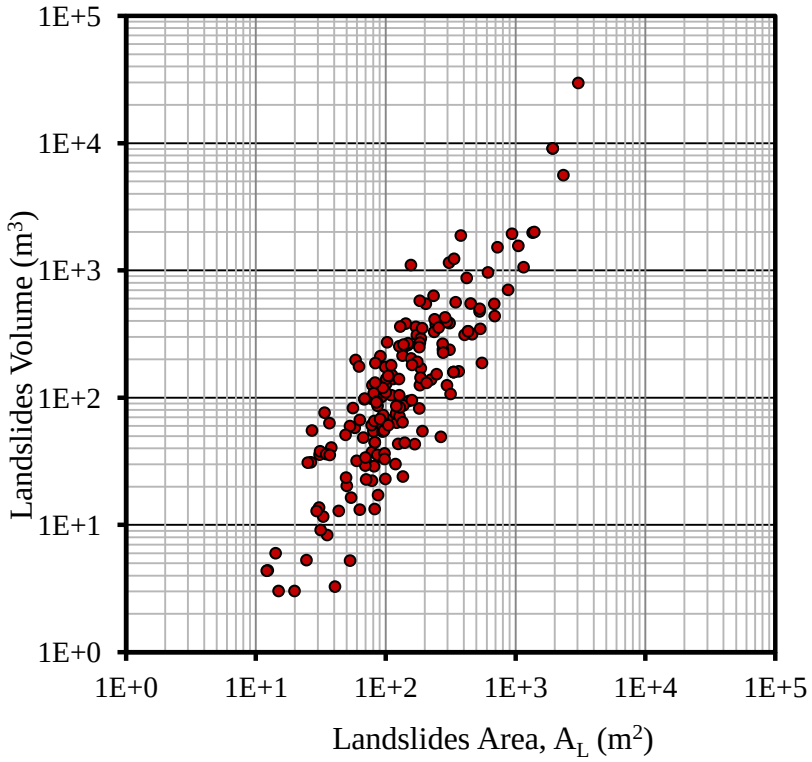

Figure 3.5 Relationship between Landslide Area and Volume

Historical data of landslide volume is also important to estimate mobilization rate or denudation rate in an area. It represents the moving failure of landslides in an area and specified time. Mobilization rate φ_L is measured by dividing total landslide volume in an a period (m^3) by the length of the period and by the extent of the study area, given in mm yr^{-1}. The extent of Purwosari area is 1.37 x 10^7 m^2 and the total landslide volume in 34 years is 95.723, 07 m^3. It indicates that mobilization rate φ_L in Purwosari area is φ_L=0.2 mm yr^{-1}. Mobilization rate is useful for many applications such as land evaluation, land suitability, and land degradation analysis. In landslide field, area and volume are usually analyzed by frequency-magnitude.

Landslide area and volume statistics were used as an approach to investigate landslide magnitude. Frquency-magnitude analysis is often used to analyze the distribution of landslide magnitude or size distribution. It indicates the frequency and what extents landslide occurred in an area. There are some evidences that the frequency area of landslides is similar to frequency-magnitude statistics of earthquake which satisfy the Gutenberg-Richter (Gutenberg and Richter, 1954)

relation:

$$\log N_{CE} = -bm + a \quad (3.1)$$

where N_{CE} is the cumulative number of earthquakes in specified area and time with magnitude greater than and equal to *m*, *a* and *b* are constants. It is valid to be applied in small region or the entire world. Equation (3.1) is equivalent to the power-law relation (Guzzetti, et al., 2002):

$$\log N_{CE} = C{A_E}^{-\alpha} \quad (3.2)$$

where *C* is constant, A_E is the earthquake rupture area and α = b from Equation 3.1. Some authors (Sugai et al., 1994; Yokoi et al., 1995) proposed that frequency-area/volume statistics of landslide is similar to frequency-magnitude statistics of earthquake which also satisfy the *power law*.

The frequency distribution of landslide area was calculated by using non cumulative distribution. There are some evidences that frequency area empirically exhibits a power law (fractal statistic). Probability density decreases with the increasing area of landslides. However, *rollover* can also be found in the Purwosari landslide database. *Rollover* phenomenon is the truncation trend of landslide extent towards probability density function. It happens in most landslide inventory data (Guzzetti, et al., 2002; Malamud et al., 2004; Van Den Eeckhaut et al., 2007). Rollover can be the result of the incompleteness of landslide data (*censoring effect*) especially small landslides (Stark and Hovius, 2001). The incompleteness is because the difficulties of interpreter to recognize small landslide area by using aerial photograph. Rollover can also be the result of the specific characteristic of landslides itself (Guzzetti et al., 2008).

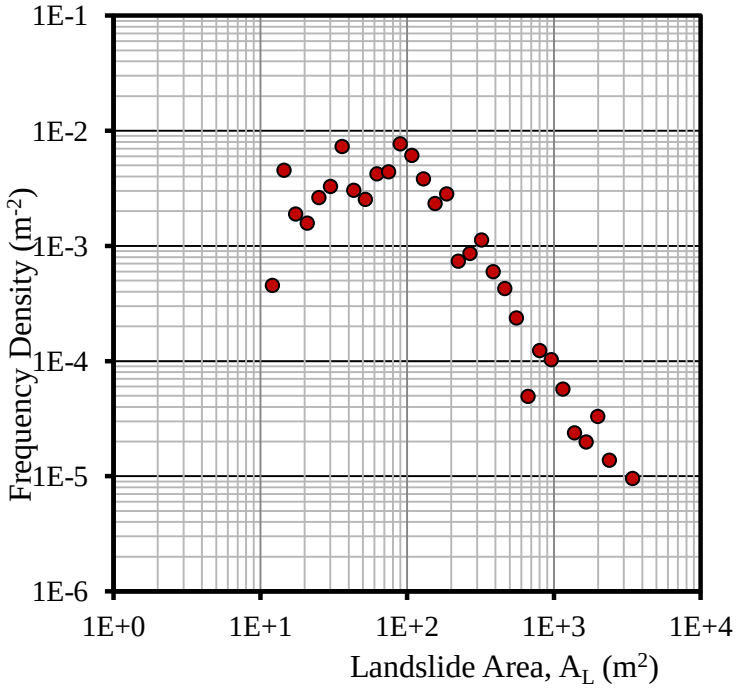

Figure 3.6 Non-cumulative Frequency-area Distribution of Purwosari Landslides

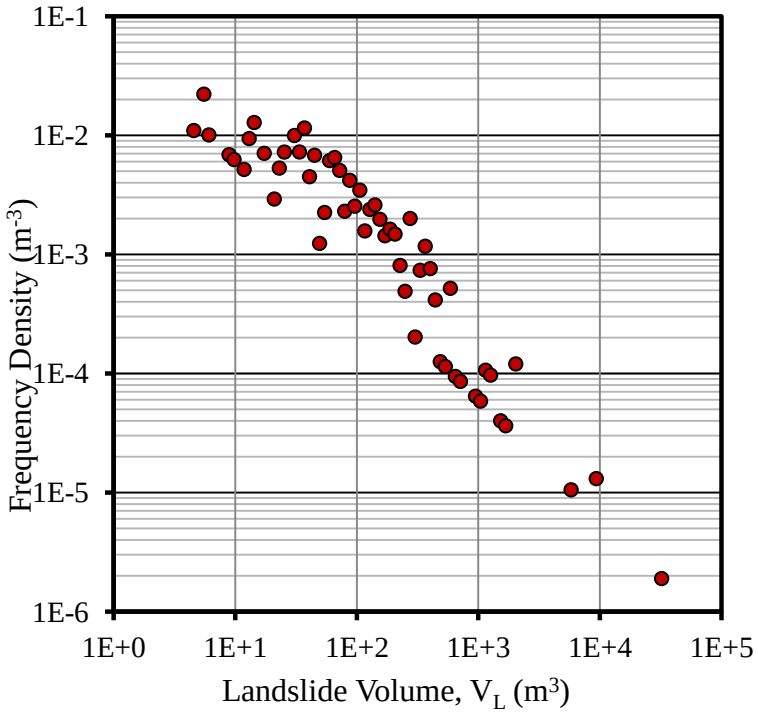

Figure 3.7 Non-cumulative Frequency-volume Distribution of Purwosari Landslides

Landslide inventory dataset in Purwosari area also exhibits *power-law* (*fractal* statistic) for area >90 m^2 based on (Guzzetti, 2002):

$$-\frac{dN_{CL}}{d_{AL}} = C`A_L{}^{-\beta} \quad (3.3)$$

with $-dN_{CL}/dA_L$ is the negative of the derivative of the cumulative distribution, A_L is landslide area, C` and β are constant. *Power-law* regression line of equation (3.3) with *R-square* 0.96 shows that landslide frequency-area has value of β=2.01 and C`=70 with the landslide area in m^2. *Rollover* phenomenon (with landslide area = 90m^2) can also be found in the dataset. This phenomenon cannot be the result of the censoring effect or incompleteness of the data because the landslide inventory dataset can be classified as complete data or nearly complete data. Thus, the author realizes that rollover phenomenon is real and exist in each of landslide datasets.

Frequency-volume statistic can be obtained by modifying Equation (3.3) with landslide volume. Small *rollover* can also be found in the volume <30m^3. Frequency-volume exhibits a *power law* with β=0.95 and C`=0.047. Figure 3.7 shows that landslide volume variation is distributed on landslides with the volume ≤600 m^3. It occurs with the landslide volume 20 $m^3 \leq V_L \leq 600$ m^3. This may be the result of different mechanism of failure and different causative factor of landslide such as lithology, geomorphology and landuse. Further investigation with complete landslide inventory from different area characteristic is still needed to confirm this issue.

3.4 ROCKFALL INVENTORY

The rockfall inventory was produced by the extensive geomorphological field survey based on the transect walk perpendicular to fall face. The main focus of the field survey were to record the coordinate location and to measure the dimension of the boulder deposits. The location was recorded by GPS plotting and the dimension of the boulder was measured by laser distance meter or measuring tape. The 521 rockfall deposits in our geomorphological inventory range in size from $18x10^{-4}$ to $3.6x10^3$ m^3 (Figure 3.8). All the rockfall data were generated as point data with an attribute of coordinate location and the volume of the boulder. The detail rockfall distribution is discussed in chapter 5 and 6.

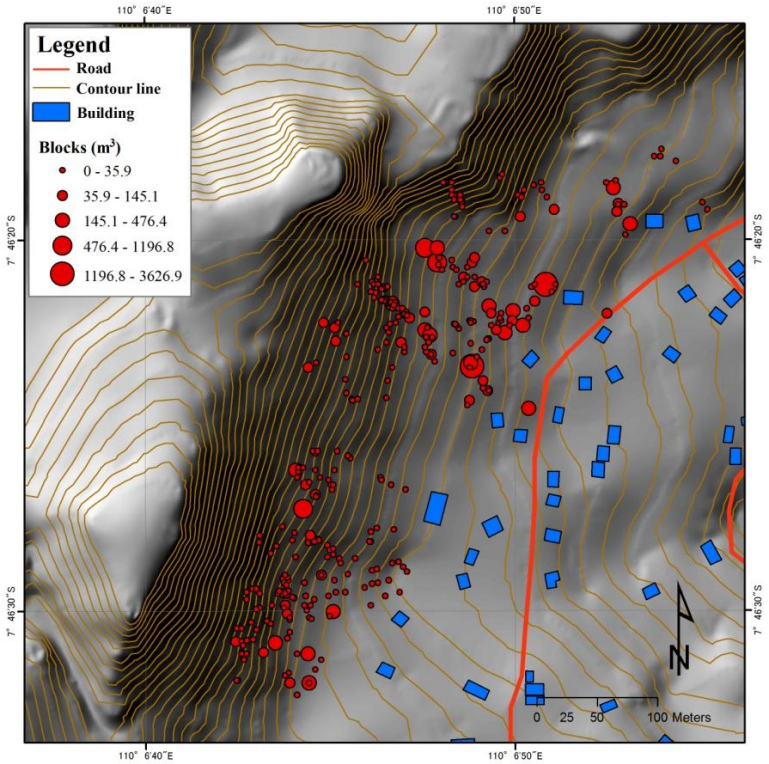

Figure 3.8 Rockfall Boulders Distribution in the Southern part of Gunung Kelir identified from Field Work

3.5 SUMMARY AND CONCLUSION

Landslide inventory mapping is aimed to provide information related to location, landslide typology, landslide extents and damage of elements at risk in. The author has combined the traditional geomorphological field survey method involving active participation from communities with the use of an innovative technology, i.e. laser range finder and GPS to identify and measure the extents of past landslide. It is later called as participatory landslide inventory mapping. Participatory landslide inventory mapping is a precise, cost-effective and less time consuming. Participants or local people in mapping activities typically showed high level of participation and engagement.

Data input into a GIS program enables post-processing, permits enhanced cadastral activities, better landslide statistics. The method is expected to solve the problem of insufficiency of landslide inventory in Indonesia. The landslide distribution will be used to generate landslide susceptibility analysis discussed in chapter 4. It is expected to support soft countermeasures tool to protect persons,

building, facilities, and infrastructures from being exposed to landslide hazard by appropriate landuse planning.

REFERENCES

Ardizzone, F., Cardinali, M., Galli, M., Guzzetti, F., Reichenbach, P. 2007. Identification and mapping of recent rainfall-induced landslides using elevation data collected by airborne Lidar. Nat. *Hazards Earth Syst. Sci*. 7:637–650.

Blochl, A., dan Braun, B. 2005. Economic Assessment of Landslide Risks in The Swabian Alb, Germany-Research Framework and First Results of Homeowners' and Experts' Surveys. *Natural Hazards and Earth System Sciences* 5, hal 389–396, 2005; European Geosciences Union.

BNPB, 2010(a). *Rencana Nasional Penanggulangan Bencana 2010-2014*. Badan Nasional Penanggulangan Bencana. Jakarta.

BNPB, 2010(b). *Rencana Strategis Badan Nasional Penanggulangan Bencana 2010-2014.* Badan Nasional Penanggulangan Bencana. Jakarta.

Booth, A.M., Roering, J.J., Perron, J.T. 2009. Automated landslide mapping using spectral analysis and high-resolution topographic data: Puget Sound lowlands, Washington, and Portland Hills, Oregon. *Geomorphology*, 109, pp. 132-147.

Brardinoni, F., Slaymaker, O., Hassan, M. A. 2003. Landslide inventory in a rugged forested watershed: a comparison between air-photo and field survey data. *Geomorphology* 54:179–196.

Brunsden, D. 1985. Landslide types, mechanisms, recognition, identification. In: Guzzetti F, ondini A.C., Cardinali M, Fiorucci F, Santangelo M, Chang K.-T (2012) Landslide inventory maps: New tools for an old problem. *Earth-Science Reviews* 112:42–66.

Cardinali, M., Reichenbach, P., Guzzetti, F., Ardizzone, F., Antonini, G., Galli, M., Cacciano, M., Castellani, M., Salvati, P. 2001. A geomorphological approach to the estimation of landslide hazards and risks in Umbria, Central Italy. *Natural Hazards and Earth System Sciences* 2:57–72.

Carrara, A., Crosta, G., Frattini, P. 2003. Geomorphological and Historical Data in Assessing Landslide Hazard. *Earth Processes and Landform* 28. hal 1125-1142.

Chen, R. F., Chang, K. J., Angelier, J., Chan, Y. C., Deffontaines, B., Lee, C. T., Lin, M. L. 2006.Topographical changes revealed by high-resolution airborne LiDAR data: the 1999 Tsaoling landslide induced by the Chi-Chi earthquake. *Engineering Geology*, 88, pp. 160-172. doi:10.1016/j.enggeo.2006.09.008.

Chigira, M., Duan, F. J, Yagi, H., Furuya, T. 2004. Using an airborne laser scanner for the identification of shallow landslides and susceptibility assessment in an area of ignimbrite overlain by permeable pyroclastics. *Landslides*, 1(3), pp. 203-209.

Crovelli, R. A. and Coe, J. A. 2009. Probabilistic Estimation of Numbers and Costs of Future Landslides in the San Francisco Bay region. *Georisk vol. 3 No. 4 hal. 206-223.*

Dahal, R.K., Hasegawa, S., Nonomura, A., Yamanaka, M., Masuda, T., Nishino, K. 2007. GIS Based Weights-of-Evidence Modeling of Rainfall Induced Landslides in Small Catchments for Landslide Susceptibility Mapping. *Environ Geol,* doi: 10.1007/s00254-007-0818-3

Derron, M. H., Jaboyedoff, M. 201). Preface to the special issue: LIDAR and DEM techniques for landslides monitoring and characterization. *Natural Hazards and Earth System Sciences*, 10 (9), pp. 1877-1879.

Dipo, T. S. 2002. Bencana Tanah Longsor Kabupaten Kulon Progo dan Upaya Mitigasi Bencana. Dalam: *Prosiding Simposium Nasional Pencegahan Bencana Alam*. ISDM Project. Yogyakarta.

Dumana, T.Y., Tolga, G., Can, T., Emrea, Ö., Kecera, M., Dogana, A., Ates, X., Durmaza, S. 2005 Landslide inventory of northwestern Anatolia, Turkey. *Engineering Geology* 77:99– 114. doi: 10.1016/j.enggeo.2004.08.005.

Fell, R., Corominas, J., Bonnard, C., Cascini, L., Leroi, E., Savage, W.Z. 2008. Guidelines for landslide susceptibility, hazard, risk zoning for land-use planning. *Engineering Geology* 102:99-111. doi: 10.1016/j.enggeo.2008.03.014.

Galli, M., Ardizzone, F., Cardinali, M., Guzzetti, F., Reichenbach, P. 2008. Comparing landslide inventory maps. *Geomorphology* 94:268–289. doi: 10.1016/j.geomorph.2006.09.023.

Glade, T., Anderson, M., Crozier, M.J. 2005. *Landslide hazard and riks*. John Wiley

& Sons Ltd.

Gutenberg, B., and Richter, C.F. 1954. *Seismicity of the earth*. 2nd ed. Princeton University Press, Princeton, N.J.

Guzzetti, F., Cardinali, M., Reichenbach, P., Carrara, A. 2000. Comparing landslide maps: a case study in the upper Tiber River Basin, Central Italy. *Environmental Management*, 25 (3):247–363.

Guzzetti, F., Malamud, B, D., Turcotte, D. L., Reichenbach, P. 2002. Power-law correlations of landslide areas in central Italy. *Earth and Planetary Science Letters*, 195, 169-183.

Guzzetti, F., Reichenbach, P., Cardinali, M., Galli, M., Ardizzone, F. 2005. Probabilistic Landslide Hazard Assessment at the Basin Scale. *Geomorphology* 72, 272-299.

Guzzetti, F., Galli, M., Reichenbach, P., Ardizzone, F., Cardinali, M. 2006. Landslide hazard assessment in the Collazzone area, Umbria, central Italy. *Natural Hazards and Earth System Sciences* 6:115–131.

Guzzetti, F., Ardizzone, F., Cardinali, M., Rossi, M., Valigi, D. 2009. Landslides Volume and Landslide Mobilization Rate in Umbria, Central Italy. *Earth and Planetary Science Letters* 279, 222-229.

Guzzetti, F., Mondini, A.C., Cardinali, M., Fiorucci, F., Santangelo, M., Chang, K. T. 2012. Landslide inventory maps: New tools for an old problem. *Earth-Science Reviews* 112:42–66. doi:10.1016/j.earscirev.2012.02.001.

Haneberg, W. C., Cole, W. F., Kasali, G. 2009. High-resolution lidar-based landslide hazard mapping and modeling, UCSF Parnassus Campus; San Francisco, USA. *Bulletin of Engineering Geology and the Environment*, 68, pp. 263-276. doi:10.1007/s10064- 009-0204-3.

Haugerud, R., Harding, D. J., Johnson, S. Y., Harless, J. L., Weaver, C. S., Sherrod, B. L. 2003. High-resolution topography of the Puget Lowland, Washington — a bonanza for earth science. *GSA Today*, 13, pp. 4-10.

Kasai, M., Ikeda, M., Asahina, T., Fujisawa, K. 2009. LiDAR-derived DEM evaluation of deep-seated landslides in a steep and rocky region of Japan. *Geomorphology*, 113, pp. 57-69. doi:10.1016/j.geomorph.2009.06.004.

Malamud, B.D., Turcotte, D.L., Guzetti, F., Reichernbach, P. 2004. Landslide

inventories and their statistical properties. *Earth Surf. Process. Landforms* 29:687–711.

Marcelino, E.V., Formaggio, A.R., Maeda, E.E. 2009. Landslide inventory using image fusion techniques in Brazil. *Applied Earth Observation and Geoinformation* 11:181–191. doi: 10.1016/j.jag.2009.01.003.

Neuhäuser, B., dan Terhorst, B. 2007. Landslide Susceptibility Assessment Using "Weights-of-Evidence" Applied to a Study Area at The Jurassic Escarpment (SW-Germany). *Geomorphology* 86, hal 12-24. Elsevier.

Nichol, E. J., Shaker, A., Wong, M. S. 2006. Application of high-resolution stereo satellite images to detailed landslide hazard assessment. *Geomorphology*, 76, pp. 68-75.

Parise, M. 2001. Landslide mapping techniques and their use in the assessment of the landslide hazard. *Phys. Chem. Earth* 26(9):697-703.

Pike, R.J. 1988. The geometric signature: quantifying landslide-terrain types from digital elevation models. *Mathematical Geology*, 20 (5), pp. 491-511.

Pusat Volkanologi dan Mitigasi Bencana Geologi. 2005. *Pengenalan Gerakan Tanah*. Diakses pada tanggal 1 Desember 2007 dari http://merapi.vsi.esdm.go.id/?static/gerakantanah/pengenalan.htm

Razak, K. A., Straatsma, M. W., van Westen, C. J., Malet, J.-P., de Jong, S.M. 2011. Airborne laser scanning of forested landslides characterization: terrain model quality and visualization. *Geomorphology*, 126, pp. 186-200.

Reichenbach, P., Guzzetti, F., Cardinali, M. 1998. Map of sites historically affected by landslides and floods in Italy, 2nd edition, CNR Gruppo Nazionale per la Difesa dalle Catastrofi Idrogeologiche Publication n. 1786.

Reichenbach, P., Galli, M., Cardinalli, M., Guzetti, F., Ardizzone, F. 2005. Geomorphological mapping to assess landslide risk: concepts, methods and applications in the Umbria Region of central Italy. In: Glade T, Anderson MG, Crozier MJ (Eds). Landslide risk assessment. John Wiley & Sons, West Sussex, England.

Salvati, P., Guzzetti, F., Reichenbach, P., Cardinali, M., Stark, C.P. 2003. Map of landslides and floods with human consequences in Italy, CNR Gruppo Nazionale per la Difesa dalle Catastrofi Idrogeologiche Publication n. 2822.

Sato, H. P., Yagi, H., Moarai, M., Iwahashi, J., Sekiguchi, T. 2007. Airborne lidar data measurement and landform classification mapping in Tomari-no-tai landslide area, Shirakami Mountains, Japan. In: Sassa, K., Fukuoka, H., Wang, F., Wang, G. (Eds.), *Progress in Landslide Science*. Springer, Berlin, pp. 237-249.

Schulz, W.H. 2004. Landslides Mapped using LIDAR Imagery, Seattle, Washington. *U.S. Geological Survey Open-File Report*, pp. 2004-1396.

Schulz, W.H. 2007. Landslide susceptibility revealed by LIDAR imagery and historical records, Seattle, Washington. *Engineering Geology*, 89, pp. 67-87.

Stark, C. P. and Hovius, N. 2001. The characterization of landslide size distributions, *Geophys. Res. Lett.*, 28, 1091–1094.

Sugai, T., Ohmori, H., Hirano, M. 1994. Rock Control on Magnitude Frequency distributions of Landslide, *Transp. Jpn. Geomorph. Union* 15, 233-251.

Suzen, M. L. dan Doyuran, V. 2004. Data Driven Bivariate Landslide Susceptibility Assessment Using GIS: a Method and Application to Asarsuyu Catchment, Turkey. *Engineering Geology* 71, hal 303-321.

van Den Eeckhaut, M., Poesen, J., Verstraeten, G., Vanacker, V., Nyssen, J., Moeyersons, J., van Beek LPH., Vandekerckhove, L. 2007. Use of LIDAR-derived images for mapping old landslides under forest. *Earth Surf. Process. Landforms* 32:754–769. doi: 10.1002/esp.1417.

van Westen, C.J., Castellanos, E., Kuriakose, S.L. 2008. Spatial Data For Landslide Susceptibility, Hazard, and Vulnerability Assessment : An Overview. *Engineering Geology* 102:112-131. doi: :10.1016/j.enggeo.2008.03.010

van Westen, C.J., Van Asch, T.W.J., Soeters, R. 2005. Landslide hazard and risk zonation; why is it still so difficult? *Bulletin of Engineering geology and the Environment* 65(2):167–184. DOI 10.1007/s10064-005-0023-0.

van Westen, C. J., Rengers. N., Soeters. R. 2003. Use of Geomorphological Information in Indirect Landslide Susceptibility Assessment. *Natural Hazard* 30: 399-419. Kluwer Academic Publishers. Netherlands.

Yokoi, Y., Carr, J.R. Watters, R.J. 1995. Fractal Character of Landslides. *Environ. Eng. Geol.*1 75-81.

CHAPTER 4

COMPARING DATA-DRIVEN LANDSLIDE SUSCEPTIBILITY MODELS GENERATED FROM PARTICIPATORY LANDSLIDE INVENTORY MAPPING

4.1 INTRODUCTION

Landslide susceptibility zoning represents a division of land which has homogeneous areas or domains and their ranking according to degrees of actual or potential landslide susceptibility (Fell *et al*., 2008; Couture, 2011). It is an important step in landslide hazard and risk analysis. There are three main approaches for landslide susceptibility zoning, i.e. knowledge driven (heuristic) approach, physically based approach, and data driven approach (statistical analysis).

Knowledge driven approach is a qualitative approach by evaluating actual landslides compared with characteristics of geology or geomorphology. Each geomorphology or geology zone is given by susceptibility ranking by the extent of actual landslide and specific geomorphological process working in an area. The susceptibility ranking is usually based on the judgement and experience of surveyor. This approach is strongly dependent on the experiences of the surveyors (Atkinson and Massari, 1998; Nagarajan et al., 2000; Huabin et al., 2005).

Physically based approach is based on the slope stability analysis by calculating safety factor in a slope. It is usually applied for a specific purpose in a small area with detail mapping scale. The detail mapping needs detail geotechnical parameters measurement and many samples because it is difficult to extrapolate geotechnical parameters in the regional scale analysis with limited data sample. The process is

laborious and time consuming because of the time and effort required for the manual handling and processing of the data. Since the detail geotechnical parameters are usually not available in the hilly and mountainous area, especially in Indonesia, it is still difficult to apply the physically based approach for regional analysis in the study area. Nowadays, data driven approach is the most feasible approach for landslide susceptibility analysis applied in the regional scale mapping, especially in Indonesia.

Recent progress and development in landslide susceptibility zoning also focus on data driven approach (statistical analysis) using GIS technology. Data driven approach is more popular, in recent decade, than knowledge driven (heuristic) approach and physically based approach because it is more objective, requires less soil parameter (less expensive), less time consuming, suitable for wide area and gives reproducible results. Data driven approach can be applied based on bivariate statistical analysis, multivariate statistical analysis and soft computing.

The bivariate statistical analysis compares each data layer of controlling factor to landslide inventory separately and assumes that the presumed controlling factors of landslide are not interrelated each other (Suzen and Doyuran, 2004). It deals with one dependent variable, i.e. landslide inventory showing polygon or area of landslide events and one independent variable, i.e. a layer indicating controlling factor of landslide. Bivariate statistic calculates the density of landslides in each class of data layer and defines the importance of each parameter. The weights for individual parameter is added by calculating landslide density per parameter class in relation to the landslide density over the whole area. Various data layers, indicating the weight of homogenous units, are then overlaid to have a final score of landslide susceptibility. The bivariate statistical analysis does not take into account the interdependence of variables, and it has to serve as a guide when exploring the data set before multivariate statistical methods are used. The weight of evidence (WoE) is one of bivariate statistical analysis, which is widely applied in landslide susceptibility zoning (Westen *et al*., 2003; Dahal *et al*., 2007; Neuhaeuser and Terhorst, 2007).

WoE was formerly applied to predict disease (Lusted, 1968) and to map mineral potential (Bonham-Carter *et al*., 1989) in geoscience application. It calculates the

weight of predictive factors (controlling factors) based on the absence or presence of landslide in the study area and assumes that the presumed controlling factors of landslide are not interrelated each other. Landslide factor would be analyzed separately with landslide events. This model is simple and less time-consuming. It needs spatial landslide inventory data and the controlling factors data related to landslides. The controlling factors are spatial data presumed as the causal factor of the occurrence of landslides and can be utilized as a spatial landslide predictor in the future.

In the other hand, multivariate statistical models evaluate the combined relationship between a dependent variable (landslide occurrence) and a series of independent variables (landslide controlling factors) simultaneously. Multivariate analysis assumes that the presumed controlling factors of landslide are interrelated each other. It means that the analysis is not only related to landslide controlling factors and landslide inventory, but also the interrelationship among landslide controlling factors. In this type of analysis, all relevant factors are sampled either on a grid basis or in slope morphometric units. For each of the sampling units, the presence or absence of landslides is determined. The resulting matrix is then analyzed using multiple regression, logistic regression, discriminant analysis, random forest or active learning. The results can be expressed in terms of probability. The logistic regression model is one of the most popular multivariate analyses in landslide susceptibility zoning.

Logistic Regression (LR) was formerly invented as a description of population growth and autocatalytic chemical reaction (Cramer, 2002). It is applied to describe the relationship between several independent variables and a dichotomous dependent variable (Hosmer and Lemeshow, 2000). Dependent variable, i.e. landslide inventory must be input as binary either 0 (no landslide) and 1 (landslides) to model landslide possibility. The variables can be either continuous and discrete or a combination of both types. It also does not necessarily have normal distributions. The result of LR ranges from 0 to 1 which is analogue to a probability value. LR was applied successfully in landslide susceptibility zoning in many regions (Olmacher and Davis, 2003; Yesilnacar and Topal, 2005; Ayalew and Yamagishi, 2005; Can *et al*., 2005; Nefeslioglu *et al*., 2008; Schicker and Moon, 2012; Das *et al*.,

2012).

Formerly, soft computing is applied as a technique in computer science whose the solution is uncertain and between 0 and 1 (Zadeh, 1994). It was applied in landslide susceptibility because soft computing techniques such as fuzzy-logic, artificial neural network (ANN), neuro-fuzzy and support vector machine can deal with several problems such as insufficient knowledge of an area of interest and incomplete data. The interrelationship between landslide events and triggering factors are also nonlinear in nature (Ercanglu, 2005). Soft computing technique such as ANN is independent of the statistical distribution of the data and does not need statistical variables (Lee *et al*., 2007).

ANN is a soft computing technique based on the capability to imitate a human being in learning a particular phenomenon. There are three layers of neurons, which are connected by weights as a network. It can generalize and predict outputs from a set of inputs that it has not previously seen. The weights of the relative importance of different factors for landslide occurrence are generated by that network. Each weight will be used to calculate a landslide susceptibility index. There were landslide susceptibility maps generated by ANN (Catani *et al*. 2005; Gomez and Kavzoglu, 2005; Ercanglu 2005; Ermini *et al*. 2005; Nefesilioglu *et al*. 2008; Pradhan and Lee 2009).

Several attempts to compare several techniques of data driven landslide susceptibility zoning were applied in many countries such as Turkey, New Zealand, Korea, Italy, India and Malaysia. Yilmaz (2009) compared conditional probability, logistic regression, ANN and support vector machine in structural mountainous area Sivas Turkey. He used 10 landslide factors, i.e. slope, distance from fault, distance from drainage, elevation, distance from road, distance from settlements, aspect, TWI, SPI and NDVI. The landslide inventory map was derived from Landsat TM satellite images 2006, aerial photographs and fieldwork. He found that ANN was more realistic with area under curve 84.6 %.

Choi *et al*., (2012) compared frequency ratio, logistic regression and artificial neural network in a hilly area underlain by biotite granite and alluvium Korea. Sixth landslide related factors, i.e. slope, aspect, curvature, proximity to lineament, land

cover and NDVI were derived from ASTER data. The landslide inventory map was derived from 1:5000 scale photographs and ASTER data. It showed that logistic regression is more realistic with area under curve 85.4% compared to frequency ratio and ANN with area under curve 84.34% and 74.29% respectively.

Pradhan and Lee (2010) also compared frequency ratio, logistic regression and artificial neural network for landslide susceptibility zoning. The area was in structural landform Klang Valley Malaysia. Eleven landslides related factors, i.e. slope, aspect, curvature, altitude, distance to rivers, distance to roads, soil, lithology, distance to fault, land cover and NDVI were used in the analysis. 398 landslides were derived from 1:5,000–1:50,000 aerial photographs 1981-2004, SPOT 5 panchromatic satellite image and landslide reports over the past 23 years using visual interpretation. The most realistic result was by using ANN with seven landslides related factors instead of 11 factors.

Garcia-Rodriguez and Malpica (2010) tried to compare logistic regression and ANN to analyze earthquake-triggered landslide susceptibility in El Salvador Central America. The study area is an earthquake prone area with hard rock including pyroclastic deposits and associated volcaniclastic; and consolidated soil. Seven factors, i.e. elevation, slope, lithology, rainfall, landuse, terrain roughness and aspect were included in the analysis. Landslide inventory consisting of 112 landslides was derived from secondary data compiled in 2001. The authors did not mention clearly the most realistic result, even though the area under the curve of logistic regression showed better results than ANN.

Schicker and Moon (2012) compared weight of evidence and logistic regression in volcanic landform Waikato region, New Zealand consisting of andesitic stratovolcanoes and rhyolitic caldera. The controlling factors considered were slope, elevation, aspect, geology, landcover, maximum monthly rainfall, mean monthly rainfall, soil, distance from fault, river and road. There were 156 past landslides obtained from secondary data represented as geomorphological map and 123 landslides obtained from 13 years (1996-2003) landslide catalogue. The authors showed that logistic regression is more realistic than weight of evidence with an area under the curve 71% and 62% respectively.

The examples above show that there were different approaches and techniques

for evaluating landslide susceptibility and no agreement has been reached both in the procedure and the use of specific controlling factors employed in the lanslide susceptibility zoning. Each approach has its own assumption and the result may differ from place to place. The different result may also be affected by different landslides controlling factors employed in the analysis, including lithology and geomorphology condition, and the completeness of landslide inventory.

Thus, bivariate, multivariate and soft computing approaches need to be compared in order to identify the most realistic landslide susceptibility approach applied in tropical region Indonesia by using complete landslide inventory. The evaluation of controlling factors will also be evaluated based on the Cramer's V value and multicollinearity analysis. The discussion of merit and demerit of each data driven method will be evaluated to propose a combination of the methods applied in Purwosari area with a complete landslide inventory mapping.

4.2 STUDY AREA

Purwosari area is located in the southern part of Central Java and covers an area of 14 km^2 (Figure 4.1). It is dominated by hilly area with large open valley striking mostly NW-SE. The lithology consists of Tertiary Oligocene-Miocene Old Andesite Formation of van Bemmelen breccia coming from Gadjah Old-Volcano in which the magma is composed by *basaltic piroxene andesites*. It consists of andesitic breccia, tuff, lapilli tuff, agglomerate and intercalated andesite lava flows (Rahardjo, *et al*., 2005). The thickness is approximately 660 meters. There is also *calcareous sandstone, limestone* and *coralline limestone* in the small western part of Purwosari area. Old Andesite Formation is a dominant lithology in Kayangan Catchment. It can be differentiated in the field by the degree of weathering. Most of landslides can be found in the Old Andesite Formation with the very intense weathering process.

The denudational landform in Purwosari is influenced by the strong gravitational movement after the geanticline of Java in the south was pushed up. It is dominated by steep topography with strong dissection and V-shape valley caused by intensively valley deepening. Rill and gully erosion are dominant features identified in this area. The soils are well developed with highly weathering and leaching process in the

gentle area.

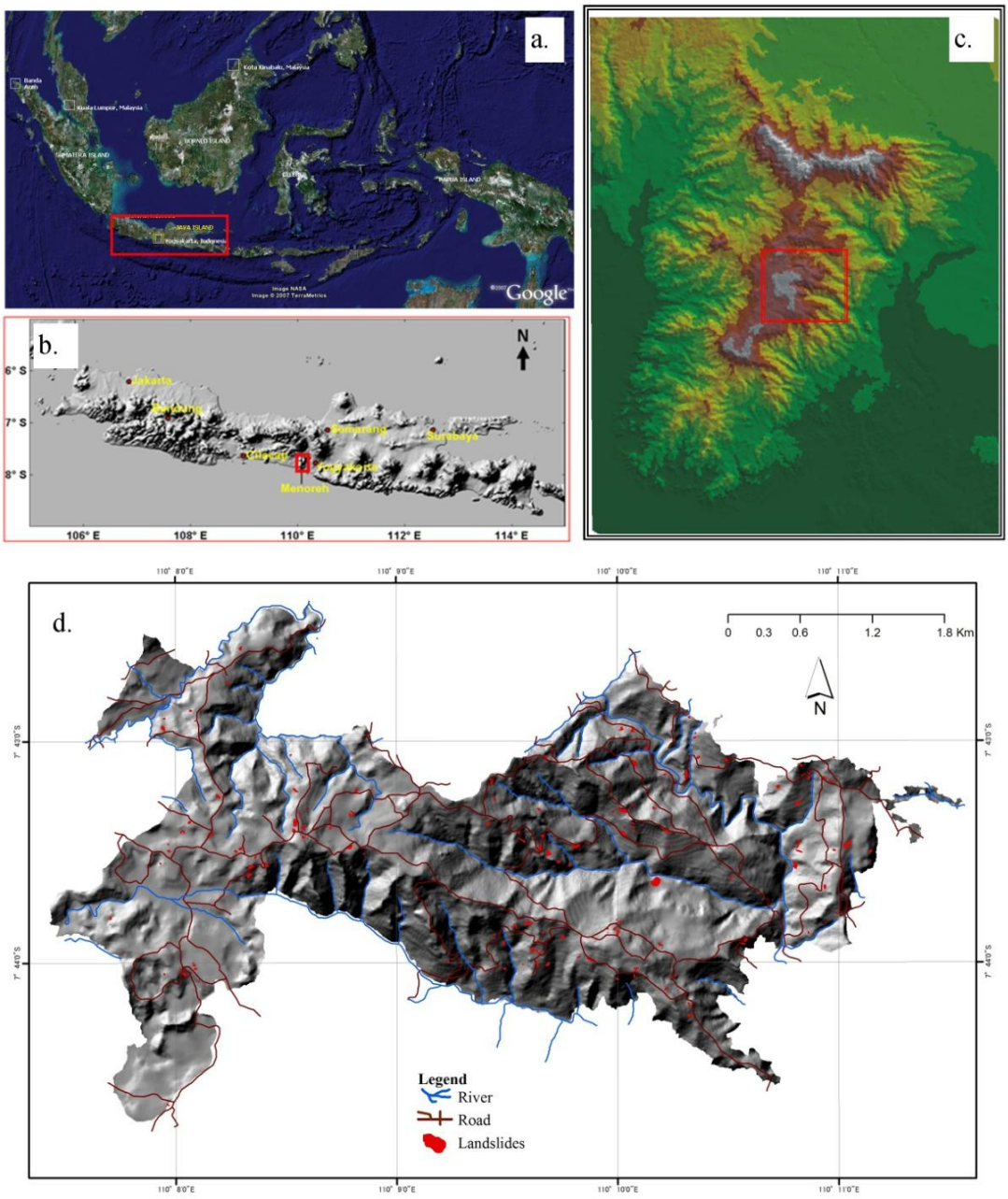

Figure 4.1 Study Area (a) geographical position of Indonesia: red rectangle shows geographical position of Java Island (b) DTM of Java Island: red rectangle shows the location of Menoreh Dome (c) DTM of Menoreh Dome: red rectangle shows Purwosari area (d) DTM of Purwosari area with landslide inventory

The average annual rainfall in Kayangan Catchment is 2478 mm and the highest rainfall intensity usually occurs from February to March with average monthly rainfall 426 mm. The high intensity of precipitation produces very intense weathering

processes and landslides. A settlement built by excavating the slope may lead to the reduction of the instability of natural slopes and can cause landslides. Settlement in the hilly area is located mostly alongside the road network.

4.3 MATERIAL AND METHODS

The evaluation of landslide susceptibility analysis includes the data driven analysis based on the weight of evidence (WoE), logistic regression (LR) and artificial neural network (ANN). It requires several data layers of controlling factors related to landslide and landslide inventory layer. Those data layers were processed in GIS environment software, i.e. ILWIS and ArcGIS.

4.3.1 DATA PREPARATION

The occurrence of most landslides is linked to controlling factors related to landslide, which reflects natural settings in the study area. Thematic maps representing various factors of landslide were generated by GIS techniques. Each controlling factor of landslide was mapped and converted to raster map with 5 meter cell size. The spatial landslide controlling factors and attribute were collected from Topography Map (Rupabumi Indonesia-RBI) Sendangagung and Wates at the scale of 1:25.000 sheet 1408-232 and 1408-214. It includes topographic related factors, water related factor, landuse and anthropogenic factors (Table 4.1).

Table 4.1 Sources and significance of the landslide controlling factors

Data Type	Factors	Source	Significance
Topographic	1. Elevation	Topographic Map (DEM)	Climate, potential energy
	2. Slope	Topographic Map (DEM)	Gravity, flow velocity
	3. Aspect	Topographic Map (DEM)	Solar insolation, evapotranspiration
	4. Plan Curvature	Topographic Map (DEM)	Converging, diverging flow

	5. Prof. Curvature	Topographic Map (DEM)	Flow acceleration, erosion/deposition
Water related	6. SPI (Stream Power Index)	Topographic Map (DEM)	Potential erosive power
	7. TWI Topographic Wetness Index)	Topographic Map (DEM)	Soil water content
	8. Distance to river	Topographic Map (DEM)	River undercutting
Landuse	9. Landuse	Topographic Map	Landslide triggering by slope cutting, trees effect on landslide
Anthropogenic	10. Distance to road	Topographic Map	Landslide triggering by road cutting, vibration of vehicles
Landslides	11. Landslides inventory	Participatory landslide inventory mapping	Landslide distribution

Acronyms: Prof.: Profile, SPI: Stream Power Index, TWI:Topographic Wetness Index

4.3.1.1 TOPOGRAPHIC FACTORS

Topographic factors include elevation, slope, aspect, plan curvature and profile curvature. Those were generated from 5 meter resolution of DTM produced by interpolation, using ILWIS linear interpolation method, from a 1:25.000 Topographical Map 1999 with contour interval 12.5 m. All of the data were initially continuous and then were sliced into different categories. The significances of topographic factors such as elevation, slope, aspect, plan curvature, and profile curvature are mainly on the gravitational related processes such as potential energy, flow direction and erosion.

Elevation is the first subdivision of the terrain related to the overall topographic setting. It represents the local relief and locates points of maximum and minimum heights within terrains. The elevation map was divided into 7 classes on a 100 m basis (Figure 4.2). The extent of classified elevation represents the steepness of the terrain. The narrow area is steeper than wide area. Elevation class 700-800 m represents high altitude of Purwosaria area and has the widest area. This area is

gentler than other elevation range classification. The density of landslide may be lower in the wide area of the elevation range class.

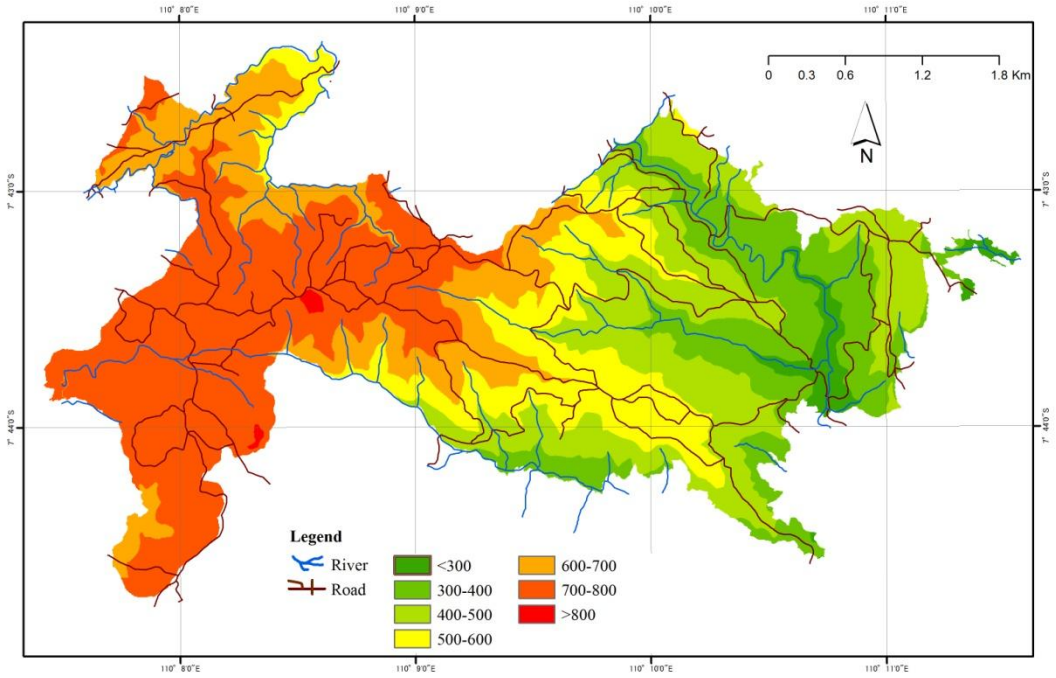

Figure 4.2 Elevation of the Study Area (in meters)

Slope gradient might be the most substantial cause of a landslide. It is expected that landslides will occur on the steepest slope as a consequence of the increasing of shear stress. It might also affect the level of pore pressure and the concentration of moisture. The slope map was divided into 5 classes. Beside represents a classification of the slope quantitatively (in degree), the division also represents the slope qualitatively (Figure 4.3). It was divided into flat-undulating (0-8), rolling (>8-15), moderately steep (>15-25), steep (>15-45), and very steep (>45).

Aspect represents the direction of the slope. It might reflect differences in soil moisture and vegetation which are related to solar insolation and evapotranspiration. Aspect was divided into 8 classes such as north, northeast, east, southeast, south, southwest, west, northwest, west and northwest (Figure 4.4).

Plan curvature represents the curvature of the corresponding normal section, which is tangential to contour. Whereas profile curvature represents the curvature of the corresponding normal section, which is tangential to flow line. Negative value represents that the normal section concavity is directed up, whereas positive

represents the opposite case.

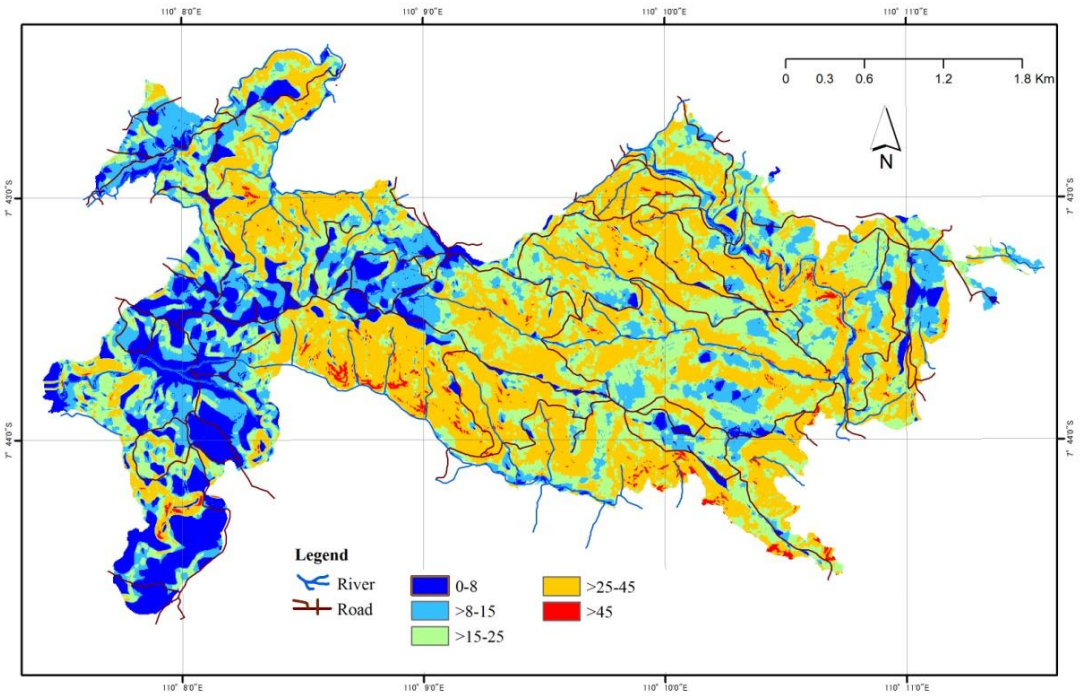

Figure 4.3 Slope of the Study Area

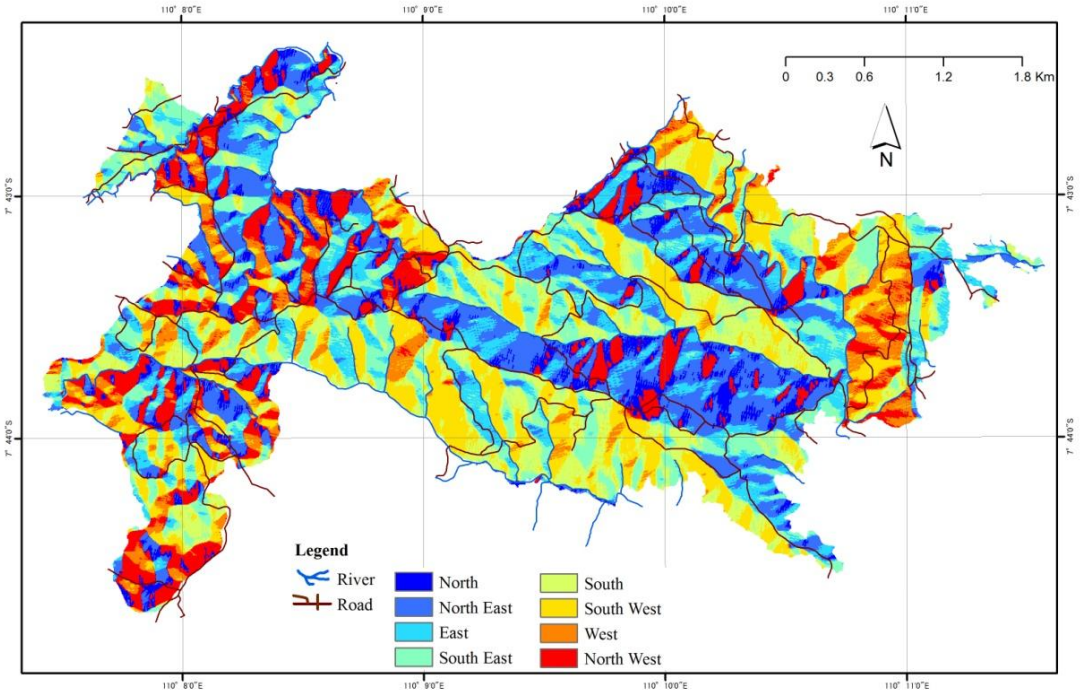

Figure 4.4 Aspect of the Study Area

Both plan curvature and profile curvature were divided into 5 classes (Figure 4.5 and 4.6). The curvature of the slope will affect the morphology or the shape of the slope. Then, it will affect the direction and acceleration of surface water flow in the terrain; and the erosion process.

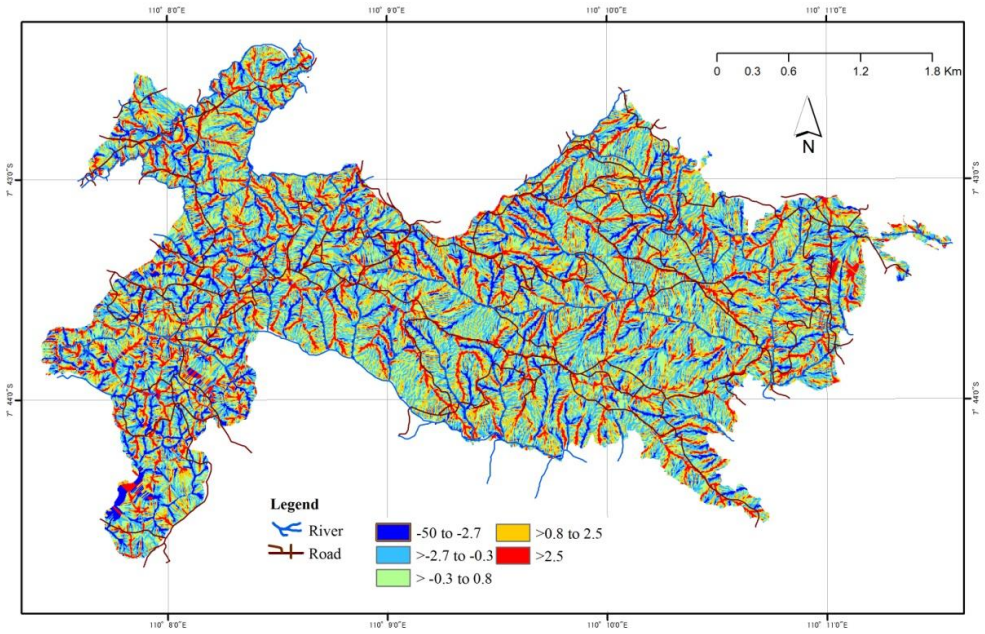

Figure 4.5 Plan Curvature of the Study Area

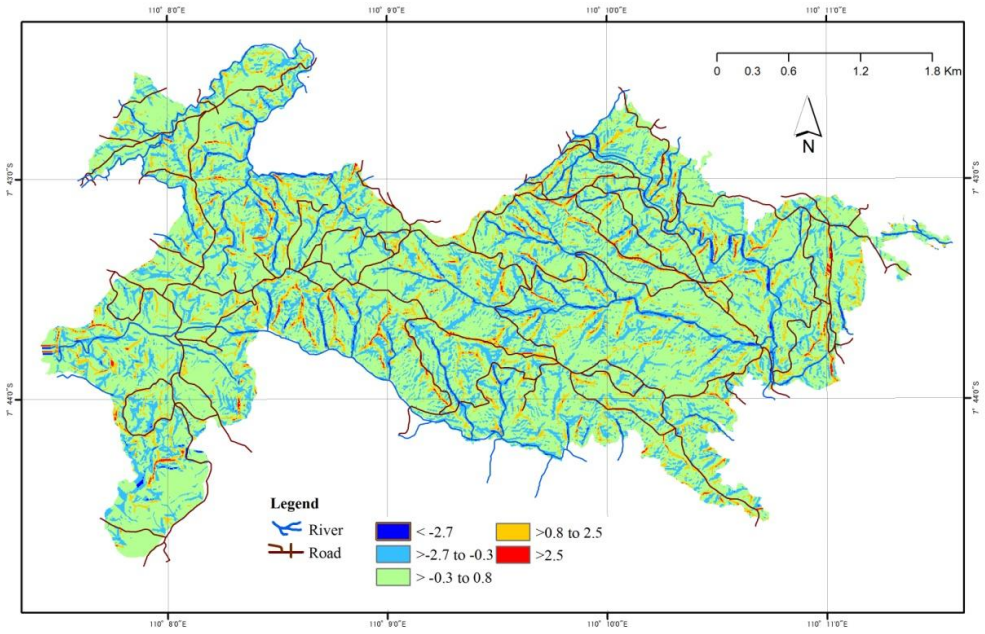

Figure 4.6 Profile Curvature of the Study Area

4.3.1.2 WATER RELATED FACTORS

Water related factors, including SPI, TWI and distance to river were also derived from DTM as a measure of surface water and sub-surface water. Surface water may cause landslide by undercutting and erosion. Subsurface water may change the water pore water pressure in the soil and cause slope instability.

SPI (Stream Power Index) was used to describe the potential flow erosion. It represents the strength of stream power and potential erosion with the idea that if a specific catchment area and steepness of the slope increase, the amount of water produced by upslope area and the velocity of water flow increase. SPI can be defined as (Hengl, et al., 2009):

$$SPI = A_f \cdot \tan\beta \qquad (4.1)$$

where A_f is the specific catchment area draining through the point and β is the slope angle. SPI was classified into 6 classes representing that higher a value is the stronger stream power (Figure 4.7).

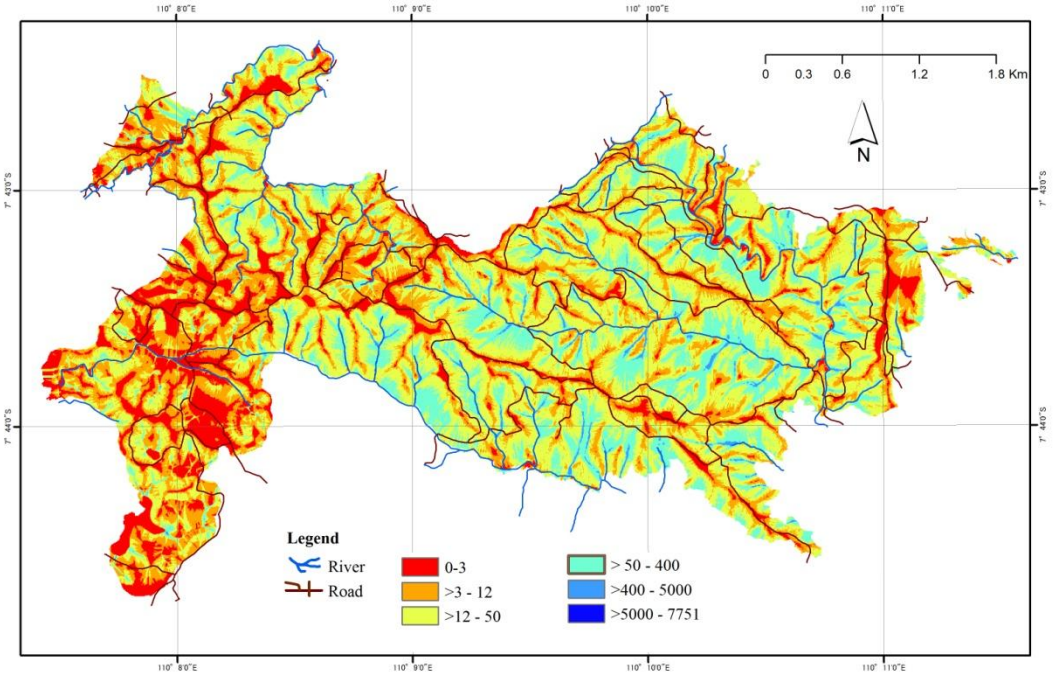

Figure 4.7 Stream Power Index of the Study Area

TWI (Topographic Wetness Index) was used as a proxy of soil water content or soil moisture (Moore et al., 1991; Quinn et al., 1991). It describes the tendency of the slope to accumulate water (Figure 4.8). A pixel with low slope angle tend to

accumulate water compare to a pixel which has a steep slope.

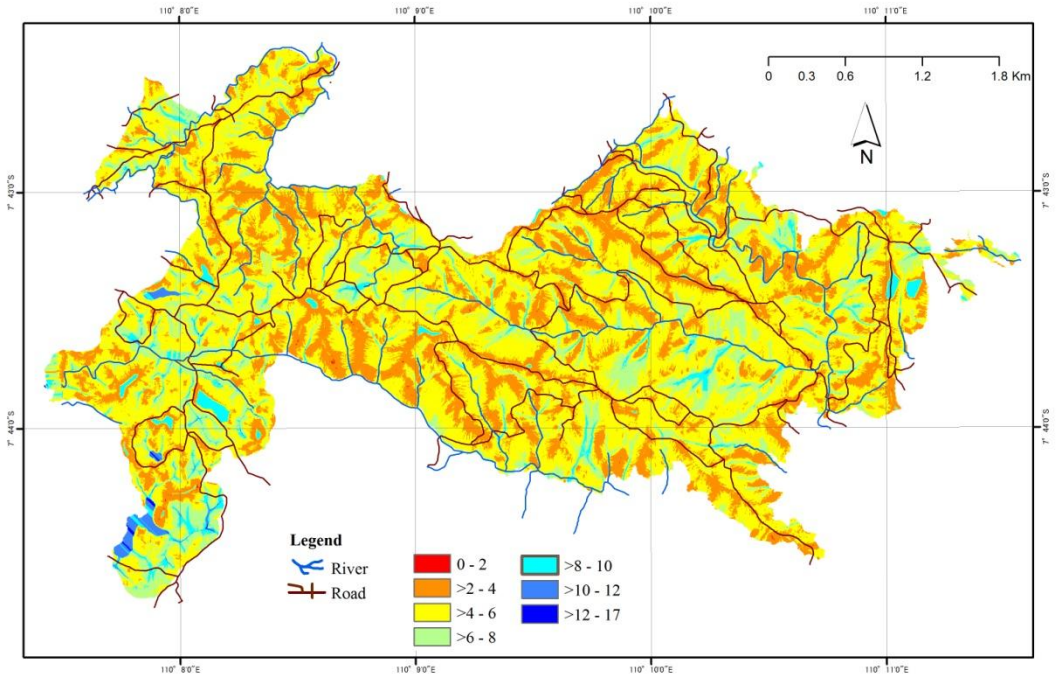

Figure 4.8 Terrain Wetness Index of the Study Area

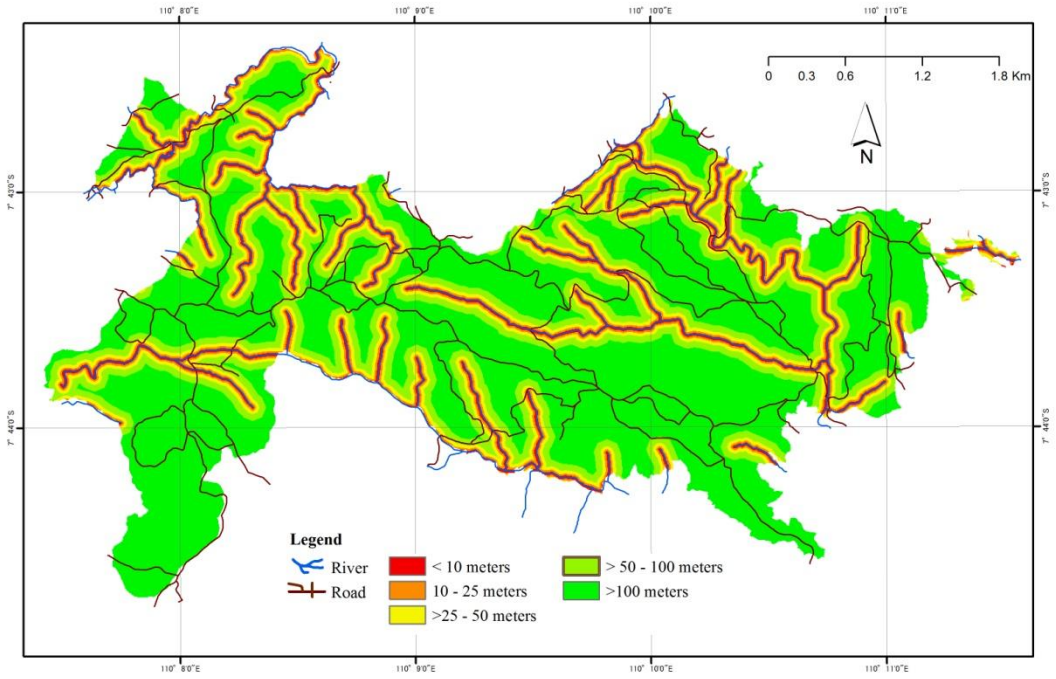

Figure 4.9 Distance to River of the Study Area

A pixel draining into many adjacent cells has also lower tendency to gather

water than a pixel draining into few adjacent cells. TWI is defined as a ratio between the slope and the catchment area:

$$TWI = \ln (A_f \, . \, \tan\beta) \qquad (4.2)$$

where A_f is the specific catchment area draining through the point, β is the slope angle, and ln was used to re-scale the value in order to produce a normalized histogram. The higher the index of TWI indicates the higher soil water content.

The distance to the river was related to erosion, which may affect landslides occurrences. It assumes that the shorter part of the river will produce more landslides. Figure 4.9 shows that the distance to the river was classified into 5 classes as follows <10 meters, 10-25 meters, >25-50 meters, > 50-100 meters, and >100 meters.

4.3.1.3 LANDUSE

Landuse is important as controlling factor responsible for landslides in the study area. The development of the settlement area by excavating the slope without measures may increase instability of the slope. Devegetation may also cause landslides because vegetation prevents erosion through the canopy and natural anchorage provided by the roots. Landuse in Purwosari can be classified as bushes, people forest, settlement, rainfed paddy field, and dry cultivated land (Figure 4.10).

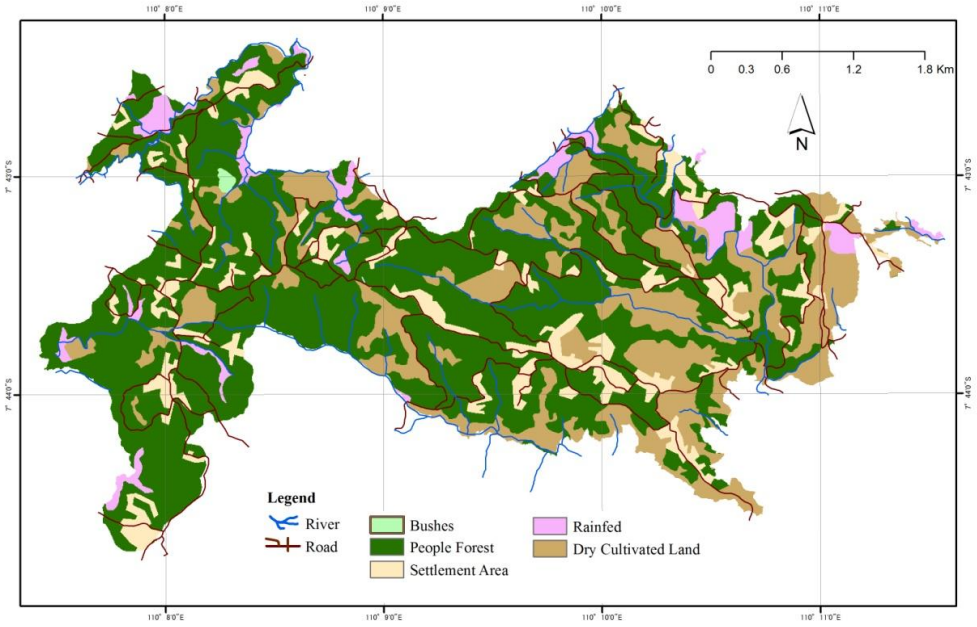

Figure 4.10 Landuse of the Study Area

4.3.1.4 DISTANCE TO ROAD

Distance to roads was included as a measure for landslide controlling factor. Excavating slope for road construction and frequent vibration generated by vehicles may cause slope failure. It may also act as a corridor of water flow during rain. Road in the study area is usually also related to housing development. House development surrounding the road is also usually built by excavating the road. The distance of excavation of a single building from the road is approximately 25 meters on average. This area may be the highest frequency of landslide events. Thus, the buffer distance of 25 meters was used to classify distance to road factor. It was classified into 5 categories such as <25 meters, 25-50 meters, >50-100 meters, >100-200 meters, and >200 meters (Figure 4.11).

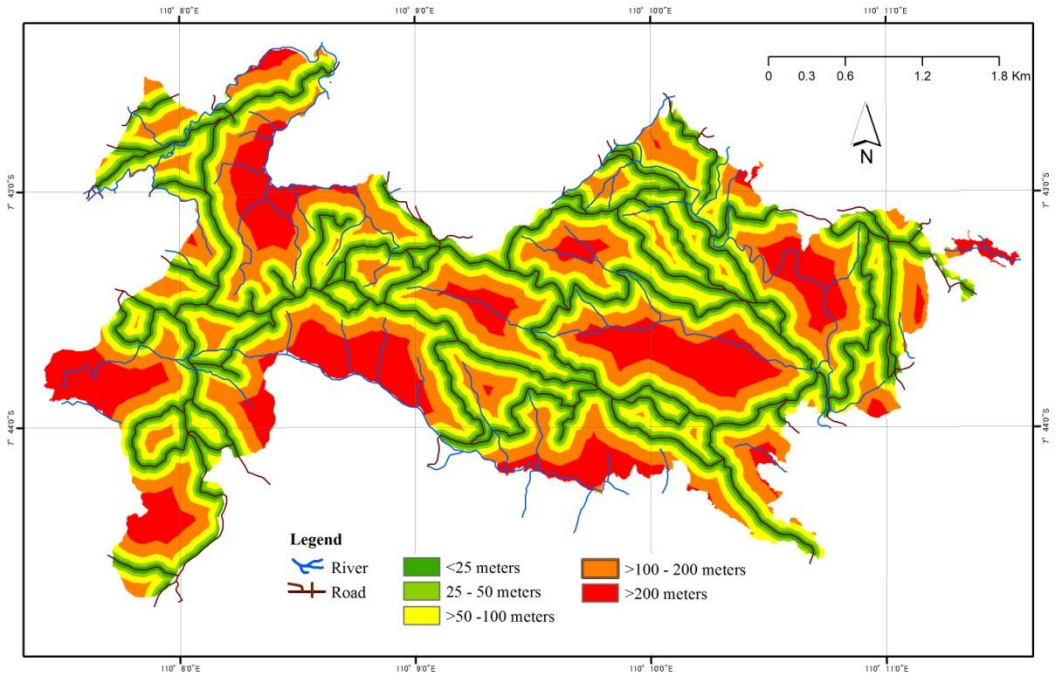

Figure 4.11 Distance to road of the Study Area

Landslide controlling factor layers and landslide inventory layer were employed to produce a landslide susceptibility map in GIS environment. Landslide inventory layer was obtained from participatory landslide inventory mapping (Chapter 3). In addition, field surveys were also carried out for verification of topographic maps and a collection of additional data.

4.3.2 LANDSLIDE SUSCEPTIBILITY METHODS

4.3.2.1 BIVARIATE - WEIGHT OF EVIDENCE

WoE compares the existing landslide distribution and various landslide controlling factors separately. It is applied to evaluate the relationship of each predictable variable controlling factor of landslide towards landslide events by using prior (unconditional) probability and posterior (conditional) probability. The prior probability is the probability of an event derived from the same events in the past for a given period of time. It is similar in geomorphological concept, widely applied for landslide analysis, "the past is the key to the future". The spatial probability of landslide in the future can be estimated based on the past landslide events. This can be evaluated by calculating the ratio of landslide events (number or area) to the total area of the study area.

New evidence or other information can be added to revise the prior probability. For example, if a landslide controlling factor is added to estimate the probability, the probability of occurrence of landslides based on this factor may change (Figure 4.12). The change probability due to additional information is called posterior probability. The conditional probability of the presence of landslide given the presence of the factor can be written as:

$$W_{ji}{}^{+} = Ln\left(\frac{P\{F_{ji}|L\}}{P\{F_{ji}|\bar{L}\}}\right) = \frac{\left(\frac{P\{F_{ji} \cap L\}}{P\{L\}}\right)}{\left(\frac{P\{F_{ji} \cap \bar{L}\}}{P\{\bar{L}\}}\right)} \tag{4.3}$$

Whereas, the conditional probability of the presence of landslide given the absence of the factor can be written as:

$$W_{ji}{}^{-} = Ln\left(\frac{P\{\bar{F}_{ji}|L\}}{P\{\bar{F}_{ji}|\bar{L}\}}\right) = \frac{\left(\frac{P\{\bar{F}_{ji} \cap L\}}{P\{L\}}\right)}{\left(\frac{P\{\bar{F}_{ji} \cap \bar{L}\}}{P\{\bar{L}\}}\right)} \tag{4.4}$$

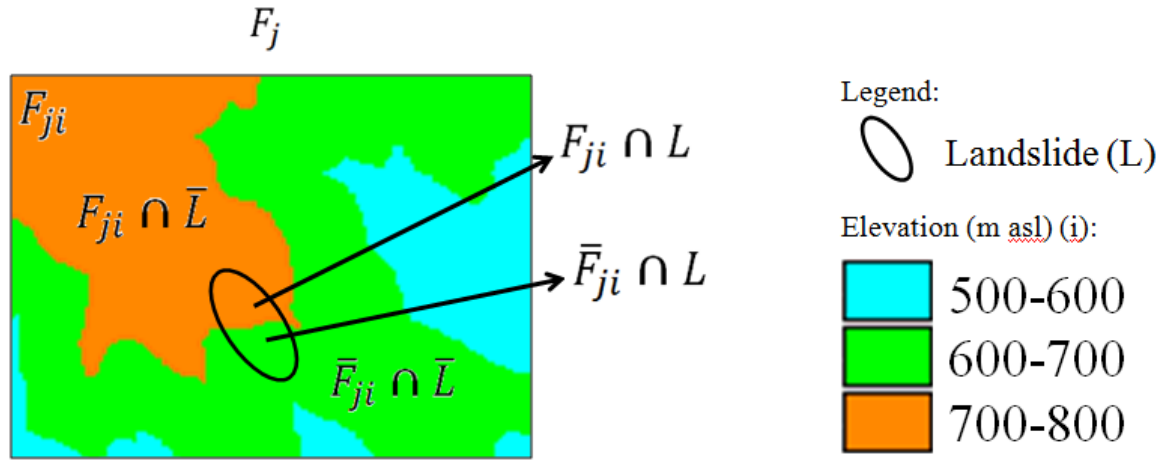

Figure 4.12 Ilustration of Weight of Evidence Method

where P : probabilitas, F_{ji} : presence of factor j class i, $\overline{F_{ji}}$: absence of factor j class i, $\bar{L}$: absence of landslide, L : presence of landslide, W_{ji}^{+} : the likelihood ratio expressing the ratio that in case of present factor F_{ji} a landslide L occur or does not occur, W_{ji}^{-} : the likelihood ratio expressing the ratio that in case of absence factor F_{ji} a landslide L occur or does not occur (Bonham-Carter, 2002). Positive correlation is shown by W_{ji}^{+} = positive and W_{ji}^{-} = negative, conversely negative correlation is shown by W_{ji}^{+} = negative and W_{ji}^{-} = positive. Landslides are not affected by the presence or absence of the factor if $W_{ji}^{+} = W_{ji}^{-} = 0$. It shows uncorrelation between landslides and controlling factor. The measure of correlation can also be measured by weight contrast as follows:

$$W_{contrast\,ji} = W_{ji}^{+} - W_{ji}^{-} \tag{4.5}$$

where weight contrast is positive showing positive spatial association and weight contrast is negative showing negative association. The total value of pixel k in weight of evidence map is determined by the total of weight contrast of landslide controlling factor j in each class i as follows:

$$P_{total}^{(k)} = \sum_{j=1}^{m} Wc_{ji(k)} \tag{4.6}$$

In GIS environment software (ILWIS), the analysis can be written in a formula base on equation as follows:

$$W_{ji}{}^{+} = Ln \frac{\frac{Npix_1}{Npix_1 + Npix_2}}{\frac{Npix_3}{Npix_3 + Npix_4}} \quad (4.7)$$

$$W_{ji}{}^{-} = Ln \frac{\frac{Npix_2}{Npix_1 + Npix_2}}{\frac{Npix_4}{Npix_3 + Npix_4}} \quad (4.8)$$

$Npix_1$ = nlsclass (4.9)

$Npix_1$ = nslide - nlsclass (4.10)

$Npix_1$ = nclass - nlsclass (4.11)

$Npix_1$ = nmap – nslide – nclass + nlsclass (4.12)

where nslide is the number of pixels with landslide in the map, nlsclass is the number of pixels with landslide in the class, nclass is the number of pixels in the class, and nmap is the total number of pixels in the map.

Table 4.2 Computed Weights for Classes of Controlling Factors Layers based on Landslide Inventory

Factor	Class	Class pixels	Landslide pixels	% Class	% Landslide	W^+	W^-	W^+-W^-
Elevation	200-300	14209	90	2.6	2.4	-0.05	0.00	-0.05
	300-400	87518	627	15.7	16.9	0.07	-0.01	0.09
	400-500	114821	890	20.6	24.0	0.15	-0.04	0.20
	500-600	80041	919	14.4	24.8	0.55	-0.13	0.68
	600-700	84530	227	15.2	6.1	-0.91	0.10	-1.01
	700-800	174536	940	31.3	25.3	-0.21	0.08	-0.30
	>800	1407	18	0.3	0.5	0.66	0.00	0.66
Slope	0-8	73453	483	13.2	13.0	-0.01	0.00	-0.02
	>8-15	98685	527	17.7	14.2	-0.22	0.04	-0.26
	>15-25	169556	1536	30.4	41.4	0.31	-0.17	0.48
	>25-45	208652	1145	37.5	30.9	-0.20	0.10	-0.30
	>45	6716	20	1.2	0.5	-0.81	0.01	-0.82
Aspect	North	34361	209	6.2	5.6	-0.09	0.01	-0.10
	North East	95117	522	17.1	14.1	-0.20	0.04	-0.23
	East	73257	447	13.2	12.0	-0.09	0.01	-0.10
	South East	81865	841	14.7	22.7	0.44	-0.10	0.54

	South	78667	620	14.1	16.7	0.17	-0.03	0.20
	South West	88579	524	15.9	14.1	-0.12	0.02	-0.14
	West	42632	315	7.7	8.5	0.10	-0.01	0.11
	Flat	62584	233	11.2	6.3	-0.58	0.05	-0.64
Plan	-50 to -2.7	55104	157	9.9	4.2	-0.85	0.06	-0.91
curvature	>-2.7 to -0.3	174196	1061	31.3	28.6	-0.09	0.04	-0.13
	>-0.3 to 0.8	137827	1051	24.7	28.3	0.14	-0.05	0.19
	>0.8 to 2.5	116071	928	20.8	25.0	0.18	-0.05	0.24
	> 2.5	73864	514	13.3	13.9	0.04	-0.01	0.05
Prof	< -2.7	6601	5	1.2	0.1	-2.18	0.01	-2.19
curvature	-2.7 to -0.3	122779	592	22.0	16.0	-0.33	0.08	-0.40
	-0.3 to 0.8	375644	2718	67.4	73.2	0.08	-0.20	0.28
	0.8 to 2.5	47110	377	8.5	10.2	0.18	-0.02	0.20
	> 2.5	4928	19	0.9	0.5	-0.55	0.00	-0.55
SPI	0-3	70561	476	12.7	12.8	0.01	0.00	0.01
	3-12	151785	1171	27.2	31.6	0.15	-0.06	0.21
	12-50	240593	1658	43.2	44.7	0.03	-0.03	0.06
	50-400	86679	350	15.6	9.4	-0.50	0.07	-0.57
	400-5000	7426	56	1.3	1.5	0.12	0.00	0.13
	5000-7751	18	0	0.0	0.0	2.11	0.00	2.11
TWI	0-2	171	1	0.0	0.0	-0.13	0.00	-0.13
	2-4	131925	905	23.7	24.4	0.03	-0.01	0.04
	4-6	318209	2302	57.1	62.0	0.08	-0.12	0.21
	6-8	83502	403	15.0	10.9	-0.32	0.05	-0.37
	8-10	19158	90	3.4	2.4	-0.35	0.01	-0.36
	10-12	3817	10	0.7	0.3	-0.94	0.00	-0.94
	12-17	280	0	0.1	0.0	-0.63	0.00	-0.63
Distance to	< 10 meter	30118	14	5.4	0.4	-2.67	0.05	-2.72
river	> 10 - 25 meter	37268	122	6.7	3.3	-0.71	0.04	-0.75
	> 25 - 50 meter	64041	324	11.5	8.7	-0.28	0.03	-0.31
	> 50 - 100 meter	115451	1005	20.7	27.1	0.27	-0.08	0.35
	> 100 meter	310184	2246	55.7	60.5	0.08	-0.12	0.20
Distance to	< 25 meter	98755	1330	17.7	35.8	0.71	-0.25	0.96
road	> 25 - 50 meter	86678	1042	15.6	28.1	0.60	-0.16	0.76
	> 50 - 100 meter	132936	682	23.9	18.4	-0.26	0.07	-0.33
	> 100 - 200 meter	139505	456	25.0	12.3	-0.72	0.16	-0.87

	> 200 meter	99188	201	17.8	5.4	-1.19	0.14	-1.34
Landuse	Bushes	933	0	0.2	0.0	-1.84	0.00	-1.84
	People forest	337305	1851	60.6	49.9	-0.20	0.25	-0.44
	Settlement	59805	1178	10.7	31.7	1.09	-0.27	1.36
	Rainfed paddy field	24510	14	4.4	0.4	-2.47	0.04	-2.51
	Dry cultivated land	132925	668	23.9	18.0	-0.29	0.08	-0.36

The result of computed weight, as shown in Table 4.2, indicates the importance of each class factor. If W_{ji}^{+} = positive and W_{ji}^{-} = negative, the factor is favorable for the occurrence of landslides, and if W_{ji}^{+} = negative and W_{ji}^{-} = positive, it is not favorable. If W_{ji}^{+} = W_{ji}^{-} = 0, the factor is not correlated with landslide. Elevation 200-300, 300-400, slope 0-8, SPI 0-3, and TWI 0.04 are examples that this factor classes is not very good for predicting landslides in the study area. The presence of profile curvature <-2.7, distance to river <10 m and distance to road >200 m is a clear indicator for the absence of landslides, as this factor had the highest negative weight -2.18, -2.67, and -1.19 respectively. Contrary, SPI 5000-7751, distance to road <25m, and settlement is a good indicator for the presence landslides. Distance to road, distance to river, curvature and middle to high class elevation are more pronounced weights than the other factors due to its higher positive and negative weights.

4.3.2.2 MULTIVARIATE – LOGISTIC REGRESSION

Logistic regression (LR) is a multivariate regression forming relation between the existing landslide distribution as a dependent variable and various landslide controlling factors as several independent variables. The variables can be either continuous or discrete, or any combination of both types, and they do not necessarily have normal distributions. The algorithm of logistic regression, estimating the probability of a certain event occurring, applies maximum likelihood estimation after transforming the dependent variable into a logit variable (Atkinson and Massari,

1998; Dai and Lee, 2002). Thus, the presence of landslide was input as 1 and the absence of landslide was input as 0.

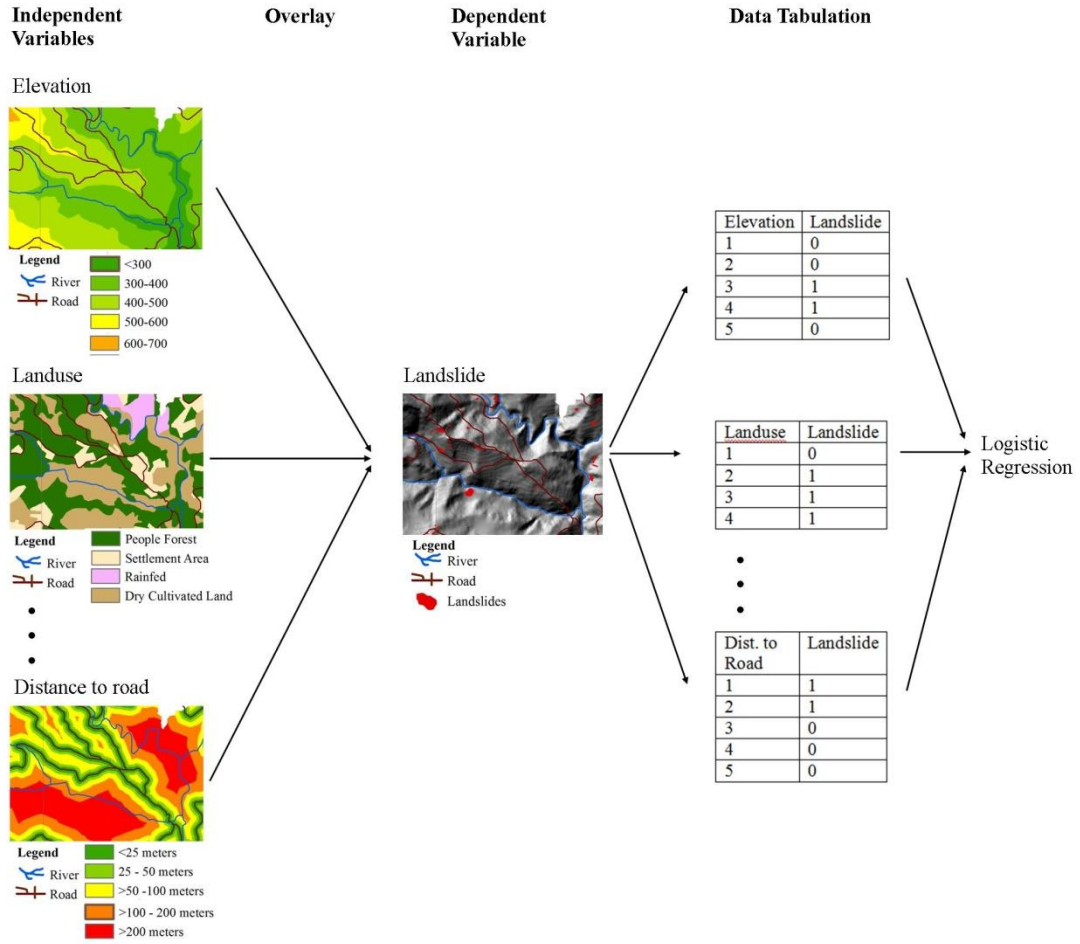

Figure 4.13 Illustration of Logistic Regression Method

Multivariate-logistic regression method compared the existing landslide distribution with various controlling factors of landslide simultaneously (Figure 4.13). The relationship of controlling factors of landslide with the existing landslides is evaluated by logistic regression equation. The logistic regression analysis can be written as follows:

$$f(z) = \pi(S = 1 | X_1, X_2, ...X_n) = \frac{1}{1 + e^{-(\beta_0 + \sum_{i=1}^{n} (\beta_i X_i)}} \quad (4.13)$$

where $\pi(S=1|X_1,X_2,...X_n)$ is a pixel affected by slope failure, which is given the presence of independent variable from X_1 to X_n, β_0 is the constant of the equation, and β_1, β_2,… β_n are the coefficient of variables $X_1,X_2...X_n$. β_0,… β_n are the unknown

coefficients which have to be estimated based on the data of independent variables of landslides by using maximum likelihood. The result represents the probability that an event will occur divided by the probability that it fails to do so, called as the odds ratio. Positive coefficient means that the event is more likely to occur and negative coefficient means that the odds of the event occurring decreases.

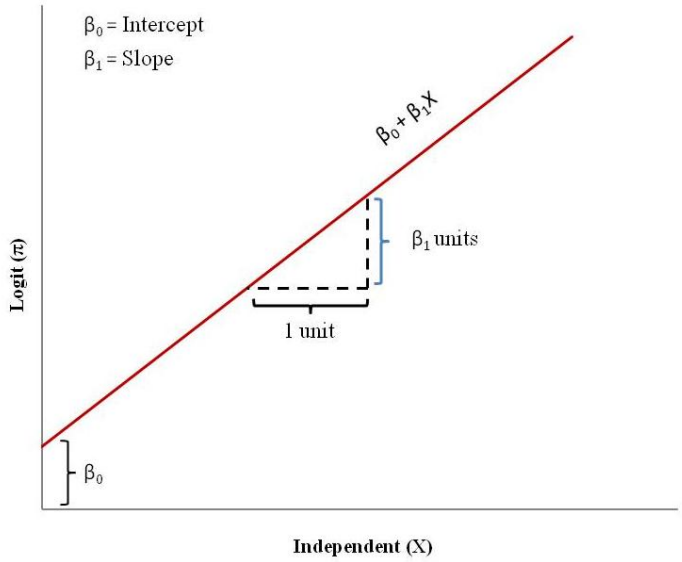

Figure 4.14 Transformation of an Exponential Curve by using the Logistic Function

Equation 4.13., as an exponential function representing non linear s curve relationship between the predictor and outcome, can be transformed into a simple linear relationship by using the logistic function (Figure 4.14). Because the logic function transforms probability to the log scale, the linearity assumption between y and x is also on the log scale. It is usually referred as the linearity of the logic assumption in the logistic regression. The natural logarithm of the odds (logit) is linearly related to the independent variables as:

$$\log it(\pi) = \left(\frac{\pi}{1-\pi}\right) = \beta_0 + \sum_{i=1}^{n}(\beta_i X_i)$$

$$= \beta_0 + \beta X \qquad (4.14)$$

The intercept, β_0, is represented by the distance from the X-axis to the point where the red line crosses the Y-axis. The slope is represented by blue distance, indicating the change in the height of the red line for each one unit change in the value of X. For the landslide susceptibility model, the slope represents the change in the logit π, meaning the change in the logit of the probability of being low or high

susceptibility for each one unit change of landslide controlling factors. Thus, determining the weight of each controlling factor class is important in landslide susceptibility zoning.

Without a prior evaluation of the importance of each controlling factor to the landslides, the weighting procedure was evaluated by a priori knowledge of investigator. For example, the steeper slopes, the higher value of weight will be given to the steeper slope class. It is simple but may lead a misleading coefficient result.

Sampling scenario is one issue in logistic regression analysis. The consideration is usually based on the number of landslide occurrences. Many studies on landslide susceptibility (Ohlmacher and Davis, 2003; Ayalew and Yamagishi, 2005; Domínguez-Cuesta *et al*, 2007) considered that landslide is a rare event because of fewer landslide presence than their absence. They applied unequal proportion of samples, e.g. Van Den Eeckhaut *et al*. (2006) who applied 1 to 5 times more absences of landslides sampling. But, some researches, e.g. Süzen and Doyuran (2004) Nefeslioglu *et al*. (2008) and Bai (2010) applied equal samples on their study.

The author has applied equal sample to estimate the regression coefficients for each independents variable to avoid the effect of unequal proportion. Logistic regression analysis was carried on by SPSS software resulting coefficients of the independent variables and intercept (Table 4.3). The independent variable which is close to 0 indicates a little impact on the occurrences of landslides.

Table 4.3 The Regression Coefficients obtained for the Ten Independent Variables

Independent variables	Coefficient
Elevation	-0.726
Slope	-0.532
Aspect	0.250
Plan Curvature	0.057
Prof Curvature	0.384
SPI (Stream Power Index)	0.539
TWI Topographic Wetness Index)	0.397
Distance to river	1.246
Landuse	0.073
Distance to road	-0.873
Intercept	-2.231

Logistic regression provides information about the quality of datasets and how

the model fits the dataset. The statistical parameters resulted on the LR is written as total number of samples, -2ln L (L=likelihood), model chi-square, Cox & Snell R Square, and Nagelkerke R Square (Table 4.4). It shows that the goodness of fit in the equation can be accepted. The value of Cox and snell R^2 and Nagelkerle R^2 indicates that the independent variables can explain the dependent variables.

Table 4.4 The overall Statistic of the Logistic Regression Model

Hosmer and Lemeshow test			-2 Log likelihood	Cox and Snell R^2	Nagelkerle R^2
X^2	df	Sig.			
40.18	8.00	0.000	3189.12	0.42	0.56

The landslide susceptibility map was computed using the logistic coefficients in ILWIS open source software by inputting controlling factor layer maps. The problem may occur if the independent variables from X_1 to X_n representing the value of pixel of class layer were nominal data. This value very much affects the result of susceptibility map.

4.3.2.3 SOFT COMPUTING – ARTIFICIAL NEURAL NETWORK

Soft computing mimic the human mind as a role model to solve problems employing modes of reasoning that is approximate rather than exact (Zadeh, 1994). Artificial neural network, applied as generic non-linear function approximators that were developed by (McCulloch and Pitts, 1943) and extensively used for pattern recognition and classification, is a soft computing technique to build a model which can generalize and predict outputs from inputs that it has not previously seen. The terminology of artificial neural network is used to describe a computational network that attempts to simulate, the networks of nerve cell (neurons) of the biological central nervous system. It consists of a connected network of processing units that are modeled on the most basic properties of the neurons in the human brain. ANN is independent from the statistical distribution and does not need specific statistical variables (Lee *et al*., 2004)

The multi-layer perceptron using a back-propagation learning algorithm is one of neural network models. It contains an input layer, output layer and hidden layers (Figure 4.14). In landslide susceptibility analysis, landslide controlling factors are considered as input layers. ANN can then be applied in the prediction of areas that

landslide is likely to occur in the future. The connection of ANN is simulated by weight connecting each layer which contains nodes or neurons (Figure 4.15). In the network, each layer has a weight matrix *w* and an output vector O_k . Each element of the input vector O_i is connected to each neuron input through the weight matrix *w*. The *ith* neuron has a summation that gathers its weighted inputs to form its own output. Finally, the neuron layer outputs form a column vector O_k .

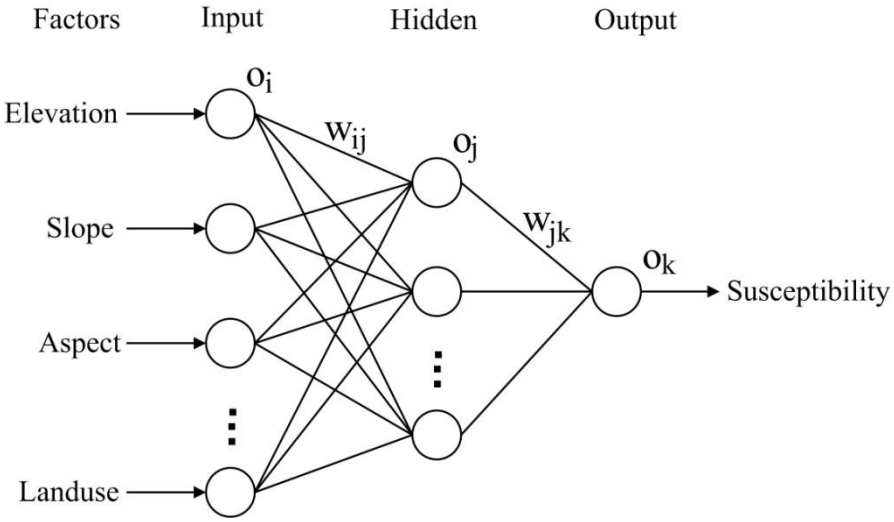

Figure 4.15 Architecture of neural network for landslide susceptibility analysis

This architectural ANN model is defined as multi-layer perceptron (MLP) using a back-propagation (BP) learning algorithm. The hidden layers nodes are important for learning and making use of interaction effects to solve complex regression and classification problems. Each node is a simple processing that responds to the weighted input according to:

$$net_j = \sum_1 w_{ij} o_i \tag{4.15}$$

where w_{ij} represents the weight between node *i* and node *j* and O_i is the output from node *i*. The output from given node *j* is then computed from :

$$o_j = f(net_j) \tag{4.16}$$

There are several function *f* such as threshold/heaviside, piecewise-linear, and sigmoid function used to the weighted sum of inputs before the signal passes to the

next layer. The value of o_j is the activation function f evaluated at the sum produced within node j, net_j. Sigmoidal function is applied to the weighted sum of inputs by using its derivative as follows:

$$f'(net_j) = f(net_j)(1 - f(net_j)) \tag{4.17}$$

After a forward pass is finished, the result of the output nodes is compared with their expected result. The difference between the output nodes and the expected result is called error. Then this error is propagated backward through the neural network and the error is minimized by changing weight via the delta rule as follows:

$$w_{ij}(n+1) = \eta(\delta_j o_i) + \alpha \Delta w_{ij} \tag{4.18}$$

where η is the learning rate parameter, δ_j is an index of the rate of change of the error and α is the momentum parameter. The forward and backward passes continue or repeated iteratively until the error of the network reaches an acceptable value.

Table 4.5 Best obtained Parameters after Multiple Trials ANN

Parameters in the model	Value
Output layer node	1
hidden layer	1
hidden layer node	20
learning rate	0.1
Momentum factor	0.5
sigmoid function constant	1
RMS	0.1
number of iteration	5000
Training RMS	0.1118
Testing RMS	0.0913

The ANN model was computed using Idrisi software. After multiple trials with different parameters, the best an ANN model was produced by using the parameters in Table 4.5. Determining these parameters can limit the development, performance and accuracy of the model (Baheer and Hajmeer, 2000). Number of hidden layers

affects the complexity of the model, period of training and the likelihood of overfitting. Learning rate affects the stability of the model, prediction of the weight (fluctuate widely) and may also decelerate the rate of training and learning. Momentum factor can affect risk of exceed the solution while training and risk of entrapment in a local minimum in the error surface. High number umber of iteration may cause overfitting.

4.4 COMPARISON OF WOE, LR AND ANN IN LANDSLIDE SUSCEPTIBILITY

4.4.1 ACCURACY EVALUATION

The best validation of landslide susceptibility zoning is comparing the landslide susceptibility model with landslide occurrences after the model finished (Neuhauser and Terhorst, 2006). It is sometimes not possible to conduct the analysis using the method due to the lack information about the accurate time of landslide occurrences. It is only possible if there is availability of landslide events in different time. However, landslide performance evaluation must be inserted when landslide model had been finished. Landslide samples (60%) were selected randomly to test the performance of landslide susceptibility maps. There are several performance evaluation in landslide susceptibility analysis, such as ROC (Receiver Operating Characteristic) curve, success rate curve and prediction rate curve.

ROC curve shows the global accuracy statistic for the model. It is usually used to measure the performance of a predictive rule and widely applied in the multivariate statistic model. The curve is obtained by plotting the sensitivities and false negatives (1-specificity). It is calculated from the analysis of the classification of the statistical unit. ROC curve only describes the statistical model to differentiate presence and absence of landslide, thus it does not consider the spatial accuracy of susceptibility map.

Success rate offers the analysis of spatial accuracy between landslide susceptibility and actual landslides (landslide inventory). It is obtained by overlaying landslide susceptibility and landslide inventory. Then, based on the frequency information from the histogram, the susceptibility value is ordered from high to low values. Joint frequency is calculated to obtain the percentage of predicted landslide and percentage of the study area. The success rate indicates how much percentage of

all landslides occur in the pixels with the highest values in the different combination maps. For example, 80 percent of all landslides are predicted by 40 percent of the pixels with the highest value in the map. Prediction rate is similar with success rate, but the susceptibility map is compared to different landslide inventory used in the model. In the present study, the success rate curve is employed to compare the mapping accuracy among three susceptibility.

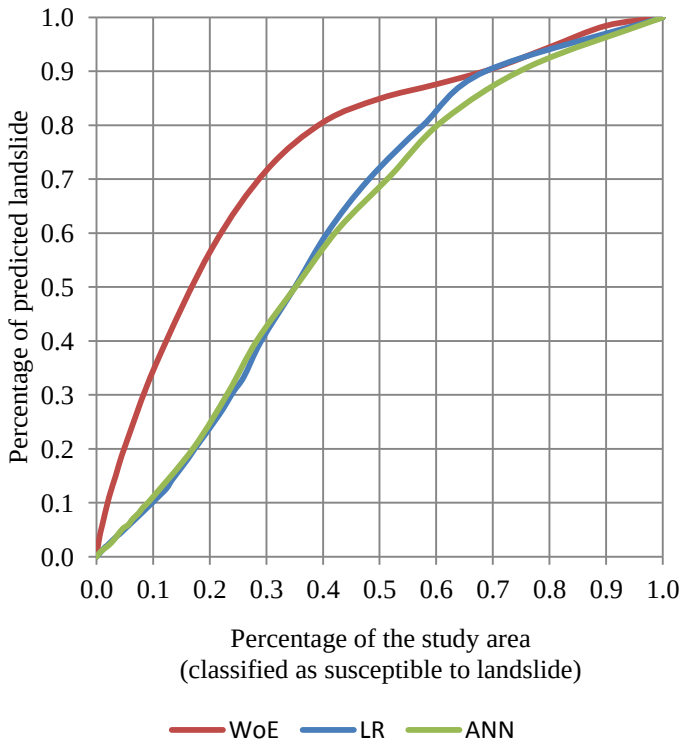

Figure 4.16 Success Rate Curve of WoE, LR, and ANN

AUC (Area Under Curve) of success rate (Figure 4.16) shows that the most realistic data driven model for Purwosari area is WoE with 79 % area (red curve). It means that 20 % or 50% of area classified into high probabilities of future landslide, there is 55% or 85% of independent landslide can be correctly predicted respectively. Whereas, ANN was less realistic with accuracy 71% and Logistic Regression indicated slight improvement in success rate at high susceptibilities. Those accuracies were obtained with the assumption that there are no a priori knowledge considered in the model.

4.4.2 LANDSLIDE SUSCEPTIBILITY MAP PERFORMANCE

The results of data driven methods were calculated probabilities which can be represented as a landslide susceptibility map. It is common that landslide susceptibility maps show the degree of susceptibility by qualitative way by dividing calculated probabilities in some classes. In this research, the calculated probabilities were split as very low, low, medium and high. Low and very low indicate that this classified area is a stable zone. Whereas, high indicates the unstable zone. Medium classification might be classified as grey zone where stable or unstable can not be clearly defined.

There is no strict rule to classify calculated probability into some classes and usually determined based on expert opinion. Several trials based on associated histogram using automated classification methods available in ArcGIS (ESRI, 2009) were applied to find the classification that suits the scale of the calculated probability. Both calculated probabilities obtained from WoE and ANN were split by natural breaks and Logistic Regression was split by geometrical interval. Natural break suit the data which have big difference in the data values and geometrical interval suits for the data which has positive or negative skewness in the data values.

The weight of WoE method has a value ranging from -12.1 to 4.87 with the normal curve distribution. Using natural breaks, the very low, low, medium, and high susceptibility zone has a value ranging from -12.09 to -4.00, -4.00 to 0.00, 0.00 to 1.00, and 1.00 to 4.87 respectively (Figure 4.17). On the susceptibility map, 6.9%, 28.3%, 40.6%, and 24.2% area are shown as very low, low, medium and high susceptibility respectively.

Table 4.6 Validation Matrix of WoE based on the Number of Pixels

		Predicted (model)	
		Stable(-12.09-0.00)	Unstable (1.00 - 4.87)
Landslide inventory	No Slide (0)	374593 (80%)	91068 (20%)
	Slide (1)	955 (35%)	1811 (65%)

Table 4.6 shows that 80% stable and 65% unstable pixels are correctly classified. Whereas, 35% stable and 25% unstable pixels are incorrectly classified. WoE has better capability to classify stable zone (80%) than unstable zone (65%).

Misclassification in the unstable zone also shows small proportion (20%).

The calculated probabilities of logistic regression method were splitted by a geometrical interval because the data value indicated negative skewness. It was classified into 0-0.75, 0.75-0.94, 0.94-0.98, and 0.98-0.99 for the very low, low, medium and high susceptibility zone respectively (Figure 4.18). The very low, low, medium and high susceptibility zone covers 12.8%, 31.9%, 27.8%, and 27.4% area respectively.

Table 4.7 Validation Matrix of LR based on the Number of Pixels

		Predicted (model)	
		Stable (0 - 0.94)	Unstable (0.98-0.99)
Landslide inventory	No Slide (0)	247757 (62%)	151085 (38%)
	Slide (1)	836 (38%)	1361 (62%)

Table 4.7 shows that 62% stable and 62% unstable pixels are correctly classified. Whereas, 38% stable and 38% unstable pixels are incorrectly classified. LR has the same capability to classify stable zone (62%) than unstable zone (62%), even though the accuracy was not so high. Misclassification in the unstable zone also shows the same proportion (38%). It has lower accuracy than WoE. This problem might be affected by the ignorance of inputting the weight of class variables during susceptibility calculation and mapping.

Table 4.8 Validation Matrix of ANN based on the Number of Pixels

		Predicted (model)	
		Stable (0-0.44)	Unstable (0.57-0.99)
Landslide inventory	No Slide (0)	292260 (76%)	91179 (24%)
	Slide (1)	1281 (64%)	719 (36%)

Similar to WoE method which has a normal curve histogram and some big difference in data value, the calculated probabilities of ANN method were split by natural breaks. The very low, low, medium, and the high susceptibility zone has a value ranging from 0 to 0.31, 0.31 to 0.44, 0.44 to 0.57, and 0.57 to 0.99 respectively (Figure 4.19). On the susceptibility map, 17.9%, 34.8%, 30.8%, and 16.5% area are shown as very low, low, medium and high susceptibility respectively.

Table 4.8 shows that 76% stable and 36% unstable pixels are correctly

classified. Whereas, 64% stable and 24% unstable pixels are incorrectly classified. Similar to WoE, ANN has better capability to classify stable zone (76%) than unstable zone (36%), even though overall the accuracy was the lowest. Misclassification in the unstable zone also shows the same proportion (24%). It has better accuracy than LR but misclassification in stable zone is very high. This problem might be affected by the difficulties in preparing the parameters in ANN model. Learning rate and iteration may cause overfitting which sometimes gives better result of RMS but not in the final susceptibility map.

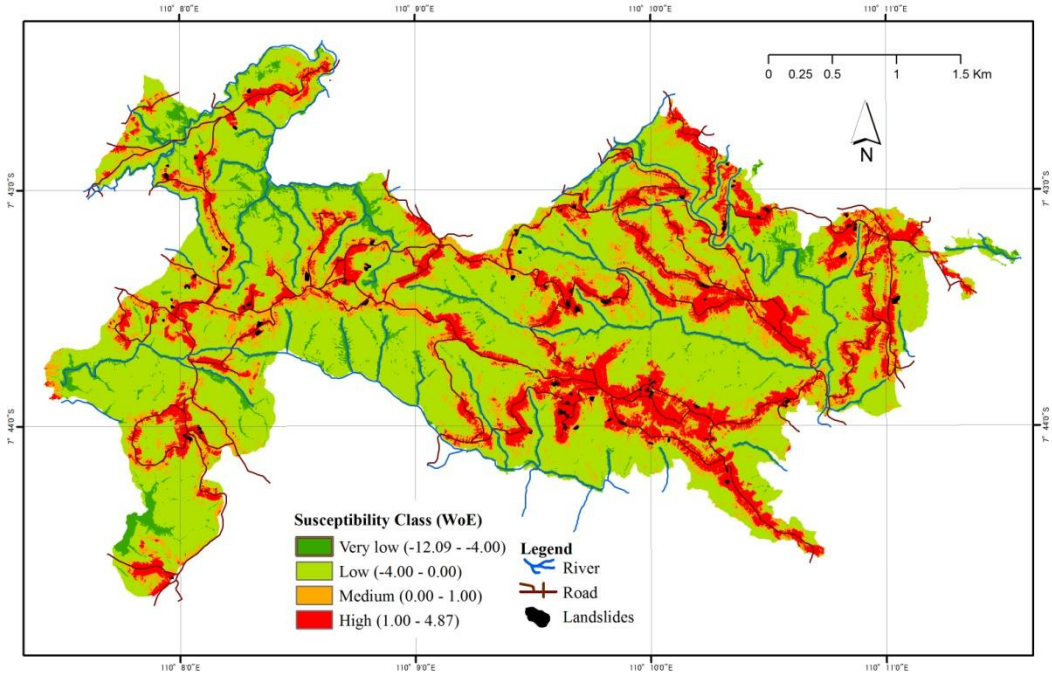

Figure 4.17 Landslide Susceptibility Map based on WoE Method

ANN has the largest very low susceptibility area, but some exaggeration may occur because ANN classify all of the area of adjacent to the valley as the very low susceptibility area. Logistic regression landslide susceptibility map can differentiate susceptibility based on the geomorphological zone, i.e. the eastern zone and the western zone. The eastern zone is more susceptible than the western zone because it has steeper relief than the western zone. It is dominated by denudation process in which weathering, erosion, and mass wasting occurred very intensive. Landslide events in the eastern zone were also larger than in the western zone.

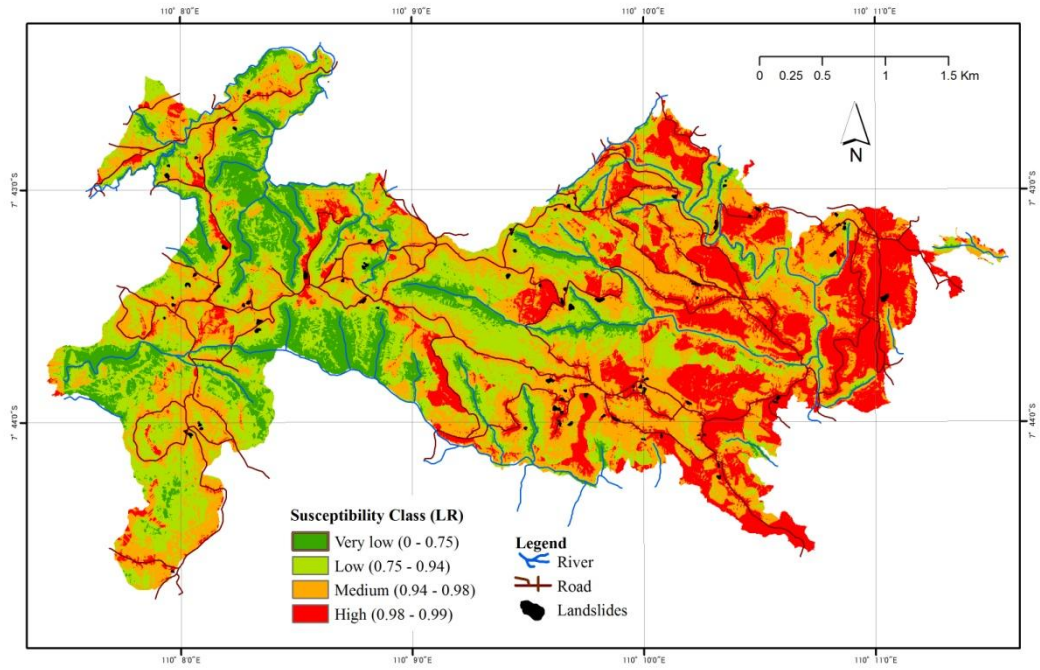

Figure 4.18 Landslide Susceptibility Map based on LR Method

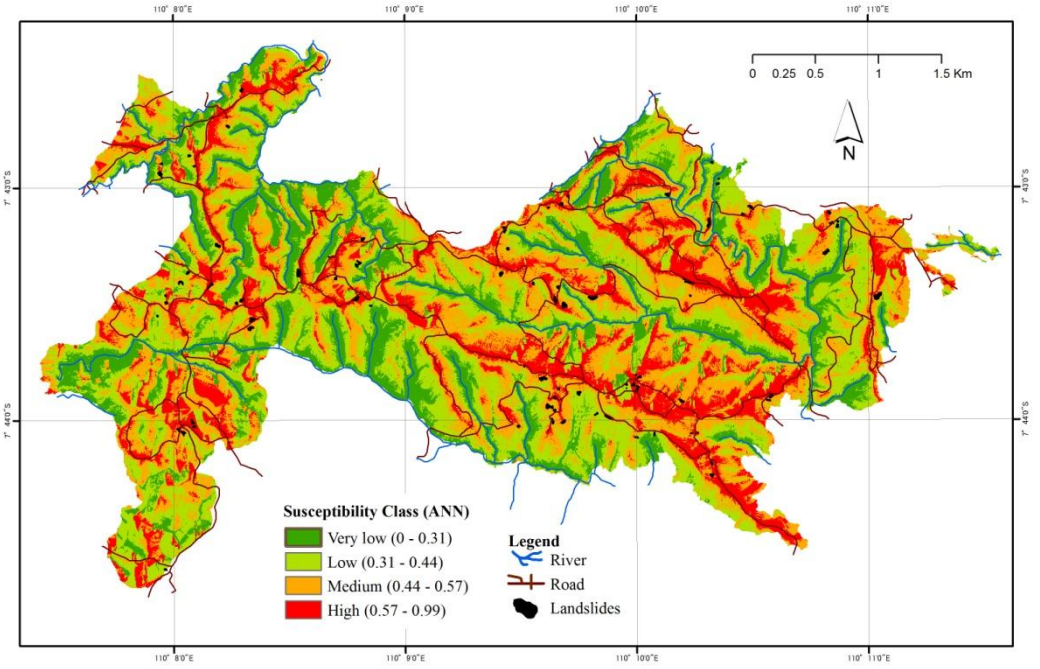

Figure 4.19 Landslide Susceptibility Map based on ANN Method

For all susceptibility maps, it generally shows that the area adjacent to valley falls to the very low susceptibility and area in the ridges and adjacent to road fall to

the high susceptibility. It showed that landuse, especially settlement area and road play very important role as landslide controlling factors.

Based on the results, there are pros-and-cons of each method in predicting landslide susceptibility zones. The WoE method has advantages as follows: 1) WoE indicates the linear relationship between landslides and its controlling factor individually; 2) sampling is not necessary; 3) WoE provides a technique to detect intercorrelation of landslide controlling factors. The disadvantages are 1) weight value may underestimates or overestimates if landslides are very small and not evenly distributed 2) the weight cannot be compared for different area.

Some advantages of logistic regression are: 1) LR has ability to explicitly identify the relationship between landslides and its controlling factors simultaneously; 2) value represents meaningful probability and can be compared for different area; 3) LR also provides a technique to detect a linear relationship of landslide controlling factors. Whereas, the disadvantages are 1) LR requires formal statistical training; 2) undersampled may significantly impact the result; 3. the final susceptibility map may be over or underestimated.

ANN has advantages as follows: 1) It requires less formal statistical training; 2) ANN can implicitly identify the complex nonlinear relationship between landslides and its controlling factors. However, the disadvantages are 1) ANN has limited ability to explicitly identify possible causal relationship; 2) ANN requires greater computational resources; 3) ANN is prone to overfitting.

4.5 Increasing Susceptibility Performance by Combining WoE and LR

Based on the comparison of the three methods, the author tried to combine WoE and logistic regression method. The author proposed to exchange the value of the independent variables from X_1 to X_n representing the value of pixel of class layer with the $W_{contrast}$ obtained from WoE method. Final map was obtained by calculating equation 4.12 with X_1 to X_n represented by landslide controlling maps with $W_{contrast}$ and $\beta_0,\ldots\ \beta_n$ value represented by the logistic regression coefficient (Table 4.10). This modification gives advantages that the final result can be compared for different area and the problem related to X_1 to X_n values when producing susceptibility map can be solved.

Two tests for conditional independence, i.e. Cramer's V and Multicollinearity diagnostic statistics were also carried out. Cramer's V coefficient (Kendall and Stuart, 1979) ranged between 0 and 1 was used to test the spatial association between parameters. It was derived from a chi-square ($\chi 2$) test using contingency tables in order to identify any interrelationships within the landslide controlling factors that may affect on statistical analysis as follows:

$$V = \sqrt{\frac{\chi^2}{Nmin(R-1, C-1)}} \tag{4.19}$$

where *N* is the sample size, *R* is the number of rows in the contingency table, and *C* is the number of the columns. Cramer's V coefficient is undertaken just on areas with landslides (Bonham-Carter, 1994).

Table 4.9 Cramer's V Values for Comparison of Multi-class Chi-square Contingency Tables

	Elevation	Slope	Aspect	Plan Curv	Prof curv	SPI	TWI	Dist to river	Landuse
Slope	0.26								
Aspect	0.24	0.20							
Plan Curv	0.10	0.13	0.09						
Prof curv	0.08	0.08	0.09	0.29					
SPI	0.25	0.40	0.22	0.30	0.18				
TWI	0.13	0.21	0.15	0.23	0.17	0.38			
Dist to river	0.21	0.10	0.11	0.13	0.21	0.18	0.18		
Landuse	0.19	0.19	0.15	0.06	0.09	0.15	0.16	0.20	
Dist to road	0.26	0.10	0.15	0.10	0.09	0.18	0.17	0.17	0.19

The result of the chi-squares tests in terms of the calculated Cramer's V value for each variable is presented in Table 4.2. The value ranges from 0 to 1 indicating that higher values reflect a stronger association. Cramer's V value >0.5 indicates a high association, 0.3 to 0.5 indicates a moderate association, 0.1 and 0.3 indicates a low association and 0 to 0.1 indicates little if any association. Table 4.2 shows that the association of slope and SPI; SPI and TWI can be categorized as moderate association, meanwhile the rest can be categorized as low to little association.

Multicollinearity diagnostic statistics, i.e. Tolerance and Variation Inflation Factors were calculated to test the multicollinearity among the landslide controlling

factors. Variable with VIF of >2 and Tolerance of <0.4 is considered as highly correlated dependent variables. Table 4.5 shows that slope, SPI, and TWI are highly correlated.

Table 4.10 Multicollinearity diagnosis indexes for independent variables.

Independent variables	Tolerance	VIF
Elevation	0.824	1.214
Slope	0.341	2.936
Aspect	0.963	1.039
Plan Curvature	0.616	1.622
Prof Curvature	0.739	1.353
SPI (Stream Power Index)	0.307	3.254
TWI Topographic Wetness Index)	0.375	2.670
Distance to river	0.811	1.233
Landuse	0.858	1.165
Distance to road	0.743	1.346

Two landslide susceptibility maps by using combination WoE and LR were produced by two scenarios. The first by using all controlling factors (case 1) and the second by excluding SPI and TWI (case 2). There were three controlling factors indicating high correlation, i.e. slope, SPI and TWI. Thus, two of which should be excluded from the analysis. The author excluded SPI and TWI as one of the scenarios because the slope is an important controlling factor to landslides. Besides, both SPI and TWI were mapped as a derivation from the slope.

Table 4.11 The Overall Statistic of the Logistic Regression Model (WoE-LR)

Cases	Hosmer and Lemeshow test			-2 Log likelihood	Cox and Snell R^2	Nagelkerle R^2
	X^2	df	Sig.			
Case 1	90.58	8	0.000	2649.37	0.499	0.665
Case 2	169.29	8	0.000	2761.59	0.484	0.645

Two cases of combined WoE-LR produce two new statistical results, i.e. statistic of datasets quality and regression coefficient. The first provides information about the quality of datasets and how the model fits the dataset. The statistical parameters resulted on the LR is written as total number of samples, -2ln L (L=likelihood), model chi-square, Cox & Snell R Square, and Nagelkerke R Square (Table 4.11). It shows that the goodness of fit in the equation can be accepted because the significance of

X^2 is larger than 0.05. The value of Cox and snell R^2 and Nagelkerle R^2 (>0.2) indicates that the independent variables can explain the dependent variables.

Interpretation of the coefficients should take the coefficients as a power to the natural log (*e*). It represents the probability that an event will occur divided by the probability that an event fails to occur. If the coefficient is positive, the transformed log value will be greater than 1, meaning that the landslide is more likely to occur. If a coefficient is negative, the odds of the landslide event decrease.

Table 4.12 The Regression Coefficients obtained for the Ten Independent Variables.

	Coefficient	
Independent variables	Case 1	Case 2
Elevation	-1.667	-1.526
Slope	-0.049	-0.147
Aspect	0.250	2.535
Plan Curvature	0.555	0.021
Prof Curvature	0.572	0.499
SPI (Stream Power Index)	-1.354	-
TWI Topographic Wetness Index)	-1.748	-
Distance to river	0.969	0.925
Landuse	3.141	3.219
Distance to road	0.982	0.782
Intercept	2.034	1.881

The result of regression coefficients, as shown in Table 4.12, indicates the importance of the independent variables. Elevation, slope, SPI, and TWI are examples that the factors are not favorable for predicting landslide events in the study area. Landuse and aspect are more pronounced coefficients than the other factors due to its higher positive value. Distance to river, distance to road, and curvature is also a good indicator for the presence landslides even though the value is not as high as landuse and aspect. Landuse strongly departs from 0 and can be inferred as a controlling factor that has a higher effect on the landslide events than any other parameter. It is reasonable that landuse change, especially housing development may pose serious slope stability problems in the study area because its construction practices. The development of the housing area by excavating slope without measures may increase instability of the slope. Devegetation may also cause landslides because vegetation prevents erosion through the canopy and natural

anchorage provided by the roots. The study of the effect of landuse change to landslides and the evaluation of devegetation to landslides will be great challenges for the future research.

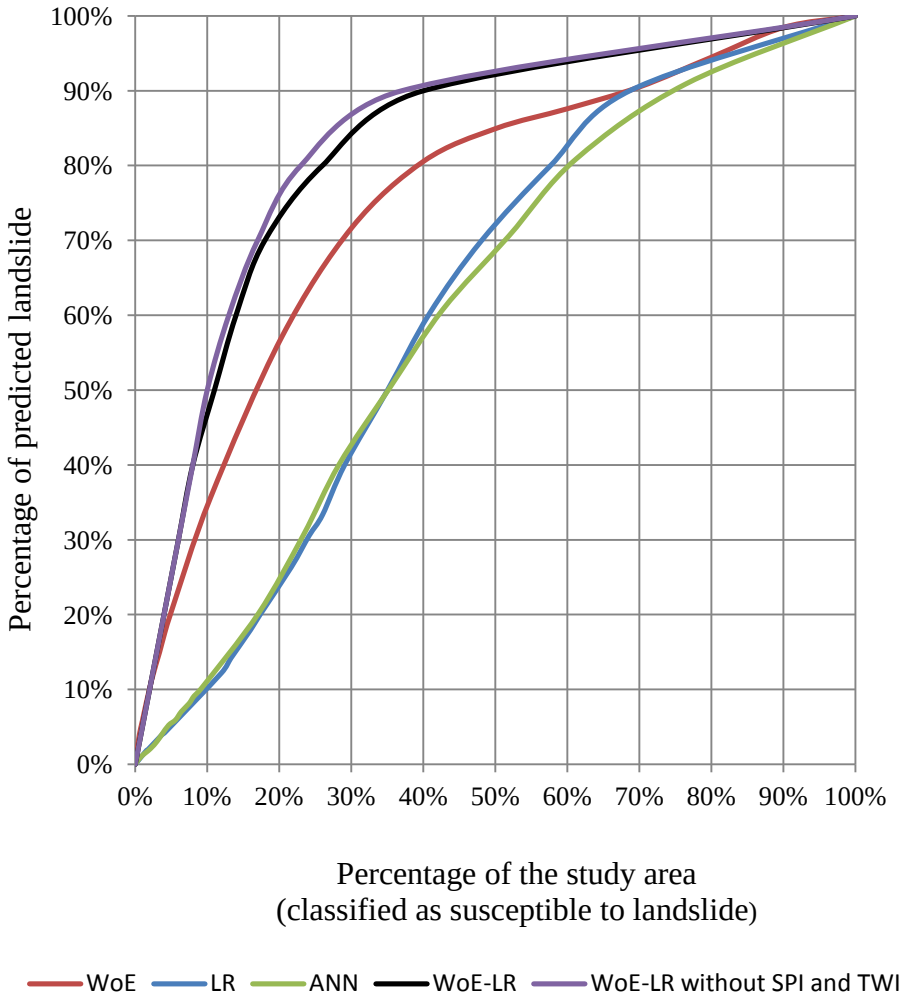

Figure 4.20 Success Rate Curves of Landslide Susceptibility (All Methods)

The result shows that by excluding SPI and TWI, the performance of landslide susceptibility map is a little bit increasing. The AUC of the first scenario is 84% and second scenario is 85% (Figure 4.20). Thus, it can be concluded that including or excluding controlling factors that has highly correlation influence the accuracy of the result. However, it does not very much influence the accuracy of the result of landslide susceptibility map in Purwosari area.

The calculated probabilities of WoE-LR method was also split as very low (0-0.2), low (0.2-0.5), medium (0.5-0.8) and high (0.8-0.99). Low and very low

indicate that this classified area is a stable zone. Whereas, high indicates unstable zone. The medium classification might be classified as grey zone where stable or unstable can not be clearly defined.

According to the above classification, most parts of Purwosari area were found in very low and low susceptible zones. The proportion of the high susceptible zones increased significantly in the settlement area and surrounding road corridor (Figure 4.21). It indicates that excavation of slope for road and building development are the major environmental factor controlling slope failures.

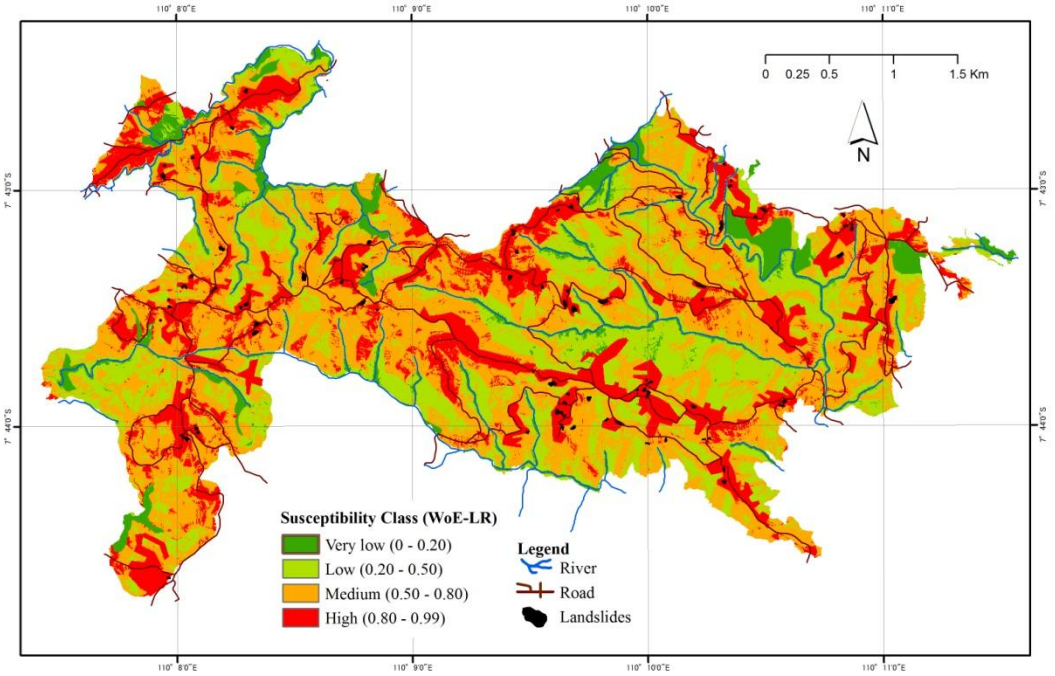

Figure 4.21 Landslide Susceptibility Map based on WoE-LR 1 (with all factors)

The distribution pattern of landslide susceptibility map using WoE-LR with all factors and minus TWI and SPI seems not so different. There were 7.36%, 26.24%, 46.05%, and 20.35% area are shown as very low, low, medium and high susceptibility respectively for the first scenario landslide susceptibility map. And for the second scenario, there were 7.46%, 27.61%, 47.96%, and 16.97% area are shown as very low, low, medium and high susceptibility respectively (Figure 4.22). The difference is on landslide susceptibility classified into high. This may affect the accuracy of mapping, the high susceptibility of scenario 2 covers a smaller area than scenario 1 and both coincide with the same area of the observed landslide area.

Table 4.13 shows that 67% stable and 98% unstable pixels are correctly classified; whereas 2% stable and 33% unstable pixels are incorrectly classified. Table 4.14 shows that 68% stable and 98% unstable pixels are correctly classified; whereas 2% stable and 32% unstable pixels are incorrectly classified.

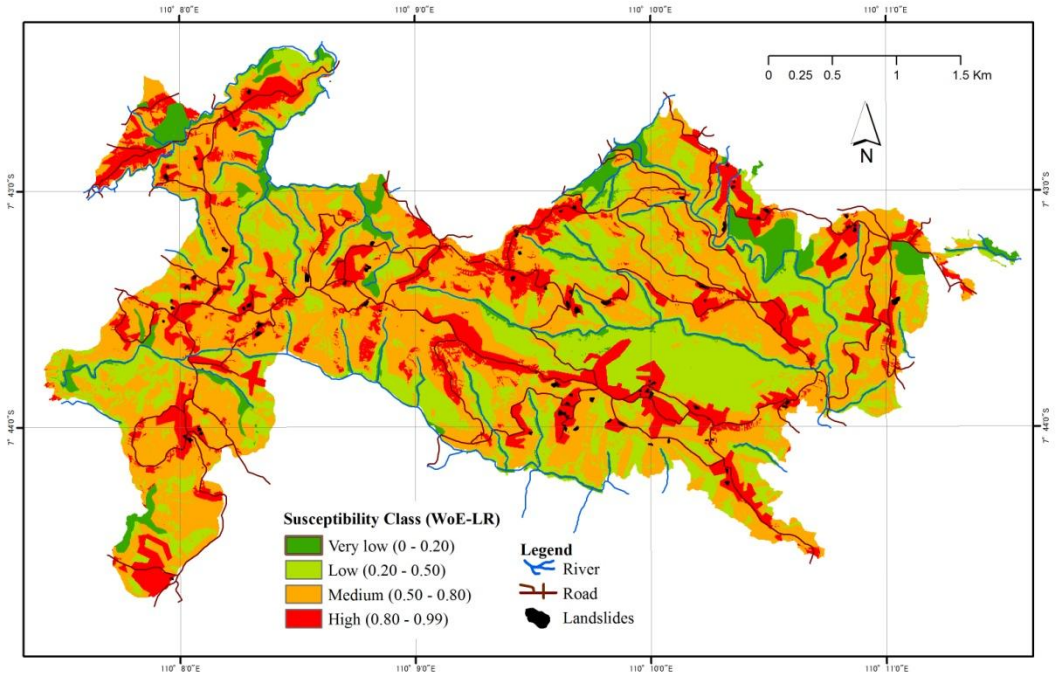

Figure 4.22 Landslide Susceptibility Map based on WoE-LR 2 (without SPI and TWI)

Table 4.13 Validation Matrix of WoE-LR based on the Number of Pixels

		Predicted (model)	
		Stable (0-0.5)	Unstable (0.8-0.99)
Landslide inventory	No Slide (0)	186649 (67%)	27379 (33%)
	Slide (1)	36 (2%)	1583 (98%)

Scenario 2 has better capability to classify stable zone (68%) than scenario 1 and has lower percentage of the misclassified unstable zone. It can be concluded that scenario 2 is better than scenario1 even though the difference is very small (1%). Misclassification in the unstable zone also shows same proportion (24%). It has better accuracy than LR but misclassification in stable zone is very high. It shows that the choice of selecting the landslide controlling factor is important and can give

an effect on the overall accuracy.

Table 4.14 Validation Matrix of WoE-LR without TWI and SPI based on the Number of Pixels

		Predicted (model)	
		Stable (0-0.5)	Unstable (0.8-0.99)
Landslide inventory	No Slide (0)	194814 (68%)	92730 (32%)
	Slide (1)	36 (2%)	1547 (98%)

Table 4.15 shows the summary of the accuracy of the three methods and the improvement method by using combined WoE-LR method. The average of true positive and true positive and true negative is better than the other methods. The average is 82.74%, 82.27%, 70.35%, 56.09%, and 52.07% for WoE-LR (case 2), WoE-LR (case 1), WoE, ANN, and LR. The average of false positive and false negative is also less than the other methods. The average is 17.26%, 17.73%, 29.65%, 43.92%, and 47.93% for WoE-LR (case 2), WoE-LR (case 1), WoE, ANN, and LR respectively.

Table 4.15 Summary of Contingency Table for All Methods in Susceptibility Zoning

Test outcome	Percentage (%)				
	WoE	LR	ANN	WoE-LR 1	WoE-LR 2
True positive	90.94	4.20	76.22	66.81	67.75
True negative	49.76	99.94	35.95	97.73	97.73
False positive	9.06	95.80	23.78	33.19	32.25
False negative	50.24	0.06	64.05	2.27	2.27

In addition, the ratio of landslide events in the grey zone for WoE-LR were also lower than the other methods except LR (Table 4.16). The number of landslides classified in the grey zone for both WoE-LR cases were also lower than the other methods, except LR. Both success rate curve and contingency table indicate that WoE-LR produce better accuracy than the other data driven methods. Since the value of WoE-LR shows the probability, it may be compared to another place with the same method employing both the same controlling factors and different controlling factors. The susceptibility map produced by either comparison of data driven methods or WoE-LR may lead to an agreement how to produce a more realistic

landslide susceptibility map in the future. Besides, landslide inventory should also be updated periodically. The fully documented landslide database will enable scientists to more accurately establish the relationship between landslides and its controlling factor which will be very useful for landslide susceptibility analysis.

Table 4.16 The ratio of Landslide Events in the Grey Zone

Mapping methods	Landslide	Grey zone	Ratio
WoE	1810	141732	0.013
LR	100	72998	0.001
ANN	1654	172346	0.010
WoE-LR 1	1599	255823	0.006
WoE-LR 2	1475	266436	0.006

4.6 CONCLUSIONS

There are different approaches and techniques for evaluating landslide susceptibility and no agreement has been reached both in the procedure and the use of specific controlling factors employed in the lanslide susceptibility mapping. Each approach has its own assumption and the result may differ from place to place. The different result may also be affected by different landslides controlling factors and the completeness of landslide inventory. Landslide susceptibility approaches need to be compared in order to identify the most realistic landslide susceptibility approach applied typically in the tropical region Indonesia by using complete landslide inventory.

The participatory landslide inventory map has been employed to generate landslide susceptibility maps based on data driven models, i.e. WoE, LR, and ANN. The merit and demerit of each data driven method have been evaluated to propose a combination of the methods applied in Purwosari area. The evaluation of controlling factors has also been discussed based on the multicollinearity analysis and Cramer's V values. Considering the accuracy and the precision evaluations, the WoE represents considerably the most realistic prediction capacities when comparing with the logistic regression and ANN. The merits and demerits of the three models were also highlighted.

The advantages and disadvantages of the models have been used to evaluate the models and to propose a technique how to improve the accuracy of the model. The author proposes landslide susceptibility zoning based on the combination of WoE and LR. Those have been produced by two scenarios based on the evaluation of controlling factors. The first by using all controlling factors and the second by excluding SPI and TWI. The result shows that WoE-LR by excluding SPI and TWI can increase the accuracy up to 5%. It also shows that the choice of selecting the landslide controlling factor is important and can give an effect on the overall accuracy.

Landuse can be inferred as a controlling factor that has a higher effect on the landslide events than any other parameter in the study area. It is reasonable that landuse change, especially housing development may pose serious slope stability problems in the study area because its construction practices. The development of the housing area by excavating slope without measures may increase instability of the slope. Devegetation may also cause landslides because vegetation prevents erosion through the canopy and natural anchorage provided by the roots. The study of the effect of landuse change to landslides and the evaluation of devegetation to landslides will be great challenges for the future research.

REFERENCES

Atkinson, P. M. and Massari, R. 1998. Generalised Linear Modelling of Susceptibility to Landsliding in The Central Apennines, Italy. *Computers & Geosciences* vol. 24, no. 4:373-385.

Ayalew, L. and Yamagishi, H. 2005. The application of GIS based logistic regression for landslide susceptibility mapping in Kakudo-Yohiko Mountains Central Japan. *Geomorphology* 65:15-31.

Bai, S-B., Wang, J., Lu, G-N., Zou, P-G., Hou, S-H., Xu, S-N. 2010. GIS-based logistic regression for landslide susceptibility mapping of the Zhongxian segment in the Three Gorges area, China. *Geomorphology*, 115, pp23-31.

Basheer, A., Hajmeer, M., 2000. Artificial neural networks: Fundamentals, computing, design, and application. *Journal of Microbiological Methods* 43, 3-31.

Bonham-Carter, G.F., 1994. *Geographic information systems for geoscientists: modeling with GIS*. Pergamon Press, Canada.

Bonham-Carter, G.F., 2002. *Geographic information systems for geoscientist: modeling with GIS*. In: Merriam, D.F. (Ed.), Computer Methods in the Geosciences. Pergamon/ Elsevier, New York,

Bonham-Carter, G.F., Agterberg, F.P., Wright, D.F., 1989. Weights of evidence modelling: a new approach to mapping mineral potential. *Statistical Applications in Earth Sciences* 89 (9), 171–183.

Can, T., Nefeslioglu, H. A., Gokceoglu, C., Sonmez, H., Duman, T. Y. 2005.Susceptibility assessments of shallow earthflows triggered by heavy rainfall at three subcatchments by logistic regression analyses. *Geomorphology*, 72, pp. 250-271.

Catani, F., Casagli, N., Ermini, L., Righini, G., Menduni, G. 2005. Landslide hazard and risk mapping at catchment scale in the Arno River basin. *Landslides* 2:329–342

Choi, J., Oh, H. J., Lee, C., Lee, S. 2012. Combining landslide susceptibility maps obtained from frequency ratio, logistic regression, and artificial networks models using ASTER images and GIS. *Engineering Geology* 124:12-23.

Couture, R. 2011. *Landslide Terminology - National Technical Guidelines and Best Practices on Landslides*. Geological Survey of Canada, Open File 6824, 12 p.

Cramer, 2002. *The Origin of Logistic Regression*. Tinbergen Institute Discussion Paper. Accessed on 29 December 2011 from http://dare.uva.nl/document/204.

Dahal, R.K., Hasegawa, S., Nonomura, A., Yamanaka, M., Masuda, T., Nishino, K. 2007. GIS Based Weights-of-Evidence Modeling of Rainfall Induced Landslides in Small Catchments for Landslide Susceptibility Mapping. *Environ Geol*, doi: 10.1007/s00254-007-0818-3

Dai, F.C., Lee, C.F. and Ngai, Y.Y 2002. Landslide Risk Assessment and Management: an Overview. *Engineering Geology* 64, page 65-87.

Das, I., Stein, A., Kerle, N., Dadhwal, V. 2012. Landslide susceptibility mapping along road corridors in the Indian Himalayas using Bayesian logistic regression models. *Geophys J Roy Astron Soc* 179:116–125

Domínguez-Cuesta, M.J., Jiménez-Sánchez, M., Berrezueta, E. 2007. Landslides in

the Central Coalfield (Cantabrian Mountains, NW Spain): geomorphological features, conditioning factors and methodological implications in susceptibility assessment. *Geomorphology* 89, 358–369.

Ercanglu, M. 2005. Landslide susceptibility assessment of SE Bartin (West Black Sea region, Turkey) by artificial neural networks. *Nat Hazard Earth Syst Sci* 5:979–992

Ermini, L., Catani, F. and Casagli, N. 2005. Artificial neural networks applied to landslide susceptibility assessment. *Geomorphology*, 66 (1-4), pp. 327-343.

ESRI (Environmental Research Systems Institute, Inc). 2009. ArcGIS Version 9.3. Redlands.

Fell, R., Corominas, J., Bonnard, C., Cascini, L., Leroi, E., Savage, W.Z. 2008. Guidelines for landslide susceptibility, hazard, risk zoning for land-use planning. *Engineering Geology* 102:99-111.

Garcia-Rodriguez, M. J., Malpica, J. A., Benito, B., Diaz, M. 2008. Susceptibility assessment of earthquake-triggered landslides in El Salvador using logistic regression. *Geomorphology* 95: 172-191.

Gomez, H. and Kavzoglu, T. 2005. Assessment of shallow landslide susceptibility using artificial neural networks in Jabonosa River Basin, Venezuela. *Engineering Geology*, 78, pp. 11-27.

Hosmer, D. W. and Lemeshow, S. 1989. *Applied Regression Analysis*. Wiley, New York, USA, 307 pp.

*Hengl, T., Maathuis, B.*H.P. and Wang, L. *Geomorphometry in ILWIS.* In: Hengl, T., Reuter, H.I. (Eds.), *geomorphometry: concepts, software, applications. Developments in soil science*, vol. 33. Elsevier, Amsterdam, pp. 497-525, *2009*.

Huabin, W., Gangjun, W., Weiya, X., Gonghui, W. 2005. GIS-based Landslide Hazard Assessment: an Overview. *Progress in Physical Geography* 29, 4 hal 548-567

Kendall, M., Stuart, A., 1979. *The Advanced Theory of Statistics: Inference and Relationship*. Griffin, London.

Lee, S., Pradhan, B. 2007. Landslide hazard mapping at Selangor, Malaysia using frequency ratio and logistic regression models. International Consortium on

Landslide 4 (1):33-41.

Lee, S., Ryu, J., Won, J., Park, H. 2004. Determination and application of weights for landslide susceptibility mapping using an artificial neural network. *Engineering Geology*, 71, pp. 289-302.

Lusted, L.B., 1968. *Introduction to Medical Decision Making*. Charles C. Thomas, Springfield III.

McCulloch, W.S., Pitts, W. 1943. A logical calculus of the ideas immanent in nervous activity. *Bull. Math. Biophys*. 5, 115–133.

Moore, I.D., Grayson, R.B., Ladson, A.R., 1991. Digital terrain modeling: a review of hydrological, geomorphological, and biological applications. *Hydrological Processes* 5 (1), 3–30.

Nagarajan, R., Roy, A., Vinod Kumar, R., Mukherjee, A., Khire, M. V. 2000. Landslide Hazard Susceptibility Mapping Based on Terrain and Climatic Factors for Tropical Monsoon Regions. *Bull Eng Geol Env* 58: 275-287. Springer-Verlaag

Nefeslioglu, H. A., Gokceoglu, C., Sonmez, H. 2008. An assessment on the use of logistic regression and artificial neural networks with different sampling strategies for the preparation of landslide susceptibility maps. *Engineering Geology*, 97, pp. 171-191.

Neuhäuser, B., dan Terhorst, B. 2007. Landslide Susceptibility Assessment Using "Weights-of-Evidence" Applied to a Study Area at The Jurassic Escarpment (SW-Germany). *Geomorphology* 86, pp 12-24. Elsevier.

Ohlmacher, G. C. and Davis, J. C. 2003. Using multiple logistic regression and GIS technology to predict landslide hazard in northeast Kansas. *USA Eng Geol* 69(33):331–343

Pradhan, B. and Lee S. 2009. Landslide risk analysis using artificial neural network model focussing on different training sites. *Int J Phys Sci* 4:001–015

Pradhan, B. and Lee, S. 2010. Landslide susceptibility assessment and factor effect analysis: backpropagation artificial neural networks and their comparison with frequency ratio and bivariate logistic regression modeling. *Environmental Modelling & Software*, 25, pp. 747-759.

Quinn, P., Beven, K., Chevallier, P., Planchon, O. 1991. The prediction of hillslope

paths for distributed hydrological modeling using digital terrain models. *Hydrological Processes* 5, 59–79.

Rahardjo, W., Sukandarrumidi, dan Rosidi, H. M. D. 1995. *Peta Geologi Lembar Yogyakarta, Jawa*. Pusat Penelitian dan Pengembangan Geologi, Bandung.

Schicker, R. and Moon, V. 2012. Comparison of bivariate and multivariate statistical approaches in landslide susceptibility mapping at regional scale. *Geomorphology* 161-162, 40-57.

Süzen M. L. and Doyuran, V. 2004. Data Driven Bivariate Landslide Susceptibility Assessment Using GIS: a Method and Application to Asarsuyu Catchment, Turkey. *Engineering Geology* 71, pp 303-321.

Van Den Eeckhaut, M., Vanwalleghem, T., Poesen, J., Govers, G., Verstraeten, G., and Vandekerckhove, L. 2006. Prediction of landslide susceptibility using rare events logistic regression: a case-study in the Flemish Ardennes, Belgium. *Geomorphology*, 76, 392– 410,

Westen van, C. J., Rengers. N., Soeters. R. 2003. Use of Geomorphology Information in Indirect Landslide Susceptibility Assessment. *Natural Hazard* 30: 399-419. Kluwer Academic Publishers. Netherlands.

Yesilnacar, E., Topal, T., 2005. Landslide susceptibility mapping A comparison of logistic regression and neural networks methods in a medium scale study, Hendek region (Turkey). *Engineering Geology* 79, 251–266.

Yilmaz, I. 2009.Landslide susceptibility mapping using frequency ratio, logistic regression, artificial neural networks and their comparison: A case study from Kat landslides (Tokat-Turkey). *Computers and Geosciences* 35, 1125-1138.

Zadeh, L. A. 1994. Fuzzy logic, neural networks and soft computing. *Fuzzy Systems* vol. 37 no. 3, pp 78-84.

CHAPTER 5

ROCKFALL SUSCEPTIBILITY BASED ON ROCKFALL SOURCE IDENTIFICATION BY USING BACK ANALYSIS OF ROCKFALL DEPOSITS INVENTORY

5.1 INTRODUCTION

Risk can be defined as ”the expected number of lives lost, persons injured, damage to property and disruption of economic activity due to a particular damaging phenomenon for a given area and reference period” (Varnes, 1984). The definition was originally used to describe landslide risk. Later, the terminology was used for all types of mass movement including rockfall.

The word “rockfall” is often distinguished from more general landslide phenomena due its typical material, size and failure mechanism. It is defined as rock fragments (Hungr and Evans, 1988) with size from a few dm^3 to 10^4 m (Levy et al., 2011) started by the detachment of blocks from their original position (Crosta and Agliardi, 2003) and followed by free falling, bouncing, rolling or sliding (Peila et al., 2007). Rockfall risk can be expressed by the simple product of hazard (temporal probability, spatial probability, reach probability), vulnerability and value of the element at risk (Fell etal., 2005; Westen et al., 2005; Agliardi et al., 2009) as follows:

$$R = \sum(H \sum(VC)) \tag{5.1}$$

where H is hazard expressed as a function of spatial probability, temporal probability and magnitude probability; V is vulnerability of particular elements at risk; and C is amount of loss of the particular elements at risk. Based on the equation 5.1, the temporal and spatial probability of rockfall are diverse in time and places. The

diverse in places is usually presented by rockfall susceptibility zoning.

There are many rockfall susceptibility zoning methodologies proposed by government agencies and or scientific society worldwide such as Switzerland (Raetzo et al., 2002), Hong Kong (GEO, 1998), Australia (AGS, 2007), Andorra (Copons et al., 2004). It includes geomorphological analysis/ rating system and trajectory-energy/velocity modeling. These provide different approaches to quantify rockfall susceptibility, hazard and risk.

Geomorphological analysis is the simplest approach and powerful to identify rockfall susceptibility. The zoning is usually based on the geomorphological unit or landform analysis. For example, Sasaki et al., (2000) generated land condition map showing geomorphologic element which is susceptible to rockfall. The division of the susceptible rockfall area was clearly defined by the geomorphological unit. However, susceptibility zoning is described in qualitative ways, subjective and needs well experienced geomorphologist as an interpreter to delimit the susceptible zone. The detail of geomorphology analysis is discussed in chapter 6.

Trajectory-energy/velocity modeling is a quantitative method which can accommodate the terminology of susceptibility quantitatively. It employs computer simulation to calculate probability of reach, velocity and the kinetic energy distribution at each point of the slope. The propagation is dependent on slope topography, lithology, mass block shape and mass. The trajectories are calculated from the input parameter that sometimes inaccurate due to unavailability of rockfall database. The susceptibility zoning is defined based on the reach probability or an energy profile to the distance. It does not represent the natural feature of the slope and the result depends on the input of the model.

Rockfall susceptibility and hazard assessment is beneficial to provide guidance on the design of structural measures and nonstructural measures as a protection system (Fell et al., 2008). Rockfall susceptibility assessment employed GIS susceptibility mapping, numerical simulations and full scale experiment (Volkwein et al., 2011). The application of rockfall susceptibility assessment usually depends on the scale of area. GIS susceptibility mapping is usually applied in regional scale, whereas numerical simulations and full scale experiment are applied in a limited area

or large scale.

A GIS rockfall model (Lan et al., 2007) is employed to infer the rockfall source by using back analysis method in this chapter. It is based on the rockfall boulder inventory and the input parameter of the characteristics of GunungKelir area. Coefficients of restitution are used to control boulder movement during impact at the end of rock movement. Sensitivity analysis is conducted to demonstrate the effect of different coefficient restitution. Once the potential of rockfall sources is identified; trajectories, frequency and energy of rockfall can be mapped.

The information of the trajectory simulation, including frequency and energy is useful to expose the spatial distribution of potentially high damage of elements at risk affected by rockfall. Thus, it is expected to provide spatial information needed for susceptibility zoning analysis when the rockfall source data is unavailable.

5.2 STUDY AREA

Gunung Kelir is located in Yogyakarta Province, Indonesia. It lies in the upper part of Menoreh Dome that is located in the central part of Java Island (Figure 5.1). The area is dominated by Tertiary Miocene Jonggrangan Formation that consists of calcareous sandstone and limestone. Bedded limestone and coralline limestone which form isolated conical hills may also be found in the highest area surrounding the study area.

Landforms in Gunung Kelir are a product of final uplifting of the Complex West Progo Dome in the Pleistocene. The evolution or chronology of Kulon Progo Dome has been well explained by van Bemmelen (1949). It was started with the rising up of geosyncline of South-Java in Eocene Period. It made the magma of Gadjah Volcano consisting of *basaltic piroxene andesites* reached up to the surface. Then, it was followed by the activity of Idjo Volcano in the south with more acid magma consisting of *hornblende-augite andesites* and *dacite* intrusions. After the strong denudation process, exposing the chamber of Gadjah Volcano, the Menoreh Volcano in the north began to be active. The material consists of *hornblende-augite andesites* without *lava flow* ended by *dacitic* intrusion and *hornblende andesite* with

doming up process. Then, in the lower Miocene, Kulon Progo dome subsided below sea level and the Jonggrangan Formation was formed by coral reef sedimentation. Finally, the complex of The Progo Dome was uplifted during Pleistocene. The uplifting caused jointing and large cracks and caused abundant rockfall and slide to the foot of Kulon Progo Dome, especially in the eastern flank of Kulon Progo Dome.

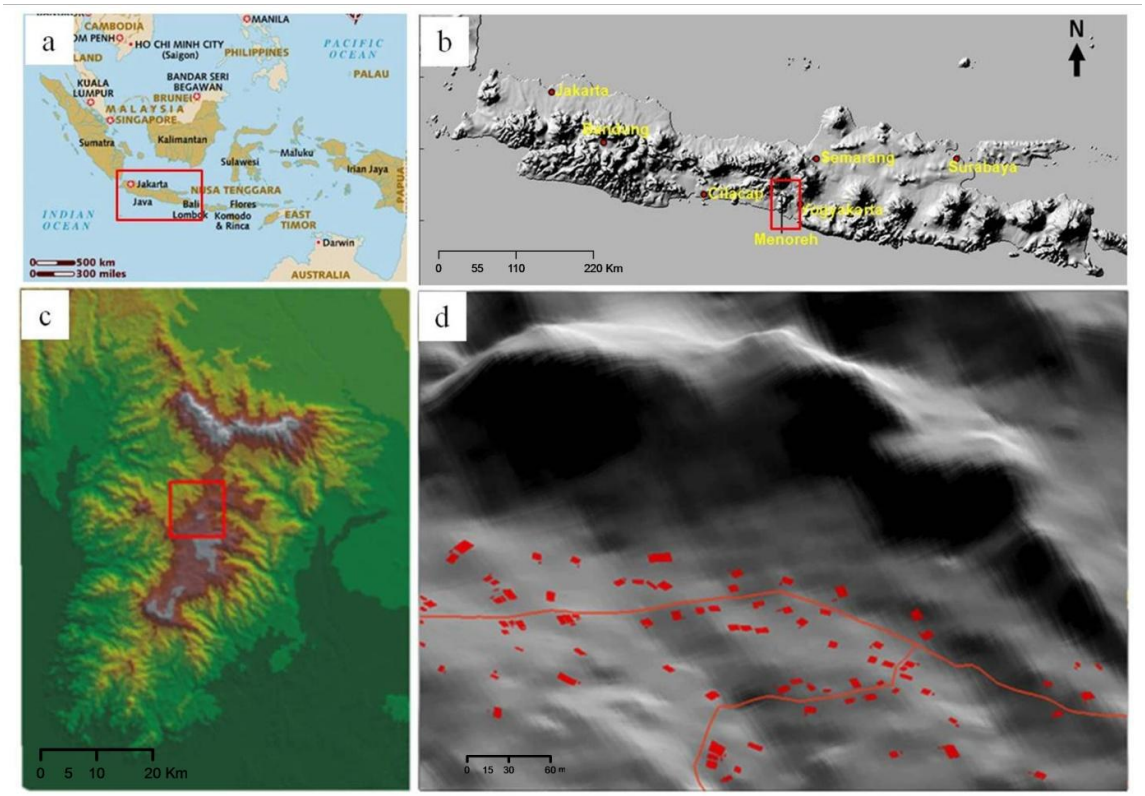

Figure 5.1 Study Area (a) geographical position of Indonesia: red rectangle shows geographical position of Java Island (b) DTM of Java Island: red rectangle shows the location of Menoreh Dome (c) DTM of Menoreh Dome: red rectangle shows Purwosari area (d) Gunung Kelir Area viewed from east: red rectangle shows building distributions and red line shows road

Gunung (Mountain) *Kelir*, of Javanese origin, literally means a curtain that is used to perform *wayang* (Javanese traditional shadow puppet). Its toponym describes a 100-200 meter high escarpment that has a maximum slope nearly 80°. The complex of Gunung Kelir consists several generic landforms which are prone to rockfall. Its mean slope gradient is 23.14° with the standard deviation 13.05°.

Altitude ranges from 297.75 to 837.5 m. There are 152 buildings exposed as elements at risk on the lower slope of the escarpment (Fig. 5.1.d).

5.3 Data and Methods

Rockfall risk analysis requires assessment of susceptibility and identification of an element at risk as well as the characteristic of rockfall deposition in a particular area. Rockfall trajectory modelling is employed to portray the susceptible area. This chapter is aimed to identify potential rockfall sources obtained from the back analysis of rockfall deposits inventory. The potential rockfall source is essential for susceptibility zoning. To achieve the primary objective, several works were conducted: 1) fieldwork, 2) DTM preprocessing, 3) rockfall modelling based on back analysis of rockfall source, and 4) sensitivity analysis.

5.3.1 Field Work and DTM Preprocessing

Fieldwork was intended to identify rockfall boulders and elements at risk used in the proposed back analysis method. A field inventory of fallen rockfall boulders of different size has been done to obtain the spatial distribution and dimension of rockfall deposition (see Figure 3.8). The rockfall boulder location was recorded by GPS and plotted in GIS layer. The size or volume of the boulder was measured in the field by laser distance meter or meter distance measurement tool. An interview using closed questionnaire was conducted to obtain the information of an element at risk. The dimension and potential rockfall source were determined to simulate rockfall trajectory, velocity, and energy. The buildings on the lower slope of the escarpment were also plotted in order to obtain the spatial distribution of elements at risk. Finally, DGPS profiling was conducted to improve the performance of DTM. DTM preprocessing was also employed to improve the quality of DTM-derived products.

The objective of DTM preprocessing was to improve the quality of DTM-derived products. The author applied DTM preprocessing proposed by Hengl et al. (2004) including reduction of padi terraces, reduction of outliers, incorporation of water bodies, and reduction of errors by error propagation (Figure 5.2). Padi terraces are usually caused by interpolation method and located in closed contour where all the surrounding pixels were assigned the same elevation value. Five meter resolution of DTM was produced by interpolation, using ILWIS linear interpolation method, from a 1:25.000 Topographical Map 1999 with contour interval 12.5 m and elevation data from DGPS profiling.

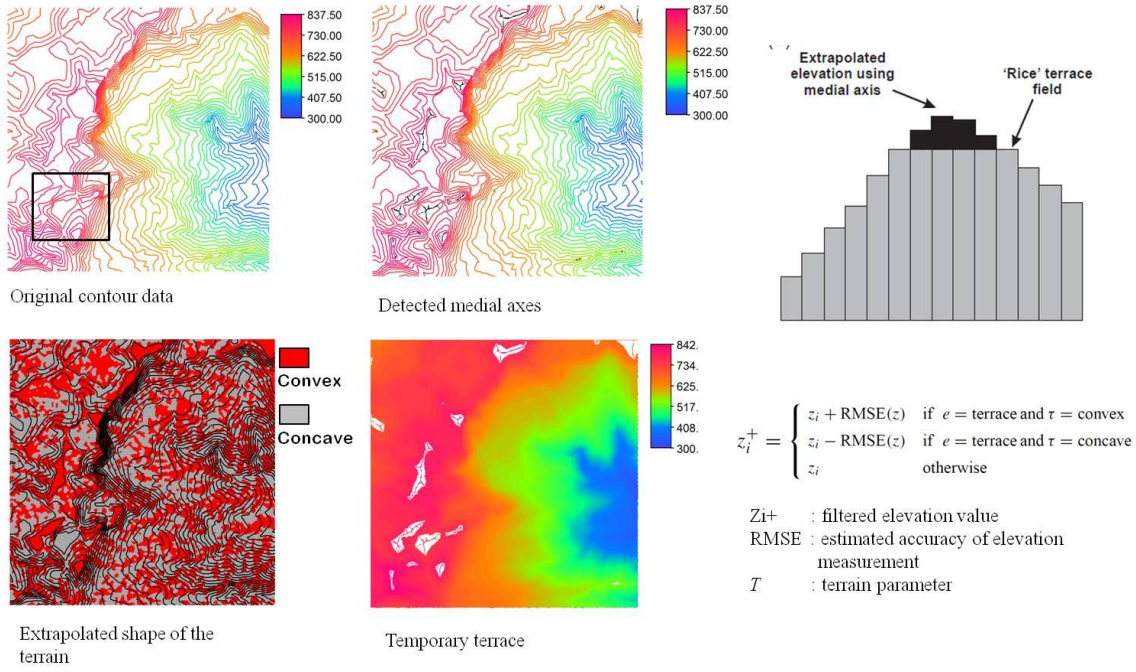

Figure 5.2 The Illustration of DTM Preprocessing

5.3.2 ROCKFALL MODELING

5.3.2.1 ROCKFALL ANALYST

GIS (Geographic Information System) is useful to determine rockfall trajectory and energy applied in regional scale. It is based on Digital Terrain Model (DTM) representing topography in raster format. The model is powerful to simulate the physical characteristics of the surface rather than the physical characteristic of the

boulder itself. The additional attribute related to geology, land use or vegetation type and rock type represented in spatial data can also be included in the model.

GIS model (Rockfall Analyst) based on lumped mass (Lan et al., 2007) was applied to model the trajectory and velocity of rockfall along the escarpment of Gunung Kelir area, Indonesia. It considers the dynamic process of rockfall based on the cell plane obtained from raster based Digital Elevation Model (DEM). DEM represents the earth surface or topography containing actual height points. GIS can produce various topographic parameters (derivative of DEM) such as slope, aspect, curvature easily. In GIS Rockfall analyst, the DEM derivatives, i.e. slope angle and aspect angle are used to construct the normal vector of each cell plane (Lan et al., 2007). It is expressed in the global Cartesian system (Figure 5.3) as:

$$u_n = (\sin\theta \sin\varphi, \sin\theta \cos\varphi, \cos\theta) \quad (5.2)$$

where u_n unit normal vector, θ is the slope angle and φ is the aspect angle.

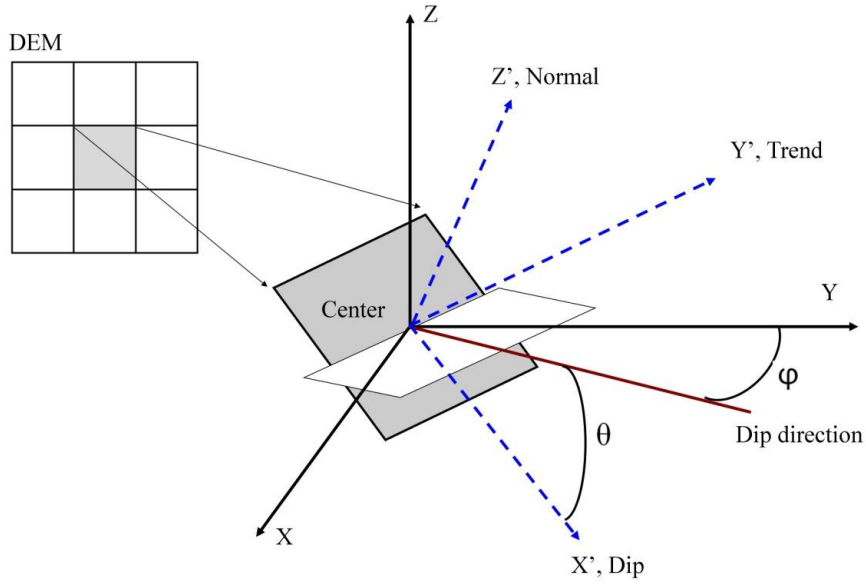

Figure 5.3 Cell Plane and Coordinate System employed in the Model (Adopted from Lan et al., 2007)

Rockfall analyst employs lumped mass approach to assess the trajectory and velocity of rockfall to reduce the excessive computational requirements in a GIS environment. It means that the rockfall simulation will not consider the size and

shape of the boulder. The rockfall process, including the modeling of free falling, bouncing and rolling or sliding is performed by discrete time steps. It is automatically determined by both cell size and particle velocity. Physical quantity of boulder such as rock position, displacement, velocity, acceleration, force and momentum is represented in 3D vector space. For instance, the flying path of boulder computed by parabolic equation which is defined as:

$$\bar{x} = \begin{bmatrix} 0 \\ 0 \\ -\frac{1}{2}gt^2 \end{bmatrix} + \begin{bmatrix} V_{x0} \\ V_{y0} \\ V_{z0} \end{bmatrix} t + \begin{bmatrix} X_0 \\ Y_0 \\ Z_0 \end{bmatrix} \quad (5.3)$$

where g is the acceleration due to gravity (9.8 m/s^2), X_0,Y_0,Z_0 is the initial position and V_{x0}, V_{y0},V_{z0} is the initial velocity of the rock in x, y, z direction. Whereas, the velocity vector of the rockfall is defined as

$$\bar{v} = \begin{bmatrix} V_{x0} \\ V_{y0} \\ V_{z0} - gt \end{bmatrix} = \begin{bmatrix} 0 \\ 0 \\ -gt \end{bmatrix} + \begin{bmatrix} V_{x0} \\ V_{y0} \\ V_{z0} \end{bmatrix} \quad (5.4)$$

In addition, coefficient restitution is also included to calculate the bouncing velocity in the intersection location between a flight path parabola and the grid cell surface. For example, rolling/sliding will occur if the velocity has decreased to some value, i.e. 0.5 m/s, after impact. It involves coefficient of normal restitution R_N and coefficient of tangential restitution R_T. Normal restitution acts in a direction perpendicular to the slope surface and tangential restitution acts in a direction parallel to the surface during each impact of the incoming velocity of the rocks. Velocities change because of the energy loss defined by both of which.

The author determined normal restitution and tangential restitution by a geological map representing elasticity of the surface material and landuse map representing vegetation cover and surface roughness respectively. The bouncing velocity vector in a local coordinate system is defined as

$$V'_{Dip} = V_{Dip} R_T \quad (5.5)$$

$$V'_{Trend} = V_{Trend} R_T \quad (5.6)$$

$$V'_N = V_N R_N \quad (5.7)$$

where V_{Dip} is the velocity components of rock in the dip direction, V_{Trend} is the velocity components of rock in the trend direction, V_N is the velocity components in

the normal direction of slope cell. Beside projectile algorithm for falling, the rolling or sliding algorithm is also determined by the interaction between rock velocity vector and the normal vector of cell plane (Lan et al., 2007). The calculation of GIS rockfall modeling is represented by vector format. It shows trajectories along the escarpment. The starting point of bolder is treated as a seeder location in the upper slope.

5.3.2.2 ROCKFALL SOURCE IDENTIFICATION

The trajectory modelling approach needs spatial distribution of the rockfall sources. However, there is no historical rockfall history recording the sources of rockfall in the study area. A field survey is also difficult to be conducted because the unavailability of track to reach the potential source location and the slope is very steep (Figure 5.4). Thus the potential source of rockfall was identified by back analysis of rockfall boulder deposits obtained from field survey.

Potential source, initially, was identified by field survey and thematic map analysis. The GIS-overlay between slope map and landuse was employed to infer the potential source area. Potential major sources were identified in landuse shrub and outcrop with slope >55. It results polygon representing a major potential area of rockfall source (Figure 5.5.a). Total 2993 point sampling were randomly generated in the potential major source area (Figure 5.5. b). It represents the potential source point which later employed as a presumed potential seeder processed in the model. The starting point of blocks was determined as a potential source of blocks and was treated as a seeder location.

Bouncing, falling, rolling/sliding including the velocity are also able to be investigated in each trajectory. Coefficient of surface parameters was also used to control boulder movement during impact at the end of rock flight. The simulation of rock fall trajectory predicts how far a boulder passes through slope. Many simulations were carried out in order to achieve best trajectories which are in good

agreement with boulder deposits. The simulation of rock fall trajectory predicts how far a boulder passes through slope. Coefficient of surface parameters, i.e. normal restitution, tangential restitution (Table 5.1) were used to control boulder movement during impact at the end of rock flight. Properties of surface material play important role to control boulder movement, i.e. bouncing velocity during impact with surface material at the end of rock flight.

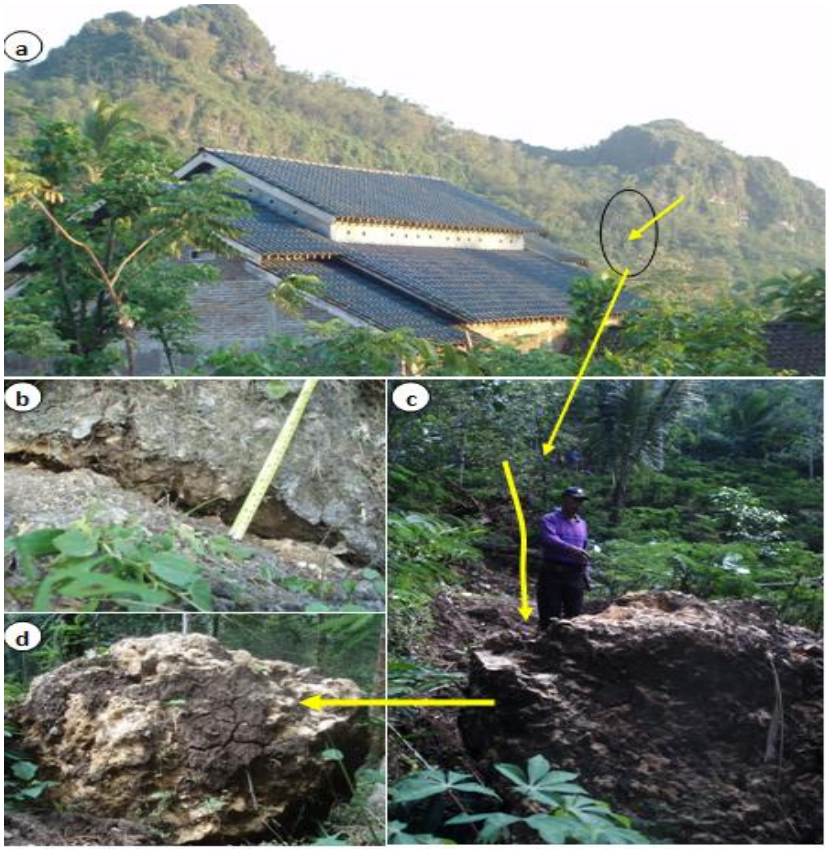

Figure 5.4 Escarpment of Gunung Kelir showing potential rockfall source (a) Crack on boulder deposits (b), potential trajectory of boulder deposits (c) and boulder deposits around 150 m from the escarpment (d) (Credit Photo: Danang Sri Hadmoko)

Table 5.1 Properties of Surface Material (Adopted from Rocscience website, 2014)

Surface Types	R_N	R_T
Sandstone face	0.53	0.9
Vegetated soil slope	0.28	0.78
Soft soil, some vegetation	0.30	0.3
Limestone face	0.31	0.71
Talus cover with vegetation	0.32	0.8

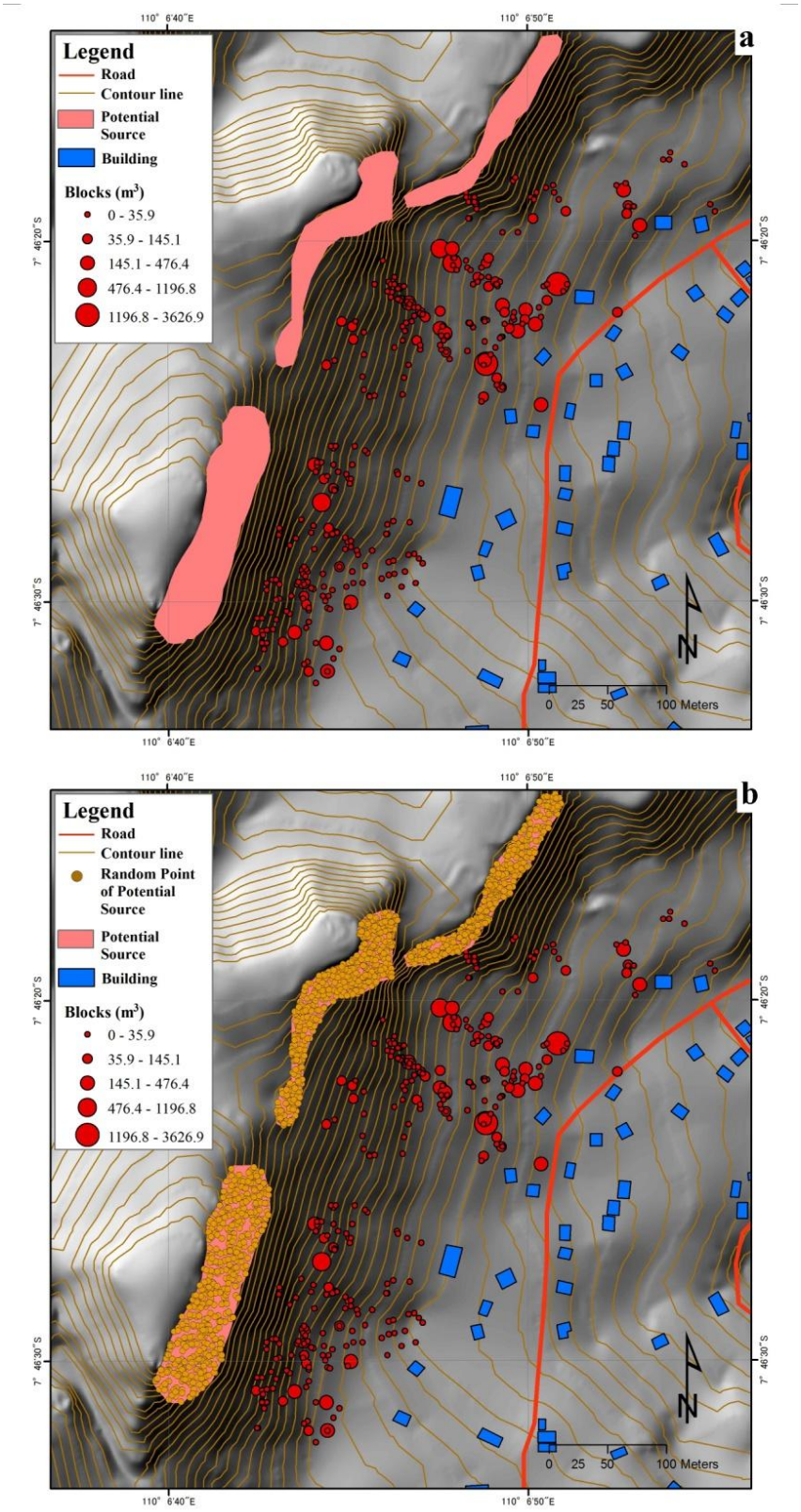

Figure 5.5 Polygon of Potential rockfall area obtained from Overlay Analysis (a) Point Random Sampling of Presumed Potential Rockfall Source (b)

However, GIS-lumped mass model is dimensionless, meaning that it does not consider the size, shape and fragmentation of the boulder. The more mechanically numerical rockfall simulation is needed as a complementary tool to analyze the trajectory which has a potency of high risk, e.g. trajectory passing a building. It should be able to model the dynamic displacement and deformation of an elastic body in any shape and consider the rigid body displacement, rotation and deformation of a block. Thus, 2D DDA was employed to confirm the reliable trajectory and dynamic behavior of boulder when travel along the slope having high risk possibility.

5.3.2.3 2D DDA

Extended 2D DDA (Chen, 2003) was employed to assess the motion behavior of the most dangerous rockfall trajectory obtained from GIS modeling. DDA is one of numerical simulation that can be applied to simulate the motion behavior of rock. It deals with the problem of rigid body movement and large deformation of a rock block system under general loading and boundary (Shi, 1988). Even though DDA is parallel to finite element, the advantage of 2D DDA is that every single block can be convex or concave in two dimensional polygon. In addition, Coulomb's law is applied to the contact interface and the simultaneous equilibrium equations are solved for each loading or time increment (Shi and Goodman, 1989). Each block can interact and deform independently.

There are six displacement variables working in DDA when a block experiences constant stresses and constant strains throughout(Shi and Goodman, 1989). The displacement (u,v) of any point (x,y) of a block can be defined as six variables as follows:

$$(u_0\ v_0\ r_0\ \varepsilon_x\ \varepsilon_y\ \gamma_{xy}) \tag{5.8}$$

where u_0,v_0 are the parallel translation (u,v) of a specific point (x_0,y_0) on the block; r_0 is the rotation angle (in radians) of the block with the rotation center at (x_0,y_0). ε_x ε_y

γ_{xy} are the normal and shear strains of the block at (x_0,y_0). Displacements (u,v) of the point (x,y) containing several mechanisms such as parallel translation, rotation, normal strain and shear strains are formulated separately. Thus, the total displacement (u,v) of the same point (x,y) is the accumulation of displacements induced by six variables (Shi, 1988) . It can be defined as:

$$\begin{bmatrix} u \\ v \end{bmatrix} = \begin{bmatrix} 1 & 0 & -(y-y_0) & (x-x_0) & 0 & (y-y_0) \\ 0 & 0 & (x-x_0) & 0 & (y-y_0) & (x-x_0) \end{bmatrix} \begin{bmatrix} u_0 \\ v_0 \\ r_0 \\ \varepsilon_x \\ \varepsilon_y \\ \gamma_{xy} \end{bmatrix} \quad (5.9)$$

2D DDA model will take an advantage of a GIS model to simulate the motion behavior of the boulder. 2D slope profile from DEM was imported to the 2D DDA to draw rock block system and to simulate the contact force of multiple falling rock. The displacement behavior of each block in the dynamic simulation can be traced and can be seen at the end of each calculation step.

5.4 Results and Discussion

5.4.1 Rockfall Trajectories based on Back Analysis of Rockfall Source

There are some difficulties to investigate the rockfall source in Gunung Kelir area because of high slope gradient and no access to reach the top of the mountain. In this research, the unknown source of rockfall was inferred from back analysis of rockfall boulder. Once the surface rasters are created and the parameters are input, the rockfall trajectory can be determined as the interaction between rock and slope. It produces line trajectory. The boulder inventory can be traced back using the trajectory to a point where the point of potential source exists. This point can be determined as the source of the rockfall. The author employed geomorphological concept, widely applied for landslide analysis, “the past is the key to the future”. It means that the past rockfall source may be the rockfall source in the future.

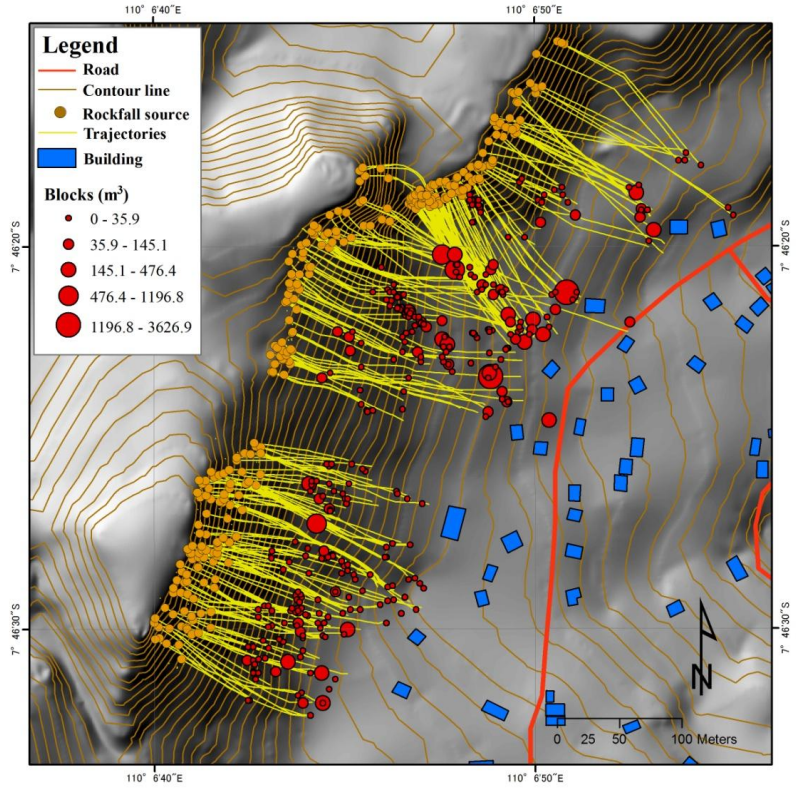

Figure 5.6 Reliable Trajectories which are in good agreement with Boulder Deposits

The simulation of rock fall trajectory predicts how far a boulder passes through slope (Figure 5.6). Many simulations with many random points of potential rockfall sources were carried out in order to achieve best trajectories which are in good agreement with boulder deposits. The simulation of rock fall trajectory predicts how far a boulder passes through slope. The distance of boulder passing through slope might be affected by the coefficient of restitution (Equation 5.5-5.7). It describes the kinematic behavior of a falling rock during an impact against the slope surface. The trajectory simulation may demonstrate significant error due to the incorrect value assigned to the Coefficient of Restitution (COR). Rockfall boulder inventory and potential rockfall source provide an opportunity to verify the result and to know what extent COR can affect the result.

5.4.2 Sensitivity Analysis

The final trajectories and the effect of COR was verified with a sensitivity

analysis. Lower and higher input of COR were employed to determine the sensitivity. Reducing and increasing both the normal and tangential restitution provides a baseline. Reducing and increasing only the normal or tangential restitution respectively gives the individual sensitivity. The selected values can be seen in Table 5.2. Six tests were employed in sensitivity analysis by changing the value of coefficient restitution i.e. R_N (+)R_T (+), R_N (-)R_T (-), R_N (+)R_T, R_N (-)R_T, R_N R_T (+), and R_N R_T (-). There were 15 rockfall sources were employed as a sample to determine the sensitivity of COR.

Table 5.2 Adjusted value of COR for Sensitivity Analysis

Surface type	R_N	R_T	R_N (+)	R_T (+)	R_N (-)	R_T (-)
Sandstone face	0.53	0.90	0.69	0.93	0.37	0.63
Vegetated soil slope	0.28	0.78	0.37	0.81	0.20	0.55
Soft soil, some vegetation	0.30	0.80	0.39	0.83	0.21	0.56
Limestone face	0.31	0.71	0.40	0.74	0.22	0.50
Talus cover with vegetation	0.32	0.80	0.42	0.83	0.22	0.56

R_N (+) = R_N +30%; R_T (+) = R_T + 0.03; R_N (-) = R_N -30%; R_T (-) = R_T -30%

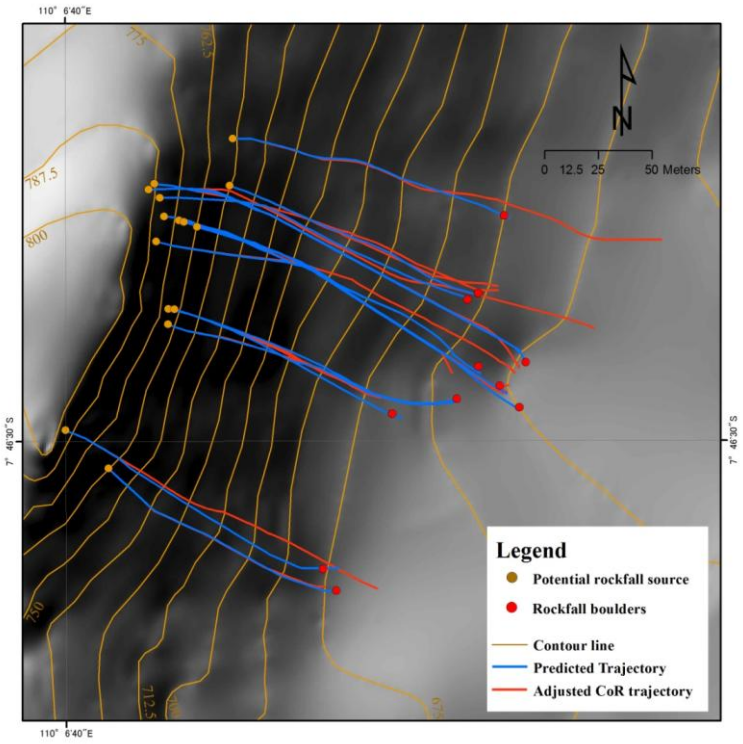

Figure 5.7 Simulation Trajectory with COR R_N (+)R_T(+)

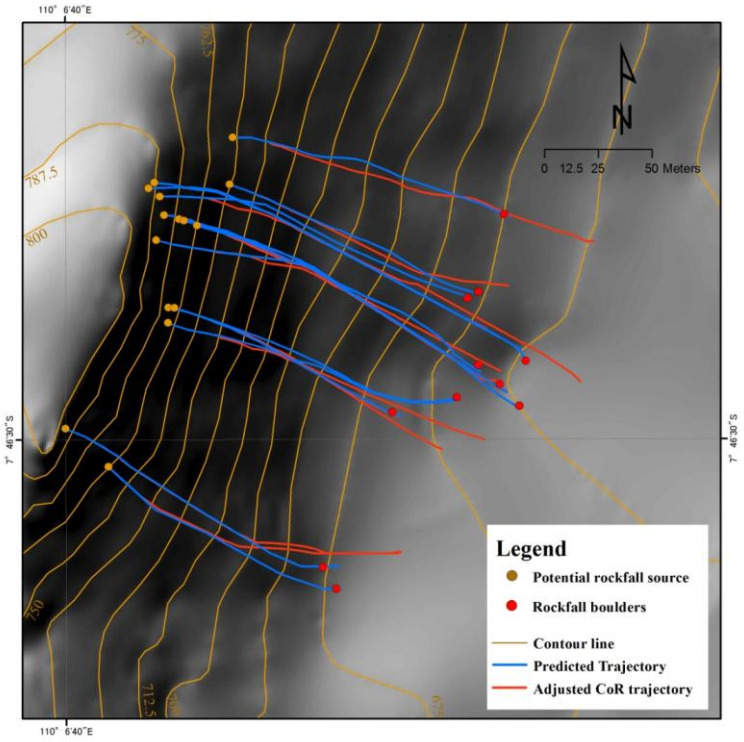

Figure 5.8 Simulation Trajectory with COR R_N (-)R_T (-)

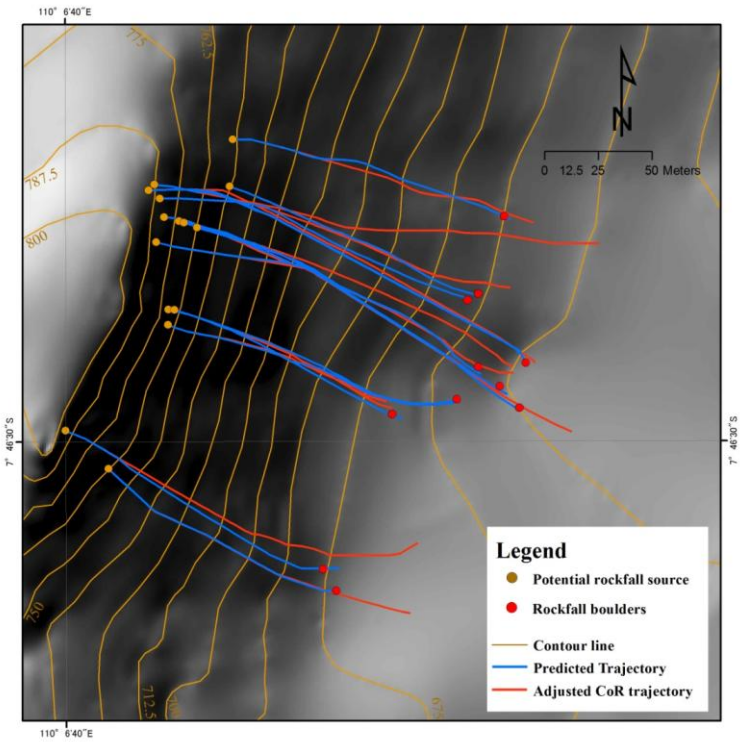

Figure 5.9 Simulation Trajectory with COR R_N (+)R_T

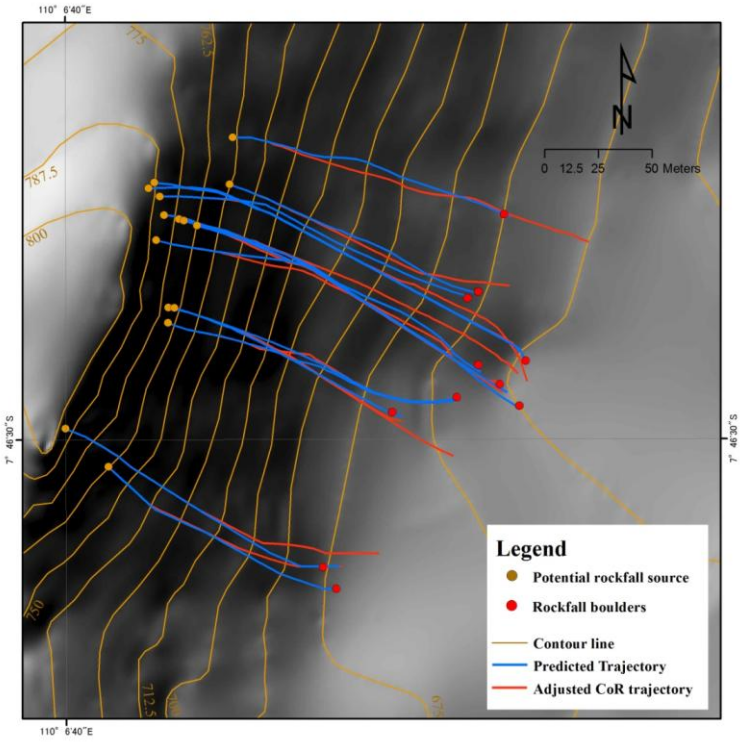

Figure 5.10 Simulation Trajectory with COR R_N (-)R_T

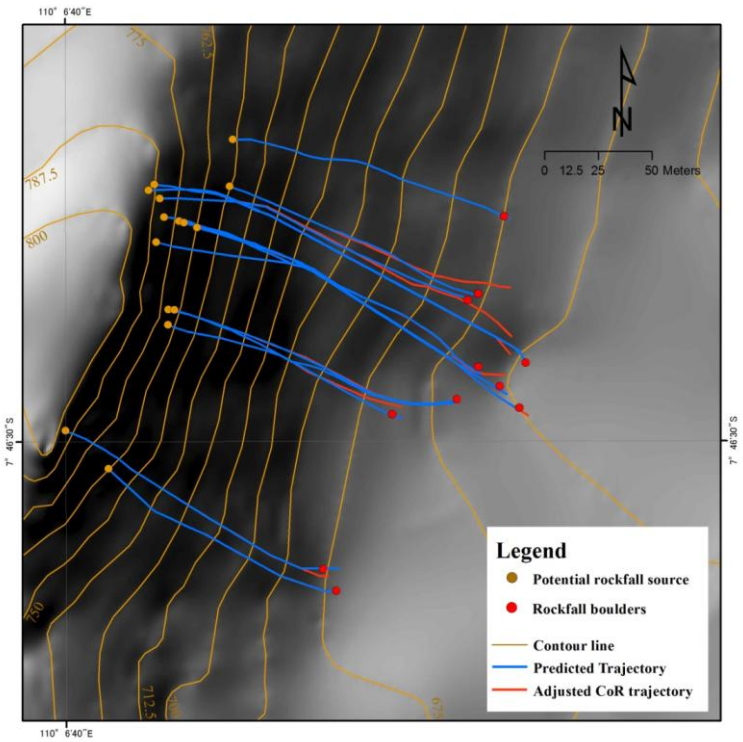

Figure 5.11 Simulation Trajectory with COR R_N R_T (+)

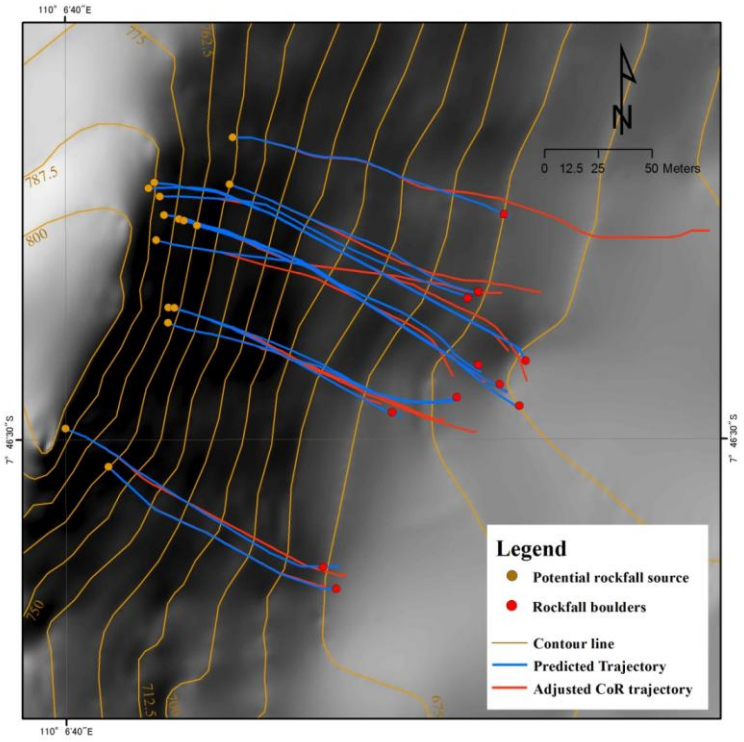

Figure 5.12 Simulation Trajectory with COR R_N R_T (-)

Table 5.3 The difference (in meter) between Predicted Trajectory and Trajectory with Adjusted COR tests

Sample no.	R_N+ R_T+	R_N- R_T-	R_N+ R_T	R_N- R_T	R_N R_T+	R_N R_T-
1	5.5	34.9	35.7	11.1	0	4.9
2	19.6	9.9	39.1	36.4	6.2	5.2
3	9.8	0.9	7.4	2.6	0.2	11.2
4	29.3	23.1	30.4	26.3	23.9	10.6
5	30.1	24.6	32.2	1.2	29	17.4
6	9.1	14.7	27.8	14.1	5.8	19.3
7	1.9	9.4	14.7	17.4	0.02	0.3
8	1.02	15.9	14.6	10.2	0.04	0.4
9	3.6	0.3	1	5.3	2.5	12.5
10	12.3	0.2	2.8	0.4	11.7	37.4
11	7.6	27.9	5.4	0.6	0.3	9.2
12	9.3	17.8	31.1	17	8.3	42.9
13	58.4	19.2	63.3	49.7	28.6	50.1
14	15.8	16.4	21.8	20.4	17.8	32.2
15	12.4	41.1	10.9	38.2	0.03	93
Average	15.05	17.09	22.55	16.73	8.96	23.11

The simulation is sensitive to change in the COR value if a slight increase or decrease COR result higher difference in rockfall travel distance. The change in normal COR affects more that the change in tangential COR. Table 5.3 shows that the maximum difference is 63.3 meters and the minimum is 0 meters. The maximum average difference is 23.11 and the minimum is 8.96. With 5 meter cell size, the difference is approximately 13, 5, and 2 pixels. It may suggest that the changing COR value may effect slightly, but it does not significantly affect the travel distance of rockfall in Gunung Kelir area. It suggests that the COR values have little effect on the travel distance and the travel distance is more affected by the source location and topography.

5.4.3 FREQUENCY AND KINETIC ENERGY

Once the rockfall sources and rockfall trajectories are determined, a rockfall susceptibility map can be directly computed based on the frequency and the kinetic energy. Frequency was computed based on the distance of trajectory lines per cell size and the kinetic energy can be computed based on the general equation relating energy to velocity:

$$E = \frac{1}{2}mV^2 \tag{5.10}$$

or

$$V = \sqrt{\frac{2E}{m}} \tag{5.11}$$

where E is energy, m is mass and V is velocity.

Rockfall frequency (Figure 5.13) was classified into 4 classes, i.e. 0-2, >2-4, >4-8, and >8. The southern part of Gunung Kelir mostly dominated by 0-2 meter/pixel. It means that 25 meter^2 can have maximum 2 lines of trajectories. Frequency >2-4 was mostly located on the middle slope of the escarpment. A few pixels were attributed as frequency >8. It occurs when the slope has the possibility to have more than one source of rockfall. The rockfall frequency can be used as susceptibility map. However, it is still difficult to apply rockfall frequency as a single

information for landuse planning. It is still difficult to divide an area into homogeneous domains only based on the frequency.

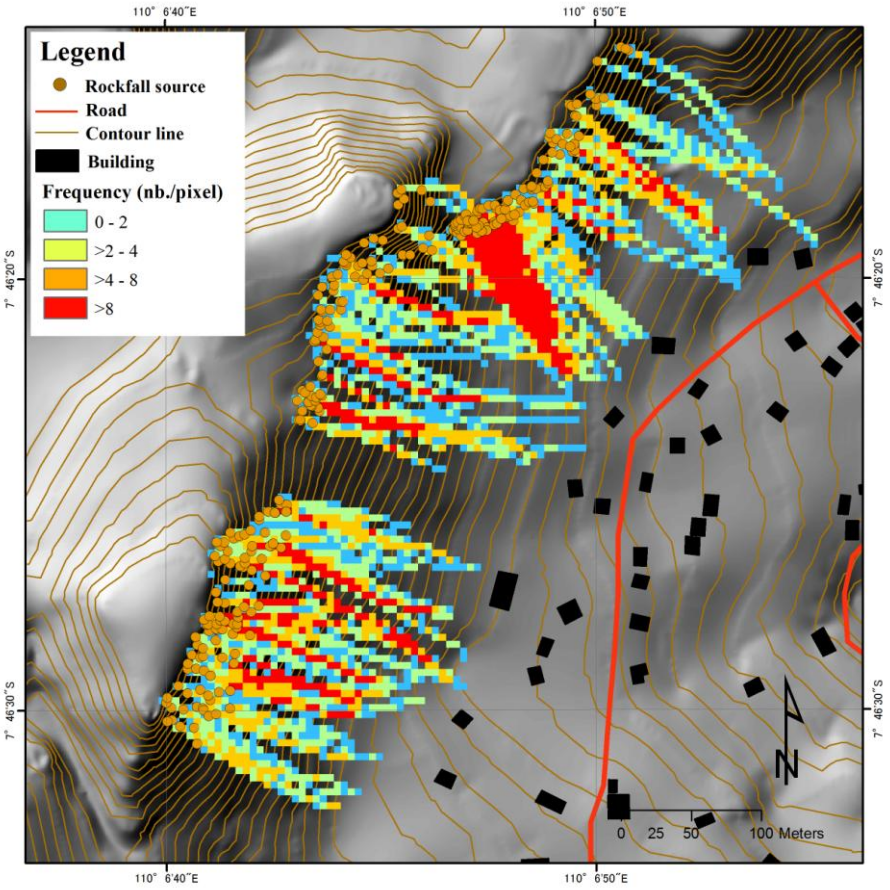

Figure 5.13 Rockfall Susceptibility Map shown as the Density of Trajectory Lines

The kinetic energy of rockfall (Figure 5.14) can also be computed and mapped based on the rockfall trajectory. Rockfall energy was classified into 4 i.e. 0-30, 30-300, 300- 600, and >600. The classification was based on the assumption of the response of a building during the impact with rockfall. It can be classified as slight damage (0-30), moderate damage (30-300), severe damage (300- 600), and totally destroyed (>600). It is easier to divide an energy map as an area which has homogeneous domains. The pattern seems that higher slope can be classified as low energy, middle slope as the highest energy and back to the lower energy in the lower part. This information can be used as susceptibility map even though both frequency and energy map still show the vague ("fuzzy") character of natural boundaries.

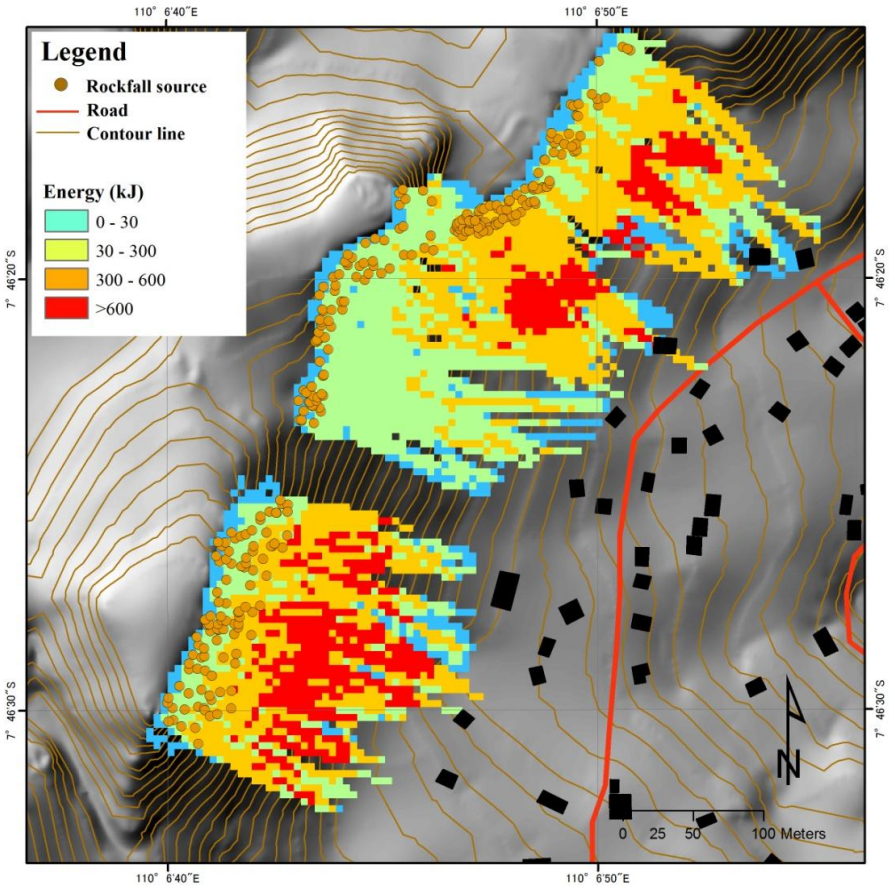

Figure 5.14 Rockfall Susceptibility Map shown as the Kinetic Energy of Rockfall Movement

The rockfall susceptibility shows that the northern part and middle part have higher susceptibility than the southern part (Figure 5.14). There are four buildings potentially obstructed by rockfall. The location of the building is 163 meters from the source of material.

More attention should be prioritized in northern and middle part that can potentially cause building damage. However, the detail of preventive measures development needs more analysis on the mechanic of rockfall process. Thus, 2D DDA was applied to explore the motion behavior of rockfall in the highest potency of high risk. There are 5 materials involved to model the motion behavior of a boulder which has the potential to damage the building in the northern part. The material properties are shown in table 3 and control parameter is shown in Table 4.

Table 5.4 Material properties of Gunung Kelir Rockfall.

	M_1	M_2	M_3	M_4	M_5
Density (ρ): g/cm^3	50000	2500	2450	2500	2450
Unit weight of rock (γ): kN/m^3	0	25	24.5	25	24.5
Elastic modulus (E) : GPa	20	20	20	20	20
Poisson's ratio (ν)	0.2	0.2	0.2	0.2	0.2
Friction angle of discontinuities (φ) : °	20	20	30	19	18
Cohesion of discontinuities (c) : MPa	0	0	0	0	0
Tensile strength of discontinuities (σ_t) : kPA	0	0	0	0	0

Table 5.5 Control Parameters of DDA.

Items	Data
Assumed maximum displacement ratio (g_2)	0.001
Total number of time steps	6000
Time steps (g_1)	0.01
Contact spring stiffness (g_0)	1.0x10^{7}kN/s

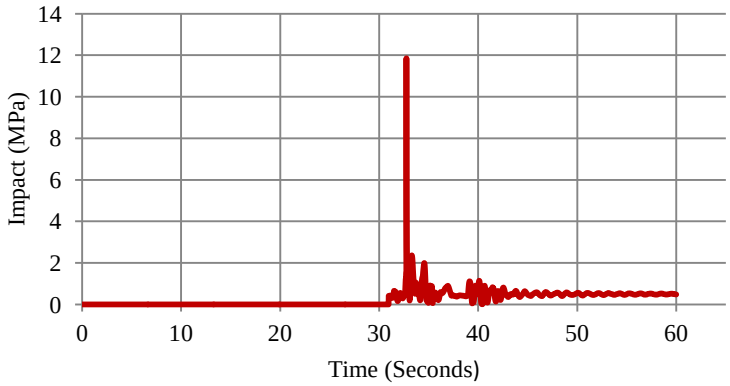

Figure 5.15 Rockfall Impact Force.

The result shows that the boulder in the northern part can potentially cause the building damage. The contact between boulder and building was introduced by small boulders with impact force 0.4 MPa at 30.95 seconds. The maximum impact force between boulders and building was 11.9 MPa (32.74 seconds after failure) (Figure 5.15 and Figure 5.16). It happened before the contact between the big boulder and the building. It was almost 80 times higher compared with the first contact between small boulders and the building. After the maximum impact force, it was followed by contact between medium boulder and the building with the maximum impact force 2.3 MPa in 33.4 seconds. Then, finally the small boulders stoped moving in 43.04

seconds with the impact force around 0.91. The velocity of the boulders is less than 15 m/s. Rolling and sliding are the most common of boulders motion.

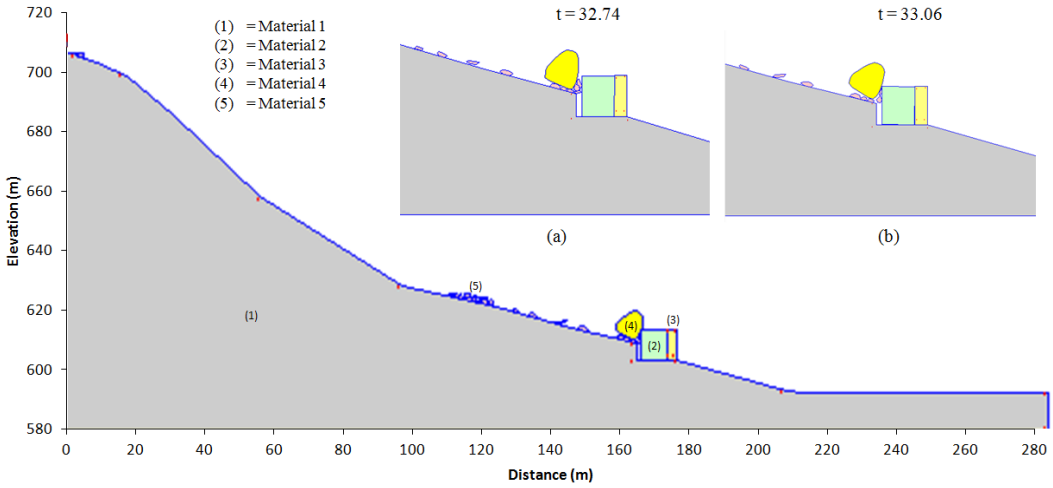

Figure 5.16 Rockfall Behavior for Potential High Risk.

5.5 CONCLUSIONS

The unavailability of rockfall source data and the difficulties to investigate the rockfall source directly are the problems to identify rockfall susceptibility in the study area. Trajectory simulation based on the rockfall deposits inventory have been investigated in this chapter. Initially, the GIS-overlay between slope map and landuse was employed to infer the potential source area. It showed that potential major sources were identified in the upper slope landuse shrub and outcrop with slope >55. Then, 2993 point sampling were randomly selected in the potential major source area.

The unknown source of rockfall was inferred from back analysis of rockfall deposits inventory. Once the surface rasters were created and the parameters were input, the rockfall trajectory has been determined as the interaction between rock and slope. It produced line trajectory. The boulder inventory was traced back using the trajectory to a point where the point of potential source existed. This point was determined as the reliable source of the rockfall.

The reliable final trajectories and the effect of COR were verified with a sensitivity analysis. The result suggested that the changing COR value may effect

slightly, but it did not significantly affect the travel distance of rockfall in Gunung Kelir area. COR values have little effect on the travel distance and the travel distance is more affected by the source location and topography.

Once the potential of rockfall sources is identified; reliable trajectories, frequency and energy of rockfall can be mapped. The rockfall susceptibility map is represented by rockfall frequency and energy. Both frequency and energy map obtained from a trajectory simulation based on the identified potential rockfall sources can represent the physical characteristic of rockfall movement and susceptibility degree. 2D DDA was applied to explore the motion behavior of rockfall in the highest potency of high risk. The result shows that the boulder in the northern part can potentially cause the building damage. More attention should be prioritized in northern and middle part that can potentially cause building damage.

REFERENCES

Agliardi, F.,Crosta, G. B., Frattini, P. Integrating rockfall risk assessment and countermeasure design by 3D modelling techniques. *Nat. Hazards Earth Syst. Sci., 9, 1059-1073*, 2009.

Australian Geomechanics Society. (2007). *Guideline for Landslide Susceptibility, Hazard and Risk Zoning for Land Use Management*. Australian Geomechanics Society Landslide Taskforce Landslide Zoning Working Group. Australian Geomechanics Society 42 (1).

Chen, G. 2003. Numerical Modelling of Rockfall using Extended DDA. *Chinese Journal of Rock Mechanics and Engineering, 22 (6):926-931*.

Copons, R., Vilaplana, J. M., Corominas, J., Altimir, J., Amigo, J. 2004. Rockfall risk management in high-density urban areas: The Andorran experience in *Landslide Hazard and Risk*, New York, John Wiley and sons, p. 673-695.

Crosta, G. B. and Agliardi, F. A methodology for physically based rockfall hazard assessment, *Nat. Hazards Earth Syst. Sci*., 3,407–422, 2003.

Fell, R., Corominas, J., Bonnard, C., Cascini, L., Leroi, E., and Savage, W. 2008.

Guidelines for landslide susceptibility, hazard and risk zoning for land use planning, *Eng. Geol.*, 102, 85–98.

Fell, R., Ho, K. K. S., Lacasse, S., and Leroi, E. A framework for landslide risk assessment and management. In: Landslide Risk Management, (Eds) Hungr, O., Fell, R., Couture, R., Eberhardt, E., Taylor and Francis, London, 3–26, 2005.

GEO. 1998. Landslides and boulder falls from natural terrains: interim risk guidelines, GEO Report 75, Geotechnical Engineering Office, Civil Engineering Department, Hong Kong, 183 pp.

Hungr, O and Evans, S. G. 1988. Engineering evaluation of fragmental rockfall hazards, Proceedings 5th International Symposium on Landslides, Lausanne, Switzerland, 1, 685–690.

Lan, H., Martin, C. D., and Lim, C. H. RockFall analyst: a GIS extension for three-dimensional and spatially distributed rockfall hazard modelling, *Computer and Geoscience*, 33, 262–279, 2007.

Levy, C., Jongmans, D., & Baillet, L. Analysis of seismic signals recorded on a prone-to-fall rock column (Vercors massif, French Alps). *Geophysical Journal International*, 186(1), 296-310, 2011.

Peila, D., Oggeri, C., Castiglia C. Ground reinforced embankments for rockfall protection: design and evaluation of full scale tests, *Landslides* 4 : 255-265, 2007.

Raetzo, H., Lateltin, O., Bollinger, D., Tripet, J.P. 2002. Hazard assessment in Switzerland – Codes of Practice for mass movements. *Bulletin of Engineering Geology and the Environment*, vol. 61, no. 3, p. 263-268.

Rocscience. 2014. Rocscience Coefficient of Restitution Table. Accessed from https://www.rocscience.com/help/rocfall/webhelp/baggage/rn_rt_table.htm.

Sasaki, Y., Dobrev, N., Wakizaka, Y. 2002. The detailed hazard map of road slopes in Japan, *Instability – Planning and Management*, London, Thomas Telford, p.

381-388.

Shi, G and Goodman, R. E. 1985. Two dimensional Discontinuous Deformation Analysis. *International Journal for Numerical and Analytical Methods in Geomechanics, vol. 9, pp. 541-556*.

Shi, G. 1989. Discontinuous deformation analysis a new numerical model for the static and dynamics of block systems. *Ph.D thesis*. Berkeley University of California.

Shi, G and Goodman, R. E. 1989. Generalization of Two-Dimensional Discontinuous Deformation Analysis for Forward Modelling. *International Journal for Numerical and Analytical Methods in Geomechanics, vol. 13, pp. 359-380*.

van Bemmelen R.W. *The geology of indonesia, Vol. II*, Government Printing Office the Hague, 1949.

Varnes, D.J. *Landslide hazard zonation*: *a review of principles and practice*. United Nations Educational, Scientific and Cultural Organization (UNESCO). Paris, 1984.

Volkwein, A., Schellenberg, K., Labiouse, V., Agliardi, F., Berger, F., Bourrier, F., Dorren, L. K. A., Gerber, W., Jaboyedoff, M. 2011. Rockfall characterisation and structural protection—a review. Nat Hazards Earth Syst 11:2617–2651.

Westen van, C. J., Asch van, T. W. J. and Soeters, R. Landslide hazard and risk zonation-why is it still so difficult?. Bull. Eng. Geol. Env. DOI 10.1007/s10064-005-0023-0, 2005.

CHAPTER 6

INTEGRATING STATISTICAL AND PHYSICAL MODEL FOR QUANTITATIVE ROCKFALL RISK ZONING BASED ON LANDFORM ANALYSIS

6.1 INTRODUCTION

Risk analysis is one of the mandatory procedure in disaster risk reduction program. A Rockfall risk reduction program may vary depend on the degree of hazard and the availability of budget and resources. Several rockfall reduction programs in practice include structural and nonstructural preventive measures, i.e. structural protection, land use planning and evacuation management. Practical considerations for the establishment of rockfall protection is an important issue for administrators and stakeholders in the rockfall prone area (Corominas et al., 2005; Jaboyedoff, et al., 2005; Fell et al, 2008). In a rockfall prone area, structural protection measures are considered, but identifying the situation and processes that may cause harm to persons, buildings, infrastructure and facilities by appropriate landuse planning is also essential. It needs spatial zoning which ranks the degree of potential rockfall susceptibility and risk.

Spatial zoning is intended to divide an area into homogeneous domains or characteristics and give a ranking based on the degree of actual or potential rockfall susceptibility, hazard or risk or capability of certain hazard-related regulations (JTC-1, 2008). Rockfall spatial zoning based on quantitative risk analysis will not be simple to achieve in practice (Crosta and Agliardi, 2003) due to the complex nature of rockfall process, the unavailability of the complete rockfall data base and insufficiency of damage data. These limitations make the quantitative rockfall risk analysis rather

difficult. Frequency, the probability of rockfall across an area, the probability of impact on elements at risk and vulnerability should be taken into account in quantitative risk analysis.

Frequency analysis requires detailed rockfall inventory which contains at least the location and the dimension of the blocks. However, complete inventory data are not available in many developing countries. Complete inventory data are mostly available in developed country, e.g. Grenoble French Alps, French (Dussauge et al., 2003), Yosemite California, USA (Wieczorek et al., 1992 and Guzzetti et al., 2003), British Columbia, Canada (Hungr et al., 1999) and Hong Kong (Chau et al., 2003). Several laws for the frequency-magnitude of rockfall have been proposed by (Hungr et al., 1999) and (Dussauge et al., 2002) based on those complete historical data. They proposed that the magnitude-frequency distribution of rockfall events follows a power law distribution. Then, it is some possibilities to relate incomplete rockfall data (e.g. missing on the event date) with the magnitude-frequency of complete historical data (Agliardi et al., 2009).

Probability across an area also defined as onset susceptibility employed several approaches based on: a) the objective of the assessment i.e. the design and evaluation of protection measures (Corominas et al., 2005, Volkwein et al., 2011), landuse planning (JTC-1, 2008; AGS, 2007); b) the method of calculation i.e. GIS techniques (Guzzetti et al., 2002; Lan et al., 2007), numerical model (Chen, 2003; Agliardi and Crosta, 2003); and c) the scale of the study area i.e. site specific/large scale (Jacopo et al., 2013), medium scale (Loye et al., 2009), small scale (Guzzetti et al., 2004; Michoud et al., 2012).

Vulnerability or degree of loss of an element at risk affected by hazard can be analyzed quantitatively by vulnerability curves derived from element at risk damage data and estimated impact energy of rockfall. However, vulnerability curves derived from historical damage data is difficult to be obtained due to unavailability of data. Thus, the empirical approach is often used to calculate rockfall vulnerability.

A landuse planning practice usually needs rockfall zoning map which can divide land into homogeneous areas or domains and can represent both physical characteristics

of rockfall movement and the characteristic of local topography. The author proposes automated landform classification to address this issue. Geomorphometry approach is employed to generate generic landform unit which is relevant to rockfall process.

The 9-unit slope model (Dalrymple et al., 1968 i.e. interfluves, seepage slope, convex creep slope, fall face, transportational midslope, colluvial footslope, alluvial footslope, channel wall and channel bed) are employed as geomorphological unit. Unsupervised fuzzy k-means is applied to classify the generic landforms class automatically and to minimize the subjectivity of the interpreter. Landform classes can pose important zones of rockfall process where energy and velocity are diverse in places.

In this chapter, the author proposes a comprehensive risk approach integrating relevant stage of quantitative rockfall risk analysis and geomorphological analysis in a scarce data environment area. Landform class is used as a mapping unit to evaluate the occurrence probability, the colliding probability and the physical vulnerability with particular boulder size in space and time. The risk to building and the risk to person inside the building are calculated based on the chance of loss (in monetary term) during a specified time.

6.2 WHAT IS LANDFORM?

Geomorphology is a study of landform (Lobeck, 1939). Furthermore, Verstappen (1983) explained that geomorphology is a science that studies landform forming earth surface, whether in the land or in the submarine that focuses on the forming process and the development in the future, and its relationship with the environment. Land surface is defined as continuous form which covers the whole globe (both subaerial and subaqueous) on the earth, moons, asteroids and other planets (Evans, 2011). Landform (or geomorphometric object) is a division of the land surface which may be discontinuous/discrete, bounded by topographic discontinuities.

A landform may have (relatively) uniform morphometry such as peak, valley, plateau, canyon, cliff, etc. It involves information about slope morphology, geomorphological processes, and topological characteristics. The classification or the name of landform, i.e. peak, valley, plateau, cliff, etc., may diverse from place to place

depends on the detail of the investigation (mapping scale concept) and the complexity of natural feature. It differs in terms of different characteristics of each landform such as shape, size, orientation, relief and contextual position.

Nowadays, land surface is usually presented as contour lines or DTMs (Digital Terrain Models). Landform classification is usually based on contour map reading, interpretation of stereoscopic aerial photograph, and DTMs analysis. Each method has pros and cons. The delineation or delimitation of land surface into a meaningful element of land surface, which has information of slope morphology, relief, geomorphological processes and topological characteristic, is called landform classification or geomorphological mapping.

Landform analysis (delineation and classification procedure) based on the stereoscopic technique of aerial photo and field investigation is very common in Indonesia. It has been applied for soil mapping, land evaluation analysis, land suitability analysis, spatial planning, and so on. There is also mentioned in Indonesia's National Standard document of Geomorphological Mapping that the technical requirement for geomorphological mapping is an interpretation of remote sensing data combined with field measurement (SNI, 2002). The standard landform classification in Indonesia is based on the ITC Classification System (Zuidam, 1983).

However, the traditional method of landform classification requires simultaneous consideration and synthesis of multiple different criteria (MacMillan and Shary, 2009) and the quality depends on the skill of interpreter. The development of landform classification has been applied mostly in soil landscape studies. Thus, the author try to automatically classify landform based on the 9-unit slope model which is appropriate to rockfall analysis. Even though, the 9-unit slope model is significant for pedogeomorphic process response (Conacher and Dalrymple, 1977), it is also relevant for preliminary rockfall risk zoning.

The detailed geomorphological information is very useful in many fields of study and application. It offers a comprehensive discussion related to another aspect. For instance, the study of hazard analysis will be very beneficial if it is analyzed in the

context of geomorphology (Panizza, 1996). Here, geomorphometric analysis can be used as a tool for incorporating disaster risk reduction and transfer measures into development planning. This provides basic ideas for planning priorities in promoting the risk management plan and strategy, and evaluating spatial planning policies. Thus, by using geomorphometry as a preliminary tool for risk assessment, the spatial planning manager can make a balance between minimizing risk and promoting some development priorities.

6.3 STUDY AREA

Gunung Kelir is located in the western part of Yogyakarta Province, Indonesia (see Figure 5.1). It lies in the upper part of Menorah Dome that is located in the central part of Java Island. The area is dominated by Tertiary Miocene Jonggrangan Formation that consists of calcareous sandstone and limestone. Bedded limestone and coralline limestone, which form isolated conical hills may also be found in the highest area surrounding the study area. Weathering, erosion, and mass movement commonly occur in the study area.

The average annual rainfall in Gunung Kelir is 2478 mm The highest rainfall intensity usually occurs from February to March Rainfall intensity fluctuation influences the geomorphology process. The degree of weathering, erosion, and landslide are mostly caused by high intensity of precipitation. Therefore, it will influence the development of landform and actually the prolonged rainfall can trigger the abundant of landslide.

Landforms in Gunung Kelir are a product of the final uplifting of the Complex West Progo Dome in the Pleistocene. The slope gradient of escarpment varies between 50° and 80°, meanwhile mean of slope gradient is 23.14°. The elevation ranges from 600 to 837.5 m. There are 152 buildings exposed as elements at risk in the lower slope of the escarpment.

There were 130 respondents that have been interviewed in order to observe socioeconomic characteristic of elements at risk in Gunung Kelir area. Most respondents (66.6%) work in agricultural sector. Cassava, ginger, corn, coffee, clove, lengkuas

(*galangale*), kunyit (*turmeric*), and groundnut are the predominant agricultural plantation in Gunung Kelir area. There are 87.7% of respondents have low income less than 1,000,000 IDR. The low-level income may affect the level of education which is relatively low with 56.9% did not graduate primary school (junior high school) and only 17.7% and 7.7% graduated from junior high school and senior high school.

The socioeconomic characteristic of the residents can affect the degree of vulnerability. There were also increasing trends in landuse change as shown by the increasing of the number of housing development. Based on the interview, there were 1, 13, 10, 30 and 73 houses that were constructed during <1931, 1931-1950, 1951-1970, 1971-1990, and 1991-2010 respectively. The increased number of housing development can increase rockfall risk in Gunung Kelir area.

6.4 AUTOMATED LANDFORM CLASSIFICATION

6.4.1 MODIFIED 9-UNIT SLOPE MODEL

Geomorphological opinion by the investigator is commonly used to classify landform through interpretation of aerial photos and field survey. However, subjectivity of investigator hinders application of this method. Therefore, unsupervised landform classification based on the 9-unit slope model is proposed in the present study. The main objective is to provide an automated landform classification, particularly for rockfall analysis. Several variables should be prepared before automated landform classification analysis. It includes morphometric and hydrological variables which can represent slope morphology, relief, geomorphological processes, and topological characteristics.

The 9-unit slope model is originally applied to pedogeomorphic process response (Conacher and Dalrymple, 1977). The original classification of 9-unit slope model should be modified if it is applied in different places. It should consider the genetic working on the specific landforms.

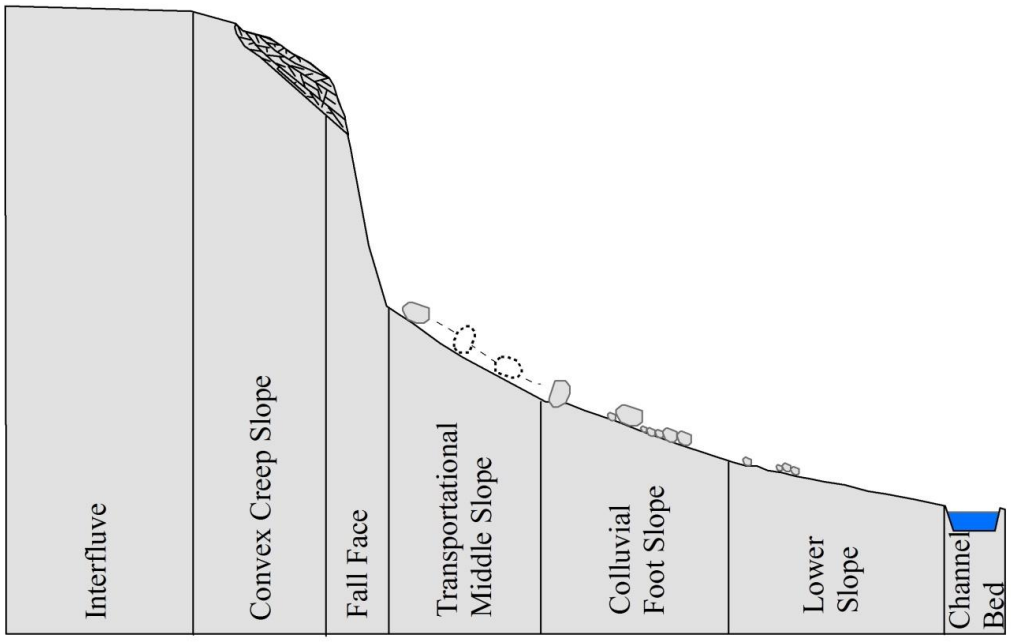

Figure 6.1 Modified 9-unit Slope Model for Preliminary Rockfall Risk Analysis

Table 6.1 Definition of Landforms modified from 9-unit Slope Model

No.	Landform Class	Definition
1	Interfluve	Divide area
2	Convex creep slope	Upper convex zone characterized by creep if soil development exists. The area adjacent to fall face is a potential rockfall source
3	Fall face	Steep slope, potential rockfall source with high weathering and cracking, dominated by falling process.
4	Transportational middle slope	A transportation zone of rockfall, characterized by concave slope, and high velocity of rockfall movement.
5	Colluvial foot sope	Convex slope, starting point of velocity decrease, and depositional region of rockfall.
6	Lower slope	Undulating to near flat zone, rockfall boulder may be found, but in small number
7	Channel bed	Stream channel

The author proposed a modified 9-unit slope model which is relevant for preliminary rockfall risk zoning (Figure 6.1). The final classification of landform elements i.e. interfluves, convex creep slope, fall face, transportational middle slope, colluvial footslope, slope and channel bed is different with the original classification of the 9-unit slope model. The definition of modified 9-unit model is described in Table 6.1.

6.4.2 MORPHOMETRIC AND HYDROLOGICAL VARIABLES

Automated landform classification needs several variables related to morphometry and hydrology. Several morphometric and hydrological variables such as slope, plan curvature, SPI (Stream Power Index) and SCI (Shape Complexity Index) (Figure 6.2-6.5) were generated based on DTM processing. Morphometric variable describe the morphology of the surface. Whereas, hydrological variable describe potential flows of material. DTM-derived products were processed in ILWIS software with several available scripts in Hengl et al. (2009).

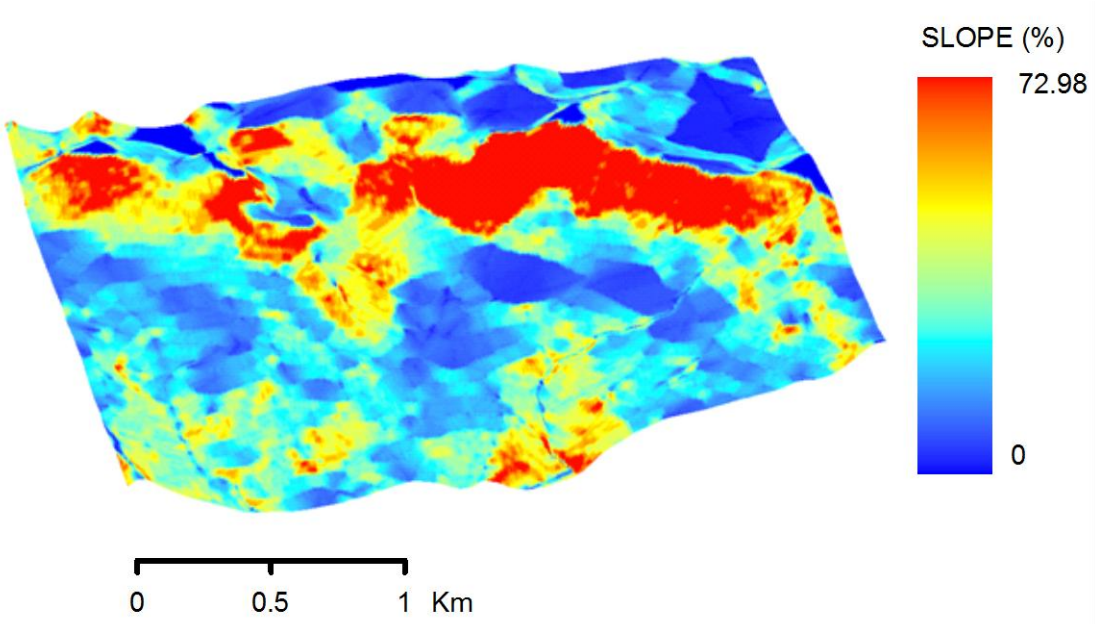

Figure 6.2 Morphometric Variable: Slope

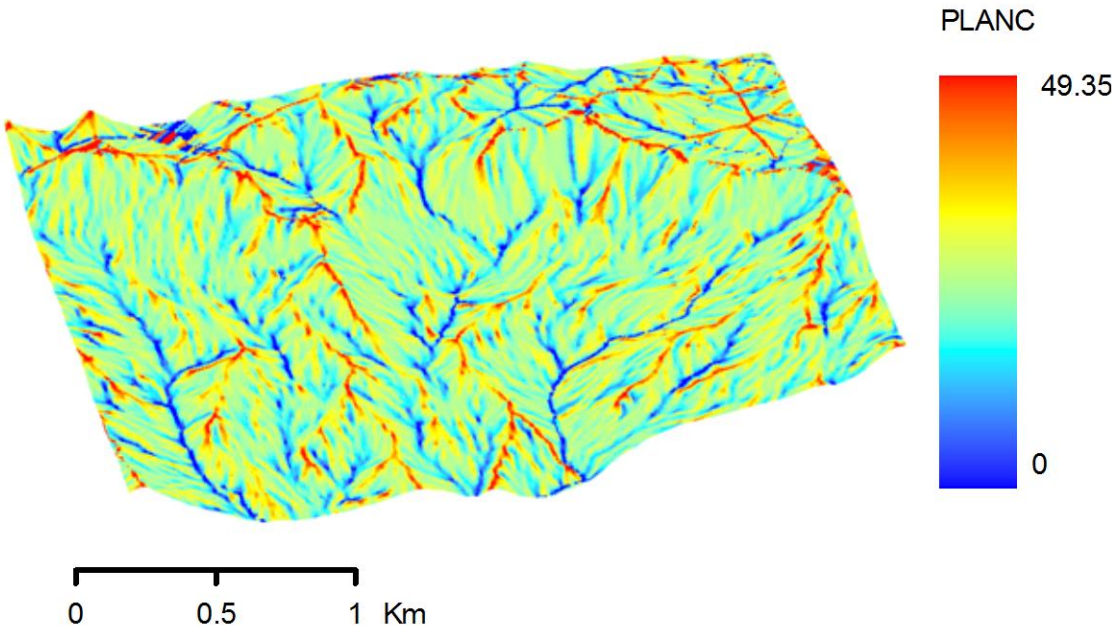

Figure 6.3 Morphometric Variable: Plan Curvature

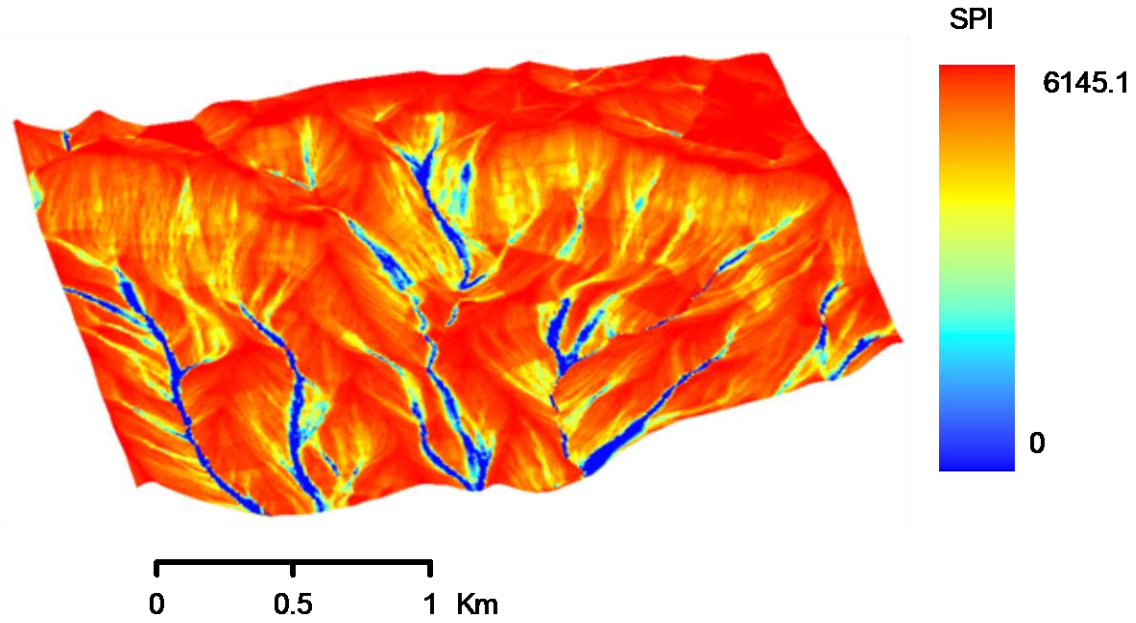

Figure 6.4 Hydrological Variables: Stream Power Index

Slope gradient might be the most substantial parameter to define landform. It represents the general morphology of landform and is used as a key variable to compute

another variables. In rockfall process, slope plays important in determining the movement of boulder and may represent the location source and deposition area of rockfall.

Plan curvature represents the curvature of the corresponding normal section, which is tangential to contour. Negative value represents that the normal section concavity is directed up, whereas positive represents the opposite case. The curvature of the slope will affect the morphology or the shape of the slope. Then, it will affect the direction and acceleration of boulder in the terrain.

SPI (Stream Power Index) was used to describe the potential flow erosion. It represents the strength of stream power and potential erosion with the idea that if a specific catchment area and steepness of the slope increase, the amount of water produced by upslope area and the velocity of water flow increase. SPI can be defined as (Hengl, et al., 2003):

$$SPI = A_f \cdot \tan\beta \qquad (6.1)$$

where A_f is the specific catchment area draining through the point and β is the slope angle.

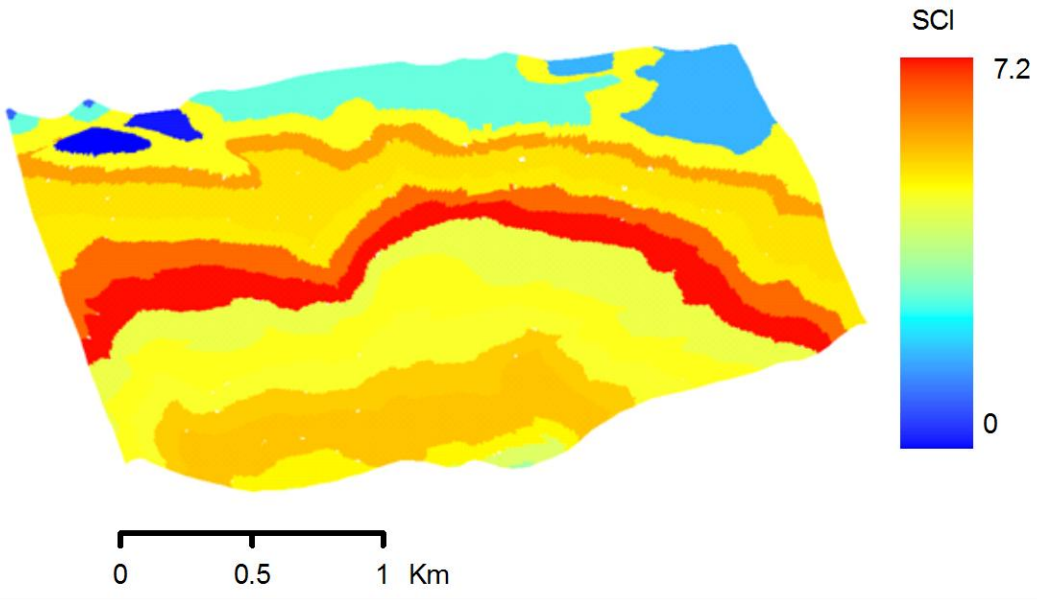

Figure 6.5 Morphometric Variables: Shape Complexity Index

Shape complexity index, sliced using an equal interval 25 m, was measured as the complexity of outline of 2-D object (Figure 6.5). It was calculated using perimeter to the boundary ratio of sliced feature:

$$SCI = \frac{P}{2r\pi} \qquad r = \sqrt{\frac{A}{\pi}} \tag{6.2}$$

where P is the perimeter of the polygon, A is the area of polygon and *r* is the radius of circle with the same surface area. SCI indicates how oval feature is. Low value of SCI represents how simple and compact a feature is. It also represents the local topological characteristics of landform.

The other morphometric variables were rockfall velocity and kinetic energy (Figure 6.6 and 6.7). There were processed by RockFall Analyst as an extension of ArcGIS (Lan et al., 2007) and discussed in chapter 5. It included modeling of rockfall trajectory by a kinematic algorithm and raster neighbourhood analysis to determine velocity and energy of rockfall. Rockfall velocity and energy analysis needed information about slope geometry and other parameters such as coefficient of restitution .

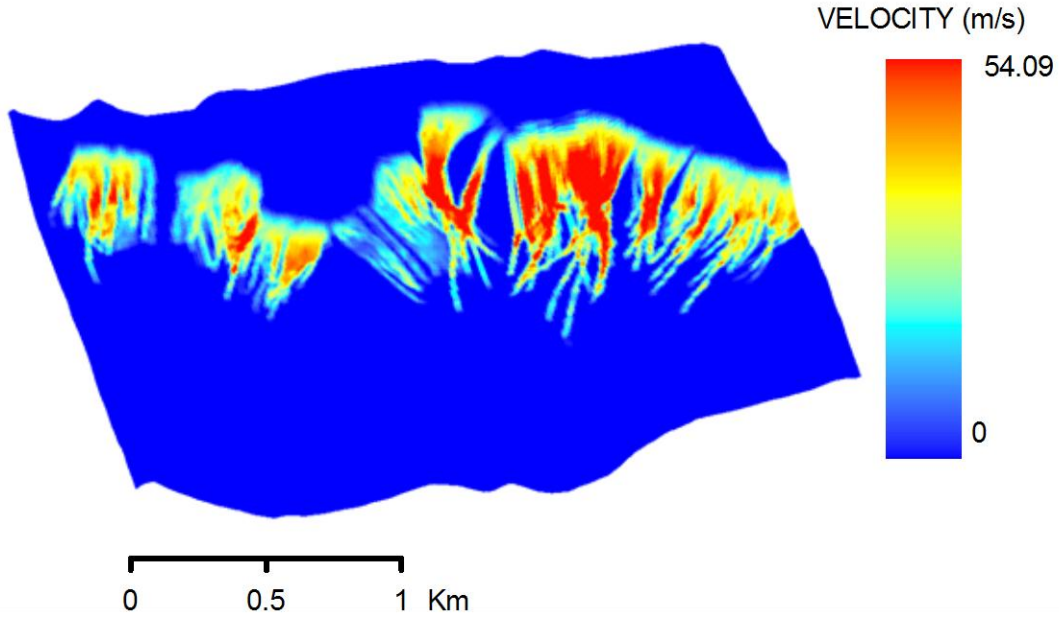

Figure 6.6 Morphometric Variable: Velocity

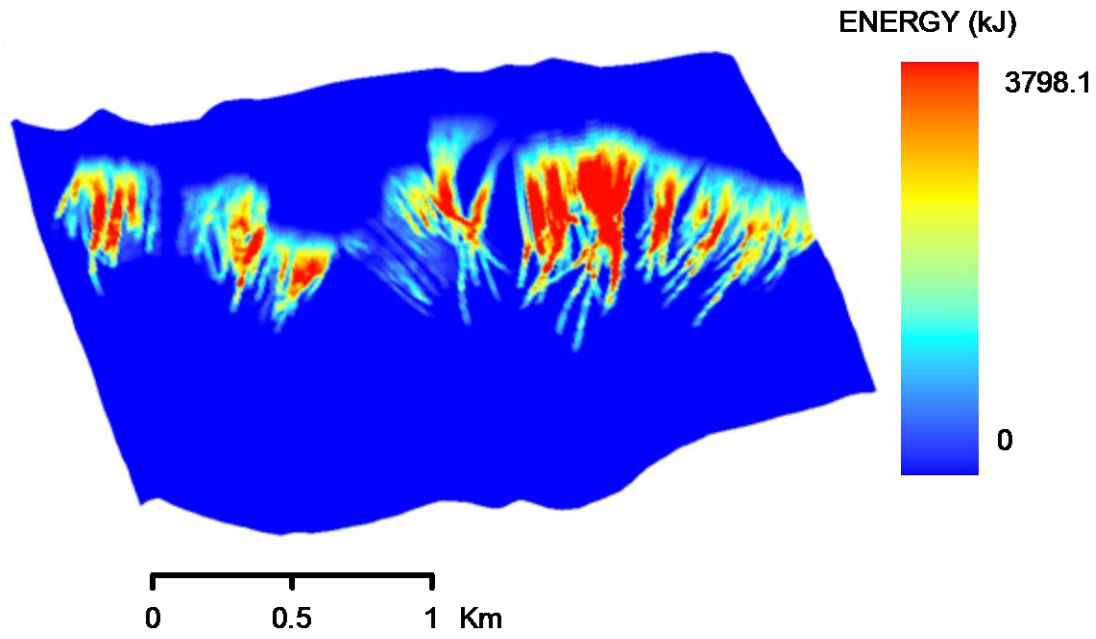

Figure 6.7 Morphometric Variable: Kinetic Energy

6.4.3 CLASSIFICATION ALGORITHM

Fuzzy k-means classification was employed to automatically delineate landform in Gunung Kelir area. It is also called as a continuous classification because of the continuity of the classes in attribute space. The method provides for class overlap which is so often found in the natural phenomenon. The degree of each an individual belongs to a given class is not expressed in binary term Yes or No. It belongs to a given class expressed by a continuous membership value that ranges in 0-1 or in 0-100. Thus, it is suitable for the situation where there is an affinity between a landform class.

The algorithm was discussed by (Irvin, et al., 1997) as an iterative procedure which start with an initial random allocation of the objects to be classified to *k* cluster. The center of each cluster, e.g. Table 6.2 is calculated as weighted average. Pixel values are reallocated among the classes based on the relative similarity between pixels value and clusters. This was calculated based on the Euclidian distance metrics. It will stop until a stable solution is reached, meaning similar pixel value are grouped together in a cluster. The membership value gives the degree of affinity which is related to the class center.

Table 6.2 Class Centres for each Morphometric Variable

Landforms	Slope (%)	PlanC	SPI	SCI	Energy (kJ)	Velocity (m/s)
Interfluve	0	0	1.0	0	0	0
Convex creep slope	6.0	5.0	3.0	5.0	0.5	0.2
Fall face	40.0	-2.0	50.0	5.5	800.0	20.0
Transportational middle slope	10.0	-1.0	30.0	7.2	1800.0	30.0
Colluvial foot slope	4.0	2.0	15.0	5.0	400.0	10.0
Lower Slope	5.0	2.0	75.0	5.0	0	0
Channel bed	5.0	-5.0	400.0	3.0	0	0
Std/variation	5.79	4.30	158.1	1.4	138.9	3.0

The landform elements were derived, as the 9-unit slope model, by using the unsupervised fuzzy k-means algorithm (Burrough et al., 2000) as

$$\mu_{ic} = \frac{[(d_{ic})^2]^{-1/(q-1)}}{\sum_{c'=1}^{k}[(d_{ic})^2]^{-1/(q-1)}} \tag{6.3}$$

where μ is the membership of *i*th object to the *c*th cluster, *d* is the distance function which is used to measure the similarity or dissimilarity between two individual observations, q is the amount of fuzziness or overlap (q=1.5). Supervised k-means classification was written and applied in ILWIS 3.3 script with an additional class center for each morphometric variable (Table 6.2).

Fuzzy k-means classification is illustrated in Figure 6.8. The 9-unit slope model was modified by excluding alluvial toe slope and seepage slope for the final landform classification. Channel wall was also modified as lower slope. Since the study area is located in the upper part of Kulon Progo Dome, the depositional process of alluvium does not work in such an area. Seepage slope was merged with interfluves because both are more related to pedogeomorphic process rather than gravitational process.

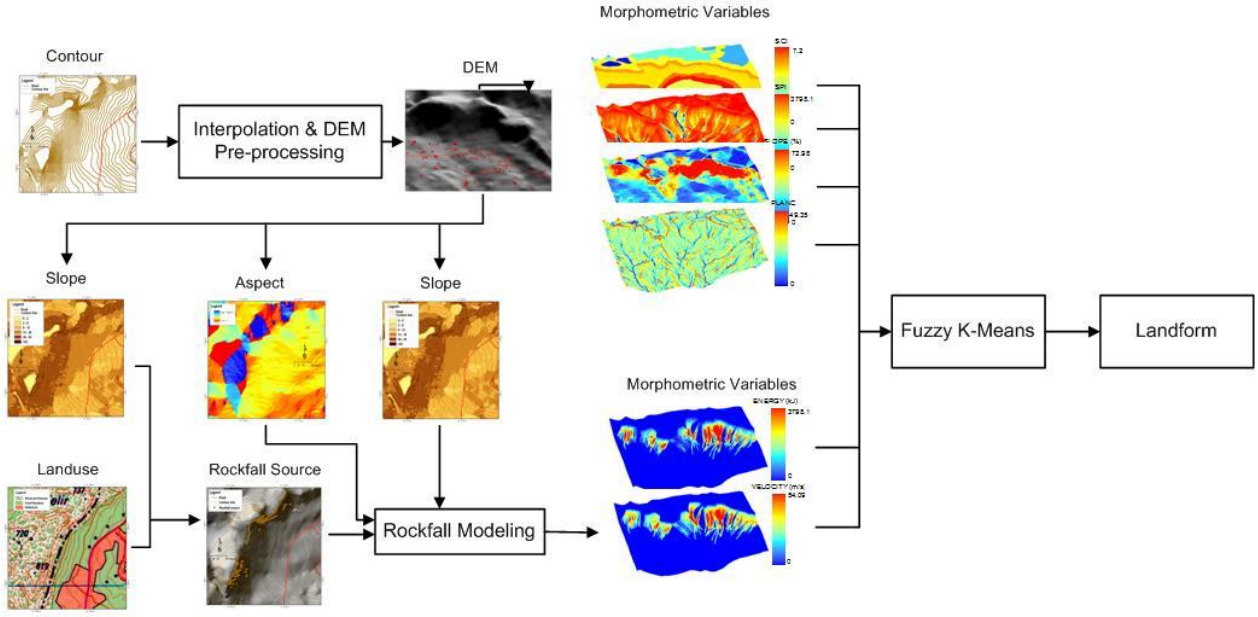

Figure 6.8 Illustration of Automated Landform Classification in Gunung Kelir area

6.4.4 PRELIMINARY RISK ZONING BASED ON LANDFORM CLASSIFICATION

Both frequency and energy map obtained from trajectory modelling represents the physical characteristic of rockfall movement. Rockfall trajectory simulation also needs many parameters and extensive field work, especially to investigate the boulder deposits along the escarpment. The problem may arise when there are no adequate data to employ trajectory modelling. Additionally, for landuse planning practice, it needs susceptibility map which can represent both physical characteristics of rockfall movement and the characteristic of local topography. The author proposed automated landform classification to address this problem. Geomorphometry approach was employed to generate generic landform unit which is relevant to rockfall process.

Geomorphometry defined as quantitative landform analysis (Pike et al., 2008) was initially applied for the assessment and mitigation of natural hazard (Pike, 1988). Dijke and Westen (1990), for example, introduced rockfall hazard assessment based on geomorphological analysis. Later, Iwahashi et al. (2001) analyzed slope movements based on landform analysis. Both utilized DTMs derived from interpolation of 1:25.000 scale contour maps to analyze geomorphological hazard. Nowadays, the interpolation of

contour map is still powerful to create medium scale mapping when better resolution DTMs are not available. However, reduction of error in interpolation of contour map is needed to obtain plausible geomorphological feature.

The result of DTM pre-procesing shows that padi terraces still exist where the sampling point of elevation data are unavailable. In addition, "flattening" topography can also be found on slopes less than 2%. Remaining padi terraces mostly occur in the transportational middle slope and flattening phenomenon mostly occurs in the interfluves. Both errors influence the plausibility of slope (Figure 6.3), but do not much influence the final classification of landform elements (Figure 6.9).

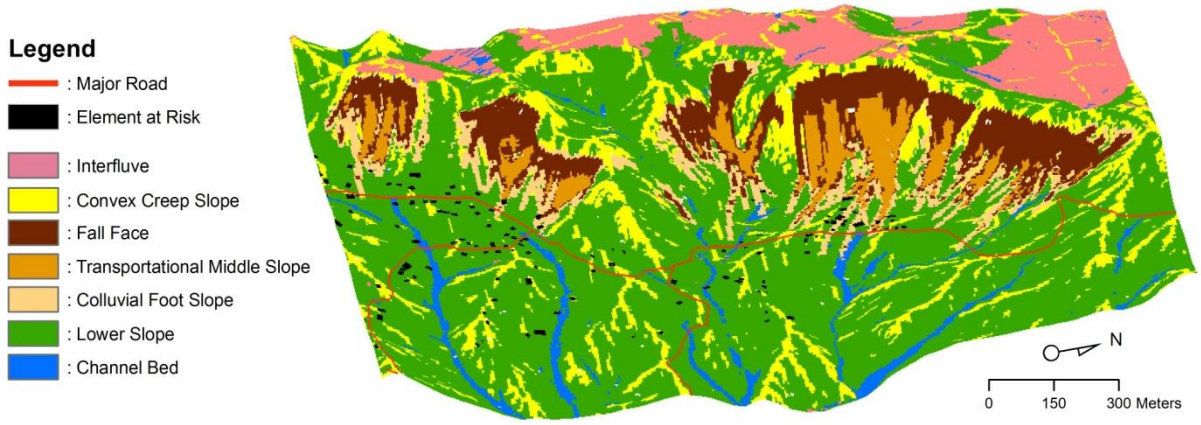

Figure 6.9 Generic Landforms in Gunung Kelir

Prior to data analysis, fundamental decision should be made in relation to the number of landform class and the selection of morphometric variables to be used. Final classification of landform elements should represent appropriate semantic description related to rockfall processes.

Modified 9-slope model was used to represent conceptual entities of rockfall deposition in each slope segment. Convex creep slopes represents a potential rockfall source. Considering that its position is adjacent to fall face, convex creep slopes and the upper part of fall face are the most potential for rockfall sources. A big boulder, which potentially fall, could be a part of convex creep slope and a part of fall face. Fall face represents Gunung Kelir escarpment which is dominated by slope >60° and falling

process. Velocity increases significantly in fall face and reaches a maximum in the transportational middle slope. In the transportational middle slope, velocity starts to decrease during the contact between boulder and surface. Bouncing, rolling and sliding are dominant in transportational middle slope. Some high velocity and high energy boulders may continue their movement to a colluvial foot slope. This depends on the local surface and the presence of an obstacle that can stop the movement of boulders.

Selecting morphometric variables should also consider rockfall processes, besides morphology shapes of the landscape. It should reflect the movement and deposition of rockfall boulders. Prior to morphometric variables selection, knowledge of rockfall process in relation to generic landforms should be utilized. Experience and former knowledge are involved during the selection of morphometric variables.

Morphometric variables derivation through DTM processing was divided into two parts, i.e. morphometric variables derived from RockFall analyst (velocity, energy) and from ILWIS script (slope, plan curvature, shape complexity index, stream power index). Rockfall velocity and energy are secondary derivative of DTM (Lan et al., 2007). The first derivatives (i.e. slope angle and aspect angle) were employed to compute the rockfall trajectory. Then, rockfall trajectory was used to model the rockfall velocity and rockfall energy by using neighborhood and geostatistical analysis. Velocity and energy of rockfall, as a result of gravitational slope phenomena, may be spatially correlated. Those which are closer tend to be more alike than those that are farther apart. The spatial autocorrelation can be performed with geostatistical techniques.

The highest velocity occurs in the transportational middle slope. Velocity gradually increases in the fall face and decreases in the colluvial footslope. Since the energy is also calculated from rockfall velocity, the spatial distribution pattern of energy is very similar to rockfall velocity. Both velocity and energy of rockfall are mostly influenced by slope geometry, coefficient of restitution, and friction angle. The first change of a pixel into zero velocity and energy of its neighborhood operation is determined as the end of boulder movements meaning that the rockfall boulders are deposited on this site.

Plan curvature and stream power index influence the pattern of the convex creep

slope and the channel bed. Shape complexity index, sliced using an equal interval 25 m, was measured as the complexity of outline of 2-D object. It was calculated using perimeter to boundary ratio of sliced feature. SCI indicates how oval feature is. Low value of SCI represents how simple and compact a feature is. SCI predominantly influences the spatial distribution of the interfluves, which has low value around 1, meaning that interfluves are more oval while convex creep slope and fall face are more longitudinal. Its effect on the other landforms is not apparent because the value of the shape complexity index in the lower slope is relatively homogeneous i.e. 4-5.

The generic landform result will depend on how well morphometric variables are selected to perform automated landform classification. It represents how well morphometric variable can describe the specific process working on a landform element. Its spatial dependency influences the application of automated landform mapping in different places and different geomorphological process.

The final classification result (Figure 6.10) was draped over DTM. The volume statistic rockfall deposit was employed to evaluate the coincidence between landform classification and rockfall frequency-magnitude. Since landform classification considers surface form and process, we argue that landform classification in a rockfall prone area exhibits scale-specifity (Evans, 2003). The magnitude (volume) and frequency of boulder deposits may have a specific scale related to each generic landform.

6.4.5 Implication for Preliminary Rockfall Risk Analysis

In the past, many people used to consider that natural hazards should be approached from the domain of engineering. However, both structural and nonstructural mitigation should be included in natural hazard mitigation comprising geomorphological, geographical, and geological approaches (Oya, 2001). Specific geomorphology features may pose a specific hazard. The most susceptible places, in order, for rockfall hazard in Gunung Kelir area are fall face, transportational middle slope, colluvial footslope and lower slope respectively each exhibits scale specifity.

Automated landform analysis and rockfall statistics can estimate the likelihood of rockfall magnitude in a specific landform. Each generic landform indicates the

susceptibility degree to rockfall events. The magnitude-frequency relation of rockfall can be calculated to estimate the annual frequency of rockfall events in each generic landform. It can be defined with reference to specific event magnitude class in a specific generic landform

Preliminary rockfall analysis can be delivered by evaluating elements at risk located in the susceptible place for rockfall hazard. There are 3 buildings located on the transportational middle slope and 10 buildings located on the colluvial footslope. This is useful information on which to base prioritization action for countermeasures policy and design. Geomorphologic analysis should be taken into account to locate structural measures (e.g. barriers, embankments, rock sheds) in suitable location. It will improve cost efficiency by optimizing budget and design. The information of building located on landforms classified as high susceptibility can also be an input to the prioritization of an evacuation procedure. Therefore, the prioritization of mitigation action based on geomorphometric analysis can meet the technical suitability and the effectiveness of selected mitigation options.

6.5 QUANTITATIVE RISK ANALYSIS

Risk can be defined as ”the expected number of lives lost, persons injured, damage to property and disruption of economic activity due to a particular damaging phenomenon for a given area and reference period” (Varnes, 1984). The definition is originally used to describe landslide risk. Later, the terminology is used for both landslides and rockfall. It can be expressed by the simple product of temporal probability, spatial probability, reach probability, vulnerability and value of the element at risk (Fell et al., 2005; Westen et al., 2005; Agliardi et al., 2009). The author improved the risk equation based on the expected volume or magnitude crossing particular landform as follows:

$$R = \sum_{j=1}^{4} \sum_{q=1}^{n_{ij}} P_r^{(ij)} . P_k^{(ij)} . V_{ij} . E_{ik} \tag{6.4}$$

where n_{ij} is the number of boulders with class volume j in landform i, $P_r^{(ij)}$ is the

temporal probability of rockfall in the magnitude scenario (i.e. boulder volume) class *j* and crossing landform *i*; $P_k^{(ij)}$ is the probability of the rockfall colliding element at risk *k* in the landform *i*, V_{ij} is the vulnerability of element at risk k collided by rockfall volume *j* in the landform *i* and E_{ik} is the economic value of the element at risk *k in* the landform *i*.

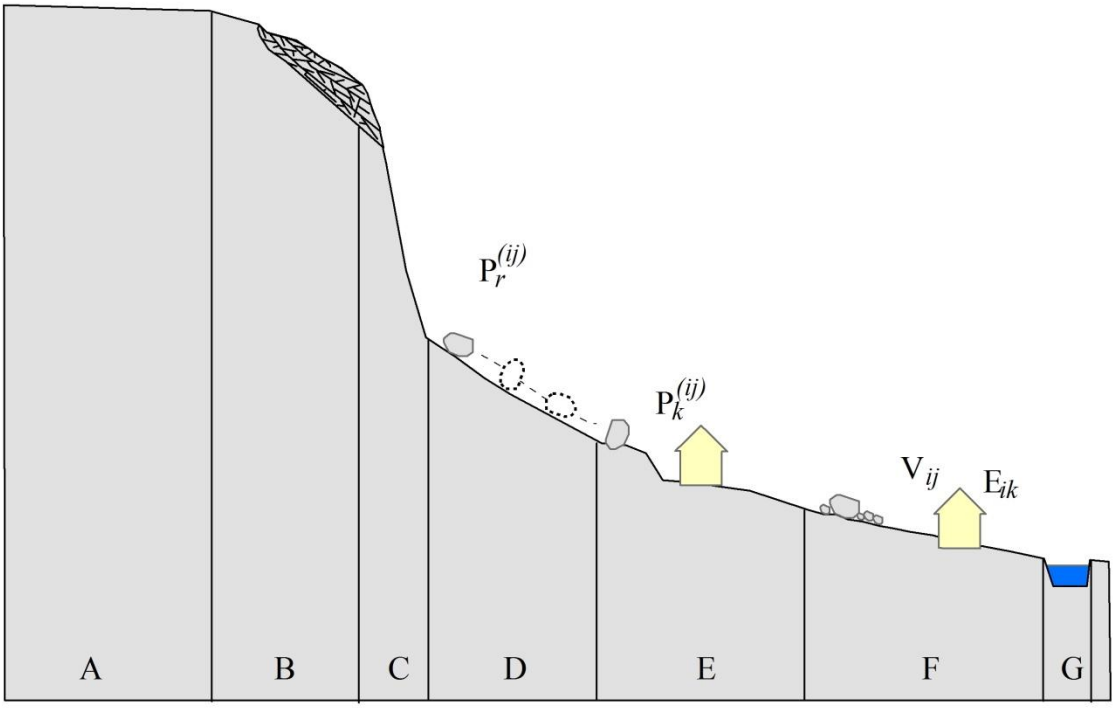

Figure 6.10 Illustration for Specific Rockfall Risk to Building based on Landform Analysis

The first two aspects of the equation 6.1 are often defined as hazard analysis (Lee and Jones, 2004). It is an estimation of spatial distribution, temporal distribution and size- frequency of rockfall which may occur in the future. The information should include the location, size (volume) or energy of the potential rockfall and any resultant detached material and the probability of their occurrence within a given period of time (JTC-1, 2008). Rockfall hazard assessment is expected to answer "when", "how frequent" and "how large" rockfall is likely to occur. Figure 6.10 illustrates the risk calculation

(equation 6.1) based on landform classes, i.e. interfluve (A), convex creep slope (B), fall face (C), transportational middle slope (D), colluvial foot slope (E), lower slope (F) and channel bed (F).

The modified 9-unit slope model (Dalrymple et al., 1968 i.e. interfluves, seepage slope, convex creep slope, fall face, transportational midslope, colluvial footslope, alluvial footslope, channel wall and channel bed) can pose important zones of rockfall process where energy and velocity are diverse in places. It can be delineated into key information for prioritization of mitigation actions. The information is useful to expose the spatial distribution of potentially high damage of elements at risk affected by rockfall. Thus, selection of preventive mitigation measure type, structural protection location, and structural protection dimension should be supported by rockfall risk assessment based on landform analysis.

6.5.1 TEMPORAL PROBABILITY

6.5.1.1 MAGNITUDE-FREQUENCY RELATION

Rockfall inventory is a key issue for hazard analysis. Research on rockfall risk is more challenging in developing country such as Indonesia, where no available rockfall catalogue is present. Inventory of rockfall boulder/blocks must be carried on by intensive fieldwork to infer the probability distribution of rockfall size. Therefore, the temporal probability of rockfall can be inferred from the magnitude-frequency distribution. It was derived from magnitude-cumulative frequency (MCF) curves constructed from rockfall inventory using graphical method (Gutenberg and Richter, 1954; Hungr et al., 1999; Dussauge-Peisser et al., 2002).

There were 16 rockfall events reported by eyewitnesses during 1970-2009 (16 events during period of 39 years) in the lower slope where the total number observed by geomorphological mapping are 58. Thus, it can be inferred that the length in years of the total 58 boulders in lower slope and in the entire area is 141 years.

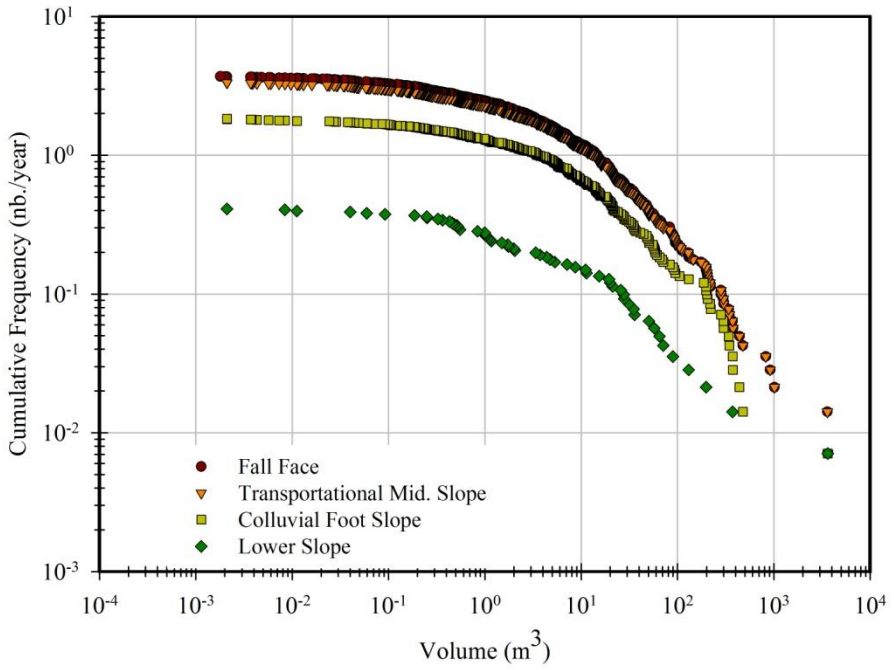

Figure 6.11 Magnitude-cumulative Frequency Curve based on Landform Class

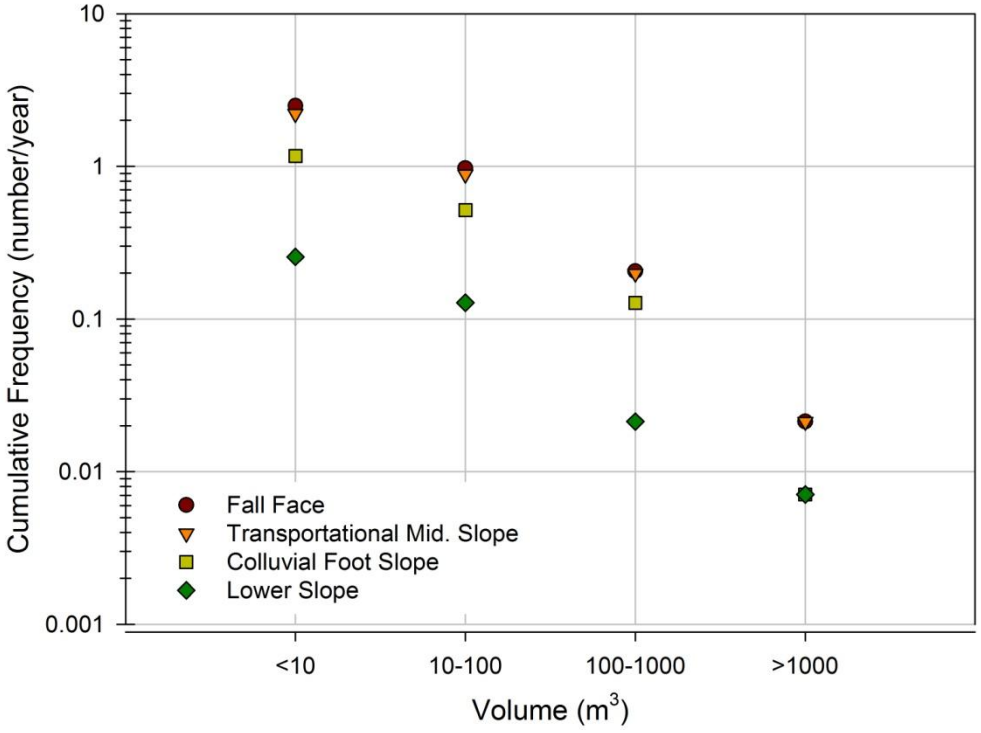

Figure 6.12 Simplified MCF Curve based on Landform and Volume Class

Magnitude-cumulative frequency curve was generated by sorting the volume of rockfall crossing each landform and accumulating the incremental frequencies from largest to smallest. The resulting magnitude-cumulative frequency (MCF) plot is shown in Figure 6.11. There were a few boulders deposited on the rockfall face, which made fall face and transportational middle slope curves is rather similar. The small difference is seen on the small volume of rockfall <1m^3. It indicates that the boulders stopped in the fall face are small boulders.

Tabel 6.3 Number of Boulders passing Landforms in Gunung Kelir Area

Landform	Vol. class (*j*)	Nb. Per class *j*	Incremental freq.
Fall Face	<10	352	2.50
	10-100	137	0.97
	100-1000	29	0.21
	>1000	3	0.02
Transp. Middle Slope	<10	312	2.21
	10-100	125	0.89
	100-1000	28	0.20
	>1000	3	0.02
Colluvial Foot Slope	<10	165	1.17
	10-100	73	0.52
	100-1000	18	0.13
	>1000	1	0.01
Lower Slope	<10	36	0.26
	10-100	18	0.13
	100-1000	3	0.02
	>1000	1	0.01

Incremental frequency (number/year) in the magnitude scenario (i.e. boulder volume) class *j* and crossing landform *i* (Fig. 6.11) can be evaluated by simplified MCF curve (Figure 6.12). For example, an incremental frequency of boulder 10-100 m^3 in the colluvial foot slope is 0.52/year. The incremental frequency of rockfall with the volume *j*

and passed landform *i* will decrease when the volume increase and decrease in the lower part of the landform arrangement (Table 6.3). However, the incremental frequency is difficult to be employed directly as temporal probability in the risk equation. Some very dangerous area with small volume boulder can have incremental frequency more than 1. It means that rockfall may occur once or more in each year. It does not represent a probability value ranging from 0 to 1. Thus, Poisson probability was employed to calculate the temporal probability of rockfall with the volume *j* and passed landform *i*.

6.5.1.2 POISSON PROBABILITY

The temporal probability of rockfall was calculated from the observation of the frequency of the past event and MCF relation. It is defined as a percent chance of one or more rockfall can reach a landform during specified time. It is similar to the hydrology analysis. In this case, rockfalls were treated as recurrent events that occur randomly and independently. Actually, this assumption does not fully accepted because once the rockfall occurs, it may change the slope morphometry which can affect the independency of future events. However, given a certain lack of understanding the physical process on the changing morphometry that control rockfall, Poisson model is one of feasible method to estimate the temporal probability of rockfall events.

The rockfall inventory data were collected and documented from field survey which is calculated in the 141-year period (521 rockfall events). The main assumption of temporal probability of rockfall is that rockfall can be considered as independent random point-events in time (Crovelli, 2000). The probability of rockfall occurrence during time *t* is:

$$P_N = P\left[N(t) \geq 1\right] \tag{6.5}$$

where N(t) is the number of rockfalls that occur during time *t* in the investigated area.

Probability model is commonly used to investigate the occurrence of independent random point-events in time i.e. Poisson model (Crovelli, 2000). The Poisson model considers naturally continuous rockfall data which is shown in Eq. 6.6.

$$P[N(t)=n]=\exp(-\lambda t)\frac{(\lambda t)^n}{n!} \qquad n=0,1,2,.... \qquad (6.6)$$

where P[N(t) = n] is the probability of experiencing *n* landslides during time *t*, λ is the estimated average rate of occurrence of rockfalls which corresponds to 1/μ, with μ is the estimated mean recurrence interval between successive failure events. The variable λ and μ can be obtained from a historical catalogue of landslide events or from a multi-temporal landslide inventory map. The probability of experiencing one or more rockfalls during time *t* (exceedance probability) as follows:

$$P[N(t)\geq 1]=1-P[N(t)=0]=1-\exp^{-\lambda t} \qquad (6.7)$$

$$P[N(t)\geq 1]=1-\exp^{\frac{-t}{\mu}} \qquad (6.8)$$

The mean recurrence interval (μ) of various predicted rockfall events can be determined by dividing the period of analysis (141 years) with the number of predicted rockfall events in each volume class *j* and crossing landform *i*. The estimated μ was used to estimated exccedance probability of having one or more rockfall in each landform (Table 6.4) by adopting a Poisson model (Eq. 6.7 and 6.8). The complete calculation of the Poisson model with *n* ranged from 1 to 352 is shown in Appendix C.

Therefore, the table of exceedance probability in different period for each landform and volume class (Table 6.4) can be used as an indication of the temporal probability of rockfall events over 100 years. For example within a 5-year period, the exceedance probability of rockfall in the volume <10, 10-100, 100-1000, and >1000 passing the lower slope are very low (0.72, 0.47, 0.10, and 0.03 respectively) compare to exceedance probability of rockfall in the volume <10, 10-100, 100-1000, and >1000 passing the transportational middle slope (1, 0.99, 0.63, and 0.1 respectively). It means that rockfall is more likely to occur on the transportational middle slope than the lower slope. The small volume of rockfall is also more likely to occur than the large one.

Table 6.4 Poisson Model for Percent Chance One or more Rockfall on each Landform, during Specified Time

Landform	Area	Number of boulders	Volume Class (*j*)	Number (n) per class *j*	Chance of one or more rockfall during specified time						
					1 yr.	5 yr.	10 yr.	25 yr.	50 yr.	100 yr.	141 yr.
Fall Face	105750	53	<10	352	0.92	1.00	1.00	1.00	1.00	1.00	1.00
			10-100	137	0.62	0.99	1.00	1.00	1.00	1.00	1.00
			100-1000	29	0.19	0.64	0.87	0.99	1.00	1.00	1.00
			>1000	3	0.02	0.10	0.19	0.41	0.65	0.88	0.95
Transportational Middle Slope	63550	211	<10	312	0.89	1.00	1.00	1.00	1.00	1.00	1.00
			10-100	125	0.59	0.99	1.00	1.00	1.00	1.00	1.00
			100-1000	28	0.18	0.63	0.86	0.99	1.00	1.00	1.00
			>1000	3	0.02	0.10	0.19	0.41	0.65	0.88	0.95
Colluvial Foot Slope	104275	199	<10	165	0.69	1.00	1.00	1.00	1.00	1.00	1.00
			10-100	73	0.40	0.92	0.99	1.00	1.00	1.00	1.00
			100-1000	18	0.12	0.47	0.72	0.96	1.00	1.00	1.00
			>1000	1	0.01	0.03	0.07	0.16	0.30	0.51	0.63
Lower Slope	285375	58	<10	36	0.23	0.72	0.92	1.00	1.00	1.00	1.00
			10-100	18	0.12	0.47	0.72	0.96	1.00	1.00	1.00
			100-1000	3	0.02	0.10	0.19	0.41	0.65	0.88	0.95
			>1000	1	0.01	0.03	0.07	0.16	0.30	0.51	0.63

6.5.2 SPATIAL PROBABILITY

The probability of colliding will differ spatially based on particular landform and the length of a building (Figure 6.13). It can also be defined as the probability of intersection of the potential rockfall trajectories from the trajectory analysis with the existing building. It needs a detailed map of building location and the length of the building. In this case, the calculation assumes that all paths have the same probability of hitting all buildings. Thus, the calculation was solely for 38 buildings that are possible to be hit by rockfall based on the trajectory analysis (Figure 6.14).

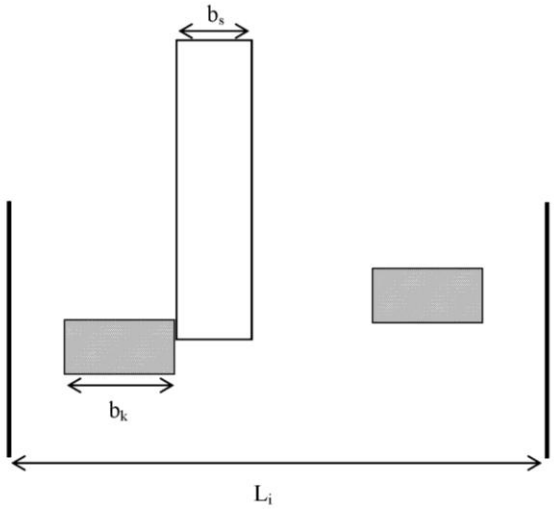

Figure 6.13 Geometrical relationship of $P_k^{(ij)}$

$P_k^{(ij)}$ was calculated using a formula based on the geometrical relationship of rockfall path, length of the building in landform *i* and the total length of landform *i*:

$$P_k^{(ij)} = \frac{b_k + b_s}{L_i} \tag{6.9}$$

where $P_k^{(ij)}$ is the probability of the rockfall colliding element at risk *k* in the landform *i*, b_k is the length of building, b_s is the path of rockfall, and L_i is the length of the possible landform corridor passed by the identified rockfall source. The path of rockfall, b_s, was estimated relative to the volume class of the rockfall given in Table 6.5.

Table 6.5 Calculated Probability of Colliding in Gunung Kelir area (One ID shows One Building)

ID	landform	Li	b_k	Path of rockfall (b_s)				Calculated probability of colliding			
				<10 m^3	10-100 m^3	100-1000 m^3	>1000 m^3	<10 m^3	10-100 m^3	100-1000 m^3	>1000 m^3
1	Lower Slope	267.75	15.4901	1.30	3.2	6.52	1.87	0.063	0.070	0.082	0.065
2	Lower Slope	267.75	15.3193	1.30	3.2	6.52	1.87	0.062	0.069	0.082	0.064
3	Colluvial Foot Slope	244.85	14.1508	1.30	3.2	6.52	1.87	0.063	0.071	0.084	0.065
4	Lower Slope	244.85	9.9404	1.30	3.2	6.52	1.87	0.046	0.054	0.067	0.048
5	Lower Slope	244.85	8.7749	1.30	3.2	6.52	1.87	0.041	0.049	0.062	0.043
6	Lower Slope	244.85	6.9371	1.30	3.2	6.52	1.87	0.034	0.041	0.055	0.036
7	Lower Slope	308.00	12.5587	1.30	3.2	6.52	1.87	0.045	0.051	0.062	0.047
8	Lower Slope	308.00	8.9677	1.30	3.2	6.52	1.87	0.033	0.039	0.050	0.035
9	Lower Slope	308.00	12.5935	1.30	3.2	6.52	1.87	0.045	0.051	0.062	0.047
10	Lower Slope	308.00	15.3069	1.30	3.2	6.52	1.87	0.054	0.060	0.071	0.056
11	Lower Slope	308.00	10.3906	1.30	3.2	6.52	1.87	0.038	0.044	0.055	0.040
12	Lower Slope	241.00	9.3985	1.30	3.2	6.52	1.87	0.044	0.052	0.066	0.047
13	Colluvial Foot Slope	308.00	9.0079	1.30	3.2	6.52	1.87	0.033	0.040	0.050	0.035
14	Lower Slope	267.75	26.0413	1.30	3.2	6.52	1.87	0.102	0.109	0.122	0.104
15	Lower Slope	267.75	24.0551	1.30	3.2	6.52	1.87	0.095	0.102	0.114	0.097
16	Lower Slope	241.00	8.3935	1.30	3.2	6.52	1.87	0.040	0.048	0.062	0.043
17	Lower Slope	241.00	11.4321	1.30	3.2	6.52	1.87	0.053	0.061	0.074	0.055
18	Lower Slope	308.00	9.4335	1.30	3.2	6.52	1.87	0.035	0.041	0.052	0.037
19	Lower Slope	241.00	9.0115	1.30	3.2	6.52	1.87	0.043	0.051	0.064	0.045

ID	landform	Li	b_k	Path of rockfall (b_s)				Calculated probability of colliding			
				<10 m^3	10-100 m^3	100-1000 m^3	>1000 m^3	<10 m^3	10-100 m^3	100-1000 m^3	>1000 m^3
20	Lower Slope	241.00	12.5213	1.30	3.2	6.52	1.87	0.057	0.065	0.079	0.060
21	Transp. Middle Slope	244.85	15.9961	1.30	3.2	6.52	1.87	0.071	0.078	0.092	0.073
22	Lower Slope	267.75	10.4239	1.30	3.2	6.52	1.87	0.044	0.051	0.063	0.046
23	Colluvial Foot Slope	244.85	13.1284	1.30	3.2	6.52	1.87	0.059	0.067	0.080	0.061
24	Colluvial Foot Slope	267.75	10.6488	1.30	3.2	6.52	1.87	0.045	0.052	0.064	0.047
25	Lower Slope	244.85	12.2034	1.30	3.2	6.52	1.87	0.055	0.063	0.076	0.057
25	Colluvial Foot Slope	308.00	13.6575	1.30	3.2	6.52	1.87	0.049	0.055	0.066	0.050
27	Lower Slope	308.00	4.1581	1.30	3.2	6.52	1.87	0.018	0.024	0.035	0.020
28	Colluvial Foot Slope	308.00	17.2770	1.30	3.2	6.52	1.87	0.060	0.066	0.077	0.062
29	Colluvial Foot Slope	308.00	10.5516	1.30	3.2	6.52	1.87	0.038	0.045	0.055	0.040
30	Colluvial Foot Slope	308.00	15.0470	1.30	3.2	6.52	1.87	0.053	0.059	0.070	0.055
31	Colluvial Foot Slope	308.00	24.9650	1.30	3.2	6.52	1.87	0.085	0.091	0.102	0.087
32	Transp. Middle Slope	308.00	15.5897	1.30	3.2	6.52	1.87	0.055	0.061	0.072	0.057
33	Lower Slope	308.00	18.6041	1.30	3.2	6.52	1.87	0.065	0.071	0.082	0.066
34	Lower Slope	308.00	15.8775	1.30	3.2	6.52	1.87	0.056	0.062	0.073	0.058
35	Transp. Middle Slope	308.00	24.9336	1.30	3.2	6.52	1.87	0.085	0.091	0.102	0.087
36	Colluvial Foot Slope	241.00	11.9446	1.30	3.2	6.52	1.87	0.055	0.063	0.077	0.057
37	Lower Slope	308.00	15.3967	1.30	3.2	6.52	1.87	0.054	0.060	0.071	0.056
38	Lower Slope	244.85	12.1212	1.30	3.2	6.52	1.87	0.055	0.062	0.076	0.057

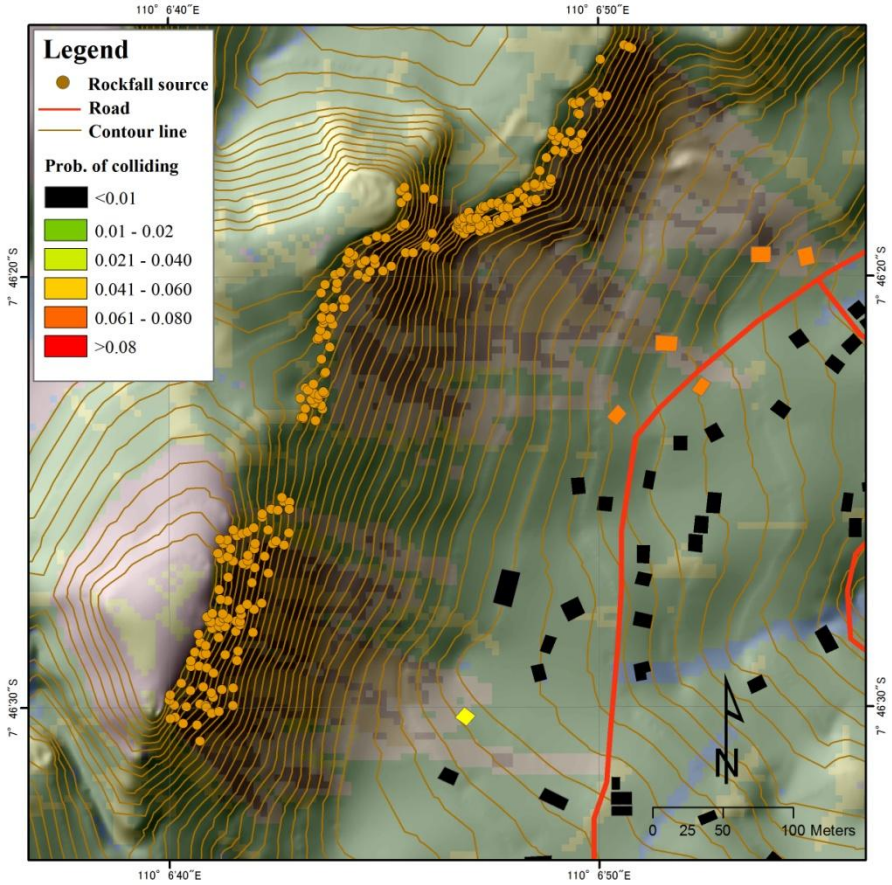

Figure 6.14 Calculated Probability of the Rockfall Colliding, an Element at Risk with Scenario Class Volume 10-100 m^3

6.5.3 VULNERABILITY AND VALUE OF ELEMENTS AT RISK

One of the important issues in risk analysis is vulnerability assessment. Recent development and debate of vulnerability analysis related to terminology (Costa and Cropp, 2012), concept (Wolf, 2012), methodological, robustness and legitimacy (Kaynia, et al., 2008; Fekete, 2011) are documented well. However, empirical quantitative vulnerability assessment of rockfall is difficult to calculate due to lack of accurate damage data.

The vulnerability of elements at risk c collided by rockfall volume *j* in the landform *i*, V_{ij}, was investigated by GIS (Geographic Information System) simulation. It considers the expected energy and the strength of a material when an element at risk / building is hit by rockfall. GIS rockfall modeling based on lumped mass (Lan, et al.,

2007) was applied to model the trajectory and energy of rockfall along the escarpment (Chapter 5).

6.5.3.1 PHYSICAL VULNERABILITY OF ROCKFALL

Ebert, et al. (2008) defines physical vulnerability as the potential damage determined by the physical structure (material and construction building) when disaster happened. Physical vulnerability was employed in this research because it directly describes the interaction between rockfall and element at risk. It is a conditional probability, given the rockfall occurs and the element at risk is on the path of rockfall movement. The classification of the physical vulnerability degree was classified based on the potential damage of building structure once hit by rockfall in a particular volume. It is expressed on a scale of 0 (no damage) to 1 (total loss of damage.

Table 6.6 The Definition of Vulnerability Index

Intensity	Type of damage	Vulnerability
I	Slight non-structural damage, stability of building structure not affected	0.01-1
II	Cracks in the wall/roof tile, stability of building structure not affected, reparation not urgent	0.2-0.3
III	Strong deformation of building structure, holes in wall, cracks in supporting structure, evacuation necessary	0.4-0.6
IV	Building structure breaks, partly destructed, evacuation necessary, reconstruction is needed partly	0.7-0.8
V	Totally destructed, evacuation necessary, complete reconstruction	0.9-1

Several factors that most affect physical vulnerability are the position of the element at risk, e.g. upper slope or down slope, the volume of the rockfall, and the velocity/energy of rockfall. Rockfall which moves slowly and/or with small volume may cause little damage to the building located on the downslope. Thus, it is important to

incorporate the volume of rockfall and the location of the element at risk in the vulnerability index. In this chapter, the author propose vulnerability index, which incorporate the volume and the location of the element at risk (with landform). Energy or velocity can be explained implicitly based on the landform analysis (Chapter 5).

Buildings in Gunung Kelir area are mostly constructed from traditional brick. The vulnerability of rockfall is often shown by the energy of rockfall impacts against loss of damage. Due to limitation on damage data, an empirical vulnerability function obtained by fitting damage and impact energy (Agliardi et al., 2009; Glade, 2003) was adapted to estimate the vulnerability degree based on landform analysis in Gunung Kelir area (Figure 6.15). The explanation of each index is shown in Table 6.6.

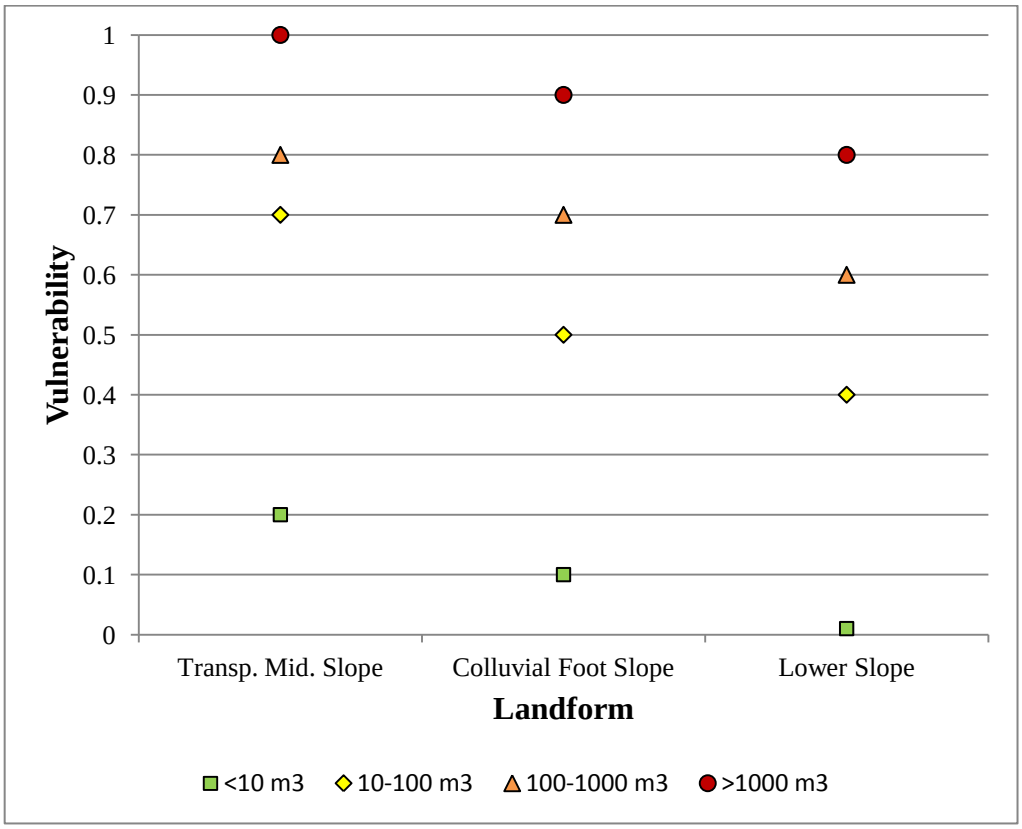

Figure 6.15 Adopted Empirical Vulnerability in Gunung Kelir Area

Vulnerability in Gunung Kelir ranges from 0.01 (slightly damage) to 1 (fully damage). It was calculated by evaluating the estimated rockfall energy and landform in each element of risk (Figure 6.16). A total loss is expected in the building impacted by

rockfall energy larger than 600 kJ which is mostly located in the transportational middle slope. Thus transportational middle slope and colluvial foot slope are expected to be high vulnerability area.

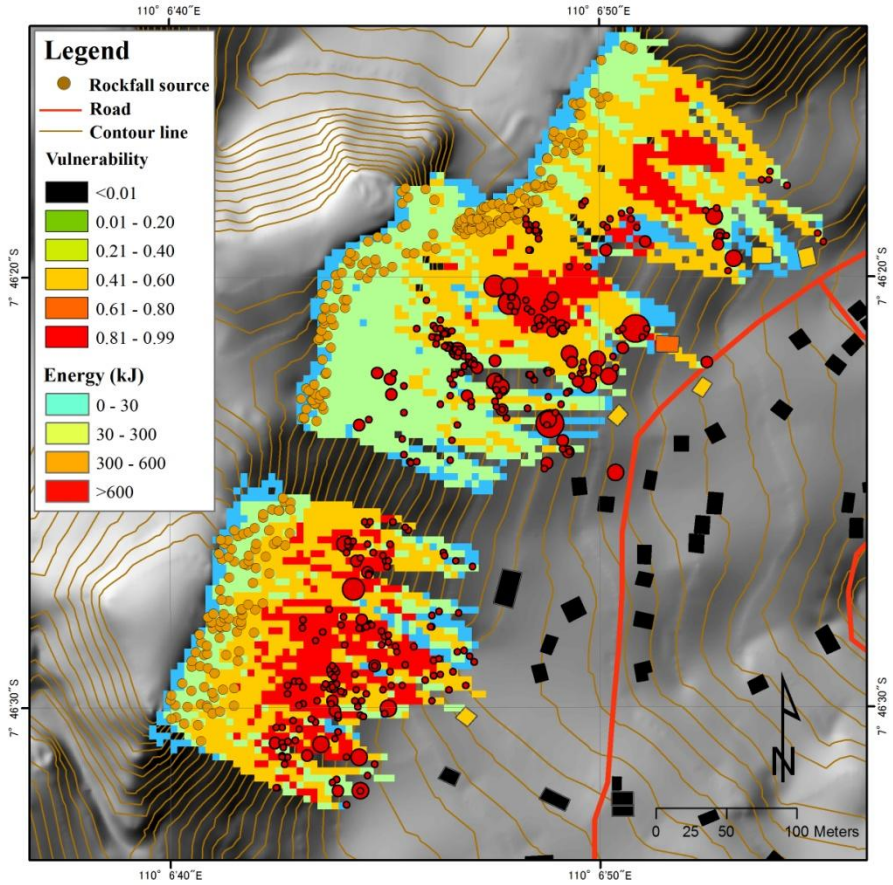

Figure 6.16 Calculated Vulnerabilty of an Element at Risk for Volume Scenario 10-100 m^3

6.5.3.2 VALUE OF ELEMENT AT RISK

There were two types of elements at risk considered in the analysis, i.e. building and population. The building represents the value of a physical assets that can be determined by the value of land and the building. The population represents the people living in the building. Both were expressed in monetary terms. The monetary term has advantages for management strategies to reduce risk based on cost benefit analysis. It is used to measure economic cost effectiveness. For example, once the risk is analyzed,

cost benefit analysis is often employed to ensure that the level of residual risk is acceptable for specific proposed land use.

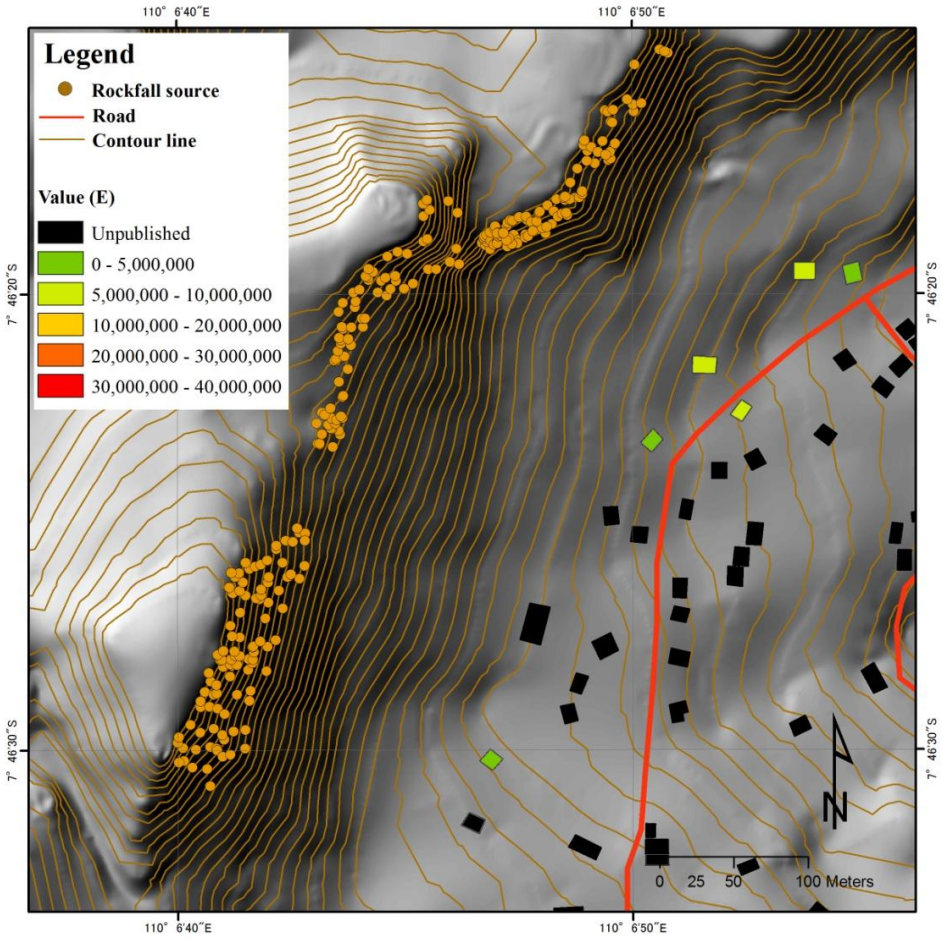

Figure 6.17 Calculated Value of Element at risk (Statistical Value of Building)

Estimating the economic losses of an element at risk is sometimes complex and problematic. Some complex analysis may include physical damage, costs of reparation/recovery process, costs of transport disruption, social costs, psychological costs, etc. To simplify the estimation, the author employed the value of building to estimate the value of element at risk. The value of building was obtained from interviews of 130 respondents living in Gunung Kelir area. It was estimated by multiplying the price of the land and building for each element at risk (Figure 6.17).

The result of vulnerability analysis shows that there is a possibility of total damage.

It may also be any of human loss of life or physical injury in Gunung Kelir area even though there was no experience of loss of life due to rockfall. The identification of human loss or physical injury is the main priorities of any risk assessment. Estimating the value of loss of life is more problematic than estimating the value of a building. It may be controversial and raise ethical and moral issues. Thus, estimating value of human life was based on the terminology of the value of statistical life-VOSL (Mooney, 1977; Jones-Lee, 1989; Marin, 1992) meaning the value of change in the risk of death, not human life itself. It is not a value of an individual is willing to pay to avoid certain death, but a value of an individual is willing to pay to reduce the risk of death.

There were methods to estimate the value of statistical life, e.g. the human capital approach and the willingness to pay (Pearce et al., 1995). The result may vary from country to country. VOSL for developed countries is in the range $1.8-$9 million, for Russia is $300,000, and for China, India and Africa are $150,000 (Pearce et al., 1995). In this research, the author used VOSL $150,000 which is equal to IDR1,650,000,000 ($1=IDR11,000). Figure 6.18 shows that the VOSL in Gunung Kelir varies from <IDR 1 billion to >7.5 billion. It depends on the number of occupants living in the building. The maximum number of occupants in each building is 10 people (Table 6.7).

The value of people was estimated based on the value of one or more persons could be killed by rockfall inside the building. It was calculated by multiplying the number of people inside the building, the average temporal-spatial probability people spending their time in the building and the VOSL. The temporal probability was divided into two groups based on the age, i.e. <16 years old and >16 years old. It was assumed that <16 years old (school year) spending 14 hours a day inside the building and >16 years spending 16 hours a day.

$$P_{(S:T)} = \frac{h}{24} \qquad (6.10)$$

where $P_{(S:T)}$ is the spatio-temporal of a person inside the building and h is the daily average time spent inside the building. For quantification of risk to people, it can be defined as:

$$R = \sum_{j=1}^{4} \sum_{q=1}^{n_{ij}} P_r^{(ij)}.P_k^{(ij)}.P_{(S:T)}.V_{ij}.E_{ik} \qquad (6.11)$$

where n_{ij} is the number of boulders with class volume j in landform i, $P_r^{(ij)}$ is the temporal probability of rockfall in the magnitude scenario (i.e. boulder volume) class j and crossing landform i; $P_k^{(ij)}$ is the probability of the rockfall colliding element at risk k in the landform i, V_{ij} is the vulnerability of element at risk k collided by rockfall volume j in the landform i and E_{ik} is the economic value of the element at risk of people inside building k *in* the landform i.

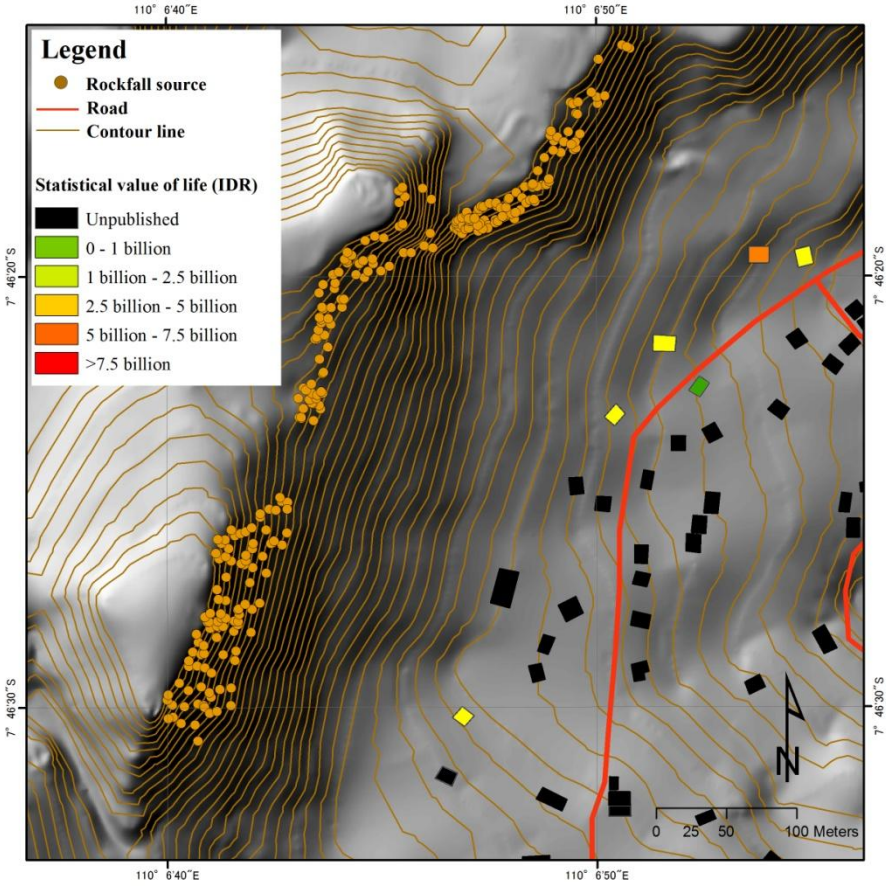

Figure 6.18 Calculated Value of Element at Risk - People inside Building (Value of Statistical Life)

Table 6.7 Estimated Value of Element at Risk (Building) and Statistical Value of Life (people inside a building)

ID	Number of Occupant	Age <16	Age>16	Av. Spatio temp. prob.	Value of element at risk (building)	Estimated Statistical value of life (US$)	Estimated Statistical value of life (IDR)
1	3	1	2	0.61	IDR 4,965,700	$275,000	IDR 3,025,000,000
2	3	0	3	0.58	IDR 6,776,160	$262,500	IDR 2,887,500,000
3	5	2	3	0.62	IDR 5,616,360	$462,500	IDR 5,087,500,000
4	5	3	3	0.75	IDR 1,958,100	$562,500	IDR 6,187,500,000
5	1	0	1	0.58	IDR 2,004,300	$87,500	IDR 962,500,000
6	5	1	4	0.60	IDR 1,062,900	$450,000	IDR 4,950,000,000
7	5	2	3	0.62	IDR 9,073,500	$462,500	IDR 5,087,500,000
8	6	1	4	0.50	IDR 1,521,250	$450,000	IDR 4,950,000,000
9	4	2	2	0.63	IDR 1,655,800	$375,000	IDR 4,125,000,000
10	5	2	3	0.62	IDR 23,752,801	$462,500	IDR 5,087,500,000
11	10	3	7	0.61	IDR 2,109,900	$912,500	IDR 10,037,500,000
12	4	2	2	0.63	IDR 2,442,240	$375,000	IDR 4,125,000,000
13	5	2	3	0.62	IDR 2,663,800	$462,500	IDR 5,087,500,000
14	3	1	2	0.61	IDR 10,691,400	$275,000	IDR 3,025,000,000
15	4	2	2	0.63	IDR 32,673,999	$375,000	IDR 4,125,000,000
16	5	2	3	0.62	IDR 2,493,600	$462,500	IDR 5,087,500,000
17	4	1	3	0.60	IDR 5,688,600	$362,500	IDR 3,987,500,000
18	3	0	3	0.58	IDR 1,772,120	$262,500	IDR 2,887,500,000
19	5	1	4	0.60	IDR 2,141,200	$450,000	IDR 4,950,000,000

ID	Number of Occupant	Age <16	Age>16	Av. Spatio temp. prob.	Value of element at risk (building)	Estimated Statistical value of life	Estimated Statistical value of life
20	4	1	3	0.60	IDR 6,450,000	$362,500	IDR 3,987,500,000
21	3	0	3	0.58	IDR 9,441,850	$262,500	IDR 2,887,500,000
22	0	0	0	0	IDR 3,968,910	$0	IDR0
23	4	2	2	0.63	IDR 4,091,100	$375,000	IDR 4,125,000,000
24	4	1	3	0.60	IDR 3,012,000	$362,500	IDR 3,987,500,000
25	3	0	3	0.58	IDR 3,028,200	$262,500	IDR 2,887,500,000
26	4	2	2	0.63	IDR 4,776,980	$375,000	IDR 4,125,000,000
27	0	0	0	0	IDR 324,900	$0	IDR0
28	3	0	3	0.58	IDR 6,558,040	$262,500	IDR 2,887,500,000
29	0	0	0	0	IDR 3,245,200	$0	IDR0
30	2	0	2	0.58	IDR 7,080,480	$175,000	IDR 1,925,000,000
31	3	0	3	0.58	IDR 9,832,000	$262,500	IDR 2,887,500,000
32	4	2	2	0.63	IDR 7,852,000	$375,000	IDR 4,125,000,000
33	4	2	2	0.63	IDR 9,118,500	$375,000	IDR 4,125,000,000
34	6	0	6	0.58	IDR 2,934,400	$525,000	IDR 5,775,000,000
35	5	5	0	0.67	IDR 5,688,000	$500,000	IDR 5,500,000,000
36	1	0	1	0.58	IDR 4,702,080	$87,500	IDR 962,500,000
37	4	0	4	0.58	IDR 27,324,001	$350,000	IDR 3,850,000,000
38	0	0	0	0	IDR 5,473,050	$0	IDR0

6.6 DISCUSSION

This study tried to estimate rockfall risk in a quantitative manner by incorporating statistical analysis of rockfall frequency and volume, landform mapping, and physical model of rockfall trajectories and energy. Risk was defined as a chance of potential economic loss during a specified time for individual building and persons inside the building.

The integration of statistical and physical model based on geomorphological analysis can evaluate both the occurrence probability in space and time, modelling trajectories of falling and the interaction between rockfall and elements at risk. In addition, landform can reflect the unique feature of landscape; thus the objective of zoning "to divide land into homogeneous areas or domains" can be achieved successfully. Each landform will represent a homogeneous area of rockfall risk ranking with the information of the occurrence probability with particular size in space and time, simplified trajectories and dynamic behavior of boulder when travel along the slope, and its interaction where elements at risk exist.

Table 6.8 and 6.9 show that landform significantly influence the rockfall risk. Higher frequency of greater events is more dominant in transportational middle slope and colluvial foot slope. It shows that landform significantly influences rockfall risk in Gunung Kelir area. For example, calculated risk building for class volume 10-100 m^3 in 5 years was estimated in average IDR 91,225; IDR 156,500 and IDR 400,400 for lower slope, colluvial foot slope and transportational middle slope respectively. Transportational middle is the landform where the chance of loss is the highest. The temporal probability of transportational middle slope is high for the middle class volume rockfall. Thus, it not only increases the temporal probability of rockfall, but also the physical vulnerability of the building.

The magnitude or the volume class of rockfall also affects the rockfall risk. Rockfall volume 10-100 m^3 may result the highest risk because both the temporal probability and the vulnerability can be categorized as medium to high class.

Table 6.8 Calculation of the Rockfall Risk to Building for 5 Years Scenario with Volume Class <10 m^3 and 10-100 m^3

ID	Landform location	P_r		P_k		Vulnerability		Value of elements at risk	Risk to building	
		<10 m^3	10-100 m^3	<10 m^3	10-100 m^3	<10 m^3	10-100 m^3		<10 m^3	10-100 m^3
1	Lower Slope	0.72	0.47	0.063	0.070	0.01	0.4	IDR 4,965,700	IDR 2,245	IDR 65,326
2	Lower Slope	0.72	0.47	0.062	0.069	0.01	0.4	IDR 6,776,160	IDR 3,032	IDR 88,328
3	Colluvial Foot Slope	1.00	0.92	0.063	0.071	0.1	0.5	IDR 5,616,360	IDR 35,337	IDR 183,773
4	Lower Slope	0.72	0.47	0.046	0.054	0.01	0.4	IDR 1,958,100	IDR 648	IDR 19,793
5	Lower Slope	0.72	0.47	0.041	0.049	0.01	0.4	IDR 2,004,300	IDR 595	IDR 18,460
6	Lower Slope	0.72	0.47	0.034	0.041	0.01	0.4	IDR 1,062,900	IDR 258	IDR 8,284
7	Lower Slope	0.72	0.47	0.045	0.051	0.01	0.4	IDR 9,073,500	IDR 2,943	IDR 87,470
8	Lower Slope	0.72	0.47	0.033	0.039	0.01	0.4	IDR 1,521,250	IDR 366	IDR 11,318
9	Lower Slope	0.72	0.47	0.045	0.051	0.01	0.4	IDR 1,655,800	IDR 538	IDR 15,997
10	Lower Slope	0.72	0.47	0.054	0.060	0.01	0.4	IDR 23,752,801	IDR 9,234	IDR 268,978
11	Lower Slope	0.72	0.47	0.038	0.044	0.01	0.4	IDR 2,109,900	IDR 577	IDR 17,537
12	Lower Slope	0.72	0.47	0.044	0.052	0.01	0.4	IDR 2,442,240	IDR 782	IDR 24,045
13	Colluvial Foot Slope	1.00	0.92	0.033	0.040	0.1	0.5	IDR 2,663,800	IDR 8,888	IDR 48,722
14	Lower Slope	0.72	0.47	0.102	0.109	0.01	0.4	IDR 10,691,400	IDR 7,871	IDR 220,163
15	Lower Slope	0.72	0.47	0.095	0.102	0.01	0.4	IDR 32,673,999	IDR 22,308	IDR 627,098
16	Lower Slope	0.72	0.47	0.040	0.048	0.01	0.4	IDR 2,493,600	IDR 723	IDR 22,588
17	Lower Slope	0.72	0.47	0.053	0.061	0.01	0.4	IDR 5,688,600	IDR 2,167	IDR 65,066
18	Lower Slope	0.72	0.47	0.035	0.041	0.01	0.4	IDR 1,772,120	IDR 445	IDR 13,690
19	Lower Slope	0.72	0.47	0.043	0.051	0.01	0.4	IDR 2,141,200	IDR 660	IDR 20,432

ID	Landforms location	P_r		P_k		Vulnerability		Value of elements at risk	Risk to building	
		<10 m^3	10-100 m^3	<10 m^3	10-100 m^3	<10 m^3	10-100 m^3		<10 m^3	10-100 m^3
20	Lower Slope	0.72	0.47	0.057	0.065	0.01	0.4	IDR 6,450,000	IDR 2,667	IDR 79,276
21	Transp. Middle Slope	1.00	0.99	0.071	0.078	0.2	0.7	IDR 9,441,850	IDR 133,384	IDR 511,318
22	Lower Slope	0.72	0.47	0.044	0.051	0.01	0.4	IDR 3,968,910	IDR 1,253	IDR 38,040
23	Colluvial Foot Slope	1.00	0.92	0.059	0.067	0.1	0.5	IDR 4,091,100	IDR 24,037	IDR 125,965
24	Colluvial Foot Slope	1.00	0.92	0.045	0.052	0.1	0.5	IDR 3,012,000	IDR 13,402	IDR 71,909
25	Lower Slope	0.72	0.47	0.055	0.063	0.01	0.4	IDR 3,028,200	IDR 1,204	IDR 35,892
26	Colluvial Foot Slope	1.00	0.92	0.049	0.055	0.1	0.5	IDR 4,776,980	IDR 23,130	IDR 120,721
27	Lower Slope	0.72	0.47	0.018	0.024	0.01	0.4	IDR 324,900	IDR 42	IDR 1,460
28	Colluvial Foot Slope	1.00	0.92	0.060	0.066	0.1	0.5	IDR 6,558,040	IDR 39,439	IDR 201,371
29	Colluvial Foot Slope	1.00	0.92	0.038	0.045	0.1	0.5	IDR 3,245,200	IDR 12,450	IDR 66,878
30	Colluvial Foot Slope	1.00	0.92	0.053	0.059	0.1	0.5	IDR 7,080,480	IDR 37,469	IDR 193,706
31	Colluvial Foot Slope	1.00	0.92	0.085	0.091	0.1	0.5	IDR 9,832,000	IDR 83,599	IDR 415,391
32	Transp. Middle Slope	1.00	0.99	0.055	0.061	0.2	0.7	IDR 7,852,000	IDR 86,109	IDR 330,871
33	Lower Slope	0.72	0.47	0.065	0.071	0.01	0.4	IDR 9,118,500	IDR 4,249	IDR 121,681
34	Lower Slope	0.72	0.47	0.056	0.062	0.01	0.4	IDR 2,934,400	IDR 1,180	IDR 34,255
35	Transp. Middle Slope	1.00	0.99	0.085	0.091	0.2	0.7	IDR 5,688,000	IDR 96,889	IDR 359,039
36	Colluvial Foot Slope	1.00	0.92	0.055	0.063	0.1	0.5	IDR 4,702,080	IDR 25,765	IDR 136,409
37	Lower Slope	0.72	0.47	0.054	0.060	0.01	0.4	IDR 27,324,001	IDR 10,679	IDR 310,922
38	Lower Slope	0.72	0.47	0.055	0.062	0.01	0.4	IDR 5,473,050	IDR 2,163	IDR 64,523

Table 6.9 Calculation of the Rockfall Risk to Building for 5 Years Scenario with Volume Class 100-1000 $m^3$and >1000 m^3

ID	Landforms location	P_r		P_k		Vulnerability		Value of elements at risk	Risk to building	
		100-1000 m^3	>1000 m^3	100-1000 m^3	>1000 m^3	100-1000 m^3	>1000 m^3		100-1000 m^3	>1000 m^3
1	Lower Slope	0.10	0.03	0.082	0.065	0.6	0.8	IDR 4,965,700	IDR 24,716	IDR 8,973
2	Lower Slope	0.10	0.03	0.082	0.064	0.6	0.8	IDR 6,776,160	IDR 33,466	IDR 12,123
3	Colluvial Foot Slope	0.47	0.03	0.084	0.065	0.7	0.9	IDR 5,616,360	IDR 156,588	IDR 11,521
4	Lower Slope	0.10	0.03	0.067	0.048	0.6	0.8	IDR 1,958,100	IDR 7,970	IDR 2,632
5	Lower Slope	0.10	0.03	0.062	0.043	0.6	0.8	IDR 2,004,300	IDR 7,581	IDR 2,428
6	Lower Slope	0.10	0.03	0.055	0.036	0.6	0.8	IDR 1,062,900	IDR 3,537	IDR 1,065
7	Lower Slope	0.10	0.03	0.062	0.047	0.6	0.8	IDR 9,073,500	IDR 34,031	IDR 11,846
8	Lower Slope	0.10	0.03	0.050	0.035	0.6	0.8	IDR 1,521,250	IDR 4,632	IDR 1,492
9	Lower Slope	0.10	0.03	0.062	0.047	0.6	0.8	IDR 1,655,800	IDR 6,222	IDR 2,167
10	Lower Slope	0.10	0.03	0.071	0.056	0.6	0.8	IDR 23,752,801	IDR 101,922	IDR 36,917
11	Lower Slope	0.10	0.03	0.055	0.040	0.6	0.8	IDR 2,109,900	IDR 7,014	IDR 2,341
12	Lower Slope	0.10	0.03	0.066	0.047	0.6	0.8	IDR 2,442,240	IDR 9,767	IDR 3,182
13	Colluvial Foot Slope	0.47	0.03	0.050	0.035	0.7	0.9	IDR 2,663,800	IDR 44,351	IDR 2,949
14	Lower Slope	0.10	0.03	0.122	0.104	0.6	0.8	IDR 10,691,400	IDR 78,727	IDR 31,061
15	Lower Slope	0.10	0.03	0.114	0.097	0.6	0.8	IDR 32,673,999	IDR 225,921	IDR 88,171
16	Lower Slope	0.10	0.03	0.062	0.043	0.6	0.8	IDR 2,493,600	IDR 9,343	IDR 2,959
17	Lower Slope	0.10	0.03	0.074	0.055	0.6	0.8	IDR 5,688,600	IDR 25,657	IDR 8,750
18	Lower Slope	0.10	0.03	0.052	0.037	0.6	0.8	IDR 1,772,120	IDR 5,558	IDR 1,812

ID	Landforms location	P_r		P_k		Vulnerability		Value of elements at risk	Risk to building	
		100-1000 m^3	>1000 m^3	100-1000 m^3	>1000 m^3	100-1000 m^3	>1000 m^3		100-1000 m^3	>1000 m^3
19	Lower Slope	0.10	0.03	0.064	0.045	0.6	0.8	IDR 2,141,200	IDR 8,355	IDR 2,694
20	Lower Slope	0.10	0.03	0.079	0.060	0.6	0.8	IDR 6,450,000	IDR 30,857	IDR 10,734
21	Transp. Middle Slope	0.63	0.10	0.092	0.073	0.8	1	IDR 9,441,850	IDR 437,241	IDR 69,521
22	Lower Slope	0.10	0.03	0.063	0.046	0.6	0.8	IDR 3,968,910	IDR 15,208	IDR 5,078
23	Colluvial Foot Slope	0.47	0.03	0.080	0.061	0.7	0.9	IDR 4,091,100	IDR 108,421	IDR 7,857
24	Colluvial Foot Slope	0.47	0.03	0.064	0.047	0.7	0.9	IDR 3,012,000	IDR 63,783	IDR 4,415
25	Lower Slope	0.10	0.03	0.076	0.057	0.6	0.8	IDR 3,028,200	IDR 14,021	IDR 4,851
26	Colluvial Foot Slope	0.47	0.03	0.066	0.050	0.7	0.9	IDR 4,776,980	IDR 103,351	IDR 7,550
27	Lower Slope	0.10	0.03	0.035	0.020	0.6	0.8	IDR 324,900	IDR 682	IDR 177
28	Colluvial Foot Slope	0.47	0.03	0.077	0.062	0.7	0.9	IDR 6,558,040	IDR 167,338	IDR 12,782
29	Colluvial Foot Slope	0.47	0.03	0.055	0.040	0.7	0.9	IDR 3,245,200	IDR 59,403	IDR 4,103
30	Colluvial Foot Slope	0.47	0.03	0.070	0.055	0.7	0.9	IDR 7,080,480	IDR 163,738	IDR 12,193
31	Colluvial Foot Slope	0.47	0.03	0.102	0.087	0.7	0.9	IDR 9,832,000	IDR 331,931	IDR 26,858
32	Transp. Middle Slope	0.63	0.10	0.072	0.057	0.8	1	IDR 7,852,000	IDR 283,846	IDR 44,915
33	Lower Slope	0.10	0.03	0.082	0.066	0.6	0.8	IDR 9,118,500	IDR 45,038	IDR 16,893
34	Lower Slope	0.10	0.03	0.073	0.058	0.6	0.8	IDR 2,934,400	IDR 12,920	IDR 4,712
35	Transp. Middle Slope	0.63	0.10	0.102	0.087	0.8	0.8	IDR 5,688,000	IDR 292,519	IDR 39,961
36	Colluvial Foot Slope	0.47	0.03	0.077	0.057	0.7	0.9	IDR 4,702,080	IDR 118,975	IDR 8,450
37	Lower Slope	0.10	0.03	0.071	0.056	0.6	0.8	IDR 27,324,001	IDR 117,728	IDR 42,689
38	Lower Slope	0.10	0.03	0.076	0.057	0.6	0.8	IDR 5,473,050	IDR 25,230	IDR 8,715

The risk to persons were also affected by the position of a building. A building located in transportational middle slope tend to have higher risk than colluvial foot slope and lower slope. Calculated risk to persons for class volume 10-100 m^3 in 5 years scenario was estimated in average IDR 41,880,000; IDR 87,721,000 and IDR 225,787,000 for lower slope, colluvial foot slope and transportational middle slope respectively (Table 6.10). It shows the high number of risk to persons, even though the number of occupants was only 4 (less than the maximum occupants (10) exist in the lower slope). The calculated risk may differ both spatially (Figure 6.19 and Figure 6.20). It means that the transportational middle slope should be paid more attention in terms of land use planning based on disaster risk reduction.

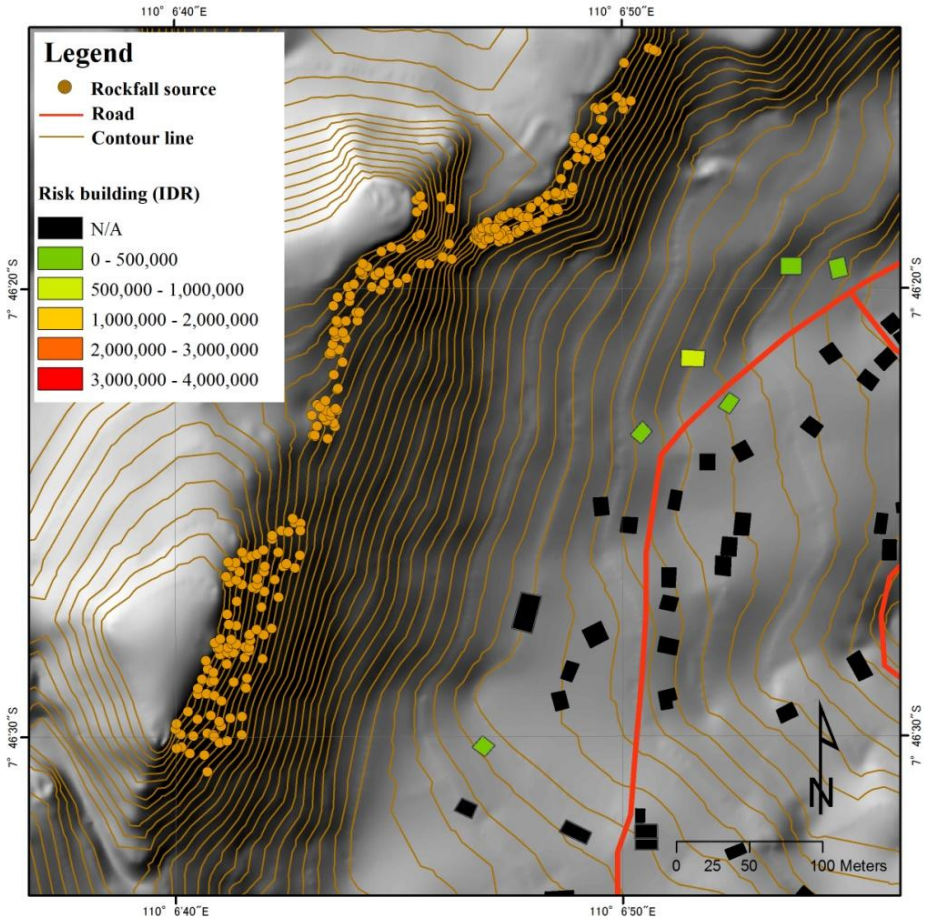

Figure 6.19 Calculated Rockfall Risk for Building for Class Volume 10-100 m^3 in 5 Years Scenario

The chance of loss is useful information for administrators to consider disaster risk reduction tool in practice. For example, if traditional structural prevention to reduce vulnerability to economic damage is not suitable (too expensive); financial risk strategies, i.e. risk transfer instrument, government disaster assistance can be further evaluated based on the existing risk analysis. Thus, the selected technical performance of the disaster risk reduction tool can be further evaluated by computing a cost-benefit ratio of applied mitigation technique. The presented quantitative risk analysis provide a general framework for reliable and reproducible results. The risk zoning based on landforms may be direcly used for land use planning and risk management in a rockfall prone area throughout the country.

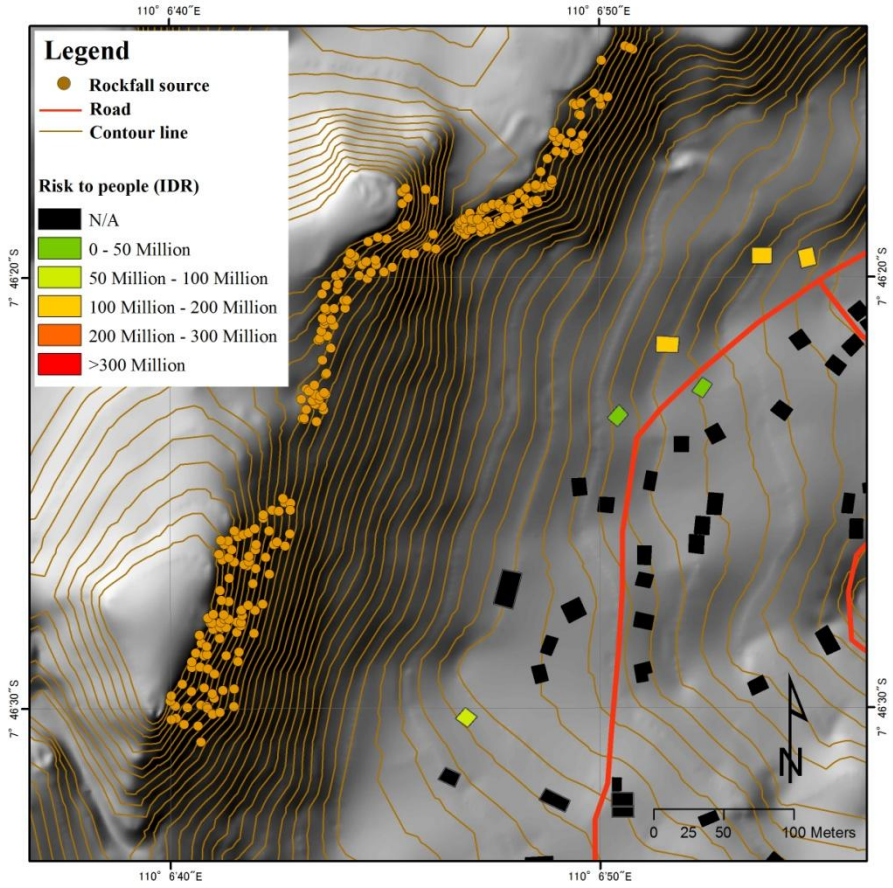

Figure 6.20 Calculated Rockfall Risk for People inside Building for Class Volume 10-100 m^3 in 5 Years Scenario

Table 6.10 Calculation of the Rockfall Risk to Persons for 5 Years Scenario with Volume Class <10 $m^3$and 10-100 m^3

ID	Landforms location	P_r		P_k		Vulnerability		Value of elements at risk	Risk to persons	
		<10 m^3	10-100 m^3	<10 m^3	10-100 m^3	<10 m^3	10-100 m^3		<10 m^3	10-100 m^3
1	Lower Slope	0.72	0.47	0.063	0.070	0.01	0.4	IDR 3,025,000,000	IDR 1,367,627	IDR 39,795,431
2	Lower Slope	0.72	0.47	0.062	0.069	0.01	0.4	IDR 2,887,500,000	IDR 1,292,181	IDR 37,638,926
3	Col. Foot Slope	1.00	0.92	0.063	0.071	0.1	0.5	IDR 5,087,500,000	IDR 32,009,317	IDR 166,468,288
4	Lower Slope	0.72	0.47	0.046	0.054	0.01	0.4	IDR 6,187,500,000	IDR 2,047,872	IDR 62,545,407
5	Lower Slope	0.72	0.47	0.041	0.049	0.01	0.4	IDR 962,500,000	IDR 285,524	IDR 8,864,638
6	Lower Slope	0.72	0.47	0.034	0.041	0.01	0.4	IDR 4,950,000,000	IDR 1,200,526	IDR 38,577,762
7	Lower Slope	0.72	0.47	0.045	0.051	0.01	0.4	IDR 5,087,500,000	IDR 1,650,400	IDR 49,044,233
8	Lower Slope	0.72	0.47	0.033	0.039	0.01	0.4	IDR 4,950,000,000	IDR 1,189,679	IDR 36,826,998
9	Lower Slope	0.72	0.47	0.045	0.051	0.01	0.4	IDR 4,125,000,000	IDR 1,341,523	IDR 39,853,553
10	Lower Slope	0.72	0.47	0.054	0.060	0.01	0.4	IDR 5,087,500,000	IDR 1,977,700	IDR 57,611,226
11	Lower Slope	0.72	0.47	0.038	0.044	0.01	0.4	IDR 10,037,500,000	IDR 2,746,749	IDR 83,428,329
12	Lower Slope	0.72	0.47	0.044	0.052	0.01	0.4	IDR 4,125,000,000	IDR 1,320,182	IDR 40,612,590
13	Col. Foot Slope	1.00	0.92	0.033	0.040	0.1	0.5	IDR 5,087,500,000	IDR 16,975,838	IDR 93,052,804
14	Lower Slope	0.72	0.47	0.102	0.109	0.01	0.4	IDR 3,025,000,000	IDR 2,227,119	IDR 62,292,407
15	Lower Slope	0.72	0.47	0.095	0.102	0.01	0.4	IDR 4,125,000,000	IDR 2,816,352	IDR 79,169,299
16	Lower Slope	0.72	0.47	0.040	0.048	0.01	0.4	IDR 5,087,500,000	IDR 1,475,258	IDR 46,084,992
17	Lower Slope	0.72	0.47	0.053	0.061	0.01	0.4	IDR 3,987,500,000	IDR 1,518,777	IDR 45,608,864
18	Lower Slope	0.72	0.47	0.035	0.041	0.01	0.4	IDR 2,887,500,000	IDR 725,466	IDR 22,306,548

ID	Landforms location	P_r		P_k		Vulnerability		Value of elements at risk	Risk to persons	
		<10 m^3	10-100 m^3	<10 m^3	10-100 m^3	<10 m^3	10-100 m^3		<10 m^3	10-100 m^3
19	Lower Slope	0.72	0.47	0.043	0.051	0.01	0.4	IDR 4,950,000,000	IDR 1,526,907	IDR 47,234,990
20	Lower Slope	0.72	0.47	0.057	0.065	0.01	0.4	IDR 3,987,500,000	IDR 1,648,715	IDR 49,009,950
21	Transp. Middle Slope	1.00	0.99	0.071	0.078	0.2	0.7	IDR 2,887,500,000	IDR 40,791,393	IDR 156,371,038
22	Lower Slope	0.72	0.47	0.044	0.051	0.01	0.4	IDR 0	IDR 0	IDR 0
23	Col. Foot Slope	1.00	0.92	0.059	0.067	0.1	0.5	IDR 4,125,000,000	IDR 24,236,013	IDR 127,009,037
24	Col. Foot Slope	1.00	0.92	0.045	0.052	0.1	0.5	IDR 3,987,500,000	IDR 17,742,243	IDR 95,197,878
25	Lower Slope	0.72	0.47	0.055	0.063	0.01	0.4	IDR 2,887,500,000	IDR 1,148,094	IDR 34,224,403
26	Col. Foot Slope	1.00	0.92	0.049	0.055	0.1	0.5	IDR 4,125,000,000	IDR 19,973,421	IDR 104,244,980
27	Lower Slope	0.72	0.47	0.018	0.024	0.01	0.4	IDR 0	IDR 0	IDR 0
28	Col. Foot Slope	1.00	0.92	0.060	0.066	0.1	0.5	IDR 2,887,500,000	IDR 17,364,914	IDR 88,663,355
29	Col. Foot Slope	1.00	0.92	0.038	0.045	0.1	0.5	IDR 0	IDR 0	IDR 0
30	Col. Foot Slope	1.00	0.92	0.053	0.059	0.1	0.5	IDR 1,925,000,000	IDR 10,186,869	IDR 52,663,654
31	Col. Foot Slope	1.00	0.92	0.085	0.091	0.1	0.5	IDR 2,887,500,000	IDR 24,551,679	IDR 121,993,672
32	Transp. Middle Slope	1.00	0.99	0.055	0.061	0.2	0.7	IDR 4,125,000,000	IDR 45,236,921	IDR 173,820,844
33	Lower Slope	0.72	0.47	0.065	0.071	0.01	0.4	IDR 4,125,000,000	IDR 1,921,933	IDR 55,045,640
34	Lower Slope	0.72	0.47	0.056	0.062	0.01	0.4	IDR 5,775,000,000	IDR 2,322,097	IDR 67,415,634
35	Transp. Middle Slope	1.00	0.99	0.085	0.091	0.2	0.7	IDR 5,500,000,000	IDR 93,686,443	IDR 347,171,923
36	Col. Foot Slope	1.00	0.92	0.055	0.063	0.1	0.5	IDR 962,500,000	IDR 5,273,987	IDR 27,922,535
37	Lower Slope	0.72	0.47	0.054	0.060	0.01	0.4	IDR 3,850,000,000	IDR 1,504,732	IDR 43,809,527
38	Lower Slope	0.72	0.47	0.055	0.062	0.01	0.4	IDR 0	IDR 0	IDR 0

Table 6.11 Calculation of the Rockfall Risk to Persons for 5 Years Scenario with Volume Class 100-1000 $m^3$and >1000 m^3

ID	Landforms location	P_r		P_k		Vulnerability		Value of elements at risk	Risk to persons	
		100-1000 m^3	>1000 m^3	100-1000 m^3	>1000 m^3	100-1000 m^3	>1000 m^3		100-1000 m^3	>1000 m^3
1	Lower Slope	0.10	0.03	0.082	0.065	0.6	0.8	IDR 3,025,000,000	IDR 15,056,648	IDR 5,465,923
2	Lower Slope	0.10	0.03	0.082	0.064	0.6	0.8	IDR 2,887,500,000	IDR 14,260,720	IDR 5,166,133
3	Col. Foot Slope	0.47	0.03	0.084	0.065	0.7	0.9	IDR 5,087,500,000	IDR 141,843,041	IDR 10,436,440
4	Lower Slope	0.10	0.03	0.067	0.048	0.6	0.8	IDR 6,187,500,000	IDR 25,186,056	IDR 8,317,112
5	Lower Slope	0.10	0.03	0.062	0.043	0.6	0.8	IDR 962,500,000	IDR 3,640,409	IDR 1,166,077
6	Lower Slope	0.10	0.03	0.055	0.036	0.6	0.8	IDR 4,950,000,000	IDR 16,472,374	IDR 4,961,430
7	Lower Slope	0.10	0.03	0.062	0.047	0.6	0.8	IDR 5,087,500,000	IDR 19,081,401	IDR 6,641,811
8	Lower Slope	0.10	0.03	0.050	0.035	0.6	0.8	IDR 4,950,000,000	IDR 15,071,090	IDR 4,853,758
9	Lower Slope	0.10	0.03	0.062	0.047	0.6	0.8	IDR 4,125,000,000	IDR 15,499,628	IDR 5,398,243
10	Lower Slope	0.10	0.03	0.071	0.056	0.6	0.8	IDR 5,087,500,000	IDR 21,830,113	IDR 7,907,029
11	Lower Slope	0.10	0.03	0.055	0.040	0.6	0.8	IDR 10,037,500,000	IDR 33,368,688	IDR 11,134,789
12	Lower Slope	0.10	0.03	0.066	0.047	0.6	0.8	IDR 4,125,000,000	IDR 16,497,303	IDR 5,374,802
13	Col. Foot Slope	0.47	0.03	0.050	0.035	0.7	0.9	IDR 5,087,500,000	IDR 84,704,582	IDR 5,632,979
14	Lower Slope	0.10	0.03	0.122	0.104	0.6	0.8	IDR 3,025,000,000	IDR 22,274,783	IDR 8,788,392
15	Lower Slope	0.10	0.03	0.114	0.097	0.6	0.8	IDR 4,125,000,000	IDR 28,521,835	IDR 11,131,305
16	Lower Slope	0.10	0.03	0.062	0.043	0.6	0.8	IDR 5,087,500,000	IDR 19,062,036	IDR 6,037,611
17	Lower Slope	0.10	0.03	0.074	0.055	0.6	0.8	IDR 3,987,500,000	IDR 17,984,794	IDR 6,133,447
18	Lower Slope	0.10	0.03	0.052	0.037	0.6	0.8	IDR 2,887,500,000	IDR 9,055,891	IDR 2,953,071

ID	Landforms location	P_r		P_k		Vulnerability		Value of elements at risk	Risk to persons	
		100-1000 m^3	>1000 m^3	100-1000 m^3	>1000 m^3	100-1000 m^3	>1000 m^3		100-1000 m^3	>1000 m^3
19	Lower Slope	0.10	0.03	0.064	0.045	0.6	0.8	IDR 4,950,000,000	IDR 19,315,452	IDR 6,228,217
20	Lower Slope	0.10	0.03	0.079	0.060	0.6	0.8	IDR 3,987,500,000	IDR 19,076,029	IDR 6,635,737
21	Transp. Middle Slope	0.63	0.10	0.092	0.073	0.8	1	IDR 2,887,500,000	IDR 133,716,715	IDR 21,260,875
22	Lower Slope	0.10	0.03	0.063	0.046	0.6	0.8	IDR 0	IDR 0	IDR 0
23	Col. Foot Slope	0.47	0.03	0.080	0.061	0.7	0.9	IDR 4,125,000,000	IDR 109,319,222	IDR 7,921,896
24	Col. Foot Slope	0.47	0.03	0.064	0.047	0.7	0.9	IDR 3,987,500,000	IDR 84,441,108	IDR 5,844,983
25	Lower Slope	0.10	0.03	0.076	0.057	0.6	0.8	IDR 2,887,500,000	IDR 13,369,464	IDR 4,625,142
26	Col. Foot Slope	0.47	0.03	0.066	0.050	0.7	0.9	IDR 4,125,000,000	IDR 89,245,554	IDR 6,519,841
27	Lower Slope	0.10	0.03	0.035	0.020	0.6	0.8	IDR 0	IDR 0	IDR 0
28	Col. Foot Slope	0.47	0.03	0.077	0.062	0.7	0.9	IDR 2,887,500,000	IDR 73,678,756	IDR 5,627,874
29	Col. Foot Slope	0.47	0.03	0.055	0.040	0.7	0.9	IDR 0	IDR 0	IDR 0
30	Col. Foot Slope	0.47	0.03	0.070	0.055	0.7	0.9	IDR 1,925,000,000	IDR 44,516,083	IDR 3,314,897
31	Col. Foot Slope	0.47	0.03	0.102	0.087	0.7	0.9	IDR 2,887,500,000	IDR 97,482,710	IDR 7,887,832
32	Transp. Middle Slope	0.63	0.10	0.072	0.057	0.8	1	IDR 4,125,000,000	IDR 149,116,749	IDR 23,596,002
33	Lower Slope	0.10	0.03	0.082	0.066	0.6	0.8	IDR 4,125,000,000	IDR 20,373,996	IDR 7,641,889
34	Lower Slope	0.10	0.03	0.073	0.058	0.6	0.8	IDR 5,775,000,000	IDR 25,427,958	IDR 9,273,739
35	Transp. Middle Slope	0.63	0.10	0.102	0.087	0.8	0.8	IDR 5,500,000,000	IDR 282,850,970	IDR 38,640,265
36	Col. Foot Slope	0.47	0.03	0.077	0.057	0.7	0.9	IDR 962,500,000	IDR 24,353,864	IDR 1,729,727
37	Lower Slope	0.10	0.03	0.071	0.056	0.6	0.8	IDR 3,850,000,000	IDR 16,588,055	IDR 6,014,984
38	Lower Slope	0.10	0.03	0.076	0.057	0.6	0.8	0	IDR 0	IDR 0

A rockfall risk zoning should include a recommendation of each zoning for different purposes. It should provide information on rockfall intensity and frequency of occurrence over a given area. Each zoning should represent the impact of the natural process in a delineated zone in order to account for conflict interest between the potential damage of a spatial extent and the future organization of the territory. The author tried to translate the rockfall risk zoning in a zoning regulating land use (Table 6.12)

Table 6.12 Proposed Landuse Planning Strategies based on Risk and Landforms

No	Landforms	Risk	Description
1.	Convex creep slope	High	Feasibility of protection is too high/difficult, development of building is forbidden
2.	Fall face	High	Feasibility of protection is too high/difficult, development of building is forbidden
3.	Tranportational Middle slope	High	Feasibility of protection is too high/difficult, development of building is forbidden
4.	Colluvial foot slope	Moderate	Protection can be afforded by group or society or government, development of building is not recommended
5.	Lower slope	Low	Protection can be afforded if necessary, development of building is allowed with conditional requirement

The proposed method allows a decision maker to have an advanced consideration to achieve specified risk measures and evaluation of their cost efficiency to optimize budget and design. The decision of the planning should account the results of the risk analysis processes. However, there is a wide range of other factors will usually need to

be considered such as financial constraints and the broader of socio-economic and political context. Disseminating the risk result into communities is a major task in the future. It can also be followed by public participation which is an essential part of the decision-making process. Involving broad ranges of groups and interest that may be affected by rockfall is important to the successful implementation of rockfall risk management strategies. Thus, involving all stakeholders in risk assessment processes i.e. collecting the rockfall data, formulation a problem and formulation the likelihood of hazard is key of successfully risk analysis.

6.7 CONCLUSIONS

This chapter shows the possibility of evaluating quantitative risk analysis based on geomorphology and rockfall blocks inventory mapping. It incorporated relevant stage of quantitative rockfall risk analysis and geomorphological analysis in a scarce data environment area. Temporal probability, probability of colliding, vulnerability and value of elements at risk were taken into account to quantitatively analyze rockfall risk.

Temporal probability was initially derived from MCF curve. However, the incremental frequency obtained from MCF curve. Rockfall that may occur once or more in each year was represented by an incremental frequency more than 1. It does not represent a probability value ranging from 0 to 1. Poisson probability was employed to solve this problem. Thus, temporal probability is defined as a percent chance of one or more rockfall can reach a landform during specified time.

Probability of colliding is defined as the probability of intersection of the potential rockfall trajectories from the trajectories analysis with the existing building. It was calculated based on the length of building, the path of rockfall, and the length of the possible landform corridor passed by identified rockfalll source. The identified rockfall source was obtained from trajectory modelling.

Vulnerability index is shown by the energy of rockfall impacts against loss of damage. An empirical vulnerability function obtained by fitting damage and impact energy was adapted to estimate the vulnerability degree based on landform analysis in Gunung Kelir area. An estimated energy was depicted from trajectory model. Building

record was plotted into energy and landform map. Then vulnerability index was estimated based on the landform and potential energy resulted from each class of rockfall volume.

Two value of elements at risk, i.e building and person are employed in this research. The value of building represents the the value of the land and the building obtained from interviews of 130 respondents living in Gunung Kelir area. The value of a person was estimated by using value of statistical life (VOSL) adapted from developing countries. The author used VOSL $150,000 which is equal to IDR1,650,000,000 ($1=IDR11,000).

The risk zoning represents a homogeneous area of rockfall risk ranking with the information of the occurrence probability with particular size in space and time, simplified trajectories and dynamic behavior of boulder when travel along the slope, and its interaction where elements at risk exist. It can be represented by landform zoning. Landform zoning can effectively represent rockfall risk zoning that can be used directly for landuse planning. Land use planning strategies based on quantitative risk analysis of landform was proposed to help policy maker to formulate a decision in a rockfall prone area. Risk analysis can give direction for policy maker to assist prioritization of evacuation; establishment of structural and or nonstructural preventive measures including spatial planning.

REFERENCES

Agliardi, F. and Crosta, G. 2003. High resolution three-dimensional numerical modelling of rockfalls. *Int. J. Rock Mech. Min., Sci.,* 40, 455–471,.

Agliardi, F., Crosta, G. B., and Frattini, P. 2009. Integrating rockfall risk assessment and countermeasure design by 3D modelling techniques, Nat. *Hazards Earth Syst. Sci*., 9, 1059-1073, doi:10.5194/nhess-9-1059-2009, 2009.

Australian Geomechanics Society (AGS). 2007. *Guideline for Landslide Susceptibility, Hazard and Risk Zoning for Land Use Management*. Australian Geomechanics Society Landslide Taskforce Landslide Zoning Working Group. Australian Geomechanics Society 42 (1).

Chau, K. T., Wong, R. H. C., Liu, J., and Lee, C. F. 2003. Rockfall Hazard Analysis for Hong Kong Based on Rockfall Inventory. *Rock Mech. Rock. Eng.* 36 (5), 383-408.

Chen. G. 2003. Numerical Modelling of Rockfall using Extended DDA. *Chinese Journal of Rock Mechanics and Engineering*, 22 (6):926-931.

Conacher, A. J. and *Dalrymple,* J. B. The nine unit land surface model: an approach to pedogeomorphic research. *Geoderma* 18, 1-154. *1977.*

Corominas, J., Copons, R., Moya, J., Vilaplana, J. M., Altimir, J., and Amig`o, J. 2005. Quantitative assessment of the residual risk in a rockfall protected area. *Landslides*, 2, 343–357.

Costa, L and Kropp J, P. 2012. Linking components of Vulnerability in Theoretic Frameworks and Case Studies. *Sustain Sci* doi 10.1007/s11625-012-0158-4

Crosta, G. B. and Agliardi, F. 2003. A methodology for physically based rockfall hazard assessment. *Nat. Hazards Earth Syst. Sci*., 3,407–422.

Crovelli, R. A. 2000. *Probabilistic Models for Estimation of Number and Cost of Landslide*. U.S. Geological Survey Open File Report 00-249. 23 pp.

Dalrymple, J.B., Blong, R.J., Conacher, A.J. 1968. A hypothetical nine unit landsurface model. *Zeitschrift für Geomorphologie* 12, 60–76.

Dijke van, J. J. and Westen van, C. J. 1990. Rockfall hazard: a geomorphologic application of neighbourhood analysis with Ilwi, *ITC Journal*, 1, 40–44.

Dussauge-Peisser, C., Helmstetter, A., Grasso, J. R., Hantz, D., Desvarreux, P., Jeannin, M., and Giraud. A. 2002. Probabilistic approach to rock fall hazard assessment: potential of historical data analysis. *Nat. Hazards Earth Syst. Sci.* 2, 15–26

Dussauge, C., Grasso, J. and Helmstetter, A. 2003. Statistical analysis of rockfall volume distributions: implications for rockfall dynamics. *J. Geophys. Res.*, 108(B6), 2286, doi:10.1029/2001JB000650.

Ebert, A., Kerle, N., & Stein, A. 2008. Urban Social Vulnerability Assessment with Physical Proxies and Spatial Metrics derived from Air- and Spaceborne Imagery and GIS Data. *Nat Hazards 48:275–294*.

Evans, I.S. scale specific landforms and aspects of the land surface. In: Evans, I. S., Dikau, R., Tokunaga, E., Ohmori, H., Hirano (Eds.), *concepts and modelling in geomorphology: international perspective*, Terrapub, Tokyo, pp. 61-84,2003.

Fekete, A. (2011). Spatial Disaster Vulnerability and Risk Assessment: Challenges in Their Quality and Acceptance. *Nat Hazards 61:1161-1178*

Fell, R., Corominas, J., Bonnard, C., Cascini, L., Leroi, E., and Savage,W. Z. 2008. Guidelines for landslide susceptibility, hazard and risk zoning for land use planning. *Eng. Geol.*, 102, 85–98,.

Fell, R., Ho, K. K. S., Lacasse, S., and Leroi, E. 2005. A framework for landslide risk assessment and management. *In: Landslide Risk Management*, edited by: Hungr, O., Fell, R., Couture, R., Eberhardt, E., Taylor and Francis, London, 3–26.

Glade, T. 2003. Vulnerability Assessment in Landslide Risk Analysis. *Die Erde* 134, 123-146.

Gutenberg, B., and Richter, C.F. 1954. *Seismicity of the earth*. 2nd ed. Princeton University Press, Princeton, N.J.

Guzzetti, F., Crosta, G., Detti, R., Agliardi, F. 2002. STONE: a computer program for three-dimensional simulation of rock-falls. *Computer & Geosciences* 28 pp. 1079-1093.

Guzzetti, F., Reichenbach, P., and Wieczorek, G. F. 2003. Rockfall hazard and risk assessment in the Yosemite Valley, California, USA. *Nat. Hazards Earth Syst. Sci.*, 3, 491–503.

Guzzetti, F., Reichenbach, P., Ghigi, S. 2004. Rockfall hazard and risk assessment along a transportation corridor in the Nera Valley, Central Italy. *Environmental Management* Vol. 34, No. 2, pp. 191–208.

Hengl, *T.*, Maathuis, B.H.P. and Wang, L. *Geomorphometry in ILWIS.* 2009. In: Hengl, T., Reuter, H.I. (Eds.), *geomorphometry: concepts, software, applications. Developments in soil science*, vol. 33. Elsevier, Amsterdam, pp. 497-525.

Hungr, O., Evans, S. G., and Hazzard, J. 1999. Magnitude and frequency of rockfalls and rock slides along the main transportation corridors of south-western British

Columbia. *Can. Geotech. J.*, 36, 224–238.

Irvin, B. J., Ventura, S. J., Slater, B. K. 1997. Fuzzy and isodata classification of landform elements from digital terrain data in Pleasant Valley, Wisconsin. *Geoderma* 77, 137-154.

Iwahashi, J., Pike, R.J. Automated classifications of topography from DEMs by an unsupervised nested-means algorithm and a three-part geometric signature. *Geomorphology* 86 (3–4), 409–440, 2007.

Jaboyedoff, M., Dudt, J. P., and Labiouse, V. 2005. An attempt to refine rockfall hazard zoning based on the kinetic energy, frequency and fragmentation degree. *Nat. Hazards Earth Syst. Sci.*, 5, 621–632,.

Jacopo, M. A. and Labiouse, V. 2013. New Cadanav methodology for quantitative rockfall hazard assessment and zoning at the Local Scale. *Landslide*. DOI 10.1007/s10346-013-0411-7.

Joint Technical Committee on Landslide and Engineered Slope (JTC-1). 2008. Guidelines for Landslide Susceptibility, Hazard and Risk Zoning for Landuse Planning. *Engineering Geology* 103, 85-98.

Jones-Lee, M. W. 1989. *The Economics of Safety and Physical Risk*. Blackwell, Oxford.

Kaynia, A. M., Papathoma-Kohle, M., Neuhauser, B., Ratzinger, K., Wenzel, H., Medina-Cetina, Z. 2008. Probabilistic Assessment of Vulnerability to Landslide: Application to the Village of Lichtenstein, Baden-Wurttemberg, Germany. *Engineering Geology 101:33-48.*

Lan, H., Martin, C. D., and Lim, C. H. 2007. RockFall analyst: a GIS extension for three-dimensional and spatially distributed rockfall hazard modeling. *Computer and Geoscience*., 33, 262–279.

Lee EM, Jones DKC. 2004. *Landslide risk assessment*. Thomas Telford, London.

Lobeck, AK. *Geomorphology*. Mc Graw-Hill Book Company Inc. New York and London.

Loye, A., Jaboyedoff, M., and Pedrazzini, A. (2009) Identification of potential rockfall source areas at a regional scale using a DEM based geomorphometric analysis.

Nat. Hazards Earth Syst. Sci., 9, 1643–1653, doi:10.5194/nhess-9-1643-2009.

MacMillan, R.A., Shary, P.A. Landforms and landform elements in geomorphometry. In: Hengl, T., Reuter, H.I. (Eds.), *Geomorphometry: Concepts, Software, Applications. Developments in Soil Science*, vol. 33. Elsevier, Amsterdam, pp. 227-254, 2009.

Marin, A. 1992. Costs and benefits of risk reduction. Appendix in *Risk: Analysis, Perception and Management*. Report of a Royal Society Study Group, London, 192—201.

Michoud, C., Derron, M. H., Horton, P., Jaboyedoff, M., Baillifard, F. J., Loye, A., Nicolet, P., Pedrazzini, A., Queyrel, A. 2012. Rockfall hazard and risk assessment along roads at a regional scale: example in Swiss Alps. *Nat. Hazards Earth Syst. Sci.*, 12, 615–629.

Mooney, G. M. (1977). *The Valuation of Human Life*. Macmillan, London.

Oya, M. *Applied geomorphology for mitigation of natural hazard*. Kluwer Academic Publisher. Dordrecht, the Netherlands, 2001.

Panizza, M. *Environmental geomorphology*. Elsevier, Amsterdam, Netherland, 1996.

Pearce, D.W. et al. 1995. The social costs of climate changes: Greenhouse damage and the benefits of control. In *Climate Change 1995: Economic and Social Dimensions of Climate Change*. Contribution of Working Group III to the Second Assessment Report of the IPCC (eds. J. P. Bruce, H. Lee and E. F. Haites). Cambridge University Press, Cambridge, 183—224.

Pike, R.J. The geometric signature: quantifying landslide-terrain types from Digital Elevation Models. *Mathematical Geology* 20, 491–511, 1988.

Samodra, G., Chen, G., Sartohadi, J., and Kasama, K. 2014. Automated landform classification in rockfall-prone area. *Earth Surface Dynamics*. 2, 339-348, doi:10.5194/esurf-2-339-2014.

SNI-Standar Nasional Indonesia (Indonesia National Standard). *Penyusunan pita geomorfologi (geomorphology mapping)*. Badan Standarisasi Nasional, 2002.

Van Westen, C. J., Van Asch, T. W. J., Soeters, R. 2005. Landslide Hazard and Risk

Zonation-Why is It still so Difficult?. *Bull. Eng. Geol. Env.* doi 10.1007/s10064-005-0023-0

Varnes, D.J. 1984. *Landslide hazard zonation: a review of principles and practice*. United Nations International, Paris.

Verstappen, H.Th. *Applied geomorphology*, Elsevier Science Publisher. Co. Amsterdam, 1983.

Volkwein, K. Schellenberg, V. Labiouse, F. Agliardi, F. Berger, F. Bourrier, L. K. A. Dorren, W. Gerber, M. Jaboyedoff. 2011.Rockfall characterisation and structural protection-a review. *Nat Hazards Earth Syst* 11:2617–2651

Wieczorek, G. F., Snyder, J. B., Alger, C. S., and Isaacson, K. A. 1992. Yosemite historical rockfall inventory. *U.S Geol. Surv. Open File Rep.*, 92– 387.

Wolf, S. 2012. Vulnerability and risk: comparing assessment approaches. *Nat Hazards 61: 1099-1113*.

Zuidam van, R.A. *Guide to geomorphological aerial photographic interpretation and mapping*. ITC. Enschede, the Netherlands, 1983.

CHAPTER 7

CONCLUSIONS AND FUTURE STUDIES

7.1 CONCLUSIONS

Spatial planning based on disaster risk reduction is one of the primary issues of the Indonesia national development agenda to promote sustainable development due to the increasing frequency of disasters and continuing environmental degradation. In terms of landslide disaster risk reduction, regional development and disaster mitigation are well approached by landslide susceptibility, hazard and risk zoning.

However, an adequate landslide inventory which is essential for hazard and risk analysis is not available in Indonesia. It is a central problem of quantitative landslide risk analysis and makes the landslide studies, especially in the risk analysis is not well developed in Indonesia. Thus, participatory landslide inventory mapping, landslide susceptibility zoning comparison and improvement, back analysis of rockfall source identification, automated landform classification in a rockfall prone area, and quantitative rockfall risk zoning based on statistical and physical model have been proposed to tackle down those issues. The research has been divided into two landslide typology i.e. landslides and rockfall.

The following major conclusions can be drawn:

1) The author has proposed participatory landslide inventory mapping by employing the traditional geomorphological field survey method involving active participation from communities with the use of an innovative technology, i.e. laser range finder

and GPS to identify and measure the extents of past landslide. It is a precise, cost-effective and less time consuming.

2) Data input of landslide inventory into a GIS program enables post-processing, permits enhanced cadastral activities, better landslide statistics. In the future, participatory landslide inventory mapping is expected to solve the problem of insufficiency of landslide inventory in Indonesia.
3) The existing data driven landslide susceptibility zoning methods i.e. WoE, LR, and ANN have been compared in order to identify the most realistic landslide susceptibility method applied typically in the tropical region Indonesia by using complete landslide inventory. Considering the accuracy and the precision evaluations, the WoE represents considerably the most realistic prediction capacities when comparing with the LR and ANN. The merits and demerits of the three models were also highlighted.
4) Based on the merits and demerits of the three methods, the author has proposed the combination of WoE-LR to improve the accuracy of the model. The result shows that WoE-LR by excluding SPI and TWI can increase the accuracy up to 5%. It also shows that the choice of selecting the landslide controlling factor is important and can give an effect on the overall accuracy.
5) Landuse can be inferred as a controlling factor that has a higher effect on the landslide events than any other parameter in the study area. It is reasonable that landuse change, especially housing development and devegetation may pose serious slope stability problems in the study area.
6) Back analysis of trajectory has been proposed to infer the potential location of rockfall sources. Rockfall sources are important to compute trajectory frequency and kinetic energy of rockfall. Sensitivity analysis of coefficients of restitution has also been employed to control the result of trajectory model. It suggests that the coefficients of restitution values have little effect on the computed trajectory.
7) The author has proposed automated landform classification to address the problems of the vagueness of rockfall frequency and energy to be used in practical landuse

planning. The modified 9-unit slope model can represent both physical characteristic of rockfall movement and the characteristic of local topography. It poses a reasonable result for preliminary rockfall risk assessment.

8) Combination of statistical and physical model has been proposed to compute rockfall risk quantitatively. Unsupervised fuzzy k means based on the modified 9-unit model was applied to classify the landform class automatically and to minimize the subjectivity of interpreter. Landform class was used as a mapping unit to evaluate the occurrence probability, the colliding probability and the physical vulnerability with particular boulder size in space and time. The risk to building and the risk to person inside the building were calculated based on the chance of loss (in monetary term) during specified time. Landform class significantly influences the calculated risk. Transportational middle slope is a landform where the chance of loss is the highest.

7.2 FUTURE STUDIES

(1) An effort of continuous landslide inventory mapping should be encouraged in the future study both in the same place and different places. The fully documented landslide database will enable scientists to more accurately establish the relationship between landslides events and both its triggering factor and controlling factor which will be very useful to understand the physical behavior of landslides.

(2) The study of the effect of landuse change to landslides and the evaluation of devegetation to landslides will be great challenges for the future research. GIS techniques and remote sensing analysis should be employed to infer the landuse change and the relation between landuse change and landslide events.

(3) Back analysis of rockfall source should be tested in different areas which have a similar genesis in order to confirm the sensitivity analysis regarding to the different landform genesis.

(4) Robust, less time consuming, less computational cost trajectory model which employs shape of boulder and the contact between boulder and surface morphology

is encouraged in order to produce “more physically sound” rockfall movement.

(5) Further studies should also employ the high accuracy of DTM, i.e. LIDAR data to obtain better accuracy of simulation and zoning.

APPENDIX A

Questionnaire and checklist for participatory landslide inventory mapping

No. Site			

FAKULTAS GEOGRAFI
UNIVERSITAS GADJAH MADA

LANDSLIDE INVENTORY MAPPING

LANDSLIDE INVENTORY
KULON PROGO REGENCY
2013

This is a research about landslide inventory mapping in Kulon Progo Regency. You will be asked to complete a short questionnaire.This questionnaire aims to collect spatial and temporal data of landslide occurred in Kulon Progo Regency. The information you provide will be used to enhance and improve landslide inventory data, susceptibility assessment, hazard assessment and risk assessment. Your answers will not be released to anyone and will remain anonymous.. All responses you provide for this study will remain confidential. When the results of the study are reported, you will not be identified by name or any other information that could be used to infer your identity. Only researchers will have access to view any data collected during this research. Your participation is voluntary and you may withdraw from this research any time you wish or skip any question you don't feel like answering.

Your refusal to participate will not result in any penalty or loss of benefits to which you are otherwise entitled to.The research intends to abide by all commonly acknowledged ethical codes. You agree to participate in this research project by filling the following questionnaire. If you have any questions, please ask the research team listed at the beginning of this questionnaire. Thank you for your time.

Guruh Samodra

NIP: 198511012010121006

Address: Mlati Jati RT 16 RW 06 Sendangadi Mlati Sleman

HP: 081227281137

CONFIDENTIAL

No. Respondent Identity : | | | |

DESCRIPTION OF INTERVIEW

RESUL OF VISITS

	FIRST VISIT	**SECOND VISIT**	**THIRD VISIT**
Date	/ /2013	/ /2013	/ /2013
Time Start	:	:	:
Time Finish	:	:	:
Result	1. Completed	1.Completed	1.Completed
	2.Partially Completed	2.Partially Completed	2.Partially Completed
	3.Respondent refuses interview/ not in place/ absent	3.Respondent refuses interview/ not in place/ absent	3.Respondent refuses interview/ not in place/ absent

ENUMERATOR AND EDITOR

	Enumerator	**Editor**
Name		

HASIL PEMERIKSAAN

Site	**No**	**Editor Note**

1. LOCATION

Name of victim	: ……
Address	: ……
Hamlet	: ……
Village	: ……
Sub District	: Girimulyo
District/Regency	: Kulon Progo
Coordinate	
X	: ……
Y	: ……
Elevation	: ……
Place where coordinate is plotted	:…… e.g. in landslide crown
Photo number	: ……
Direction of photoshoot	: ……
Photograph note	: ……

2. DATE WHEN LANDSLIDE OCCURED

Date/month/year	: ……
Date (Javanese Calendar)	: ……
Time (hh:mm:ss)	: ……

3. LANDSLIDE TYPOLOGY

(Please circle the choices below)

Landslide Material

1. Rock 2. earth 3. debris 4……..

Process

1. fall 2. topple 3. slide (rotational) 4. slide (translational)
5. lateral spread 6.flow

Landslide velocity (qualitative judgement)

1. fast 2. slow

nb: (engineering soil) ➔ fine material consist of at least 50% sand particle, loam and clay

Another characteristic:

Slope : ……

Landuse where landslide occured (please circle the choice below based on field investigation)

1. bushes 2. forest 3. settlement 4. paddy field
5. rainfed 6. field 7. others …….

Types of plants ……

The cause of landslide:……

4. LANDSLIDE GEOMETRY

Length L_r : ……. m L_d : ……. m L : ……. m
Width W_r : ……. m W_d : ……. m
Depth D_r : ……. m D_d : ……. m

Volume : $\frac{1}{6}\pi L_d W_d D_d$ Volume : ……. m^3

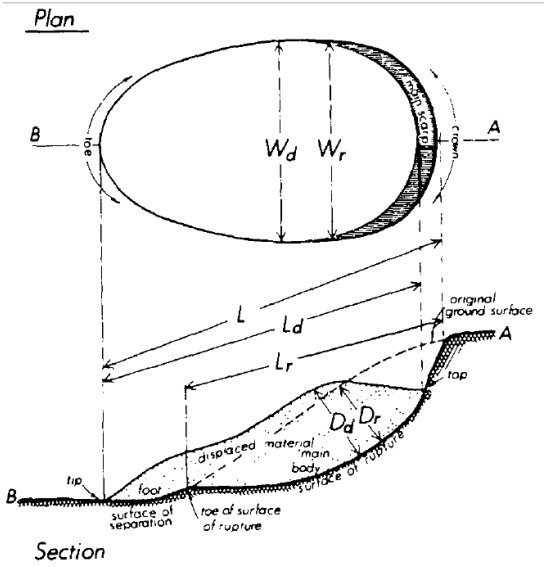

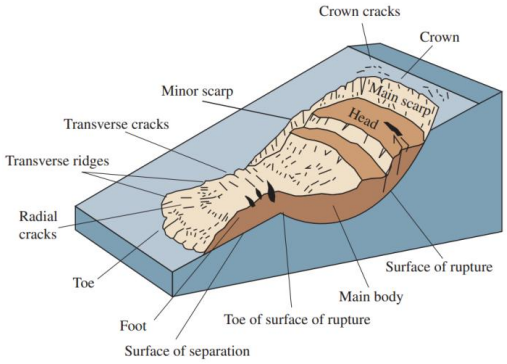

Figure A.1. Ideal scheme of landslide geometry *rotational slide* (*slump*)

5. LOSSES

death	: ……..	
property	: ……..	lost estimation (IDR) : ……
plantation	: ……..	lost estimation (IDR) : ……
livestock	: ……..	lost estimation (IDR) : ……
others	: ……..	lost estimation (IDR) : ……

FIELD OBSERVATION CHECKLIST

Location Description

1. Village :
2. Sub District :
3. Regency :
4. Coordinate :X=
   :Y=
5. Picture/Photograph number :
6. Slope :
7. Landslide prone area : Yes/No

Physical Building Condition

1. Building Age :
2. Wall Material :
3. Construction Type :
4. Building Structure :
5. Floor Material :
6. Roof Material :
7. Building Condition :
8. Distance to Major Road :
9. Additional Information :

APPENDIX B

Coefficients of restitution table (adapted from: https://www.rocscience.com/help/rocfall/webhelp/baggage/rn_rt_table.htm)

R_N (Normal)				R_T (Tangential)				Type	Verification	Location	Reference
Min	Max	Mean	Standard Deviation	Min	Max	Mean	Standard Deviation				
0.370	0.420			0.870	0.920			Hard surface paving	Tested using simulated rockfalls of similar size and shape of a previous rockfall.	Glenwood Canyon, Colorado, USA	Pfeiffer, T.J., and Bowen, T.D., "Computer Simulation of Rockfalls." Bulletin of Association of Engineering Geologists. Vol. 26, No. 1. 1989. pp135-146
0.330	0.370			0.830	0.870			Bedrock or boulders with little soil or vegetation			
0.300	0.330			0.830	0.870			Talus with little vegetation			
0.300	0.330			0.800	0.830			Talus with some vegetation			
0.280	0.320			0.800	0.830			Soft soil slope with little vegetation			
0.280	0.320			0.780	0.820			Vegetated soil slope			
		0.315	0.064			0.712	0.116	Limestone face	Tested on restoration-blasting slopes made of four types of materials; blast-generated rock fragments,	Limestone quarry in England	Robotham, M.E., and Wang, H., and Walton, G., "Assessment of risk from rockfall from active and
		0.303	0.080			0.615	0.170	Partially vegetated limestone scree			

		0.315	0.064	0.712	0.116	Uncovered limestone blast pile	partially vegetated scree on berms, uncovered blast piles, and vegetated quarry waste.		abandoned quarry slopes." Institution of mining and Metallurgy, Section A. 1995.104(Jan-April), pp A25-A33
		0.251	0.029	0.489	0.141	Vegetated covered limestone pile			
		0.276	0.079	0.835	0.087	Chalk face		Chalk quarry in England	
		0.271	0.018	0.596	0.085	Vegetated chalk scree			
		0.530		0.990		Clean hard bedrock			Hoek, Evert. "Unpublished notes" NSERC Industrial Research Professor of Rock Engineering, Department of Civil Engineering, University of Toronto, St George Street, Toronto, Ontario, Canada M5S 1A4
		0.400		0.900		Asphalt roadway			
		0.350		0.850		Bedrock outcrops with hard surface, large boulders			
		0.320		0.820		Talus cover			
		0.320		0.800		Talus cover with vegetation			
		0.300		0.800		Soft soil, some vegetation			
0.370	0.420					Smooth hard surfaces and paving	Developed by observation and literature review	Colordado, USA	Pfeiffer, T.J., and Higgens, J.D., "Rockfall

0.330	0.370				Most bedrock and boulder fields	Hazard Analysis Using the Colorado Rockfall Simulation." Transportation Research Record 1288, TRB, National Research Council, Washington, D.C., 1990, pp117-126.
0.300	0.330				Talus and firm soil slopes	
0.280	0.300				Soft soil slopes	
		0.830	0.870		Most bedrock surfaces and talus with no vegetation	
		0.820	0.850		Most talus slopes with some low vegetation	
		0.800	0.830		Vegetated talus slopes and soil slopes with spares vegetation	

APPENDIX C

Poisso model for percent chance of one or more rockfall in Gunung Kelir, during a specified time

Past years (t*)=141		Time-years (t)						
Number of rockfall (n)	Mean recurrence interval (years) μ	1	5	10	25	50	100	141
1	141.000	0.7%	3.5%	6.8%	16.2%	29.9%	50.8%	63.2%
2	70.500	1.4%	6.8%	13.2%	29.9%	50.8%	75.8%	86.5%
3	47.000	2.1%	10.1%	19.2%	41.3%	65.5%	88.1%	95.0%
4	35.250	2.8%	13.2%	24.7%	50.8%	75.8%	94.1%	98.2%
5	28.200	3.5%	16.2%	29.9%	58.8%	83.0%	97.1%	99.3%
6	23.500	4.2%	19.2%	34.7%	65.5%	88.1%	98.6%	99.8%
7	20.143	4.8%	22.0%	39.1%	71.1%	91.6%	99.3%	99.9%
8	17.625	5.5%	24.7%	43.3%	75.8%	94.1%	99.7%	100.0%
9	15.667	6.2%	27.3%	47.2%	79.7%	95.9%	99.8%	100.0%
10	14.100	6.8%	29.9%	50.8%	83.0%	97.1%	99.9%	100.0%
11	12.818	7.5%	32.3%	54.2%	85.8%	98.0%	100.0%	100.0%
12	11.750	8.2%	34.7%	57.3%	88.1%	98.6%	100.0%	100.0%
13	10.846	8.8%	36.9%	60.2%	90.0%	99.0%	100.0%	100.0%
14	10.071	9.5%	39.1%	63.0%	91.6%	99.3%	100.0%	100.0%
15	9.400	10.1%	41.3%	65.5%	93.0%	99.5%	100.0%	100.0%
16	8.813	10.7%	43.3%	67.8%	94.1%	99.7%	100.0%	100.0%
17	8.294	11.4%	45.3%	70.1%	95.1%	99.8%	100.0%	100.0%
18	7.833	12.0%	47.2%	72.1%	95.9%	99.8%	100.0%	100.0%
19	7.421	12.6%	49.0%	74.0%	96.6%	99.9%	100.0%	100.0%
20	7.050	13.2%	50.8%	75.8%	97.1%	99.9%	100.0%	100.0%
21	6.714	13.8%	52.5%	77.4%	97.6%	99.9%	100.0%	100.0%
22	6.409	14.4%	54.2%	79.0%	98.0%	100.0%	100.0%	100.0%
23	6.130	15.1%	55.8%	80.4%	98.3%	100.0%	100.0%	100.0%
24	5.875	15.7%	57.3%	81.8%	98.6%	100.0%	100.0%	100.0%
25	5.640	16.2%	58.8%	83.0%	98.8%	100.0%	100.0%	100.0%
26	5.423	16.8%	60.2%	84.2%	99.0%	100.0%	100.0%	100.0%
27	5.222	17.4%	61.6%	85.3%	99.2%	100.0%	100.0%	100.0%
28	5.036	18.0%	63.0%	86.3%	99.3%	100.0%	100.0%	100.0%
29	4.862	18.6%	64.2%	87.2%	99.4%	100.0%	100.0%	100.0%
30	4.700	19.2%	65.5%	88.1%	99.5%	100.0%	100.0%	100.0%
31	4.548	19.7%	66.7%	88.9%	99.6%	100.0%	100.0%	100.0%
32	4.406	20.3%	67.8%	89.7%	99.7%	100.0%	100.0%	100.0%

33	4.273	20.9%	69.0%	90.4%	99.7%	100.0%	100.0%	100.0%
34	4.147	21.4%	70.1%	91.0%	99.8%	100.0%	100.0%	100.0%
35	4.029	22.0%	71.1%	91.6%	99.8%	100.0%	100.0%	100.0%
36	3.917	22.5%	72.1%	92.2%	99.8%	100.0%	100.0%	100.0%
37	3.811	23.1%	73.1%	92.7%	99.9%	100.0%	100.0%	100.0%
38	3.711	23.6%	74.0%	93.2%	99.9%	100.0%	100.0%	100.0%
39	3.615	24.2%	74.9%	93.7%	99.9%	100.0%	100.0%	100.0%
40	3.525	24.7%	75.8%	94.1%	99.9%	100.0%	100.0%	100.0%
41	3.439	25.2%	76.6%	94.5%	99.9%	100.0%	100.0%	100.0%
42	3.357	25.8%	77.4%	94.9%	99.9%	100.0%	100.0%	100.0%
43	3.279	26.3%	78.2%	95.3%	100.0%	100.0%	100.0%	100.0%
44	3.205	26.8%	79.0%	95.6%	100.0%	100.0%	100.0%	100.0%
45	3.133	27.3%	79.7%	95.9%	100.0%	100.0%	100.0%	100.0%
46	3.065	27.8%	80.4%	96.2%	100.0%	100.0%	100.0%	100.0%
47	3.000	28.3%	81.1%	96.4%	100.0%	100.0%	100.0%	100.0%
48	2.938	28.9%	81.8%	96.7%	100.0%	100.0%	100.0%	100.0%
49	2.878	29.4%	82.4%	96.9%	100.0%	100.0%	100.0%	100.0%
50	2.820	29.9%	83.0%	97.1%	100.0%	100.0%	100.0%	100.0%
51	2.765	30.4%	83.6%	97.3%	100.0%	100.0%	100.0%	100.0%
52	2.712	30.8%	84.2%	97.5%	100.0%	100.0%	100.0%	100.0%
53	2.660	31.3%	84.7%	97.7%	100.0%	100.0%	100.0%	100.0%
54	2.611	31.8%	85.3%	97.8%	100.0%	100.0%	100.0%	100.0%
55	2.564	32.3%	85.8%	98.0%	100.0%	100.0%	100.0%	100.0%
56	2.518	32.8%	86.3%	98.1%	100.0%	100.0%	100.0%	100.0%
57	2.474	33.3%	86.8%	98.2%	100.0%	100.0%	100.0%	100.0%
58	2.431	33.7%	87.2%	98.4%	100.0%	100.0%	100.0%	100.0%
59	2.390	34.2%	87.7%	98.5%	100.0%	100.0%	100.0%	100.0%
60	2.350	34.7%	88.1%	98.6%	100.0%	100.0%	100.0%	100.0%
61	2.311	35.1%	88.5%	98.7%	100.0%	100.0%	100.0%	100.0%
62	2.274	35.6%	88.9%	98.8%	100.0%	100.0%	100.0%	100.0%
63	2.238	36.0%	89.3%	98.9%	100.0%	100.0%	100.0%	100.0%
64	2.203	36.5%	89.7%	98.9%	100.0%	100.0%	100.0%	100.0%
65	2.169	36.9%	90.0%	99.0%	100.0%	100.0%	100.0%	100.0%
66	2.136	37.4%	90.4%	99.1%	100.0%	100.0%	100.0%	100.0%
67	2.104	37.8%	90.7%	99.1%	100.0%	100.0%	100.0%	100.0%
68	2.074	38.3%	91.0%	99.2%	100.0%	100.0%	100.0%	100.0%
69	2.043	38.7%	91.3%	99.3%	100.0%	100.0%	100.0%	100.0%
70	2.014	39.1%	91.6%	99.3%	100.0%	100.0%	100.0%	100.0%
71	1.986	39.6%	91.9%	99.3%	100.0%	100.0%	100.0%	100.0%
72	1.958	40.0%	92.2%	99.4%	100.0%	100.0%	100.0%	100.0%

73	1.932	40.4%	92.5%	99.4%	100.0%	100.0%	100.0%	100.0%
74	1.905	40.8%	92.7%	99.5%	100.0%	100.0%	100.0%	100.0%
75	1.880	41.3%	93.0%	99.5%	100.0%	100.0%	100.0%	100.0%
76	1.855	41.7%	93.2%	99.5%	100.0%	100.0%	100.0%	100.0%
77	1.831	42.1%	93.5%	99.6%	100.0%	100.0%	100.0%	100.0%
78	1.808	42.5%	93.7%	99.6%	100.0%	100.0%	100.0%	100.0%
79	1.785	42.9%	93.9%	99.6%	100.0%	100.0%	100.0%	100.0%
80	1.763	43.3%	94.1%	99.7%	100.0%	100.0%	100.0%	100.0%
81	1.741	43.7%	94.3%	99.7%	100.0%	100.0%	100.0%	100.0%
82	1.720	44.1%	94.5%	99.7%	100.0%	100.0%	100.0%	100.0%
83	1.699	44.5%	94.7%	99.7%	100.0%	100.0%	100.0%	100.0%
84	1.679	44.9%	94.9%	99.7%	100.0%	100.0%	100.0%	100.0%
85	1.659	45.3%	95.1%	99.8%	100.0%	100.0%	100.0%	100.0%
86	1.640	45.7%	95.3%	99.8%	100.0%	100.0%	100.0%	100.0%
87	1.621	46.0%	95.4%	99.8%	100.0%	100.0%	100.0%	100.0%
88	1.602	46.4%	95.6%	99.8%	100.0%	100.0%	100.0%	100.0%
89	1.584	46.8%	95.7%	99.8%	100.0%	100.0%	100.0%	100.0%
90	1.567	47.2%	95.9%	99.8%	100.0%	100.0%	100.0%	100.0%
91	1.549	47.6%	96.0%	99.8%	100.0%	100.0%	100.0%	100.0%
92	1.533	47.9%	96.2%	99.9%	100.0%	100.0%	100.0%	100.0%
93	1.516	48.3%	96.3%	99.9%	100.0%	100.0%	100.0%	100.0%
94	1.500	48.7%	96.4%	99.9%	100.0%	100.0%	100.0%	100.0%
95	1.484	49.0%	96.6%	99.9%	100.0%	100.0%	100.0%	100.0%
96	1.469	49.4%	96.7%	99.9%	100.0%	100.0%	100.0%	100.0%
97	1.454	49.7%	96.8%	99.9%	100.0%	100.0%	100.0%	100.0%
98	1.439	50.1%	96.9%	99.9%	100.0%	100.0%	100.0%	100.0%
99	1.424	50.4%	97.0%	99.9%	100.0%	100.0%	100.0%	100.0%
100	1.410	50.8%	97.1%	99.9%	100.0%	100.0%	100.0%	100.0%
101	1.396	51.1%	97.2%	99.9%	100.0%	100.0%	100.0%	100.0%
102	1.382	51.5%	97.3%	99.9%	100.0%	100.0%	100.0%	100.0%
103	1.369	51.8%	97.4%	99.9%	100.0%	100.0%	100.0%	100.0%
104	1.356	52.2%	97.5%	99.9%	100.0%	100.0%	100.0%	100.0%
105	1.343	52.5%	97.6%	99.9%	100.0%	100.0%	100.0%	100.0%
106	1.330	52.8%	97.7%	99.9%	100.0%	100.0%	100.0%	100.0%
107	1.318	53.2%	97.8%	99.9%	100.0%	100.0%	100.0%	100.0%
108	1.306	53.5%	97.8%	100.0%	100.0%	100.0%	100.0%	100.0%
109	1.294	53.8%	97.9%	100.0%	100.0%	100.0%	100.0%	100.0%
110	1.282	54.2%	98.0%	100.0%	100.0%	100.0%	100.0%	100.0%
111	1.270	54.5%	98.0%	100.0%	100.0%	100.0%	100.0%	100.0%
112	1.259	54.8%	98.1%	100.0%	100.0%	100.0%	100.0%	100.0%

113	1.248	55.1%	98.2%	100.0%	100.0%	100.0%	100.0%	100.0%
114	1.237	55.4%	98.2%	100.0%	100.0%	100.0%	100.0%	100.0%
115	1.226	55.8%	98.3%	100.0%	100.0%	100.0%	100.0%	100.0%
116	1.216	56.1%	98.4%	100.0%	100.0%	100.0%	100.0%	100.0%
117	1.205	56.4%	98.4%	100.0%	100.0%	100.0%	100.0%	100.0%
118	1.195	56.7%	98.5%	100.0%	100.0%	100.0%	100.0%	100.0%
119	1.185	57.0%	98.5%	100.0%	100.0%	100.0%	100.0%	100.0%
120	1.175	57.3%	98.6%	100.0%	100.0%	100.0%	100.0%	100.0%
121	1.165	57.6%	98.6%	100.0%	100.0%	100.0%	100.0%	100.0%
122	1.156	57.9%	98.7%	100.0%	100.0%	100.0%	100.0%	100.0%
123	1.146	58.2%	98.7%	100.0%	100.0%	100.0%	100.0%	100.0%
124	1.137	58.5%	98.8%	100.0%	100.0%	100.0%	100.0%	100.0%
125	1.128	58.8%	98.8%	100.0%	100.0%	100.0%	100.0%	100.0%
126	1.119	59.1%	98.9%	100.0%	100.0%	100.0%	100.0%	100.0%
127	1.110	59.4%	98.9%	100.0%	100.0%	100.0%	100.0%	100.0%
128	1.102	59.7%	98.9%	100.0%	100.0%	100.0%	100.0%	100.0%
129	1.093	59.9%	99.0%	100.0%	100.0%	100.0%	100.0%	100.0%
130	1.085	60.2%	99.0%	100.0%	100.0%	100.0%	100.0%	100.0%
131	1.076	60.5%	99.0%	100.0%	100.0%	100.0%	100.0%	100.0%
132	1.068	60.8%	99.1%	100.0%	100.0%	100.0%	100.0%	100.0%
133	1.060	61.1%	99.1%	100.0%	100.0%	100.0%	100.0%	100.0%
134	1.052	61.3%	99.1%	100.0%	100.0%	100.0%	100.0%	100.0%
135	1.044	61.6%	99.2%	100.0%	100.0%	100.0%	100.0%	100.0%
136	1.037	61.9%	99.2%	100.0%	100.0%	100.0%	100.0%	100.0%
137	1.029	62.2%	99.2%	100.0%	100.0%	100.0%	100.0%	100.0%
138	1.022	62.4%	99.3%	100.0%	100.0%	100.0%	100.0%	100.0%
139	1.014	62.7%	99.3%	100.0%	100.0%	100.0%	100.0%	100.0%
140	1.007	63.0%	99.3%	100.0%	100.0%	100.0%	100.0%	100.0%
141	1.000	63.2%	99.3%	100.0%	100.0%	100.0%	100.0%	100.0%
142	0.993	63.5%	99.3%	100.0%	100.0%	100.0%	100.0%	100.0%
143	0.986	63.7%	99.4%	100.0%	100.0%	100.0%	100.0%	100.0%
144	0.979	64.0%	99.4%	100.0%	100.0%	100.0%	100.0%	100.0%
145	0.972	64.2%	99.4%	100.0%	100.0%	100.0%	100.0%	100.0%
146	0.966	64.5%	99.4%	100.0%	100.0%	100.0%	100.0%	100.0%
147	0.959	64.7%	99.5%	100.0%	100.0%	100.0%	100.0%	100.0%
148	0.953	65.0%	99.5%	100.0%	100.0%	100.0%	100.0%	100.0%
149	0.946	65.2%	99.5%	100.0%	100.0%	100.0%	100.0%	100.0%
150	0.940	65.5%	99.5%	100.0%	100.0%	100.0%	100.0%	100.0%
151	0.934	65.7%	99.5%	100.0%	100.0%	100.0%	100.0%	100.0%
152	0.928	66.0%	99.5%	100.0%	100.0%	100.0%	100.0%	100.0%

153	0.922	66.2%	99.6%	100.0%	100.0%	100.0%	100.0%	100.0%
154	0.916	66.5%	99.6%	100.0%	100.0%	100.0%	100.0%	100.0%
155	0.910	66.7%	99.6%	100.0%	100.0%	100.0%	100.0%	100.0%
156	0.904	66.9%	99.6%	100.0%	100.0%	100.0%	100.0%	100.0%
157	0.898	67.2%	99.6%	100.0%	100.0%	100.0%	100.0%	100.0%
158	0.892	67.4%	99.6%	100.0%	100.0%	100.0%	100.0%	100.0%
159	0.887	67.6%	99.6%	100.0%	100.0%	100.0%	100.0%	100.0%
160	0.881	67.8%	99.7%	100.0%	100.0%	100.0%	100.0%	100.0%
161	0.876	68.1%	99.7%	100.0%	100.0%	100.0%	100.0%	100.0%
162	0.870	68.3%	99.7%	100.0%	100.0%	100.0%	100.0%	100.0%
163	0.865	68.5%	99.7%	100.0%	100.0%	100.0%	100.0%	100.0%
164	0.860	68.7%	99.7%	100.0%	100.0%	100.0%	100.0%	100.0%
165	0.855	69.0%	99.7%	100.0%	100.0%	100.0%	100.0%	100.0%
166	0.849	69.2%	99.7%	100.0%	100.0%	100.0%	100.0%	100.0%
167	0.844	69.4%	99.7%	100.0%	100.0%	100.0%	100.0%	100.0%
168	0.839	69.6%	99.7%	100.0%	100.0%	100.0%	100.0%	100.0%
169	0.834	69.8%	99.8%	100.0%	100.0%	100.0%	100.0%	100.0%
170	0.829	70.1%	99.8%	100.0%	100.0%	100.0%	100.0%	100.0%
171	0.825	70.3%	99.8%	100.0%	100.0%	100.0%	100.0%	100.0%
172	0.820	70.5%	99.8%	100.0%	100.0%	100.0%	100.0%	100.0%
173	0.815	70.7%	99.8%	100.0%	100.0%	100.0%	100.0%	100.0%
174	0.810	70.9%	99.8%	100.0%	100.0%	100.0%	100.0%	100.0%
175	0.806	71.1%	99.8%	100.0%	100.0%	100.0%	100.0%	100.0%
176	0.801	71.3%	99.8%	100.0%	100.0%	100.0%	100.0%	100.0%
177	0.797	71.5%	99.8%	100.0%	100.0%	100.0%	100.0%	100.0%
178	0.792	71.7%	99.8%	100.0%	100.0%	100.0%	100.0%	100.0%
179	0.788	71.9%	99.8%	100.0%	100.0%	100.0%	100.0%	100.0%
180	0.783	72.1%	99.8%	100.0%	100.0%	100.0%	100.0%	100.0%
181	0.779	72.3%	99.8%	100.0%	100.0%	100.0%	100.0%	100.0%
182	0.775	72.5%	99.8%	100.0%	100.0%	100.0%	100.0%	100.0%
183	0.770	72.7%	99.8%	100.0%	100.0%	100.0%	100.0%	100.0%
184	0.766	72.9%	99.9%	100.0%	100.0%	100.0%	100.0%	100.0%
185	0.762	73.1%	99.9%	100.0%	100.0%	100.0%	100.0%	100.0%
186	0.758	73.3%	99.9%	100.0%	100.0%	100.0%	100.0%	100.0%
187	0.754	73.5%	99.9%	100.0%	100.0%	100.0%	100.0%	100.0%
188	0.750	73.6%	99.9%	100.0%	100.0%	100.0%	100.0%	100.0%
189	0.746	73.8%	99.9%	100.0%	100.0%	100.0%	100.0%	100.0%
190	0.742	74.0%	99.9%	100.0%	100.0%	100.0%	100.0%	100.0%
191	0.738	74.2%	99.9%	100.0%	100.0%	100.0%	100.0%	100.0%
192	0.734	74.4%	99.9%	100.0%	100.0%	100.0%	100.0%	100.0%

193	0.731	74.6%	99.9%	100.0%	100.0%	100.0%	100.0%	100.0%
194	0.727	74.7%	99.9%	100.0%	100.0%	100.0%	100.0%	100.0%
195	0.723	74.9%	99.9%	100.0%	100.0%	100.0%	100.0%	100.0%
196	0.719	75.1%	99.9%	100.0%	100.0%	100.0%	100.0%	100.0%
197	0.716	75.3%	99.9%	100.0%	100.0%	100.0%	100.0%	100.0%
198	0.712	75.4%	99.9%	100.0%	100.0%	100.0%	100.0%	100.0%
199	0.709	75.6%	99.9%	100.0%	100.0%	100.0%	100.0%	100.0%
200	0.705	75.8%	99.9%	100.0%	100.0%	100.0%	100.0%	100.0%
201	0.701	76.0%	99.9%	100.0%	100.0%	100.0%	100.0%	100.0%
202	0.698	76.1%	99.9%	100.0%	100.0%	100.0%	100.0%	100.0%
203	0.695	76.3%	99.9%	100.0%	100.0%	100.0%	100.0%	100.0%
204	0.691	76.5%	99.9%	100.0%	100.0%	100.0%	100.0%	100.0%
205	0.688	76.6%	99.9%	100.0%	100.0%	100.0%	100.0%	100.0%
206	0.684	76.8%	99.9%	100.0%	100.0%	100.0%	100.0%	100.0%
207	0.681	77.0%	99.9%	100.0%	100.0%	100.0%	100.0%	100.0%
208	0.678	77.1%	99.9%	100.0%	100.0%	100.0%	100.0%	100.0%
209	0.675	77.3%	99.9%	100.0%	100.0%	100.0%	100.0%	100.0%
210	0.671	77.4%	99.9%	100.0%	100.0%	100.0%	100.0%	100.0%
211	0.668	77.6%	99.9%	100.0%	100.0%	100.0%	100.0%	100.0%
212	0.665	77.8%	99.9%	100.0%	100.0%	100.0%	100.0%	100.0%
213	0.662	77.9%	99.9%	100.0%	100.0%	100.0%	100.0%	100.0%
214	0.659	78.1%	99.9%	100.0%	100.0%	100.0%	100.0%	100.0%
215	0.656	78.2%	100.0%	100.0%	100.0%	100.0%	100.0%	100.0%
216	0.653	78.4%	100.0%	100.0%	100.0%	100.0%	100.0%	100.0%
217	0.650	78.5%	100.0%	100.0%	100.0%	100.0%	100.0%	100.0%
218	0.647	78.7%	100.0%	100.0%	100.0%	100.0%	100.0%	100.0%
219	0.644	78.8%	100.0%	100.0%	100.0%	100.0%	100.0%	100.0%
220	0.641	79.0%	100.0%	100.0%	100.0%	100.0%	100.0%	100.0%
221	0.638	79.1%	100.0%	100.0%	100.0%	100.0%	100.0%	100.0%
222	0.635	79.3%	100.0%	100.0%	100.0%	100.0%	100.0%	100.0%
223	0.632	79.4%	100.0%	100.0%	100.0%	100.0%	100.0%	100.0%
224	0.629	79.6%	100.0%	100.0%	100.0%	100.0%	100.0%	100.0%
225	0.627	79.7%	100.0%	100.0%	100.0%	100.0%	100.0%	100.0%
226	0.624	79.9%	100.0%	100.0%	100.0%	100.0%	100.0%	100.0%
227	0.621	80.0%	100.0%	100.0%	100.0%	100.0%	100.0%	100.0%
228	0.618	80.2%	100.0%	100.0%	100.0%	100.0%	100.0%	100.0%
229	0.616	80.3%	100.0%	100.0%	100.0%	100.0%	100.0%	100.0%
230	0.613	80.4%	100.0%	100.0%	100.0%	100.0%	100.0%	100.0%
231	0.610	80.6%	100.0%	100.0%	100.0%	100.0%	100.0%	100.0%
232	0.608	80.7%	100.0%	100.0%	100.0%	100.0%	100.0%	100.0%

233	0.605	80.8%	100.0%	100.0%	100.0%	100.0%	100.0%	100.0%
234	0.603	81.0%	100.0%	100.0%	100.0%	100.0%	100.0%	100.0%
235	0.600	81.1%	100.0%	100.0%	100.0%	100.0%	100.0%	100.0%
236	0.597	81.2%	100.0%	100.0%	100.0%	100.0%	100.0%	100.0%
237	0.595	81.4%	100.0%	100.0%	100.0%	100.0%	100.0%	100.0%
238	0.592	81.5%	100.0%	100.0%	100.0%	100.0%	100.0%	100.0%
239	0.590	81.6%	100.0%	100.0%	100.0%	100.0%	100.0%	100.0%
240	0.588	81.8%	100.0%	100.0%	100.0%	100.0%	100.0%	100.0%
241	0.585	81.9%	100.0%	100.0%	100.0%	100.0%	100.0%	100.0%
242	0.583	82.0%	100.0%	100.0%	100.0%	100.0%	100.0%	100.0%
243	0.580	82.2%	100.0%	100.0%	100.0%	100.0%	100.0%	100.0%
244	0.578	82.3%	100.0%	100.0%	100.0%	100.0%	100.0%	100.0%
245	0.576	82.4%	100.0%	100.0%	100.0%	100.0%	100.0%	100.0%
246	0.573	82.5%	100.0%	100.0%	100.0%	100.0%	100.0%	100.0%
247	0.571	82.7%	100.0%	100.0%	100.0%	100.0%	100.0%	100.0%
248	0.569	82.8%	100.0%	100.0%	100.0%	100.0%	100.0%	100.0%
249	0.566	82.9%	100.0%	100.0%	100.0%	100.0%	100.0%	100.0%
250	0.564	83.0%	100.0%	100.0%	100.0%	100.0%	100.0%	100.0%
251	0.562	83.1%	100.0%	100.0%	100.0%	100.0%	100.0%	100.0%
252	0.560	83.3%	100.0%	100.0%	100.0%	100.0%	100.0%	100.0%
253	0.557	83.4%	100.0%	100.0%	100.0%	100.0%	100.0%	100.0%
254	0.555	83.5%	100.0%	100.0%	100.0%	100.0%	100.0%	100.0%
255	0.553	83.6%	100.0%	100.0%	100.0%	100.0%	100.0%	100.0%
256	0.551	83.7%	100.0%	100.0%	100.0%	100.0%	100.0%	100.0%
257	0.549	83.8%	100.0%	100.0%	100.0%	100.0%	100.0%	100.0%
258	0.547	84.0%	100.0%	100.0%	100.0%	100.0%	100.0%	100.0%
259	0.544	84.1%	100.0%	100.0%	100.0%	100.0%	100.0%	100.0%
260	0.542	84.2%	100.0%	100.0%	100.0%	100.0%	100.0%	100.0%
261	0.540	84.3%	100.0%	100.0%	100.0%	100.0%	100.0%	100.0%
262	0.538	84.4%	100.0%	100.0%	100.0%	100.0%	100.0%	100.0%
263	0.536	84.5%	100.0%	100.0%	100.0%	100.0%	100.0%	100.0%
264	0.534	84.6%	100.0%	100.0%	100.0%	100.0%	100.0%	100.0%
265	0.532	84.7%	100.0%	100.0%	100.0%	100.0%	100.0%	100.0%
266	0.530	84.8%	100.0%	100.0%	100.0%	100.0%	100.0%	100.0%
267	0.528	84.9%	100.0%	100.0%	100.0%	100.0%	100.0%	100.0%
268	0.526	85.1%	100.0%	100.0%	100.0%	100.0%	100.0%	100.0%
269	0.524	85.2%	100.0%	100.0%	100.0%	100.0%	100.0%	100.0%
270	0.522	85.3%	100.0%	100.0%	100.0%	100.0%	100.0%	100.0%
271	0.520	85.4%	100.0%	100.0%	100.0%	100.0%	100.0%	100.0%
272	0.518	85.5%	100.0%	100.0%	100.0%	100.0%	100.0%	100.0%

273	0.516	85.6%	100.0%	100.0%	100.0%	100.0%	100.0%	100.0%
274	0.515	85.7%	100.0%	100.0%	100.0%	100.0%	100.0%	100.0%
275	0.513	85.8%	100.0%	100.0%	100.0%	100.0%	100.0%	100.0%
276	0.511	85.9%	100.0%	100.0%	100.0%	100.0%	100.0%	100.0%
277	0.509	86.0%	100.0%	100.0%	100.0%	100.0%	100.0%	100.0%
278	0.507	86.1%	100.0%	100.0%	100.0%	100.0%	100.0%	100.0%
279	0.505	86.2%	100.0%	100.0%	100.0%	100.0%	100.0%	100.0%
280	0.504	86.3%	100.0%	100.0%	100.0%	100.0%	100.0%	100.0%
281	0.502	86.4%	100.0%	100.0%	100.0%	100.0%	100.0%	100.0%
282	0.500	86.5%	100.0%	100.0%	100.0%	100.0%	100.0%	100.0%
283	0.498	86.6%	100.0%	100.0%	100.0%	100.0%	100.0%	100.0%
284	0.496	86.7%	100.0%	100.0%	100.0%	100.0%	100.0%	100.0%
285	0.495	86.8%	100.0%	100.0%	100.0%	100.0%	100.0%	100.0%
286	0.493	86.8%	100.0%	100.0%	100.0%	100.0%	100.0%	100.0%
287	0.491	86.9%	100.0%	100.0%	100.0%	100.0%	100.0%	100.0%
288	0.490	87.0%	100.0%	100.0%	100.0%	100.0%	100.0%	100.0%
289	0.488	87.1%	100.0%	100.0%	100.0%	100.0%	100.0%	100.0%
290	0.486	87.2%	100.0%	100.0%	100.0%	100.0%	100.0%	100.0%
291	0.485	87.3%	100.0%	100.0%	100.0%	100.0%	100.0%	100.0%
292	0.483	87.4%	100.0%	100.0%	100.0%	100.0%	100.0%	100.0%
293	0.481	87.5%	100.0%	100.0%	100.0%	100.0%	100.0%	100.0%
294	0.480	87.6%	100.0%	100.0%	100.0%	100.0%	100.0%	100.0%
295	0.478	87.7%	100.0%	100.0%	100.0%	100.0%	100.0%	100.0%
296	0.476	87.7%	100.0%	100.0%	100.0%	100.0%	100.0%	100.0%
297	0.475	87.8%	100.0%	100.0%	100.0%	100.0%	100.0%	100.0%
298	0.473	87.9%	100.0%	100.0%	100.0%	100.0%	100.0%	100.0%
299	0.472	88.0%	100.0%	100.0%	100.0%	100.0%	100.0%	100.0%
300	0.470	88.1%	100.0%	100.0%	100.0%	100.0%	100.0%	100.0%
301	0.468	88.2%	100.0%	100.0%	100.0%	100.0%	100.0%	100.0%
302	0.467	88.3%	100.0%	100.0%	100.0%	100.0%	100.0%	100.0%
303	0.465	88.3%	100.0%	100.0%	100.0%	100.0%	100.0%	100.0%
304	0.464	88.4%	100.0%	100.0%	100.0%	100.0%	100.0%	100.0%
305	0.462	88.5%	100.0%	100.0%	100.0%	100.0%	100.0%	100.0%
306	0.461	88.6%	100.0%	100.0%	100.0%	100.0%	100.0%	100.0%
307	0.459	88.7%	100.0%	100.0%	100.0%	100.0%	100.0%	100.0%
308	0.458	88.7%	100.0%	100.0%	100.0%	100.0%	100.0%	100.0%
309	0.456	88.8%	100.0%	100.0%	100.0%	100.0%	100.0%	100.0%
310	0.455	88.9%	100.0%	100.0%	100.0%	100.0%	100.0%	100.0%
311	0.453	89.0%	100.0%	100.0%	100.0%	100.0%	100.0%	100.0%
312	0.452	89.1%	100.0%	100.0%	100.0%	100.0%	100.0%	100.0%

313	0.450	89.1%	100.0%	100.0%	100.0%	100.0%	100.0%	100.0%
314	0.449	89.2%	100.0%	100.0%	100.0%	100.0%	100.0%	100.0%
315	0.448	89.3%	100.0%	100.0%	100.0%	100.0%	100.0%	100.0%
316	0.446	89.4%	100.0%	100.0%	100.0%	100.0%	100.0%	100.0%
317	0.445	89.4%	100.0%	100.0%	100.0%	100.0%	100.0%	100.0%
318	0.443	89.5%	100.0%	100.0%	100.0%	100.0%	100.0%	100.0%
319	0.442	89.6%	100.0%	100.0%	100.0%	100.0%	100.0%	100.0%
320	0.441	89.7%	100.0%	100.0%	100.0%	100.0%	100.0%	100.0%
321	0.439	89.7%	100.0%	100.0%	100.0%	100.0%	100.0%	100.0%
322	0.438	89.8%	100.0%	100.0%	100.0%	100.0%	100.0%	100.0%
323	0.437	89.9%	100.0%	100.0%	100.0%	100.0%	100.0%	100.0%
324	0.435	90.0%	100.0%	100.0%	100.0%	100.0%	100.0%	100.0%
325	0.434	90.0%	100.0%	100.0%	100.0%	100.0%	100.0%	100.0%
326	0.433	90.1%	100.0%	100.0%	100.0%	100.0%	100.0%	100.0%
327	0.431	90.2%	100.0%	100.0%	100.0%	100.0%	100.0%	100.0%
328	0.430	90.2%	100.0%	100.0%	100.0%	100.0%	100.0%	100.0%
329	0.429	90.3%	100.0%	100.0%	100.0%	100.0%	100.0%	100.0%
330	0.427	90.4%	100.0%	100.0%	100.0%	100.0%	100.0%	100.0%
331	0.426	90.4%	100.0%	100.0%	100.0%	100.0%	100.0%	100.0%
332	0.425	90.5%	100.0%	100.0%	100.0%	100.0%	100.0%	100.0%
333	0.423	90.6%	100.0%	100.0%	100.0%	100.0%	100.0%	100.0%
334	0.422	90.6%	100.0%	100.0%	100.0%	100.0%	100.0%	100.0%
335	0.421	90.7%	100.0%	100.0%	100.0%	100.0%	100.0%	100.0%
336	0.420	90.8%	100.0%	100.0%	100.0%	100.0%	100.0%	100.0%
337	0.418	90.8%	100.0%	100.0%	100.0%	100.0%	100.0%	100.0%
338	0.417	90.9%	100.0%	100.0%	100.0%	100.0%	100.0%	100.0%
339	0.416	91.0%	100.0%	100.0%	100.0%	100.0%	100.0%	100.0%
340	0.415	91.0%	100.0%	100.0%	100.0%	100.0%	100.0%	100.0%
341	0.413	91.1%	100.0%	100.0%	100.0%	100.0%	100.0%	100.0%
342	0.412	91.2%	100.0%	100.0%	100.0%	100.0%	100.0%	100.0%
343	0.411	91.2%	100.0%	100.0%	100.0%	100.0%	100.0%	100.0%
344	0.410	91.3%	100.0%	100.0%	100.0%	100.0%	100.0%	100.0%
345	0.409	91.3%	100.0%	100.0%	100.0%	100.0%	100.0%	100.0%
346	0.408	91.4%	100.0%	100.0%	100.0%	100.0%	100.0%	100.0%
347	0.406	91.5%	100.0%	100.0%	100.0%	100.0%	100.0%	100.0%
348	0.405	91.5%	100.0%	100.0%	100.0%	100.0%	100.0%	100.0%
349	0.404	91.6%	100.0%	100.0%	100.0%	100.0%	100.0%	100.0%
350	0.403	91.6%	100.0%	100.0%	100.0%	100.0%	100.0%	100.0%
351	0.402	91.7%	100.0%	100.0%	100.0%	100.0%	100.0%	100.0%
352	0.401	91.8%	100.0%	100.0%	100.0%	100.0%	100.0%	100.0%